Methods in Molecular Biology™

VOLUME 239

Cell Migration in Inflammation and Immunity

Methods and Protocols

Edited by

Daniele D'Ambrosio
Francesco Sinigaglia

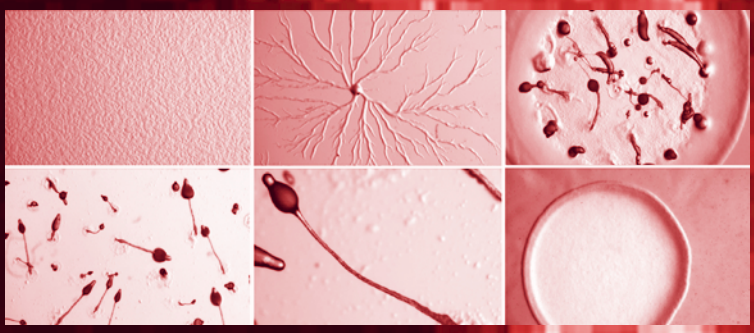

HUMANA PRESS

Cell Migration in Inflammation and Immunity

METHODS IN MOLECULAR BIOLOGY™

John M. Walker, SERIES EDITOR

252. **Ribozymes and siRNA Protocols, Second Edition,** edited by *Mouldy Sioud, 2004*
251. **HPLC of Peptides and Proteins:** *Methods and Protocols,* edited by *Marie-Isabel Aguilar, 2004*
250. **MAP Kinase Signaling Protocols,** edited by *Rony Seger, 2004*
249. **Cytokine Protocols,** edited by *Marc De Ley, 2004*
248. **Antibody Engineering:** *Methods and Protocols,* edited by *Benny K. C. Lo, 2004*
247. ***Drosophila* Cytogenetics Protocols,** edited by *Daryl S. Henderson, 2004*
246. **Gene Delivery to Mammalian Cells:** *Volume 2: Viral Gene Transfer Techniques,* edited by *William C. Heiser, 2004*
245. **Gene Delivery to Mammalian Cells:** *Volume 1: Nonviral Gene Transfer Techniques,* edited by *William C. Heiser, 2004*
244. **Protein Purification Protocols, Second Edition,** edited by *Paul Cutler, 2004*
243. **Chiral Separations:** *Methods and Protocols,* edited by *Gerald Gübitz and Martin G. Schmid, 2004*
242. **Atomic Force Microscopy:** *Biomedical Methods and Applications,* edited by *Pier Carlo Braga and Davide Ricci, 2004*
241. **Cell Cycle Checkpoint Control Protocols,** edited by *Howard B. Lieberman, 2004*
240. **Mammalian Artificial Chromosomes:** *Methods and Protocols*, edited by *Vittorio Sgaramella and Sandro Eridani, 2003*
239. **Cell Migration in Inflammation and Immunity:** *Methods and Protocols,* edited by *Daniele D'Ambrosio and Francesco Sinigaglia, 2003*
238. **Biopolymer Methods in Tissue Engineering,** edited by *Anthony P. Hollander and Paul V. Hatton, 2003*
237. **G Protein Signaling:** *Methods and Protocols,* edited by *Alan V. Smrcka, 2003*
236. **Plant Functional Genomics**: *Methods and Protocols*, edited by *Erich Grotewold, 2003*
235. ***E. coli* Plasmid Vectors**: *Methods and Applications*, edited by *Nicola Casali and Andrew Preston, 2003*
234. **p53 Protocols**, edited by *Sumitra Deb and Swati Palit Deb, 2003*
233. **Protein Kinase C Protocols**, edited by *Alexandra C. Newton, 2003*
232. **Protein Misfolding and Disease:** *Principles and Protocols*, edited by *Peter Bross and Niels Gregersen, 2003*
231. **Directed Evolution Library Creation**: *Methods and Protocols*, edited by *Frances H. Arnold and George Georgiou*, *2003*
230. **Directed Enzyme Evolution**: *Screening and Selection Methods*, edited by *Frances H. Arnold and George Georgiou*, *2003*
229. **Lentivirus Gene Engineering Protocols**, edited by *Maurizio Federico, 2003*
228. **Membrane Protein Protocols**: *Expression, Purification, and Characterization*, edited by *Barry S. Selinsky, 2003*
227. **Membrane Transporters:** *Methods and Protocols,* edited by *Qing Yan, 2003*
226. **PCR Protocols, Second Edition,** edited by *John M. S. Bartlett and David Stirling, 2003*
225. **Inflammation Protocols,** edited by *Paul G. Winyard and Derek A. Willoughby, 2003*
224. **Functional Genomics:** *Methods and Protocols,* edited by *Michael J. Brownstein and Arkady B. Khodursky, 2003*
223. **Tumor Suppressor Genes:** *Volume 2: Regulation, Function, and Medicinal Applications*, edited by *Wafik S. El-Deiry, 2003*
222. **Tumor Suppressor Genes:** *Volume 1: Pathways and Isolation Strategies,* edited by *Wafik S. El-Deiry, 2003*
221. **Generation of cDNA Libraries:** *Methods and Protocols*, edited by *Shao-Yao Ying, 2003*
220. **Cancer Cytogenetics:** *Methods and Protocols,* edited by *John Swansbury, 2003*
219. **Cardiac Cell and Gene Transfer:** *Principles, Protocols, and Applications,* edited by *Joseph M. Metzger, 2003*
218. **Cancer Cell Signaling:** *Methods and Protocols,* edited by *David M. Terrian, 2003*
217. **Neurogenetics:** *Methods and Protocols,* edited by *Nicholas T. Potter, 2003*
216. **PCR Detection of Microbial Pathogens:** *Methods and Protocols,* edited by *Konrad Sachse and Joachim Frey, 2003*
215. **Cytokines and Colony Stimulating Factors:** *Methods and Protocols,* edited by *Dieter Körholz and Wieland Kiess, 2003*
214. **Superantigen Protocols,** edited by *Teresa Krakauer, 2003*
213. **Capillary Electrophoresis of Carbohydrates,** edited by *Pierre Thibault and Susumu Honda, 2003*
212. **Single Nucleotide Polymorphisms:** *Methods and Protocols,* edited by *Pui-Yan Kwok, 2003*
211. **Protein Sequencing Protocols, Second Edition,** edited by *Bryan John Smith, 2003*
210. **MHC Protocols,** edited by *Stephen H. Powis and Robert W. Vaughan, 2003*
209. **Transgenic Mouse Methods and Protocols,** edited by *Marten Hofker and Jan van Deursen, 2003*
208. **Peptide Nucleic Acids:** *Methods and Protocols,* edited by *Peter E. Nielsen, 2002*
207. **Recombinant Antibodies for Cancer Therapy:** *Methods and Protocols,* edited by *Martin Welschof and Jürgen Krauss, 2002*
206. **Endothelin Protocols,** edited by *Janet J. Maguire and Anthony P. Davenport, 2002*
205. ***E. coli* Gene Expression Protocols,** edited by *Peter E. Vaillancourt, 2002*
204. **Molecular Cytogenetics:** *Protocols and Applications,* edited by *Yao-Shan Fan, 2002*
203. ***In Situ* Detection of DNA Damage:** *Methods and Protocols,* edited by *Vladimir V. Didenko, 2002*
202. **Thyroid Hormone Receptors:** *Methods and Protocols,* edited by *Aria Baniahmad, 2002*
201. **Combinatorial Library Methods and Protocols,** edited by *Lisa B. English, 2002*
200. **DNA Methylation Protocols,** edited by *Ken I. Mills and Bernie H. Ramsahoye, 2002*
199. **Liposome Methods and Protocols,** edited by *Subhash C. Basu and Manju Basu, 2002*
198. **Neural Stem Cells:** *Methods and Protocols,* edited by *Tanja Zigova, Juan R. Sanchez-Ramos, and Paul R. Sanberg, 2002*
197. **Mitochondrial DNA:** *Methods and Protocols,* edited by *William C. Copeland, 2002*
196. **Oxidants and Antioxidants:** *Ultrastructure and Molecular Biology Protocols,* edited by *Donald Armstrong, 2002*
195. **Quantitative Trait Loci:** *Methods and Protocols*, edited by *Nicola J. Camp and Angela Cox, 2002*
194. **Posttranslational Modifications of Proteins:** *Tools for Functional Proteomics*, edited by *Christoph Kannicht, 2002*
193. **RT-PCR Protocols,** edited by *Joe O'Connell, 2002*

METHODS IN MOLECULAR BIOLOGY™

Cell Migration in Inflammation and Immunity

Methods and Protocols

Edited by

Daniele D'Ambrosio

and

Francesco Sinigaglia

BioXell S.p.A., Milan, Italy

Humana Press  **Totowa, New Jersey**

999 Riverview Drive, Suite 208
Totowa, New Jersey 07512

www.humanapress.com

This publication is printed on acid-free paper. ∞
ANSI Z39.48-1984 (American Standards Institute)

Permanence of Paper for Printed Library Materials.

Cover illustration: Figures 1 and 3 from Chapter 8, "Analyzing Chemotaxis Using *Dicytostelium discoideum* as a Model System" by Mark A. Landree and Peter N. Devreotes.

Production Editor: Wendy S. Kopf.
Cover design by Patricia F. Cleary.

For additional copies, pricing for bulk purchases, and/or information about other Humana titles, contact Humana at the above address or at any of the following numbers: Tel.: 973-256-1699; Fax: 973-256-8341; E-mail: humana@humanapr.com; or visit our Website: www.humanapress.com

Printed in the United States of America. 10 9 8 7 6 5 4 3 2 1

Library of Congress Cataloging in Publication Data

e-ISBN 1-59929-435-2

ISSN: 1064-3745

Cell migration in inflammation an immunity : methods and protocols / edited by Daniele D'Ambrosio and Francesco Sinigaglia.
p. cm. -- (Methods in molecular biology ; 239)
Includes bibliographical references and index.
ISBN 1-58829-102-2
1. Chemokines--Laboratory manuals. 2. Chemokines--Receptors--Laboratory manuals. 3. Leucocytes--Motility--Laboratory manuals. 4. Inflammation--Mediators--Laboratory manuals. I. D'Ambrosio, Daniele. II. Sinigaglia, Francesco. III. Series.

QR185.8.C45C44 2003
616',0473--dc21

2003045270

Preface

Chemokines and their receptors play a central role in the pathogenesis of numerous, perhaps all, acute and chronic inflammatory diseases. About 50 distinct chemokines produced by a variety cell types and tissues either constitutively or in response to inflammatory stimuli are involved in a plethora of biological processes. These small secreted proteins exert their exquisitely variegated functions upon binding to a family of seven-transmembrane spanning G-protein coupled receptors (GPCRs) composed of almost 20 distinct entities. The biological activities of chemokines range from the control of leukocyte trafficking in basal and inflammatory conditions to the regulation of hematopoiesis, angiogenesis, tissue architecture, and organogenesis. The basis for such diversified activities rests, on one hand, upon the ubiquitous nature of chemokine production and chemokine receptor expression. Virtually every cell type can produce chemokines and expresses a unique combination of chemokine receptors. On the other hand, chemokine receptors make use of a flexible and complex network of intracellular signaling machineries that can regulate a variety of cellular functions ranging from cell migration, growth, and differentiation to death.

As knowledge of the size of chemokine and chemokine receptor families rapidly reaches completeness, much is still to be uncovered in terms of functional architecture of the chemokine system. The disparity between the large number of chemokines and that smaller number of receptors is balanced by the promiscuity in ligand–receptor interactions, with multiple chemokines binding to the same receptor and several chemokines binding to more than one receptor. Although most investigators now agree that this apparent redundancy in the chemokine system may actually be a powerful way to diversify their biological activities, we still do not fully understand how this can be achieved.

Evidence for the role of many chemokines and receptors in the pathogenesis of different acute or chronic inflammatory diseases is rapidly increasing. Optimistically, every chemokine receptor may be an interesting pharmacological target for therapeutic intervention. The challenge for the future is to identify the unique pathogenic process and specific disease in which any given chemokine receptor may potentially be implicated. The rapidly expanding knowledge of viral strategies for manipulation of the chemokine system lends support to the notion that chemokines have a crucial biological role. From the revolutionary discovery of chemokine receptors as coreceptors for HIV, and more recently smallpox, a whole range of virally encoded chemokine receptor

analogs, chemokine receptor agonists and antagonists, and chemokine inhibitors has been identified, each hinting at the potent effects and potential benefits of manipulating the chemokine system. These findings, together with the knowledge that chemokine receptors belong to the superfamily of GPCRs that constitute a large fraction of current targets for therapeutic intervention in human diseases, explain why these receptors have become the focus of great interest in the pharmaceutical industry.

The aim of *Cell Migration in Inflammation and Immunity* is to provide a range of protocols and practical approaches to the study of chemokine receptor biology. Innovative techniques and useful protocols are illustrated by leading scientists in the field. Our hope is to provide a useful guide to researchers with various levels of experience who wish to investigate the many areas of chemokine receptor biology ranging from cloning and characterization of novel receptors, to the use of animal models to dissect chemokine receptor function in vivo. This book strives to cover a wide range of chemokine receptor biology, with an emphasis on experimental approaches useful in dissecting their involvement in the pathogenesis of both acute and chronic inflammatory diseases. Each manuscript provides a detailed description of methods and background information, and also includes a short but useful bibliography for a more in depth analysis of each specific topic.

We would like to thank Ms. Angela Evans for her excellent assistance with the preparation of this collection of manuscripts.

Daniele D'Ambrosio
Francesco Sinigaglia

Contents

Preface ..... *v*
Contributors ..... *ix*

1 Chemotaxis and Interaction with Vascular or Lymphatic Endothelium
Silvano Sozzani, Annunciata Vecchi, Paola Allavena, and Alberto Mantovani ***1***

2 Analysis of Integrin-Dependent Rapid Adhesion Under Laminar-Flow Conditions
Carlo Laudanna ***17***

3 Posttranslational Processing of Chemokines
Paul Proost, Frank Mahieu, Evemie Schutyser, and Jo Van Damme ***27***

4 Chemotactic Profiling of Lymphocyte Subpopulations
Lucia Colantonio, Andrea Iellem, and Daniele D'Ambrosio ***45***

5 Measurement of the Levels of Polymerized Actin (F-Actin) in Chemokine-Stimulated Lymphocytes and GFP-Coupled cDNA Transfected Lymphoid Cells by Flow Cytometry
Miguel Vicente-Manzanares, Mariano Vitón, and Francisco Sánchez-Madrid ***53***

6 Evaluation of Rho Family Small G-Protein Activity Induced by Integrin Ligation on Human Leukocytes
Angela Gismondi, Fabrizio Mainiero, and Angela Santoni ***69***

7 Reconstructing Leukocyte Migration in 3D Extracellular Matrix by Time-Lapse Videomicroscopy and Computer-Assisted Tracking
Peter Friedl and Eva-B. Bröcker ***77***

8 Analyzing Chemotaxis Using *Dictyostelium discoideum* as a Model System
Mark A. Landree and Peter N. Devreotes ***91***

9 Conditional Transgenic Models to Study Chemokine Biology
Sergio A. Lira, Borna Mehrad, Shu-Cheng Chen, Petronio Zalamea, David J. Kinsley, Maria T. Wiekowski, Elizabeth Coronel, Galya Vassileva, Denise Manfra, and Kristian K. Jensen ***105***

10 Intravital Microscopy as a Tool for Studying Recruitment and Chemotaxis
Denise C. Cara and Paul Kubes ***123***

11 Tracking Antigen-Specific Lymphocytes In Vivo
Claire L. Adams, Catherine M. Rush, Karen M. Smith, and Paul Garside 133

12 Analysis of Homing-Receptor Expression on Infiltrating Leukocytes in Disease States
Margherita Mariani and Paola Panina-Bordignon 147

13 Interaction of Viral Chemokine Inhibitors with Chemokines
Antonio Alcami 167

14 Discovery of Small-Molecule Antagonists of Chemokine Receptors: *Screening Strategy and Assays*
Maria Elena Fuentes 181

15 Visualization and Analysis of Adhesive Events in Brain Microvessels by Using Intravital Microscopy
Gabriela Constantin 189

16 Animal Models to Study Chemokine Receptor Function In Vivo: *Mouse Models of Allergic Airway Inflammation*
Clare M. Lloyd and Jose-Carlos Gutierrez-Ramos 199

17 Assessing the Role of Multiple Phosphoinositide 3-Kinases in Chemokine Signaling: *Use of Dominant Negative Mutants Controlled by a Tetracycline-Regulated Gene Expression System*
Adam P. Curnock, Yannis Sotsios, and Stephen G. Ward 211

18 In Vitro and In Vivo Models to Study Chemokine Regulation of Angiogenesis
Giovanni Bernardini, Domenico Ribatti, Gaia Spinetti, Lucia Morbidelli, Marina Ziche, Angela Santoni, Maurizio C. Capogrossi, and Monica Napolitano 223

19 Real Time In Vitro Assay for Studying Chemoattractant-Triggered Leukocyte Transendothelial Migration Under Physiological Flow Conditions
Guy Cinamon and Ronen Alon 233

20 Generation of Monoclonal Antibodies Against Chemokine Receptors
Leonor Kremer and Gabriel Márquez 243

21 Detection of High-Affinity α4-Integrin Upon Leukocyte Stimulation by Chemoattractants or Chemokines
Jason R. Chan and Myron I. Cybulsky 261

Index *269*

Contributors

CLAIRE L. ADAMS • *Division of Immunology, Infection, and Inflammation, Western Infirmary, University of Glasgow, Glasgow, UK*

ANTONIO ALCAMI • *Department of Medicine and Division of Virology, Department of Pathology, University of Cambridge, Cambridge, UK*

PAOLA ALLAVENA • *Istituto di Ricerche Farmacologiche Mario Negri, Milan, Italy*

RONEN ALON • *Department of Immunology, The Weizmann Institute of Science, Rehovot, Israel*

GIOVANNI BERNARDINI • *Department of Experimental Medicine and Pathology, University of Rome "La Sapienza," Rome, Italy*

EVA-B. BRÖCKER • *Department of Dermatology, University of Wuerzburg, Wuerzburg, Germany*

MAURIZIO C. CAPOGROSSI • *Instituto Dermopatico Dell'Immacolata, Instituto di Ricovero e Cura Carrattere Scientifico (IRCCS), Rome, Italy*

DENISE C. CARA • *Department of Physiology and Biophysics, Health Sciences Center, University of Calgary, Calgary, Canada*

JASON R. CHAN • *Department of Laboratory Medicine and Pathobiology, Toronto General Research Institute, University of Toronto, Toronto, Canada*

SHU-CHENG CHEN • *Department of Immunology, Schering-Plough Research Institute, Kenilworth, NJ*

GUY CINAMON • *Department of Immunology, The Weizmann Institute of Science, Rehovot, Israel*

LUCIA COLANTONIO • *BioXell S.p.A., Milan, Italy*

GABRIELA CONSTANTIN • *Department of Pathology, University of Verona, Verona, Italy*

ELIZABETH CORONEL • *Department of Immunology, Schering-Plough Research Institute, Kenilworth, NJ*

ADAM P. CURNOCK • *Department of Pharmacy and Pharmacology, University of Bath, Bath, UK*

MYRON I. CYBULSKY • *Department of Laboratory Medicine and Pathobiology, Toronto General Research Institute, University of Toronto, Toronto, Canada*

DANIELE D'AMBROSIO • *BioXell S.p.A., Milan, Italy*

PETER N. DEVREOTES • *Department of Cell Biology, Johns Hopkins University School of Medicine, Baltimore, MD*

Peter Friedl • *Department of Dermatology, University of Wuerzburg, Wuerzburg, Germany*
Maria Elena Fuentes • *Roche Bioscience, Palo Alto, CA*
Paul Garside • *Division of Immunology, Infection, and Inflammation, Western Infirmary, University of Glasgow, Glasgow, UK*
Angela Gismondi • *Department of Experimental Medicine and Pathology, University of Rome La Sapienza, Rome, Italy*
Jose-Carlos Gutierrez-Ramos • *Millennium Pharmaceuticals Inc., Cambridge, MA*
Andrea Iellem • *BioXell S.p.A., Milan, Italy*
Kristian K. Jensen • *Department of Immunology, Schering-Plough Research Institute, Kenilworth, NJ*
David J. Kinsley • *Department of Immunology, Schering-Plough Research Institute, Kenilworth, NJ*
Leonor Kremer • *Department of Immunology and Oncology, Centro Nacional de Biotecnología/CSIC, Autonomous University of Madrid, Madrid, Spain*
Paul Kubes • *Department of Physiology and Biophysics, Health Sciences Center, University of Calgary, Calgary, Canada*
Mark A. Landree • *Department of Cell Biology, Johns Hopkins University School of Medicine, Baltimore, MD*
Carlo Laudanna • *Department of Pathology, Faculty of Medicine, University of Verona, Verona, Italy*
Sergio A. Lira • *Immunobiology Center, Mount Sinai School of Medicine, New York, NY*
Clare M. Lloyd • *Leukocyte Biology Section, Division of Biomedical Sciences, Faculty of Medicine, Imperial College, London, UK*
Frank Mahieu • *Laboratory of Molecular Immunology, Rega Institute, Katholieke Universiteit Leuven, Leuven, Belgium*
Fabrizio Mainiero • *Department of Experimental Medicine and Pathology, University of Rome La Sapienza, Rome, Italy*
Denise Manfra • *Department of Immunology, Schering-Plough Research Institute, Kenilworth, NJ*
Alberto Mantovani • *Istituto di Ricerche Farmacologiche Mario Negri, Department of General Pathology, University of Milan, Milan, Italy*
Margherita Mariani • *BioXell S.p.A., Milan, Italy*
Gabriel Márquez • *Departments of Immunology and Oncology, Centro Nacional de Biotecnología/CSIC, Autonomous University of Madrid, Madrid, Spain*

Borna Mehrad • *Department of Immunology, Schering-Plough Research Institute, Kenilworth, NJ*
Lucia Morbidelli • *Institute of Pharmacological Sciences, University of Siena, Italy*
Monica Napolitano • *Laboratory of Vascular Pathology, Instituto Dermopatico Dell'Immacolata, Instituto di Ricovero e Cura Carrattere Scientifico (IRCCS), Rome, Italy*
Paola Panina-Bordignon • *BioXell S.p.A., Milan, Italy*
Paul Proost • *Laboratory of Molecular Immunology, Rega Institute, Katholieke Universiteit Leuven, Leuven, Belgium*
Domenico Ribatti • *Department of Human Anatomy and Histology, University of Bari, Italy*
Catherine M. Rush • *Division of Immunology, Infection, and Inflammation, Western Infirmary, University of Glasgow, Glasgow, UK*
Francisco Sanchez-Madrid • *Immunology Service, Hospital Universitario de la Princesa, UAM, Madrid, Spain*
Angela Santoni • *Department of Experimental Medicine and Pathology, University of Rome La Sapienza, Rome, Italy*
Evemie Schutyser • *Laboratory of Molecular Immunology, Rega Institute, Katholieke Universiteit Leuven, Leuven, Belgium*
Karen M. Smith • *Division of Immunology, Infection, and Inflammation, Western Infirmary, University of Glasgow, Glasgow, UK*
Yannis Sotsios • *Department of Pharmacy and Pharmacology, University of Bath, Bath, UK*
Silvano Sozzani • *Istituto di Ricerche Farmacologiche Mario Negri, Milan, Italy and Department of Biotechnology, Section of General Pathology, University of Brescia, Italy*
Gaia Spinetti • *Laboratory of Vascular Pathology, Instituto Dermopatico Dell'Immacolata, Instituto di Ricovero e Cura Carrattere Scientifico (IRCCS), Rome, Italy*
Jo Van Damme • *Laboratory of Molecular Immunology, Rega Institute, Katholieke Universiteit Leuven, Leuven, Belgium*
Galya Vassileva • *Department of Immunology, Schering-Plough Research Institute, Kenilworth, NJ*
Annunciata Vecchi • *Istituto di Ricerche Farmacologiche Mario Negri, Milan, Italy*
Miguel Vicente-Manzanares • *Immunology Service, Hospital Universitario de la Princesa, UAM, Madrid, Spain*
Mariano Vitón • *Immunology Service, Hospital Universitario de la Princesa, UAM, Madrid, Spain*

Stephen G. Ward • *Department of Pharmacy and Pharmacology, University of Bath, Bath, UK*
Maria T. Wiekowski • *Department of Immunology, Schering-Plough Research Institute, Kenilworth, NJ*
Petronio Zalamea • *Department of Immunology, Schering-Plough Research Institute, Kenilworth, NJ*
Marina Ziche • *Institute of Pharmacological Sciences, University of Siena, Italy*

1

Chemotaxis and Interaction with Vascular or Lymphatic Endothelium

Silvano Sozzani, Annunciata Vecchi, Paola Allavena, and Alberto Mantovani

1. Introduction

Leukocyte recruitment has been recognized as an early event in inflammatory processes since the late 19th century. Accumulation and trafficking of leukocytes in tissues under physiological and pathological conditions are orderly (typically neutrophils precede mononuclear cells) and selective because, in certain states, one or more leukocyte subsets are recruited preferentially (e.g., eosinophils in allergy). The current paradigm of recruitment is that of a multistep process involving the action of chemotactic signals ***(1,2)***.

Classical chemoattractants include complement components, formyl peptides, and leukotriene B4. In addition, various cytokines are able to elicit directional migration of leukocytes. Whereas molecules, such as monocyte colony-stimulating factor (M-CSF), tumor necrosis factor, and vascular endothelial growth factor (VEGF), exert chemotactic activity, the main chemotactic cytokines are a superfamily of molecules known as chemokines (for chemotactic cytokines). However, the in vivo role of M-CSF and VEGF as chemoattractants is well established.

Several independent lines of work lead to the identification of chemokines such as monocyte chemotactic protein-1 (MCP-1) and related molecules. In the early 1970s it had already been noted that supernatants of activated blood mononuclear cells contained attractants active on monocytes and neutrophils ***(3)***. Subsequently, a chemotactic factor active on monocytes was identified in culture supernants of mouse ***(4)*** and human ***(5,6)*** tumor lines and was called tumor-derived chemotactic factor (TDCF) human ***(5–7)***. At the time, TDCF was rather unique in that it was active on monocytes but not on neutrophils ***(6)*** and

From: *Methods in Molecular Biology, vol. 239: Cell Migration in Inflammation and Immunity*
Edited by: D. D'Ambrosio and F. Sinigaglia © Humana Press Inc., Totowa, NJ

had a low molecular weight ***(5,6)***. Moreover, correlative evidence suggested its involvement in the regulation of macrophage infiltration in murine and human tumors ***(5,6,8)***. A molecule with similar cellular specificity and physicochemical properties was independently identified in the culture supernatant of smooth muscle cells (SMDCF) ***(9)***. The *JE* gene had been identified as an immediate–early platelet-derived growth factor (PDGF)-inducible gene in fibroblasts ***(10,11)***. Thus, in the mid-1980s, a gene (*JE*) was in search of function and a monocyte-specific attractant was waiting for molecular definition. In 1989, MCP-1 was successfully purified from supernatants of a human glioma ***(12)***, a human monocytic leukemia ***(13)*** and a human sarcoma cell line ***(14–16)***: sequencing and molecular cloning revealed its relationship with the long-known *JE* gene ***(17–19)***.

Here, we will focus on selected methods used to investigate chemoattractants at large, with emphasis on chemokines. In particular, classic protocols used for studying cell movement including chemotaxis will be presented, along with methods for transendothelial migration and reverse transmigration. In particular, sources of vascular endothelium and the generation of lymphatic endothelial cultures are discussed. In vivo approaches to monitor leukocyte traffic are discussed elsewhere in this volume; here, we will describe the air-pouch model as a simple in vivo recruitment system.

2. Materials

2.1. Chemotaxis

1. Micro 48-well Boyden chamber (Neuroprobe).
2. Humidified 5% CO_2 incubator.
3. Peripheral mononuclear cells (PBMCs).
4. 5-μm Polycarbonate filters.
5. Glass slides.
6. RPMI 1640 medium (Biochrom KG) + 0.2% bovine serum albumin (BSA).
7. Chemoattractants.
8. Diff-Quik (Harleco).

2.2. Polarization Assay

1. Purified leukocytes (monocytes, neutrophils, lymphocytes).
2. RPMI 1640 medium (Biochrom KG) + 1% fetal calf serum (FCS) (Hyclone).
3. 10X Concentration chemoattractants.
4. 10% (v/v) Formaldehyde.
5. Humidified 5% CO_2 incubator.

2.3. In Vivo Air-Pouch Model

1. Animals: CD1 mice, either sex.
2. Iota carrageenan, 1% in sterile, apirogen saline.

3. Syringes, 5 mL, with a 25G needle.
4. Plastic Pasteur pipets, 3 mL.
5. Hemocytometer.
6. Test tubes.
7. Centrifuge.
8. Sterile apirogen saline.

2.4. Adhesion to Endothelium

1. Endothelial cells (ECs) obtained with a well-established methodology ***(20)***.
2. Tissue culture medium, M199 with 20% FBS +50 µg/mL endothelial cell growth supplement (ECGS) (Collaborative Research) + 100 µg/mL heparin (Sigma). This is referred to as a complete medium.
3. Freshly isolated eukocytes.
4. 96-Well plates (Falcon, Becton Dickinson).
5. Cotton fiocs (Johnson and Johnson).
6. ^{51}Cr (Amersham, 37 MBq, 1 µCi).
7. Humidified 5% CO_2 incubator.
8. Gamma counter windowed for ^{51}Cr.
9. Phosphate-buffered saline (PBS) (Biochrom KG).

2.5. Transendothelial Migration

1. ECs obtained with a well-established methodology ***(20)***.
2. Tissue culture medium, M199 with 20% FBS +50 µg/mL ECGS (Collaborative Research) + 100 µg/mL heparin (Sigma). This is referred to as complete medium.
3. Freshly isolated leukocytes.
4. Single-well Boyden chambers (Neuroprobe).
5. Nitrocellulose filter (12-mm diameter , 5-µm pore, Sartorius).
6. Polyvinyl-pirrolidonet (PVP)-free polycarbonate filter (12-mm diameter, 5-µm pore, Sartorius).
7. Fibronectin (Sigma).
8. 24-Well plates (Falcon, Becton Dickinson).
9. Cotton fiocs (Johnson and Johnson).
10. ^{51}Cr (Amersham, 37 MBq, 1 µCi).
11. Humidified 5% CO_2 incubator.
12. Gamma counter windowed for ^{51}Cr.
13. PBS (Biochrom KG).

2.6. Reverse Transmigration In Vitro

1. ECs obtained with a well-established methodology ***(20)***.
2. Tissue culture medium, M199 with 20% FBS +50 µg/mL ECGS (Collaborative Research) + 100 µg/mL heparin (Sigma). This is referred to as a complete medium.
3. Freshly isolated leukocytes.
4. Single-well Boyden chambers (Neuroprobe).

5. Nitrocellulose filter (12-mm diameter, 5-µm pore, Sartorius).
6. PVP-free polycarbonate filter (12-mm diameter, 5-µm pore, Sartorius).
7. Fibronectin (Sigma).
8. 24-Well plates (Falcon, Becton Dickinson).
9. Cotton fiocs (Johnson and Johnson).
10. ^{51}Cr (Amersham, 37 MBq, 1 µCi).
11. Humidified 5% CO_2 incubator.
12. Gamma counter windowed for ^{51}Cr.
13. PBS (Biochrom KG).
14. Stripping buffer: 20 m*M* NH_4OH, 0.5% (v/v) Triton X-100.

2.7. Endothelial Cells

2.7.1. Generation of Endothelioma Cell Lines

Note: All culture reagents are from Gibco unless otherwise specified.

1. 15 Days' gestation fetuses.
2. 0.05% Trypsin + 0.02% EDTA.
3. Dulbecco's modified Eagle's medium (DMEM) medium + 20% FCS.
4. 6- and 12-Well tissue culture plates.
5. Retrovirus vector N-TKmT.
6. G418.
7. Ca^{2+}- and Mg^{2+}-free PBS or saline.

2.7.2. Generation of Lymphatic Endothelial Cell Lines

Note: All culture reagents are from Gibco unless otherwise specified.

1. Incomplete Freund adjuvant (Sigma).
2. 0.05% Trypsin + 0.02% ethylenediamine tetraacetic acid (EDTA).
3. DMEM medium + 10% FCS (HyClone).
4. Nonessential amino acids (NEAA).
5. Na Pyruvate (NaPyr).
6. 6-Well tissue culture plates and T25 flasks (Falcon).
7. Ca^{2+}- and Mg^{2+}-free PBS or saline.
8. Supernatant of Sarcoma 180.
9. ECGS (Sigma).
10. Heparin (Sigma).
11. Gelatin (Sigma) solution (1% in PBS).
12. Collagenase CLS type I (Worthington Biochem).

3. Methods

3.1. Chemotaxis

Chemotaxis is defined as the directional locomotion of cells sensing a gradient of the stimulus. Chemotaxis has been extensively studied with leukocytes

that are "professional migrants," but a variety of cell types, including fibroblasts, melanoma cells, keratinocytes, and vascular endothelial cells, exhibit directional locomotion in vitro. Two main techniques have been used to measure migration in vitro: migration under agarose and chemotaxis across porous membranes. Although the former approach may more closely resemble the in vivo conditions, the latter is easier to quantitate and allows analysis of directional versus random locomotion. We will therefore focus on the description of migration through a porous membrane using the modified Boyden microchamber method ***(21,22)***.

1. Aliquot 25 µL chemoattractant in each lower well. The 25-µL volume may have some variations (2–3 µL more or less), depending on the microchamber used. It is worth calibrating the lower wells in advance, so that having seeded the chemoattractant, the liquid in the lower well forms a small convex surface that guarantees a perfect adhesion of the filter, avoiding air-bubble formation.
2. Put the filter (25 × 85 mm) on the lower compartment. To avoid confusion in filter orientation, cut an angle of the filter.
3. Mount the silicon trimming and cover piece. Press the cover piece tightly to avoid air bubbles.
4. Seed 50 µL cell suspension (1.5×10^6 cells) in the upper well by leaning the pipet tip on the border of the well and quickly ejecting the cell suspension.
5. Incubate the chamber at 37°C in 5% CO_2 for 1.5 h.
6. Unscrew and turn over the chamber. Hold the upper compartment tightly and remove the lower compartment, keeping the silicon trimming and the filter adhered to the upper compartment of the chamber. At this point, the migrated cells are on the upper surface of the filter.
7. Lift the filter and hold it with a clamp on each end (clamps purchased from the manufacturer of the chamber—Neuroprobe, Maryland, USA).
8. Wash the opaque side of the filter, where the nonmigrated cells remain, by passing this side over PBS. Do not immerse the entire filter in PBS or the migrated cells will be lost.
9. Remove all nonmigrating cells by scraping the opaque surface of the filter against the special rubber policeman (purchased from the manufacturer).
10. Stain the filter with Diff-Quik.
11. Place the filter on glass slides and cout the migrated cells present on the bright surface of the filter. Count 5–10 microscopic fields at ×1000 final magnification.

3.2. Polarization Assay

The early phase of leukocyte response to chemotactic factors is characterized by shape change. Chemoattract stimulation results in the formation of a frontal lamellipodia that contains all of the machinery for cell movement and a rear uropode ***(23)***. This front-tail polarization is rapid, being detectable within minutes, and can easily be observed at the microscope without the need of any special equipment. Leukocyte polarization is not chemotaxis. However, for

the measurement of cell polarization, it is a predictive, and inexpensive, way to investigate chemotactic factors ***(23)***.

1. Prepare cells (10^6/mL) in RPMI 1640 with 1% FCS and prepare 200 µL samples (use at least duplicate tubes).
2. Prepare agonists (e.g., fMLP, C5a; Sigma) at a 10X concentration.
3. Prewarm cells at 37°C for 5 min.
4. Add the agonists in a volume of 20 µL.
5. Stimulate the cells at 37°C for 10 min.
6. Stop the stimulation by the addition of an equal volume (200 µL) of ice-cold 10% (v/v) formaldhyde.
7. The readout of the experiment is the evaluation of the percentage of polarized cells (head/tail) at the microscope (×400). At least 200 total cells per sample need to be counteted.

3.3. In Vivo Air-Pouch Model

In vivo leukocyte recruitment can be easily investigated by the use of the air-pouch model. This technique consists in the creation of a pouch in the back of the mice. The pouch needs to be prepared some days in advance by the the injection of sterile air, to allow the internal formation of an epithelial layer ***(24)***. The advantage of this technique is that a chemotactic factor or a pleyotropic inflammatory agent can be injected locally and cell recruitment can be evaluated by the collection of the local essudate. Cytokines (e.g., chemokines), lipid mediators, and other components of the inflammatory reaction can also be tested in the inflammatory essadute. In our experience, this technique works at the best when pro-inflammatory mediators are inoculated (e.g., endotoxin, interleukin-1, carrageenan). In these conditions, infiltration of mononuclear cells (monocytes and lymphocytes) as well granulocytes is easily detected. Interleukin (IL)-8 and C5a also represent active in vivo chemotactic signals that provide clear results. On the contrary, recruitment of monocytes by chemokines may represent a more difficult task.

1. Inject mice subcutaneously on their back with 5 mL of sterile air (syringes are prepared under a laminar-flow hood).
2. After 3 d, inject the pouches again with 3 mL of sterile air.
3. On d 6, inject 1 mL of 1% carrageenan into the pouches. Controls are injected with 1 mL of saline.
4. On d 7 (24 h later), sacrifice animals. Incise the skin on the back and gently detach it to expose the surface of the air sac. Carefully inject the pouch with 1 mL saline; then, make a small incision in the upper part, recover the liquid with a plastic Pasteur pipet, and immediately put it in a test tube in ice.
5. Record the total amount of liquid collected. Take an aliquot (usually 100 µL) for counting the cells; if differential counting is needed, spin the cells in a cytocentrifuge and stain with Diff-Quik.

6. If measurement of soluble factors has to be performed, centrifuge the remaining fluid at 500*g* for 10 min at 4°C, and collect and store the supernatants at –20°C until use.

The method described here uses carrageenan as a local stimulus for leukocyte recruitment; other stimuli may be used as well, basically following the same protocol. It must be noted, however, that water-soluble stimuli (e.g., proteins) must be prepared in 0.5% sterile (endotoxin-free) carboxymethylcellulose to avoid the fast absorption of the agent from the local site of injection. The carrageenan injection cause a recruitment that lasts a long time, for 7 d, whereas other stimuli (e.g., IL-1β, recruit cells for shorter times. For IL-1β or IL-8, peak cell recruitment is observed at 4 h. Conditions here reported refer to CD1 mice. If other strains of mice are used, experimental conditions need to be validated.

3.4. Adhesion to Endothelium

The emigration of leukocytes from blood to tissues is essential for mediating immune surveillence and mounting inflammatory responses. The interaction of leukocytes with endothelial cells (ECs) can be divided into four sequential steps: tethering, triggering, strong adhesion, and migration. The selectin family of adhesion molecules mediates tethering; strong adhesion is mediated by the integrin family, which need to be activated (triggering), and, finally, migration is induced by local promigratory factors, including some cytokines and chemokines ***(25,26)***. We have studied the adhesive properties and transendothelial migration of leukocytes, but this method may also apply for investigation of other cell types (e.g., tumor cells). Protocols 5 and 6 describe radioisotopic assays for monitoring adhesion and transendothelial migration, based on an assay described in **ref. *27***. Some leukocytes (e.g., dendritic cells, lymphocytes) have a peculiar trafficking pattern from tissues into the lumen of blood or lymphatic vessels. To mimick this basal-to-apical process of migration in vitro, we established a transmigration assay, described in **ref. *20***—the reverse transmigration assay.

1. Various leukocyte subsets (neutrophils, monocytes, natural killer [NK] cells, or lymphocytes) are separated from buffy coats of normal blood donors, as described ***(22,28)***.
2. Resuspend cells at 10^7 cells/mL in RPMI 1640 medium +10% FBS (complete medium) and label by incubation with 100 µCi ^{51}Cr for 1 h at 37°C.
3. After labeling, wash extensively and resuspend in complete medium.
4. Culture ECs in 96-well plates (1×10^4/well) in order to reach a confluent monolayer in 36–48 h. Stimulate designed wells with IL-1 (10 ng/mL) during the last 18 h of culture.
5. Incubate ECs with 100 µL ^{51}Cr-labeled cells resuspended at 107 cells/mL and incubate at 37°C for 30 min.

6. Carefully remove the supernantant and wash the cells twice to remove nonadherent cells.
7. Incubate the adherent cells with 100 µL of NaOH 1 *M* + 1% sodium dodecyl sulfate (SDS) for 5 min and count radioactivity using a gamma counter. Express cell adhesion as percentage of input cells.

The spontaneous adhesion of resting leukocytes to unstimulated ECs varies for different subsets. For instance, the adhesion of NK cells is usually 5–15%, a value intermediate between that of monocytes (20–40%) and the very low value of T-cells and polymorphonuclear cells (PMNs) (<5%). With monocytes and NK cells, there is usually a high degree of variability among different donors.

The adhesive capacity of leukocytes to ECs can be modulated by various signals. When ECs are stimulated with IL-1, leukocyte adhesion increases, as ECs express new adhesion molecules. The identification of adhesion molecules involved in the interaction of leukocytes and ECs is performed by the addition of blocking monoclonal antibodies (mAbs)—most of which are commercially available—specific for the adhesion structures expressed by leukocytes or ECs. Studies with specific mAbs have demonstrated that adhesion through resting ECs is mediated by the LFA-1/ICAM-1,2 pathway, whereas through IL-1, activated ECs involved both LFA-1/ICAM-1 and VLA-4/VCAM-1 for monocytes and lymphoid cells, and neutrophils use only the first pathway, being VLA-4 negative.

Cytokines can also affect leukocytes directly. IL-2 and IL-12, for instance, increases NK cell adhesion to ECs, whereas IL-4 has inhibitory activity.

3.5. Transendothelial Migration

1. Coat PVP-free polycarbonate filters with 1 mL of 10 µg/mL fibronectin in PBS at room temperature for 2 h) in 24-well plates.
2. Aspirate fibronectin and add 10^5 ECs in 2 mL of M199 complete medium and grow to confluence (5–6 d).
3. Place 0.2 mL of complete medium in the lower compartment of each Boyden chamber.
4. Mount the first uncoated filter and on top the second filter coated with ECs.
5. Immediately add 0.15 mL of complete medium. Drying should be avoided.
6. Assemble and screw the upper compartment of the chamber.
7. Label PBMCs (100 µCi ^{51}Cr at 4°C for 1 h) and seed cells [$(3–6) \times 10^5$ in 0.15 mL of complete medium] into the upper compartment of the chamber.
8. Incubate the chamber at 37°C for 60 min.
9. Remove the chambers from the incubator.
10. Collect the medium containing nonadherent cells in a 3-mL vial (fraction A).
11. Gently wash the EC monolayers with 0.5 mL warm medium and collect it (fraction B).

12. Scrape (gently) the EC monolayer and adherent leukocytes with cotton fiocs and transfer to vials (fraction C).
13. Transfer the double filter system to vials together with the medium of the lower compartment (fraction D).
14. Measure radioactivity in each fraction. Fractions A+B represent nonadherent cells. Fraction D represent migrated cells. Because migrated cells had first adhered to ECs, total number of adherent cells is calculated by summing fractions C+D.

The spontaneous transendothelial migration varies for different leukocytes subsets. Usually, only a proportion (about 30%) of EC-adherent leukocytes effectively transmigrate during the assay. When ECs are activated with IL-1, a greater number of cells adhere and transmigrate, but the proportion of transmigrated cells over the input does not dramatically change (usually 30% of EC-adherent leukocytes). It should be noted that IL-1 does not change the state of confluence of the monolayer, as determined by staining.

The identification of adhesion molecules involved in the interaction of leukocytes and EC is performed by the addition of blocking mAbs—most of which are commercially available—specific for the adhesion structures expressed by leukocytes or ECs. Studies with specific mAbs have demonstrated that, like adhesion, transmigration through resting ECs is mediated by the LFA-1/ICAM-1,2 pathway, whereas though IL-1, activated ECs involved both LFA-1/ICAM-1 and VLA-4/VCAM-1 for monocytes and lymphoid cells, and neutrophils use only the first pathway, being VLA-4 negative. In addition, PECAM (CD31) is a molecule expressed both by leukocytes and ECs, and plays a major role during transmigration ***(25)***. Chemoattractants can be seeded in the lower compartment to increase leukocyte transmigration.

3.6. Reverse Transmigration In Vitro

1. Culture EC to confluent monolayers on fibronectin-precoated PVP-free polycarbonate filters in 24-well plates as described in **Subheading 3.5., item 1**.
2. Treat one-half of the filters with 1 mL of stripping buffer for 30 s.
3. Quickly remove the stripping buffer and the digested EC monolayer (ECM) and wash twice with complete medium. Cover the exposed ECM with 1 mL of complete medium. Drying should be avoided.
4. Place 0.2 mL of complete medium in the lower compartment of each Boyden chamber. Mount the first filter, coated with ECs, upside down, and on top of the second filter coated with ECM.
5. Assemble and screw the upper compartment of the chamber.
6. Immediately add 0.15 mL of complete medium. Drying should be avoided.
7. ^{51}Cr-labeled leukocytes are seeded [$(3–6) \times 10^5$ in 0.15 mL of complete medium] into the upper compartment of the chamber.
8. Incubate the chamber at 37°C for 60 min.

9. Remove the chambers from the incubator.
10. Collect the medium present in the upper chamber (fraction A) and wash the ECM layer with 0.5 mL warm medium (fraction B).
11. Collect the ECM-adherent cells with cotton fiocs (fraction C), and the transmigrated cells in the lower compartment (fraction D).
12. Measure radioactivity in each fraction. Fraction A+fraction B represent the non-adherent cells. Fraction C + D represent the adherent cells.
13. Fraction D represents the migrated cells. Please note that in the reverse assay, the transmigrated cells comprise only the radioactivity present in the lower compartment.

3.7. Endothelial Cells

3.7.1. Mouse Vascular Endothelial Cells: Generation of PMT-Transformed Lines

Normal ECs of human and murine origin are cumbersome to obtain and culture. EC lines have been generated sporadically, and, in our experience, at least some of them lack important functions of normal ECs. The polyoma middle T (PmT) oncogene transforms mouse ECs ***(29)*** and can be used to generate immortalized EC cell lines, possibly representative of microvascular elements. These lines retain many properties of normal ECs, including production of and responsiveness to cytokines ***(30–32)***.

All procedures must be performed with sterile material in aseptic conditions.

1. Remove fetuses or organs of interest from six to eight fetuses of 15 d gestation.
2. Cut organ or fetus in small pieces and trypsinize (trypsin 0.05% + EDTA 0.02%, 20 min at 37°C).
3. Collect supernatants and add the same volume of DMEM medium with 20% FCS.
4. Centrifuge at 300*g* for 10 min.
5. Resuspend the pellet in 2–5 mL of DMEM + 10% FCS (complete medium), count, and bring the suspension to $(0.5–1) \times 10^6$ cells/mL.
6. Distribute 2 mL of cell suspensions to each well of 12-well plates and incubate at 37°C in 5% CO_2.
7. After 24 h, remove medium and add about 105 neo colony-forming units (CFU) of the retrovirus vector N-TKmT per well in 1 mL of complete medium. The virus is produced by the GP+E cell line obtained through the courtesy of Dr. E. Wagner (Wien, Austria).
8. After 2 h, remove medium and add fresh complete medium.
9. After 72 h, select PmT-infected neomycin-resistant cells with G418, 800 µg/mL.
10. Change the medium twice a week, keeping G418 at 800 µg/mL.
11. Check wells for G418-resistant cells. They usually are observed after 15–20 d.
12. When cells are confluent, wash the wells throroughly two times with PBS Ca^{2+}- and Mg^{2+}-free or with saline, add 0.3 mL of trypsin 0.05% + EDTA 0.02% for 2–3 min at 37°C, resuspend the detached cells, and add 1 mL of complete medium.

Transfer all of the suspension to one well of a six-well plate and bring to the final volume of 3 mL, with G418 at the 800-µg/mL final concentration.

13. Check cells for the growth every day.
14. When confluent, pass the cells 1:3.

At this stage, cells should not be diluted too much, even if they are growing very well. Confluent monolayers can usually be kept 1–2 d without damage for the cells. On the other hand, if cells are diluted too much, they stop growing and can either remain quiescent for some time and eventually grow again, or die. Maintain selection with G418.

Following this protocol, we have obtained stable cell lines from the heart, brain, and whole embryo of C57Bl. Cell lines show a cobblestone morphology at confluency and maintain a monolayer structure without overgrowth. Cells are positive for CD31/PECAM-1 antigen, show rapid uptake of fluorescinated acetylated low-density lipoprotein, produce IL-6 constitutively, and are negative or weakly positive for factor-VIII-related antigen. Transmission electron microscopy revealed that they were uniformly negative for the presence of Weibel–Palade bodies.

Transformed cells maintain many characteristics of normal endothelial cells, such as CD31 expression, modulation of adhesion molecules by cytokines, and cytokine production ***(31)***. They do not constitutively express ICAM-1, VCAM-1, E-selectin, and P-selectin; however, they can be induced, with the exception of ICAM-1, by exposure to tumor necrosis factor-α (TNF-α) and lipopolysaccharide (LPS), but not IL-1.

Endothelioma cells produce IL-6 and CCL2/JE, whose production can be increased by IL-1 exposure.

Lines originated from embryo tissues infected in vitro with the PmT oncogene of the polyoma virus have been growing in this laboratory since the early 1990s. They represent an easy and reliable source of endothelial cells of murine origin, suitable for studies on EC biology ***(30,33)***.These lines do not need exogeneous growth factors for proliferation. All lines have been frozen, stored in liquid nitrogen, and put again in culture without problems. PmT murine EC lines originated by hemangiomas ***(34,35)*** have been used to generate mAbs against EC-specific antigens expressed constitutively, such as CD31 or induced by cytokines (e.g., VCAM-1 and ELAM-1) ***(36)***. EC lines from different organs can be useful to study the potential diversity of the microvasculature of different organs.

3.7.2. Lymphatic Endothelial Cells: Isolation and Culture

The lymphatic vessels, by channeling fluid and leukocytes from the periphery into the lymph nodes, play a central role in the development of the immune

response. Despite their importance in homeostasis and diseases, the difficulties in enriching and culturing lymphatic endothelial cells limit studies on their biology. Recently, isolation, characterization, and short-term culture of human *(37)* and mouse *(38)* lymphatic cells have been reported, but after very few passages, cells stop growing and die. We report here a metodology to isolate and stabilize in vitro mouse lymphatic endothelial cells.

All procedures must be performed with sterile material in aseptic conditions.

1. Inject intraperitoneally 0.2 mL of a 1:1 mixture of incomplete Freund adjuvant and PBS to DBA/2 mice
2. Inject mice for the second time 15 d later, as in **step 1**.
3. After an additional 15–30 d, recover hyperplastic lymphatic vessels from the liver and diaphragm, where they appear as small white spots.
4. Treat with collagenase (0.1% in Dulbecco's phosphate buffer, 3–5 mL), incubate at 37°C in 5% CO_2 for 45 min and centrifuge at 300*g* for 10 min.
5. Resuspend the pellet in 2–5 mL of complete medium (DMEM + 10% FCS + NEAA + NaPyr + 20% of S180 supernatant + 100 μg/mL ECGS + 100 μg/mL heparin).
6. Check cultures on the microscope. After 7–10 d, clusters of adherent growing cells with a cobblestonelike morphology can be found.
7. Recover cells with trypsin/EDTA when subconfluent and plate on gelatin-coated flasks.
8. Check cultures on the microscope. When confluent pass the cells 1/3–1/5.

Following this protocol, we have obtained a cell line that shows a cobblestone morphology at confluency and maintains a monolayer structure without overgrowth. These cells, called MELCs (mouse endothelial lymphatic cells), were studied for lymphatic endothelial markers and found positive for Flt-4 in Western and florescein activated cell sorter (FACS) analysis and for podoplanin and D6 in reverse transcription–polymerase chain reaction; they have been checked for the expression of endothelial markers and adhesion molecules, relevant for the physiological circulation of leukocytes from tissues to secondary lyphoid organs through the lymphatics. MELCs were found to express CD34, ICAM-1, VCAM, and JAM-1, but not CD31, VE-cadherin and E-selectin (TNF-α induced) and to produce IL-6 and CCL2. Upon stimulation with TNF-α, they upregulate the expression of adhesion molecules such as ICAM-1 and VCAM and produce increased amounts of IL-6 and CCL2.

Cells from lymphatic hyperplasia, cultured with appropriate supplements as reported here, are able to grow in culture for more than 30 passages. They maintain the reported markers and response to TNF-α during in vitro culture. MELCs have also been cloned by limiting dilution and clones mantained the markers of the original population. Cells have been frozen, stored in liquid nitrogen, and put again in culture without problems. Hyperplasia of the lymphatic vessel can be induced by the protocol reported also in other mouse strains (C57Bl/6

and Balb/c). MELCs are now a suitable source of lymphatic endothelial cells for in vitro studies of their biology.

Acknowledgments

This work was supported by Associazione Italiana per la Ricerca sul Cancro (AIRC) and Centro di Eccellenza per l'Innovazione Diagnostica e Terapeutica (IDET).

References

1. Butcher, E. C. (1991) Leukocyte–endothelial cell recognition: three (or more) steps to specificity and diversity. *Cell* **67,** 1033–1036.
2. Mantovani, A., Bussolino, F., and Dejana, E. (1992) Cytokine regulation of endothelial cell function. *FASEB J.* **6,** 2591–2599.
3. Ward, P. A., Remold, H. G., and David, J. R. (1970) The production by antigen-stimulated lymphocytes of a lekotactic factor distinct from migration inhibitory factor. *Cell Immunol.* **1,** 162–174.
4. Meltzer, M. S., Stevenson, M. M., and Leonard, E. J. (1977) Characterization of macrophage chemotaxis in tumor cell cultures and comparison with lymphocyte-derived chemotactic factors. *Cancer Res.* **37,** 721–725.
5. Bottazzi, B., Polentarutti, N., Acero, R., et al. (1983) Regulation of the macrophage content of neoplasms by chemoattractants. *Science* **220,** 210–212.
6. Bottazzi, B., Polentarutti, N., Balsari, A., et al. (1983) Chemotactic activity for mononuclear phagocytes of culture supernatants from murine and human tumor cells: evidence for a role in the regulation of the macrophage content of neoplastic tissues. *Int. J. Cancer* **31,** 55–63.
7. Bottazzi, B., Ghezzi, P., Taraboletti, G., et al. (1985) Tumor-derived chemotactic factor(s) from human ovarian carcinoma: evidence for a role in the regulation of macrophage content of neoplastic tissues. *Int. J. Cancer* **36,** 167–173.
8. Mantovani, A., Bottazzi, B., Colotta, F., Sozzani, S., and Ruco, L. (1992) The origin and function of tumor-associated macrophages. *Immunol. Today* **13,** 265–270.
9. Valente, A. J., Fowler, S. R., Sprague, E. A., Kelley, J. L., Suenram, C. A., and Schwartz, C. J. (1984) Initial characterization of a paripheral blood mononuclear cell chemoattractant derived from cultured arterial smooth muscle cells. *Am. J. Pathol.* **117,** 409–417.
10. Zullo, J. N., Cochran, B. H., Huang, A. S., and Stiles, C. D. (1985) Platelet-derived growth factor and double-stranded ribonucleic acids stimulate expression of the same genes in 3T3 cells. *Cell* **43,** 793–800.
11. Rollins, B. J., Morrison, E. D., and Stiles, C. D. (1988) Cloning and expression of JE, a gene inducible by platelet-derived growth factor and whose product has cytokine-like properties. *Proc. Natl. Acad. Sci. USA* **85,** 3738–3742.
12. Yoshimura, T., Robinson, E. A., Tanaka, S., Appella, E., Kuratsu, J., and Leonard, E. J. (1989) Purification and amino acid analysis of two human glioma-derived monocyte chemoattractants. *J. Exp. Med.* **169,** 1449–1459.

13. Matsushima, K., Larsen, C. G., DuBois, G. C., and Oppenheim, J. J. (1989) Purification and characterization of a novel monocyte chemotactic and activating factor produced by a human myelomonocytic cell line. *J. Exp. Med.* **169,** 1485–1490.
14. Zachariae, C. O., Anderson, A. O., Thompson, H. L., et al. (1990) Properties of monocyte chemotactic and activating factor (MCAF) purified from a human fibrosarcoma cell line. *J. Exp. Med.* **171,** 2177–2182.
15. Van Damme, J., Decock, B., Lenaerts, J. P., et al. (1989) Identification by sequence analysis of chemotactic factors for monocytes produced by normal and transformed cells stimulated with virus, double-stranded RNA or cytokine. *Eur. J. Immunol.* **19,** 2367–2373.
16. Graves, D. T., Jiang, Y. L., Williamson, M. J., and Valente, A. J. (1989) Identifcation of monocyte chemotactic activity produced by malignant cells. *Science* **245,** 1490–1493.
17. Furutani, Y., Nomura, H., Notake, M., et al. (1989) Cloning and sequencing of the cDNA for human monocyte chemotactic and activating factor (MCAF). *Biochem. Biophys. Res. Commun.* **159,** 248–255.
18. Yoshimura, T., Yuhki, N., Moore, S. K., Appella, E., Lerman, M. I., and Leonard, E. J. (1989) Human monocyte chemoattractant proein-1 (MCP-1). Full-length cDNA cloning, expression in mitogen-stimulation blood mononuclear meukocytes, and sequence similarity to mouse competence gene JE. *FEBS Lett.* **244,** 487–493.
19. Bottazzi, B., Colotta, F., Sica, A., Nobili, N., and Mantovani, A. (1990) A chemoattractant expressed in human sarcoma cells (tumor-derived chemotactic factor, TDCF) is identical to monocyte chemoattractant protein-1/monocyte chemotactic and activating factor (MCP-1/MCAF). *Int. J. Cancer* **45,** 795–797.
20. D'Amico, G., Bianchi, G., Bernasconi, S., et al. (1998) Adhesion, transendothelial migration, and reverse transmigration of in vitro cultured dendritic cells. *Blood* **92,** 207–214.
21. Falk, W., Goodwin, R. H. Jr., and Leonard, E. J. (1980) A 48-well microchemotaxis assembly for rapid and accurate measurement of leukocyte migration. *J. Immunol. Methods* **33,**239–245.
22. Sozzani, S., Luini, W., Molino, M., et al. (1991) The signal transduction pathway involved in the migration induced by a monocyte chemotactic cytokine. *J. Immunol.* **147,** 2215–2221.
23. Wilkinson, P. C. (1998) Assays of leukocyte locomotion and chemotaxis. *J. Immunol. Methods* **216,** 139–153.
24. Romano, M., Sironi, M., Toniatti, C., et al. (1997) Role of IL-6 and its soluble receptor in induction of chemokines and leukocyte recruitment. *Immunity* **6,** 315–325.
25. Springer, T. A. (1994) Traffic signal for lymphocyte recirculation and leukocyte emigration: the multistep paradigm. *Cell* **76,** 301–314.
26. Adams, D. H. and Shaw, S. (1994) Leucocyte–endothelial interactions and regulation of leucocyte migration. *Lancet* **343,** 831–836.
27. Bianchi, G., Sironi, M., Ghibaudi, E., et al. (1993) Migration of natural killer cells across endothelial cell monolayers. *J. Immunol.* **151,** 5135–5144.

28. Allavena, P., Paganin, C., Martin Padura, I., et al. (1991) Molecules and structures involved in the adhesion of natural killer cells to vascular endothelium. *J. Exp. Med.* **173,** 439–448.
29. Williams, R. L., Courtneidge, S. A., and Wagner, E. F. (1988) Embryonic lethalities and endothelial tumors in chimeric mice expressing polyoma virus middle T oncogene. *Cell* **52,** 121–131.
30. Bussolino, F., De Rossi, M., Sica, A., et al. (1991) Murine endothelioma cell lines transformed by polyoma middle T oncogene as target for and producers of cytokines. *J. Immunol.* **147,** 2122–2129.
31. Garlanda, C., Parravicini, C., Sironi, M., et al. (1994) Progressive growth in immunodeficient mice and host cell recruitment by mouse endothelial cells transformed by polyoma middle-sized T antigen: implications for the pathogenesis of opportunistic vascular tumors. *Proc. Natl. Acad. Sci. USA* **91,** 7291–7295.
32. Taraboletti, G., Belotti, D., Dejana, E., Mantovani, A., and Giavazzi, R. (1993) Endothelial cell migration and invasiveness are induced by a soluble factor produced by murine endothelioma cells transformed by polyoma virus middle T oncogene. *Cancer Res.* **53,** 3812–3816.
33. Bocchietto, E., Guglielmetti, A., Silvagno, F., et al. (1993) Proliferative and migratory responses of murine microvascular endothelial cells to granulocyte-colony-stimulating factor. *J. Cell Physiol.* **155,** 89–95.
34. Vecchi, A., Garlanda, C., Lampugnani, M. G., et al. (1994) Monoclonal antibodies specific for endothelial cells of mouse blood vessels. Their application in the identification of adult and embryonic endothelium. *Eur. J. Cell Biol.* **63,** 247–254.
35. Piali, L., Albelda, S. M., Baldwin, H. S., Hammel, P., Gisler, R. H., and Imhof, B. A. (1993) Murine platelet endothelial cell adhesion molecule (PECAM-1)/CD31 modulates beta 2 integrins on lymphokine-activated killer cells. *Eur. J. Immunol.* **23,** 2464–2471.
36. Hahne, M., Jager, U., Isenmann, S., Hallmann, R., and Vestweber, D. (1993) Five tumor necrosis factor-inducible cell adhesion mechanisms on the surface of mouse endothelioma cells mediate the binding of leukocytes. *J. Cell Biol.* **121,** 655–664.
37. Kriehuber, E., Breiteneder-Geleff, S., Groeger, M., et al. (2001) Isolation and characterization of dermal lymphatic and blood endothelial cells reveal stable and functionally specialized cell lineages. *J. Exp. Med.* **194,** 797–808.
38. Mancardi, S., Stanta, G., Dusetti, N., et al. (1999) Lymphatic endothelial tumors induced by intraperitoneal injection of incomplete Freund's adjuvant. *Exp. Cell Res.* **246,** 368–375.

2

Analysis of Integrin-Dependent Rapid Adhesion Under Laminar-Flow Conditions

Carlo Laudanna

1. Introduction

Adhesion molecules mediate recognition of the blood vessels by circulating leukocytes and support their selective targeting to different organs ***(1)***. In the vessels, the blood flow imposes peculiar conditions by generating a wall shear stress that opposes leukocyte stable arrest on the endothelium. As the rapidness of integrin activation is mandatory to leukocyte adhesion to the blood vessels, any analysis of adhesion triggering relevant to leukocyte in vivo migration should be performed under flow conditions. Here, a method is illustrated to quantitatively analyze the rapid induction of integrin-dependent lymphocyte adhesion by chemokines under flow conditions. Glass capillary tubes are cocoated with purified ligands for selectins and integrins and with chemokines, thus reconstituting the minimal requirement to support tethering, rolling, and arrest under flow conditions, with a physiologic wall shear stress of 2 dynes/cm^2. PNAd, ICAM-1, and the chemokine CCL21 are used as paradigmatic adhesion molecules and physiologic proadhesive agonist. Naive lymphocytes isolated from mouse lymph nodes are used as the cell model. The procedure for quantitative analysis is discussed.

2. Materials

1. Human tonsils (from the Pediatric Department).
2. Mouse spleens (from Balb/c mice).
3. Tissue potter or blade grinder.
4. CNBr-activated Sepharose™ 4B Fast Flow (Amersham-Pharmacia, code 17-0981-01) (*see* **Table 1**).

From: *Methods in Molecular Biology, vol. 239: Cell Migration in Inflammation and Immunity*
Edited by: D. D'Ambrosio and F. Sinigaglia

Table 1
Characteristics of CNBr-Activated Sepharose 4 Fast Flow

Mean particle size	90 µm
Particle size range	45–165 µm
Bead structure	Highly crosslinked 4% agarose, spherical
Linear flow[a]	150 cm/h at 100 kPa
Coupling capacity	13–26 mg chymotrypsinogen/mL drained gel
Swelling factor	4–5 mL drained gel/g
pH stability	2–11

[a]At 25°C in water in an XK 50/60 column, 25-cm bed height. The flow rate after coupling may differ depending on the ligand.

5. MECA 79, antiperipheral lymph node addressin (PNAd)-associated carbohydrate epitope mAb (rat IgM; ATCC number: 9479) ***(2)***.
6. Y.N.1.7 (rat anti-mouse ICAM-1; from Professor E. C. Butcher, Stanford University).
7. Coupling buffer: 50 m*M* Tris-HCl, pH 8.3, 150 m*M* NaCl.
8. Ethanolamine (Sigma).
9. 50 m*M* Tris-HCl, 0.5 *M* NaCl, pH 8.0.
10. 50 m*M* glycine, 0.5 *M* NaCl, pH 4.0.
11. Phosphate-buffered saline (PBS).
12. Disposable polypropylene minicolumns: filter pore size, 15 µm; length, 11.3 cm; total volume, 7.5 mL; reservoir, 4.5 mL (Spectra/Chrom®, code 104705).
13. Lysis buffer for PNAd and ICAM-1 purification: 0.4% 3-[(cholamido-propyl1) dimethyl-ammonio]-propanesulfonate (CHAPS) (Boehringer Manneheim), 25 m*M* Tris-HCl, pH 8.0, 150 m*M* NaCl, 1 m*M* $CaCl_2$, 1 m*M* $MgCl_2$, 2 m*M* NaN_3; add 1 tablet of protease inhibitor cocktail tablet "Complete, Mini" (Roche Diagnostic GmbH) to 10 mL of buffer.
14. Wash buffer A: 0.04 % CHAPS, 50 m*M* Tris-HCl, pH 8.0, 0.5 *M* NaCl, 1 m*M* $CaCl_2$, 1 m*M* $MgCl_2$, 1 m*M* NaN_3.
15. Wash buffer B: 50 m*M* *N*-octyl β-D-glucopyranoside (Sigma, cat. no. O-9882), 50 m*M* Tris-HCl, pH 8.0, 0.5 *M* NaCl, 1 m*M* $CaCl_2$, 1 m*M* $MgCl_2$, 1 m*M* NaN_3.
16. Elution buffer: 50 m*M* *N*-octyl β-D-glucopyranoside, 0.2 *M* acetic acid, 0.5 *M* NaCl, 2 m*M* NaN_3 (pH 8.0).
17. 3 *M* Tris-HCl, pH 8.5.
18. Dot blot standard equipment.
19. Dry milk.
20. Enzymatic-chemiluminescence (ECL) (Pierce).
21. Pipets, microcapillary calibrated tubes, 100 µL, color-coded blue (produced by Drummond Scientific Co., Broomall, PA, USA, cat. no. 2-000-100; purchased from Sigma, code P-1174) (*see* **Fig. 1**).

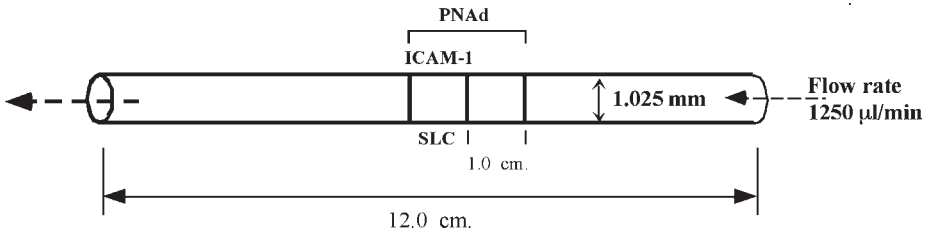

Fig. 1. Dimensions of the capillary tube and example of coating.

22. Polypropylene tubes connected to microperfusion needles ("Butterfly") (G 23, 0.63 × 19 mm; tube internal volume = 0.46 mL).
23. Digital pump with microliter-precise setting capability.
24. 10 mL polypropylene syringe without needle.
25. Adhesion buffer: PBS, pH 7.2, 1 m*M* $CaCl_2$, 1 m*M* $MgCl_2$, 10% heat-inactivated fetal calf serum (FCS).
26. CCL21 (SLC, 6Ckine, TCA-4, Exodous-2) (from PeproTech).
27. Inverted microscope with ×10 and ×20 phase-contrast objectives, connected to a high-resolution black-and-white CCD video camera (Sony, Hamamatsu, Ikegami), monitor (Sony), and analogic S-VHS (400 lines) or digital (540 lines) VCR (Panasonic) with time-stamp capability for image recording and analysis (better if with SMPTE; *see* **Note 1**).

3. Methods

In this section, the described methods (1) purify native PNAd from human tonsils and native ICAM-1 from mouse spleens, (2) coat the internal surface of glass capillary tubes with purified adhesion molecules to generate a surface able to support tethering, rolling, and full arrest under flow, (3) produce and maintain a laminar flow to perform under flow adhesion assays, and (4) analyze and quantify the recorded data. Complex reagents and solutions, described in **Subheading 2.**, are reported as item 1, 2, 3, and so forth.

3.1. Affinity Purification of Adhesion Molecules

3.1.1. Tissue Disruption

Human PNAd supports tethering and rolling of both human and mouse leukocytes. Mouse ICAM-1 mediates stable arrest of either mouse as well as human leukocytes ***(3,4)***. Thus, human PNAd and muse ICAM-1 can be indifferently used for assays with human or murine leukocytes. Tonsils and spleens are stored frozen at –80°C. Five to ten human tonsils (corresponding to approx 25–35 g of tissues) or 100–200 mouse spleens (corresponding to about 40–50 g

of tissue) are disrupted on ice by homogenization with a potter or a blade grinder and then lysed for 45 min in 30 mL of ice-cold, freshly made lysis buffer, with occasional stirring. Unlysed nuclei and cell debris are removed by centrifugation at 4°C for 10 min at 10,000*g*, followed by centrifugation of the supernatant at 4°C for 45 min at 150,000*g*. The supernatants are then collected as tonsil or spleen lysates (*see* **Note 2**).

3.1.2. Preparation of the Affinity Column

CNBr-preactivated 4% agarose matrix is used (*see* **Table 1** for the characteristics of the CNBr-activated beads).

1. Dialyze MECA 79 (for PNAd purification) or Y.N.1.7 (for ICAM-1 purification) against the coupling buffer.
2. Suspend 1 g of CNBr-activated matrix in 1 m*M* HCl for 30 min and allow to swell at room temperature.
3. Wash twice in 100 mL of cold 1 m*M* HCl.
4. Wash with 50 mL of coupling buffer.
5. Mix the washed gel with 10–15 mg of dialyzed MECA 79 or Y.N.1.7 and incubate overnight at 4°C. (The coupling can also be performed at room temperature for 3–4 h.) Keep the gel suspended by rotation or slow stirring.
6. Wash the coupled gel in 50 mL of 1 *M* ethanolamine.
7. Resuspend the coupled gel in 50 mL of 1 *M* ethanolamine and leave for 4 h at room temperature to block unused activated sites.
8. Wash the gel four times with alternating 50 m*M* Tris-HCl, 0.5 *M* NaCl, pH 8.0, and 50 m*M* glycine, 0.5 *M* NaCl, pH 4.0 buffers.
9. Wash the gel with 50 mL of PBS containing 2 m*M* NaN_3.
10. Pack the gel (approx 4 mL of drained gel) into a disposable column with a bottom filter (*see* **Note 3**).

3.1.3. Purification of Adhesion Molecules from Tissue Lysates

The entire procedure is done by gravity and at 4°C.

1. Wash the column with 20 mL of wash buffer A.
2. Wash the column with 5 mL of lysis buffer.
3. Run the tissue lysates *twice* on the column.
4. Wash the column with 40 mL of wash buffer A to remove the unbound proteins.
5. Wash the column with 10 mL of wash buffer B.
6. Elute bound PNAd or ICAM-1 with 5 mL of elution buffer by collecting 0.5-mL fractions immediately neutralized with 50 µL of Tris buffer or 5 µL of 10 *M* NaOH.

The fractions containing purified PNAd or ICAM-1 are then identified by dot-blot analysis. Usually, fractions 2–4 contain most of the protein. Fractions are stored at 4°C (*see* **Note 4**).

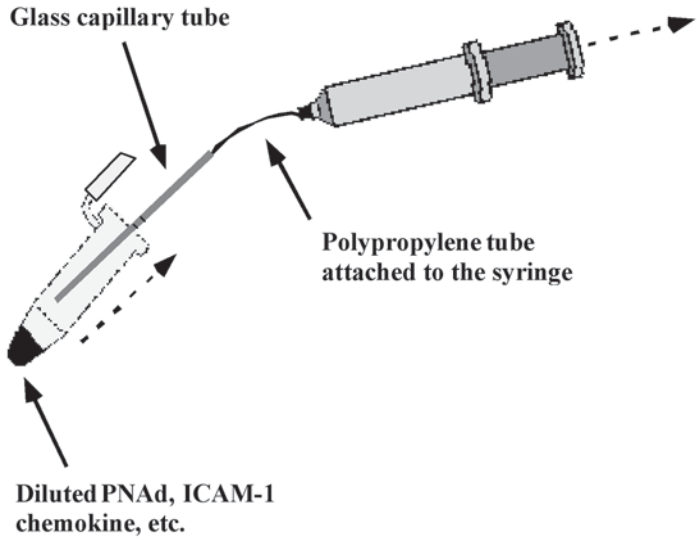

Fig. 2. Schematic drawing of the procedure for capillary coating. Proportions are not respected.

3.2. Cocoating Capillary Tubes with Adhesion Molecules and Chemokines

Glass capillary tubes are used to establish a biological surface permissive to lymphocytes tethering, rolling, and arrest under flow. In **Fig. 1**, the standard dimensions of the tube are reported and an example of organization of the coated areas is given. **Figure 2** depicts the manual procedure for the coating.

1. Identify two distinct sections of the capillary tube (each one 1 cm long) by marking the external surface of the tube with a pen. The section should be identified in the middle of the tube.
2. Immediately before use, dilute the human PNAd in 30 µL of PBS; dilution should be under the critical micelle concentration of *N*-octyl β-D-glucopyranoside (*see* **Note 4**).
3. Suck diluted PNAd into the tube according to **Fig. 2**. Completely coat both of the 1-cm-long sections and seal off the ends of the tube to prevent evaporation. Coating should be done at 4°C for at least 12 h.
4. Wash the tube twice with PBS; to prevent contamination of uncoated areas, washing has to be done always in the direction of the laminar flow.
5. Immediately before use, dilute mouse ICAM-1 in 15 µL of PBS (*see* **Note 4**).
6. Suck diluted ICAM-1 to coat the 1-cm-long downstream section of the tube and seal off the ends of the tube. Care should be taken to prevent contamination of the

upstream section, which has to be coated only with PNAd. Coating should be done at 4°C for at least 12 h.
7. Wash the tube twice with PBS.
8. Suck 15 µL of CCL21 (2 µ*M* in PBS) to coat only the 1-cm-long downstream section of the tube (now cocoated with PNAd and ICAM-1). Coat for 30–60 min at room temperature.
9. Immediately before the experiment, wash the tube three times with PBS containing 10% heat-inactivated FCS.

The upstream 1-cm section of tube is now coated only with PNAd, whereas the downstream 1-cm section is cocoated with PNAd, ICAM-1, and chemokine.

3.3. Under Flow Adhesion Assay

The coating described in **Subheading 3.2.** supports interaction and stable arrest of L-selectin, LFA-1, and CCR7-positive cells, such as naïve lymphocytes. Murine naive lymphocytes (approx 50% B, 50% T) are isolated from mouse (Balb/c) lymph nodes and resuspended in adhesion buffer (**item 25**) at 10^6/mL. The assay is done at room temperature.

1. Place 10 mL of lymphocyte suspension in a disposable 10-mL polypropylene syringe connected to a 15-cm-long polypropylene tube (**item 22**).
2. Connect the syringe to the upstream end of the coated capillary tube; connect the downstream end of the capillary to a second 15-cm-long polypropylene tube; connect the downstream polypropylene tube to a 15-mL Falcon tube to collect the cells.
3. The entire setting has to be fixed on the inverted microscope to focus from the bottom the coated sections of the capillary tube; by using ×20 magnification, an area of 0.2 mm^2 is visualized at video; phase-contrast optics improves the image quality. The syringe is placed on the digital pump.
4. Set the digital pump to provide a flow rate of 75 mL/h, corresponding to 1250 µL/min. By applying this flow rate to the capillary tube (with a diameter of 1.025 mm), a wall shear stress (WSS) of 2 dynes/cm^2 is obtained (considering the cell suspension a Newtonian fluid with a viscosity 0.01 *P*) (*see* **Note 5**).
5. Start the video recording and cell transfusion; 2–3 min are normally necessary to establish a stable laminar flow and see interacting cells. During the experiment, care has to be taken to record, as much as possible, separate fields for at least 30 s.

3.4. Analysis and Quantification of Interacting Cells

The described experimental setting reproduces some of the physiological behaviors of homing lymphocytes, including tethering, rolling, and sticking. Quantitative differences such as duration of tethering, speed of rolling, and efficiency of stable adhesion can be quantified. To limit the description to chemokine-triggered integrin-dependent rapid adhesion, we will focus only on stable arrest analysis.

1. Quantitative definition of integrin-dependent stable arrest is a little arbitrary and has to be defined depending of the experimental setting. For instance, in the presence of L-selectin-mediated rolling, a stable adhesion of 10 s can be considered integrin activation; in contrast, in the presence of P-selectin–PSGL-1 mediated interaction, rolling is much slower ***(5)*** and can be occasionally scored as stable arrest if a too stringent temporal parameter is adopted. Here, we will consider a stable arrest of at least 10 s as a manifestation of integrin triggering under flow.
2. The experiments are analyzed by evaluating for at least 30 s as much as possible of the areas of the coated tube. This will provide much data for statistical analysis. Start by looking at a noncoated section in order to evaluate eventual background, nonspecific interactions. Next, evaluate the efficiency of PNAd in supporting tethering and rolling by counting the number of tethering and rolling cells in 30 s.
3. If a cell does not make a complete rotation on itself, score as tethering, otherwise score as rolling. Normally, an only-tethering cell interacts with the surface for less than 1 s. Individual cells stable adherent for less than 10 s has to be considered not arrested but still rolling. In the case of coating with a low number of sites of PNAd, the number of tethering cells tends to be higher than the number of rolling cells. Occasional full arrest for 10 or more seconds has to be scored as nonspecific, integrin-mediated adhesion.
4. Move to the section cocoated with PNAd, ICAM-1, and chemokines. Count in each 0.2-mm^2 area the number of total interacting cells, including teething, rolling, and arrested cells. Analyze frame by frame the fields to precisely evaluate the duration of full adhesion of single cells. This is important to distinguish between full adherent cells from only-rolling cells. Various cells adherent in the same field can be analyzed one by one by going backward and forward with the VCR.
5. The number of interacting cells in noncoated areas (nonspecific interaction) is subtracted form the number of cells interacting on PNAd alone. The number of cells arrested on PNAd is subtracted from the number of cells arrested on ICAM-1 and chemokines. The data can be either expressed as total number of only-rolling or full arrested cells in 0.2 mm^2 in 30 s or as a percentage of arrested cells of the total interacting cells in 0.2 mm^2 in 30 s (*see* **Note 6**.)

4. Notes

1. Identification of single frames by a time code is critical for the accurate measurement of dynamic events. The most accurate time code has been established by the Society of Motion Pictures and Television Engineers (SMPTE), which identifies each frame with a unique address in the form hours:minutes:seconds:frames. Notably, in the PAL system, 1 s of recording contains 25 frames; in the SECAM system, 1 s contains 24 frames; in the NTSC system, 1 s contains 30 frames (precisely 29.97). Consequently, the duration of a single frame is 40 ms, for PAL; it is 41.6 ms for SECAM, and it is 33.33 ms for NTSC. Thus, in the PAL system, a frame identified as 00:02:25:15 is positioned at 2 min, 25 s, and 15 frames (that is 2' 25" 600 ms) after the beginning of the recording. The time code is essential for quantifica-

tion of leukocyte behavior under flow. For example, a cell that started to move after 20 frames was adherent for only 800 ms (in PAL) and, thus, was a rolling cell.

2. It is better to proceed with protein purification immediately after tissue lysate preparation. If necessary, it is possible to store the lysates at –80°C. To prevent protein aggregation and precipitation (which will reduce the purification efficiency and clog the affinity column), rapidly freeze the lysates in liquid N_2 before storing them at –80°C.
3. When choosing the disposable polypropylene minicolumns, pay attention to order columns with a filter pore size of 15 µm (Spectra/Chrom, code 104705). Note that the Sepharose 4 Fast Flow particle size range is 45–165 µm (*see* **Table 1**). The MECA 79 column appears to be rather unstable and not suitable for more than two purifications, even if care is taken to correctly wash and prevent contamination. The Y.N.1.7 can be reused several times.
4. It is very important to buffer the fractions immediately after their collection. Never freeze the fractions. Dilutions must be made immediately before the coating, to prevent rapid reduction of the titer by adsorption of the protein to the wall of the tube used for the dilution. Coating can be also done at 37°C for 3–4 h, but more care has to be taken to prevent evaporation. The specific activity of the ICAM-1 preparation may be determined in static adhesion assay by making several dilutions of the purified protein to identify the dilution providing the lowest ratio between background binding in the absence of agonist and binding induced by agonists. The specific activity of the PNAd preparation has to be evaluated under flow. The most accurate way to coat the tubes is by calculating the number of molecules immobilized in 1 μm^2. This is particularly important with integrin ligands. This will allow precise evaluation of the role of different modalities of integrin activation in determine the rapid and stable arrest under flow ***(4)***. The number of molecules immobilized can be determined by using ^{125}I-mAbs, as reported ***(6)***.
5. The wall shear stress (WSS) can be modified to study the efficiency among different selectins, integrins, and chemokines in mediating tethering, rolling, and arrest under flow. This can be combined with changes in the density of immobilized ligands and agonists to perform a more informative analysis.

   The WSS is calculated using the following:

$$\mathrm{WSS} = \mathrm{WSR} \times P \tag{1}$$

   where WSR is the wall shear rate and P is the viscosity (0.01 for PBS);

   The WSR is calculated using:

$$\mathrm{WSR} = 8V_m/D \tag{2}$$

   where V_m is the fluid mean velocity and D is the diameter of the tube (1.025 mm in our case);

   The V_m is extracted using:

$$Q = V_m \, \pi \, D^2/4 \times 10^{-6} \tag{3}$$

   where Q is the flow rate (75 mL/h in our case) and D is the diameter of the tube (1.025 mm).

Note: WSS is in dyn/cm^2; WSR is in s^{-1}; P is in Poise; V_m is mm/s; D is in mm; Q is in mL/s. Thus, a flow rate of 75 mL/h corresponds to 0.021 mL/s and this is the value to be used in formula (3) to extract the V_m. The V_m value is then applied to formula (2) to calculate WSR, which is finally used to calculate the WSS from formula (1).

6. Other controls can be used also. For instance, chemokines should be immobilized on sections of the tube uncoated and coated only with PNAd without ICAM-1, to evaluate nonspecific, but agonist-triggered, integrin binding. Moreover, a section of the tube should also be coated with ICAM-1 and PNAd but without chemokine, to evaluate a basal state of integrin activation in absence of agonist. The possibility of selectin to integrin transactivation may also be explored. Obviously, other ligands and chemokines may be used following the same directions. Notably, VCAM-1 does not support tethering and rolling unless coimmobilized with chemokines *(7)*.

Acknowledgments

The author thanks Professor E. C. Butcher for providing purified MECA 79 and Y.N.1.7. This work was supported by Cofinanziamento MIUR and University of Verona, Progetto Sanità 1996/97, Fondazione Cassa di Risparmio, Ministero della Sanità (Ricerca Finalizzata), and CNR, and by a grant from Italian Association for Cancer Research (AIRC) 2001.

References

1. Butcher, E. C., Williams, M., Youngman, K., Rott, L., and Briskin, M. (1999) Lymphocyte trafficking and regional immunity. *Adv. Immunol.* **72,** 209–253.
2. Streeter, P. R., Rouse, B. T. N., and Butcher, E. C. (1999) Immunohistologic and functional characterization of a vascular addressin involved in lymphocyte homing into peripheral lymph nodes. *J. Cell. Biol.* **107,** 1853–1862.
3. Campbell, J. J., Hedrick, J., Zlotnik, A., Siani, M. A., Thompson, D. A., and Butcher, E. C. (1998) Chemokines and the arrest of lymphocytes rolling under flow conditions. *Science* **279,** 381–384.
4. Constantin, G., Majeed, M., Giagulli, C., et al. (2000) Chemokines trigger immediate β2 integrin affinity and mobility changes: differential regulation and roles in lymphocyte arrest under flow. *Immunity* **13,** 759–769.
5. Norman, K. E., Katapodis, A. G., Thoma, G., et al. (2000) P-Selectin glycoprotein ligand-1 supports rolling on E- and P-selectin in vivo. *Blood* **96,** 3585–3593.
6. Lawrence, M. B. and Springer, T. A. (1991) Leukocytes roll on a selectin at physiologic flow rates: distinction from and prerequisite for adhesion through integrins. *Cell* **65,** 859–873.
7. Grabovsky, V., Feigelson, S., Chen, C., et al. (2000) Subsecond induction of α4 integrin clustering by immobilized chemokines stimulates leukocyte tethering and rolling on endothelial vascular cell adhesion molecule 1 under flow conditions. *J. Exp. Med.* **192,** 495–506.

3

Posttranslational Processing of Chemokines

Paul Proost, Frank Mahieu, Evemie Schutyser, and Jo Van Damme

Introduction

Under physiological and pathological conditions, low-molecular-mass *chemo*tactic cyto*kines* or *chemokines* provide a chemotactic gradient for the directional migration of specific leukocyte subclasses. In vivo, leukocyte migration requires a network of molecules, including cytokines, chemokines, leukocyte adhesion molecules such as selectins and integrins, and proteases ***(1–3)***. This complex network provides different levels of specificity based on ligand–receptor interactions. Selectins will interact with specific glycoprotein receptors, integrins with endothelial cell adhesion molecules, and chemokines with a limited number of specific chemokine receptors. Cytokines and chemokines will alter the expression level of cellular receptors, activate adhesion molecules, and induce the release of proteases. These proteases will not only help to degrade the extracellular matrix, but more recent evidence points toward a regulatory function for proteases on cytokine and chemokine activity ***(1,4)***.

Purification of chemokines from natural sources allows for the identification of N- or C-terminally truncated and/or glycosylated proteins ***(5–10)***. In most cases, N-terminal truncations of chemokines lead to alterations in specific activity and/or receptor specificity. Some chemokines, such as platelet basic protein, only possess chemotactic activity after N-terminal processing ***(11,12)***. In addition, activation of leukocytes by chemokines results in either the secretion of proteolytic enzymes from intracellular stores (e.g., gelatinase B in neutrophil granulocytes) or in the *de novo* synthesis of proteases (e.g., in tumor cells or monocytes) ***(1)***. A number of proteases are constitutively available in body fluids such as plasma, are continuously present in active forms on the membranes of most leukocytes and endothelial cells and/or are secreted by leukocytes.

From: *Methods in Molecular Biology, vol. 239: Cell Migration in Inflammation and Immunity*
Edited by: D. D'Ambrosio and F. Sinigaglia © Humana Press Inc., Totowa, NJ

Therefore, they are likely to interact with possible chemokine substrates. Recently, a number of observed natural chemokine truncations have been mimicked by the incubation of intact natural, recombinant, or synthetic chemokines with purified proteases ***(4,13–22)***. This chapter describes the purification, identification, and synthesis of posttranslationally modified chemokines and, subsequently, the methods used to investigate the susceptibility of chemokines to proteolytic processing. For in vitro assays used to study receptor specificity and biological activity of posttranslationally modified chemokines, we refer to Chapters 1, 4, 13, and 18 in this volume.

2. Materials

2.1. Leukocyte Purification

1. Plasmasteril (Fresenius, Bad Homburg, Germany), Lymphoprep (Nycomed, Oslo, Norway).
2. Inducers: Bacterial lipopolysaccharide (LPS from *Escherichia coli* 0111:B4; Difco Laboratories, Detroit, MI, USA), double-stranded RNA (polyI-C; P-L Biochemicals Inc., Milwaukee, WI, USA), and cytokines (e.g., interleukin-1 [IL-1] and interferon-γ [IFN-γ]).
3. Fetal calf serum (FCS) and Hanks' balanced salt solution (HBSS).

2.2. Buffers (All Filtered Through 0.2-µm Filters)

1. PBS: 2.7 m*M* KCl, 1.5 m*M* KH_2PO_4, 138 m*M* NaCl, 8 m*M* Na_2HPO_4, pH 7.4.
2. Assay buffer for incubation with gelatinase B: 100 m*M* Tris-HCl, pH 7.5, 100 m*M* NaCl, 10 m*M* $CaCl_2$.
3. Assay buffer for incubation with CD26/DPP IV: 50 m*M* Tris-HCl , pH 7.5, 1 m*M* EDTA.

2.2.1. Buffers for Chromatography

1. Heparin–Sepharose loading and wash buffer: 50 m*M* Tris-HCl, pH 7.4, 50 m*M* NaCl.
2. Heparin–Sepharose elution buffer: 50 m*M* Tris-HCl, pH 7.4, 2 *M* NaCl.
3. Mono S loading buffer: 50 m*M* formic acid, pH 4.0.
4. Mono S elution buffer: 50 m*M* formic acid, pH 4.0, 1 *M* NaCl.

2.3. Media and Columns Chromatography

2.3.1. Media and Columns

1. Dialysis membranes with a relative molecular mass (M_r) cutoff of 3500.
2. CPG (controlled pore glass, particle size, 120–200 mesh; pore size, 35 nm; Serva, Heidelberg, Germany) and silicic acid (Matrex Silica; particle size, 35–70 µm; pore size, 10 nm; Amicon Inc., Beverly, MA, USA).
3. Heparin–Sepharose, Mono S, and Resource RPC columns (Amersham Biosciences, Uppsala, Sweden).

4. C-8 reversed-phase high-performance liquid chromatography (RP-HPLC) columns: 1 × 50-mm, 2.1 × 220-mm, or 4.6 × 220-mm Brownlee Aquapore RP-300 (Applied Biosystems, Foster City, CA, USA).

2.4. Protein Sequencing and Mass Spectrometry (MS) Equipment

1. 491 Procise cLC protein sequencer and reagents (Applied Biosystems).
2. Analytical high-performance liquid chromatography (HPLC) coupled to an electrospray ion-trap MS (Esquire LC-MS; Bruker/Daltonics, Bremen, Germany) with postcolumn flow splitter (Acurate; LC Packings, Amsterdam, The Netherlands).
3. C18 ZipTips (Millipore, Bedford, MA, USA).
4. Ultrapure solvents: Water, methanol, acetonitrile, trifluoroacetic acid (TFA), and acetic acid.

2.5. Chemical Synthesis of Chemokines

1. 433A Peptide synthesizer (Applied Biosystems).
2. Reagents: Amino acids with an Fmoc (fluorenyl methoxy carbonyl)-protected α-amino group and extra side-chain protecting groups on the following amino acids: trityl on Asn, Cys, Gln and His; *tert*-butyl on Ser, Thr and Tyr; *t*-butyloxycarbonyl on the ε-amino group of Lys; *tert*-butyl ester on Asp and Glu; 2,2,5,7,8-pentamethylchroman-6-sulfonyl on Arg.
3. Deprotection mixture: Dissolve 0.75 g crystalline phenol in 10 mL concentrated trifluoroacetic acid (TFA). Add 0.25 mL ethanedithiol, 0.5 mL thioanisole, and 0.5 mL ultrapure water.
4. Folding buffer: 150 m*M* Tris-HCl, pH 8.6, containing 2 *M* urea, 0.3 m*M* oxidized glutathione, 3 m*M* reduced glutathione, and 1 m*M* EDTA.

2.6. Proteases

1. Dipeptidyl peptidase IV (DPP IV)/CD26: Natural soluble and membrane-bound DPP IV, purified to homogeneity as described ***(23)*** and kindly provided by Dr. S. Scharpé (Lab. Medical Biochemistry, Univerity of Antwerp, Belgium).
2. Neutrophil-derived matrix metalloprotease 9 (MMP-9) or gelatinase B was purified by Dr. P.E. Van den Steen (Lab. Molecular Immunology, Rega Institute, University of Leuven, Belgium) as described ***(13)***.

3. Methods

3.1. Isolation of Proteolytically Processed Natural Chemokines

Semipurified peripheral blood mononuclear cells (PBMCs) are obtained from fresh human buffy coats (25–100 pooled buffy coats from the blood transfusion centers of Antwerp and Leuven, Belgium) by density gradient centrifugation. One volume of leukocytes is layered on top of three volumes of sodium metrizoate (Lymphoprep) and centrifuged without using the brake of the centrifuge at 500*g* for 45 min at 4°C. The mononuclear cell layer is washed with

Table 1
Influence of Serum Concentrations on the Induction of IP-10 in PBMCs

	IP-10 Production (ng/mL) in the Presence of		
Inducer	0% FCS	2% FCS	10% FCS
IFN-γ (ng/mL)			
200	2.6[a]	35	25
67	2.3	11	14
20	<2	8.6	16
0	<2	<2	<2
PolyI-C (μg/mL)			
30	<2	4.7	6
10	<2	4.5	6.6

[a]IP-10 concentrations measured by enzyme-linked immunosorbent assay in the supernatant of PBMC cultures (2×10^6 cells/mL) after 8.5 h incubation with or without IFN-γ or polyI-C at 37°C and 5% CO_2.

PBS and diluted to 5×10^6 cells/mL in HBSS with or without 2% FCS. The PBMC suspension is stimulated with endogenous (e.g., the cytokines IL-1 or IFN-γ) and/or exogenous (e.g., bacterial LPS, polyI-C, or plant lectins) stimuli for 8–120 h. Alternatively, chemokines are produced by primary cultures (e.g., fibroblasts) or tumor cell lines in stationary cultures upon induction with cytokines, plant, bacterial, and/or viral components.

Even after optimal induction, cell lines and freshly isolated leukocytes or platelets produce only small (μg/L supernatant) amounts of most chemokines. The addition of serum often significantly increases the amount of chemokine produced but complicates subsequent purification steps. For instance, IP-10 production levels augment by a factor of 5–10 if 2% FCS is added to the culture medium of PBMC in addition to the stimulus (IFN-γ or polyI-C) (*see* **Table 1**). In the past, different strategies were used for the isolation of chemokines. We have developed a four-step purification procedure that allows several chemokines to be isolated at the same time from complex protein mixtures (*see* **Fig. 1**).

3.1.1. Concentration of Cell-Derived Conditioned Media and Biological Fluids

Because of the large volumes of conditioned medium (typically 3–10 L) or biological fluids (e.g., serum, ascites) to be processed, an initial concentration step is essential in the purification procedure. Concentration can be achieved by adsorption to controlled pore glass (CPG) ***(24)*** or to silicic acid ***(25)*** using a batch procedure (*see* **Note 1**). The conditioned medium is incubated with silicic

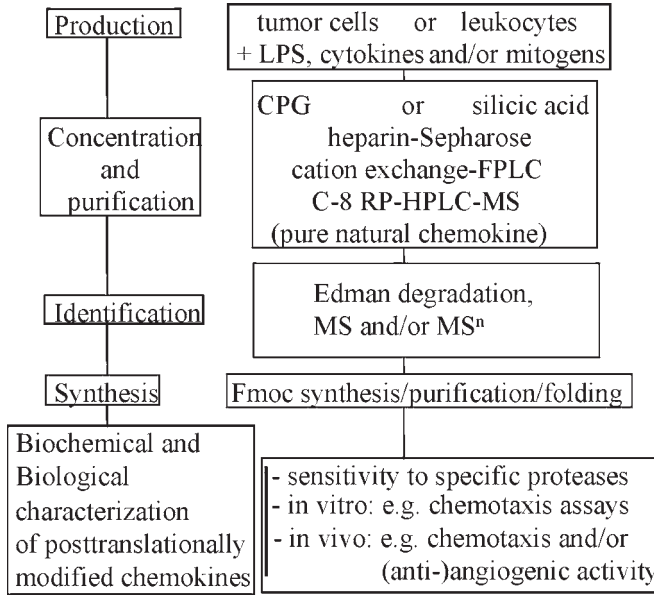

Fig. 1. Schematic representation of the strategy used for the isolation, identification and characterization of chemokines.

acid (10 g/L) or CPG (1/30 v/v) for 2 h at 4°C and neutral pH in spinner flasks. The silicic acid particles are washed with PBS (pH 7.4) and with PBS containing 1 *M* NaCl (pH 7.4) at 4°C. Chemokines are eluted from the silicic acid in two steps. The first elution is performed by washing for 30 min at 4°C with 50% (v/v) ethylene glycol in 1.4 *M* NaCl (four times) and remaining proteins are eluted in 0.3 *M* glycine-HCl (pH 2.0). The ethylene glycol is removed by dialysis and proteins may be concentrated another 10-fold against 20 m*M* Tris-HCl, pH 7.4, containing 15% polyethylene glycol (PEG 20,000).

Proteins bound on CPG are washed with PBS (pH 7.4) and 10 m*M* glycine-HCl (pH 3.5) and eluted from the glass beads in one step with 0.3 *M* glycine-HCl (pH 2.0) at 4°C.

The eluate can be further concentrated by dialysis against polyethylene glycol until the volume is reduced another 10-fold. Both silicic acid- and CPG-eluted proteins are finally dialyzed against heparin–Sepharose loading buffer and stored at –20°C until further purification.

Both adsorption procedures result, additional to the concentration, in a first partial purification of chemokines. Generally, better purification yields are obtained on CPG compared to silicic acid. However, the use of CPG is limited by its cost and the small amount of protein that can be adsorbed to the beads. Therefore, adsorption to silicic acid is preferred for the purification of conditioned

medium containing serum or biological fluids, whereas CPG is ideal for the purification of serum-free cell supernatant. In the latter case, recovery of the expensive CPG matrix can be obtained by cleaning with nitric acid.

3.1.2. Affinity Purification of Chemokines

Most chemokines bind to heparin. Therefore, heparin-affinity chromatography is an efficient technique for removing the bulk of contaminating proteins from crude chemokine preparations. Concentrated eluates of the silicic acid or CPG adsorption steps are applied to heparin–Sepharose columns in loading buffer. The columns are extensively washed with loading buffer and chemokines are eluted with a NaCl gradient (50 m*M* to 2 *M* NaCl). **Figure 2** shows the affinity purification of a pH 2.0 eluate of MG-63 cell conditioned medium (3 L) after adsorption to CPG. Whereas about 40% of the CPG-eluted protein

---

Fig. 2. (*opposite page*) Purification of monocyte chemotactic proteins (MCPs) from concentrated MG-63 osteosarcoma cell conditioned medium by heparin–Sepharose chromatography, Mono S cation-exchange fast protein liquid chromatography (FPLC), and C-8 RP-HPLC. MG-63 cells were stimulated with a cytokine mixture and the cell supernatant was adsorbed to CPG. The CPG eluate was dialyzed against 50 m*M* Tris-HCl, pH 7.4; 50 m*M* NaCl and loaded on a heparin–Sepharose column. Proteins were eluted in a NaCl gradient (0.05–2 *M* NaCl) and the protein concentration was measured by a Coomassie blue G-250 protein assay, using bovine serum albumin as a standard (**A**). Fractions were tested at various concentrations for neutrophilic granulocyte chemotactic activity (expressed in units/mL) in the migration test under agarose ***(26)***. One unit corresponds to the amount of granulocyte chemotactic protein (GCP) that results in a half-maximal migration distance under agarose. Monocyte chemotaxis was performed under agarose with 1/50 dilutions of the different fractions. The activity of the MCPs was indicated as the percentage of the migration distance of monocytes to 10^{-7} *M* FMLP (arbitrarily taken as 100%). The amount of MCP-1 immunoreactivity (ng/mL) in every fraction was determined with a specific radioimmunoassay (RIA) using polyclonal rabbit–anti-human MCP antisera ***(27)***.

Heparin–Sepharose fractions containing monocyte chemotactic activity were dialyzed against 50 m*M* formate, pH 4.0, and loaded on a Mono S column. Proteins were eluted in a linear NaCl gradient and MCP-1 immunoreactivity was measured with a RIA (**B**). The activity of the MCPs was determined in a microchamber assay ***(26)***. The chemotactic index (C.I.) was calculated by dividing the number of cells that migrated toward the samples by the number of cells that migrated to the control medium.

The monocyte chemotactic proteins that eluted from the Mono S column at 0.4 *M* NaCl and 0.5 *M* NaCl were further purified by C-8 RP-HPLC. Fractions derived from both HPLC columns were subjected to sodium dodecyl sulfate–polyacrylamide gel electrophoresis (SDS-PAGE) under reducing conditions and silver stained (**C**). The higher M_r bands on the left half of the gel and the lower M_r bands on the right half of the gel correspond to proteins purified from the 0.4 *M* and 0.5 *M* NaCl Mono S fractions, respectively. The M_r of the marker proteins are indicated on the left lane in (kDa).

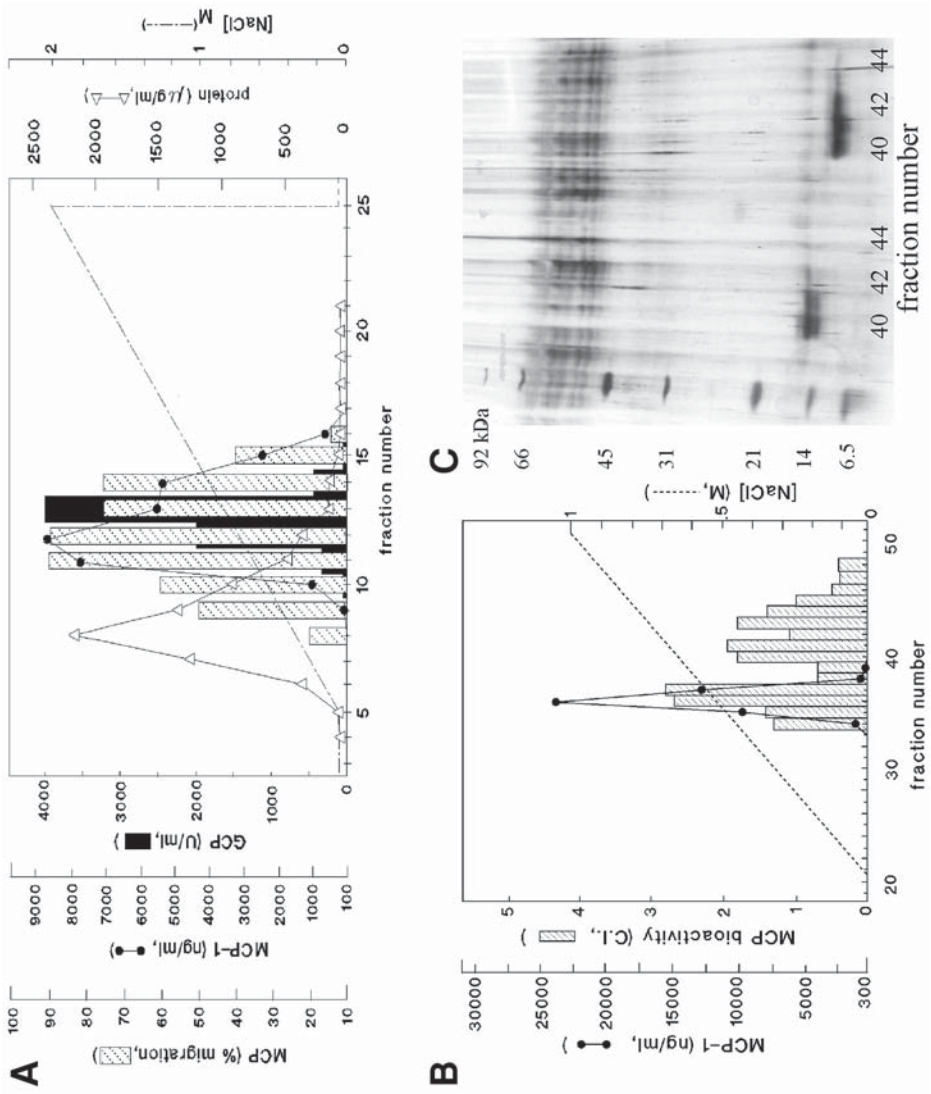
A
MCP (% migration, ▨)
MCP-1 (ng/ml, ●—●)
GCP (U/ml, ■)
protein (μg/ml, △—△)
[NaCl] M (------)
fraction number
B
MCP-1 (ng/ml, ●—●)
MCP bioactivity (C.I., ▨)
[NaCl] (M, ------)
fraction number
C
92 kDa
66
45
31
21
14
6.5
40 42 44 40 42 44
fraction number

(77 mg) is recovered in the void volume, less than 5% of the MCP-1 protein is lost (not shown). The majority of contaminating proteins that bound to the column elute in the first part of the NaCl gradient before the chemokine activity. Most monocyte and neutrophilic granulocyte chemotactic activity elutes between 0.4 and 1.0 *M* of the NaCl gradient (*see* **Note 2**).

3.1.3. Ion-Exchange Chromatography

Because of the high p*I* of most chemokines, cation-exchange chromatography is a very useful technique for fractionating chemokines and removing most of the remaining contaminants. Generally, a few heparin–Sepharose or antibody-affinity column fractions containing the peak of chemotactic and/or chemokine immunoreactivity are pooled, dialyzed against loading buffer, and applied on the Mono S column at a flow rate of 1 mL/min (Amersham Biosciences). The column is washed with 20 column volumes of loading buffer and the proteins are eluted from the ion exchanger in a NaCl salt gradient (0–1 *M* in 30 min) (*see* **Note 3**).

For example, upon cation-exchange chromatography of the MG-63 cell-derived leukocyte chemotactic activity (*see* **Fig. 2A**), three peaks containing monocyte chemotactic activity (eluting at ± 0.4–0.5 *M*, 0.6 *M*, and 0.7 *M* NaCl) (*see* **Fig. 2B**) and two zones of granulocyte chemotactic activity (eluting at ± 0.6 *M* and 0.85 *M* NaCl) (not shown) are fractionated. The first peak (at 0.4 to 0.5 *M* NaCl) of monocyte chemotactic activity corresponds to the C–C chemokine MCP-1; the second one contains the C–C chemokines MCP-2 and MCP-3 (not shown). The granulocyte chemotactic activity is the result of several N-terminally processed forms of the C–X–C chemokines GRO-α, GRO-γ, IL-8, and the C–X–C chemokine GCP-2 (granulocyte chemotactic protein-2) ***(5)***.

3.1.4. Reversed-Phase Chromatography

Fractions from the ion-exchange column containing chemotactic activity can further be purified to homogeneity by analytical C-8 RP-HPLC without prior dialysis. The column is washed with 0.1% TFA in Milli-Q water (Millipore) and proteins are eluted with a gradient from 0% to 80% acetonitrile in 0.1% TFA. Proteins are detected by their ultraviolet (UV) adsorption spectrum (at 214 nm) and/or by splitting a fraction (0.5–2%) of the eluent to be analyzed on an electrospray MS. At this stage, the coupling of the HPLC to a MS allows for the direct and accurate (± 1 Da) measurement of the M_r of most of the eluted chemokines (*see* **Note 4**).

3.2. Biochemical Identification of Chemokines

For control of protein purity, chemokines are routinely subjected to SDS-PAGE and/or to electrospray ion-trap MS. Column fractions are analyzed by

SDS-PAGE under reducing conditions on Tris-tricine gels. The stacking, spacer and separating gels contain respectively 5% T (w/v% of acrylamide monomer + bisacrylamide) and 5% C (5% bisacrylamide in total acrylamide), 10% T and 3.3% C, and 13% T and 5% C, and proteins are stained with silver. Electrospray ion-trap MS is performed either on-line on a small portion of the HPLC eluent or separately on diluted fractions.

The N-terminal sequence of RP-HPLC-purified chemokines is determined by classical Edman degradation on an automated pulsed liquid-phase protein sequencer. Because of the high sensitivity of currently available protein sequencers (high femtomole to low picomole level), 10 ng of chemokine is usually sufficient for identification (*see* **Note 5**). The combination of the N-terminal sequence with the results from MS allow for the detection of glycosylation(s) and/or N- or C-terminal truncations of chemokines.

The use of subsequent ion-exchange chromatography and RP-HPLC purification may result in the separation of multiple truncated or glycosylated forms (e.g., glycosylated and unglycosylated isoforms of MCP-1 with a relative molecular mass ranging from 10 to 16 kDa on SDS-PAGE [0.4 and 0.5 *M* NaCl cation-exchange fractions each further purified by RP-HPLC; *see* **Fig. 2B,C**]). The 15–16-kDa band corresponds to different glycosylated MCP-1 forms (*see* **Fig. 3A**), whereas the 10-kDa band on SDS-PAGE corresponds to unglycosylated MCP-1 (theoretical average M_r of 8664.0) (*see* **Fig. 3B**). Although the SDS-PAGE analysis would predict about 5- to 6-kDa large sugar moieties, the M_r of the most glycosylated MCP-1-form was not larger that 9710 (*see* **Fig. 3A**). The presence of several sugar units (e.g., *N*-acetylglucosamine [GlcNAc] or *N*-acetylgalactosamine [GalNAc] in combination with a six-carbon sugar [galactose, mannose, or glucose] and one or more sialic acid or *N*-acetylneuraminic acid [NeuNAc] units) is deduced from the mass spectra.

3.3. Chemical Synthesis of (Truncated) Chemokines

Because purification of natural posttranslationally modified chemokines often yields low microgram amounts of protein and because most modifications consist of truncations rather than glycosylations, chemical peptide synthesis is an alternative for the production of significant (milligram) amounts of modified chemokines. An additional advantage of chemical synthesis is the possibility of stopping the synthesis at specific peptide chain lengths, which results in the generation of multiple N-terminally truncated forms of one chemokine during a single synthesis run. Solid-phase Fmoc peptide synthesis was performed on an automated peptide synthesizer equipped with a conductivity cell that allows one to follow the efficacy of the deprotection reactions and allows one to program conditional double couplings if the deprotection proceeds slowly. In order to avoid complex mixtures of incompletely synthesized peptides, each coupling

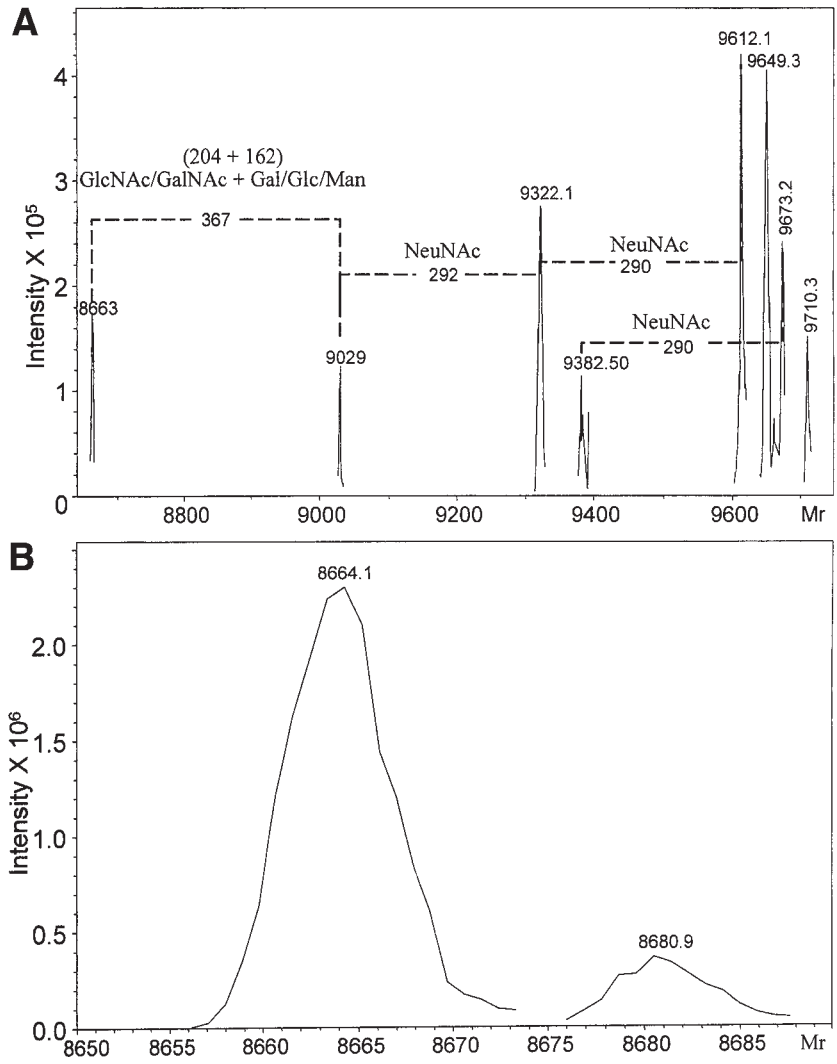

Fig. 3. Mass spectrometry of natural human MCP-1. Mass-spectrometric analysis of the proteins in fractions 40 of the RP-HPLC columns shown in **Fig. 2C**. Fraction 40 from the first RP-HPLC purification (of the 0.4 *M* ion-exchange fraction; *see* **Fig. 2C**) contains multiple glycosylated isoforms of natural human MCP-1. The peak at 8663 corresponds to unglycosylated MCP-1. The additional M_r of 367 is the sum of two sugar units (i.e., *N*-acetylglucosamine [GlcNAc] or *N*-acetylgalactosamine [GalNAc] in combination with a six-carbon sugar [galactose, mannose, or glucose]. The further addition of sialic acid units (M_r of 291) explains most of the other peaks. In (**B**) (derived from the 0.5 *M* NaCl ion exchange fraction), the M_r of the major protein corresponds exactly to the theoretical M_r of intact unglycosylated MCP-1; the minor peak probably results from an oxidation at the single methionine in MCP-1.

step is followed by a capping step with acetic anhydride. The capping procedure blocks the N-terminus when the coupling reactions are inefficient. This results in the synthesis of chemokines with the expected sequence that are only contaminated with amino-terminally acetylated incompletely synthesized chemokines.

The side-chain protection groups and solid-phase resin are cleaved from the protein in the deprotection mixture for 1.5 to 3 h at room temperature under nitrogen (*see* **Note 6**). The peptides are filtered through a medium-porosity glass filter and precipitated into cold (4°C) methyl *t*-butyl ether (MTBE). After centrifugation at 2000*g*, the peptide precipitate is washed at least three times with cold MTBE, finally dissolved in ultrapure water, lyophilized, and stored at –20°C until purification.

Three naturally occurring N-terminal variants of the C–C chemokine LD78β were synthesized in one synthesis run. Impurities are removed by RP-HPLC on a Resource RPC column and the M_r of the peptides is determined by on-line LC-MS (*see* **Fig. 4A–C**). Fractions containing the peptide with the correct M_r are pooled, lyophilized, incubated in folding buffer for 2 h at room temperature (*see* **Note 7**), and repurified by C-8 or Resource RPC RP-HPLC coupled to a mass spectrometer. **Figure 5** shows the total ion current (TIC) chromatogram and the sum of the chromatogram tracks for the three major ions of intact synthetic LD78β. The formation of the two disulfide bridges is evidenced by the reduction of the M_r of the proteins by 4 Da (*see* **Fig. 4D,E**). Purified proteins are stored at –20°C until use.

3.4. Chemokine Processing In Vitro

Numerous proteolytically processed chemokines have been identified from natural sources. Multiple observed truncations result from cleavages at conserved sites. Chemokines such as GCP-2, RANTES, eotaxin, the macrophage-derived chemokine macrophage-derived chemokine (MDC), and the macrophage inflammatory protein-1α (MIP-1α) variant LD78β have a conserved Pro at the penultimate N-terminal position. Although this amino acid protects proteins against most aminopeptidases, a form of all these chemokines lacking the two N-terminal amino acids has been identified from natural sources ***(5–9)***. Thus, enzymes that remove Xaa-Pro dipeptides N-terminally from proteins are likely to be involved in the processing. The number of proteases with this substrate specificity is limited, the most omnipresent one in human plasma (25 U/L) being the serine protease dipeptidyl peptidase IV (DPP IV) or CD26 ***(28)***. CD26/DPP IV is a membrane-bound protease that is found on endothelial cells and lymphocytes and also occurs in a soluble active form without membrane anchor (e.g., in blood and seminal plasma). Therefore, chemokines (5 μ*M*) that contain the expected consensus sequence can be tested by incubation with different concentrations of this protease (0.25–250 U/L) in 50 m*M* Tris-HCl, pH

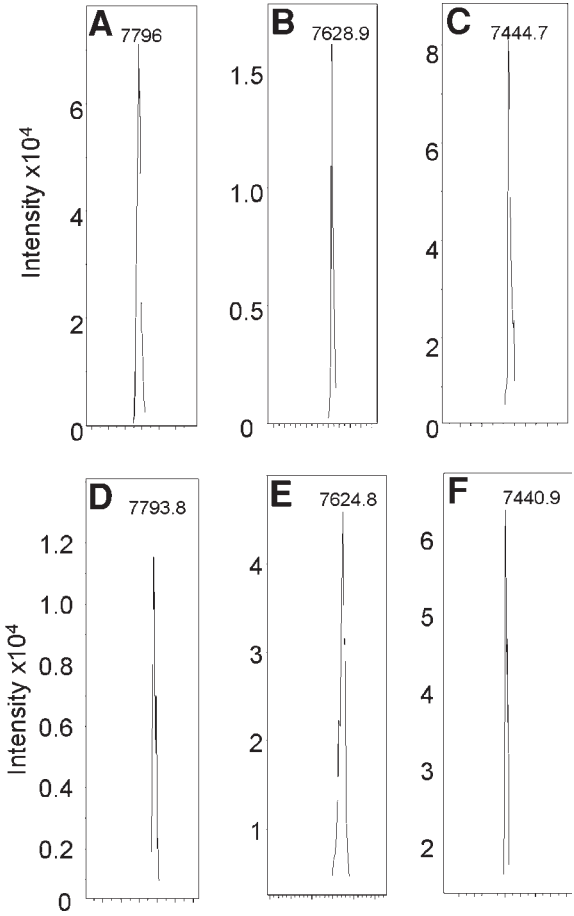

Fig. 4. Mass-spectrometric analysis of synthetic LD78β isoforms. The M_r and purity of synthetic unfolded (**A–C**) and folded (**D** and **E**) LD78β(1–70) (**A** and **D**), LD78β(3–70) (**B** and **E**), and LD78β(5–70) (**C** and **F**) were determined by electrospray ion-trap MS. The figure shows the deconvoluted uncharged M_r of the proteins (average of 100–500 spectra).

7.5; 1 m*M* EDTA at 37°C and by sampling (5 µL) at several time intervals (*see* **Note 8**) ***(29)***. After the reaction is stopped in 0.1% TFA, samples are desalted on C18 ZipTips. Prior to the application of the chemokine, the ZipTips are washed 10 times with 10 µL water/acetonitrile (50/50) and 10 times with 10 µL of 0.1% TFA in water. The samples are pipetted over the tips and washed 10 times with each of the following solvents (a) 0.1% TFA in water, (b) 0.1% acetic acid in water, and (c) 0.1% acetic acid in water/methanol (95/5). The chemo-

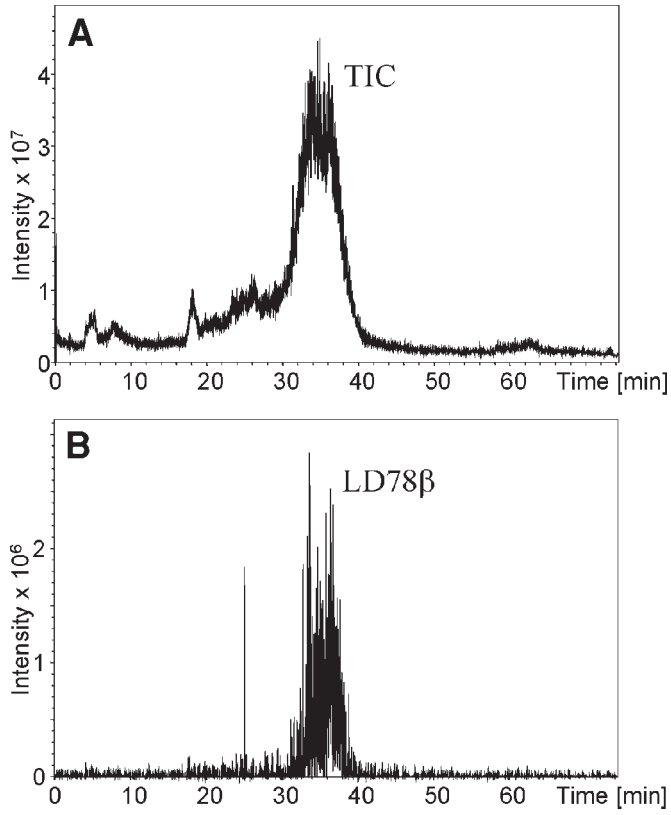

Fig. 5. Purification of folded intact LD78β. Intact synthetic LD78β was incubated for 2 h in folding buffer at room temperature and subjected to a Resource RPC column coupled on-line to an ion-trap MS and eluted in a linear acetonitrile gradient in 0.1% TFA. (**A**) The total ion current (TIC) chromatogram; (**B**) the sum of the chromatogram tracks for the three major ions of intact synthetic LD78β (ions of 1300, 1560, and 1949 that correspond respectively to six, five, and four times protonated peptide).

kines are eluted from the C18 ZipTips in 2 × 10 µL of 0.1% acetic acid in water/acetonitrile (50/50) and injected on an ion-trap MS at a flow rate of 5 µL/min. The percent conversion of intact to truncated chemokines is calculated from the relative intensity of the signals on the MS (*see* **Fig. 6**) (*see* **Note 9**). In order to control that no other contaminating protease is responsible for the degradation of the chemokines, chemokines are incubated with CD26/DPP IV that is inactivated prior to the incubation with the chemokine with the specific irreversible CD26/DPP IV inhibitor bis(4-acetamidophenyl) 1-((*S*)-prolyl)pyrrolidine-2-(*R*,*S*)-phosphonate ***(30)*** (*see* **Fig. 6**, lower right panel).

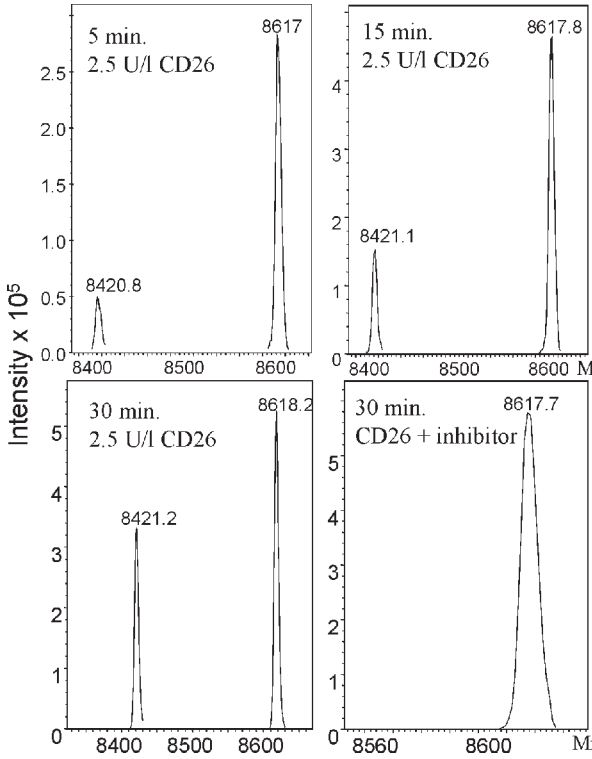

Fig. 6. Kinetics of processing of IP-10 by CD26/DPP IV. Recombinant human IP-10 (5 μ*M*) was incubated with 2.5 U/L CD26/DPP IV at 37°C and samples were taken after different time intervals. In addition, CD26/DPP IV was inactivated with the specific irreversible inhibitor bis(4-acetamidophenyl) 1-((*S*)-prolyl)pyrrolidine-2-(*R*,*S*)-phosphonate and subsequently incubated with 5 μ*M* IP-10 for 30 min (negative control).

Another protease that is likely to be involved in the processing of chemokines is the endoprotease MMP9/gelatinase B. Gelatinase B is rapidly (within minutes) released from the granules of neutrophil granulocytes upon stimulation with C–X–C chemokines that contain the ELR motif (such as IL-8 and GCP-2) during inflammatory processes ***(1)***. To test its role in chemokine processing, pure protein is incubated in vitro at 37°C with gelatinase in assay buffer and analyzed by SDS-PAGE, automated Edman degradation, or MS (discussed earlier). If MS is used for the analysis of the truncation of the chemokine, Tween-20 cannot be added to the incubation mixture because this detergent interferes with the analysis. Tween-20 is normally added if small amounts of protease or chemokine (100 ng or less) are incubated with gelatinase B to prevent the chemokine and protease from sticking to the incubation tubes. In this case, the cleavage

sites and percent conversion are calculated from the sequences and yields of the Edman degradation, respectively ***(13)***.

For use in bioassays, large amounts of the truncated chemokines can be generated by chemical synthesis or by incubating intact (natural or recombinant) proteins overnight with the protease involved. The truncated chemokines are repurified by C-8 RP-HPLC (*see* **Subheading 3.1.4.**) and the purity of the truncated chemokines is checked by electrospray MS. Chemokines are lyophilized and dissolved in 0.9% NaCl or PBS, pH 7.4, and stored at –70°C until use.

4. Notes

1. Chemokine purification and recovery vary significantly depending on both the biological fluid and adsorbant. Therefore, different batches of conditioned media and of silicic acid or CPG have to be tested before purification on large scale (e.g., by measuring the recovery of the chemokines by enzyme-linked immunosorbent assay [ELISA] before adsorption and after elution).
2. If available, antibody-affinity chromatography columns form an alternative for heparin–Sepharose chromatography. However, these columns have the disadvantage that they will only bind one or a limited number of chemokines.
3. If small (< 20 µg) amounts of protein have to be purified by ion-exchange chromatography, 0.01% (v/v) Tween-20 can be added to the loading and elution buffers to prevent loss of proteins because of aspecific interactions with tubings and collection vials. However, if Tween-20 is used, MS for the identification of the proteins is disturbed because Tween-20 remains in the protein samples even after an additional RP-HPLC purification.
4. As an ion-pairing agent, TFA increases the resolution of the RP-HPLC separation. However, TFA reduces the sensitivity of the detection on the MS and results in the generation of fewer protonated ions on the MS. TFA may be replaced by 0.1% formic acid or 0.1% acetic acid in order to measure the M_r of small amounts of chemokine.
5. Because the N-terminal glutamine of natural MCPs is converted into pyroglutamic acid, N-terminally intact MCPs are blocked for Edman degradation. In order to obtain internal sequence information from these chemokines, pure proteins have to be digested chemically (e.g., upon incubation with 75% formic acid for 48 h at 37°C) or with proteases. The sequences of the proteolytic fragments are determined by Edman degradation or deduced from the fragmentation spectra after LC-MS^n (random fragmentation of specific peptides isolated on the mass spectrometer followed by M_r determination of the generated fragments).
6. The length of the deprotection reaction depends largely on the number of arginines in the peptide because the side-chain protection group of Arg (the 2,2,5,7,8-pentamethylchroman-6-sulfonyl group) is slowly removed.
7. For every chemokine, the optimal protein concentration that results in efficient folding has to be determined. High chemokine concentrations during the folding result in the formation of interchain instead of intrachain disulfide bridges.

8. EDTA is added to the incubation buffer to ensure that low undetectable (by SDS-PAGE) contamination of natural CD26/DPP IV preparations with metalloproteases do not interfere with the assay.
9. Desalt and analyze the protease-treated chemokines as soon as possible by MS. Overnight storage of chemokines at low concentrations results in reduction of the signal because of the sticking of the protein to the tubes.

Acknowledgments

This work was supported by the Fund for Scientific Research of Flanders (FWO-Vlaanderen), the Concerted Research Actions of the Regional Government of Flanders, and the InterUniversity Attraction Pole Initiative of the Belgian Federal Government. P.P. holds a Postdoctoral Research Fellowship of the FWO-Vlaanderen.

References

1. Opdenakker, G., Van den Steen, P. E., and Van Damme, J. (2001) Gelatinase B: a tuner and amplifier of immune functions. *TRENDS Immunol.* **22,** 571–579.
2. Springer, T. A. (1994) Traffic signals for lymphocyte recirculation and leukocyte emigration: the multistep paradigm. *Cell* **76,** 301–314.
3. Baggiolini, M., Dewald, B., and Moser, B. (1997) Human chemokines: an update. *Annu. Rev. Immunol.* **15,** 675–705.
4. De Meester, I., Korom, S., Van Damme, J., and Scharpé, S. (1999) CD26, let it cut or cut it down. *Immunol. Today* **20,** 367–375.
5. Proost, P., De Wolf-Peeters, C., Conings, R., Opdenakker, G., Billiau, A., and Van Damme, J. (1993) Identification of a novel granulocyte chemotactic protein (GCP-2) from human tumor cells. *In vitro* and *in vivo* comparison with natural forms of GRO, IP-10, and IL-8. *J. Immunol.* **150,** 1000–1010.
6. Struyf, S., De Meester, I., Scharpé, S., et al. (1998) Natural truncation of RANTES abolishes signaling through the CC chemokine receptors CCR1 and CCR3, impairs its chemotactic potency and generates a CC chemokine inhibitor. *Eur. J. Immunol.* **28,** 1262–1271.
7. Mochizuki, M., Bartels, J., Mallet, A. I., Christophers, E., and Schröder, J.-M. (1998) IL-4 induces eotaxin: a possible mechanism of selective eosinophil recruitment in helminth infection and atopy. *J. Immunol.* **160,** 60–68.
8. Pal, R., Garzino-Demo, A., Markham, P. D., et al. (1997) Inhibition of HIV-1 infection by the beta-chemokine MDC. *Science* **278,** 695–698; comments, *Science* **281,** 487 (1998).
9. Menten, P., Struyf, S., Schutyser, E., et al. (1999) The LD78β isoform of MIP-1α is the most potent CCR5 agonist and HIV-1-inhibiting chemokine. *J. Clin. Invest.* **104,** R1–R5.
10. Proost, P., Struyf, S., Couvreur, M., et al. (1998) Post-translational modifications affect the activity of the human monocyte chemotactic proteins MCP-1 and MCP-

2: identification of MCP-2(6–76) as a natural chemokine inhibitor. *J. Immunol.* **160,** 4034–4041.
11. Walz, A., Dewald, B., von Tscharner, V., and Baggiolini, M. (1989) Effects of the neutrophil-activating peptide NAP-2, platelet basic protein, connective tissue-activating peptide III and platelet factor 4 on human neutrophils. *J. Exp. Med.* **170,** 1745–1750.
12. Van Damme, J., Rampart, M., Conings, R., et al. (1990) The neutrophil-activating proteins interleukin-8 and beta-thromboglobulin: in vitro and in vivo comparison of NH_2-terminally processed forms. *Eur. J. Immunol.* **20,** 2113–2118.
13. Van den Steen, P. E., Proost, P., Wuyts, A., Van Damme, J., and Opdenakker, G. (2000) Neutrophil gelatinase B potentiates interleukin-8 tenfold by aminoterminal processing, whereas it degrades CTAP-III, PF-4, and GRO-α and leaves RANTES and MCP-2 intact. *Blood* **96,** 2673–2681.
14. Oravecz, T., Pall, M., Roderiquez, G., et al. (1997) Regulation of the receptor specificity and function of the chemokine RANTES (regulated on activation, normal T cell expressed and secreted) by dipeptidyl peptidase IV (CD26)-mediated cleavage. *J. Exp. Med.* **186,** 1865–1872.
15. Proost, P., De Meester, I., Schols, D., et al. (1998) Amino-terminal truncation of chemokines by CD26/dipeptidylpeptidase IV: conversion of RANTES into a potent inhibitor of monocyte chemotaxis and HIV-1-infection. *J. Biol. Chem.* **273,** 7222–7227.
16. Proost, P., Struyf, S., Schols, D., et al. (1998) Processing by CD26/dipeptidyl-peptidase IV reduces the chemotactic and anti-HIV-1 activity of stromal-cell-derived factor-1α. *FEBS Lett.* **432,** 73–76.
17. Proost, P., Struyf, S., Schols, D., et al. (1999) Truncation of macrophage-derived chemokine by CD26/dipeptidyl-peptidase IV beyond its predicted cleavage site affects chemotactic activity and CC chemokine receptor 4 interaction. *J. Biol. Chem.* **274,** 3988–3999.
18. Struyf, S., Proost, P., Schols, D., et al. (1999) CD26/dipeptidyl-peptidase IV down-regulates the eosinophil chemotactic potency, but not the anti-HIV activity of human eotaxin by affecting its interaction with CC chemokine receptor 3. *J. Immunol.* **162,** 4903–4909.
19. Proost, P., Menten, P., Struyf, S., Schutyser, E., De Meester, I., and Van Damme, J. (2000) Cleavage by CD26/dipeptidyl peptidase IV converts the chemokine LD78β into a most efficient monocyte attractant and CCR1 agonist. *Blood* **96,** 1674–1680.
20. Proost, P., Schutyser, E., Menten, P., et al. (2001) Aminoterminal truncation of CXCR3 agonists impairs receptor signaling and lymphocyte chemotaxis, while preserving anti-angiogenic properties. *Blood* **98,** 3554–3561.
21. McQuibban, G. A., Gong, J. H., Tam, E. M., McCulloch, C. A., Clark-Lewis, I., and Overall, C. M. (2000) Inflammation dampened by gelatinase A cleavage of monocyte chemoattractant protein-3. *Science* **289,** 1202–1206.
22. Lee, J. K., Lee, E. H., Yun, Y. P., et al. (2002) Truncation of NH2-terminal amino acid residues increases agonistic potency of leukotactin-1 on CC chemokine receptors 1 and 3. *J. Biol. Chem.* **277,** 14,757–14,763.

23. De Meester, I., Vanhoof, G., Lambeir, A.-M., and Scharpé, S. (1996) Use of immobilized adenosine deaminase (EC3.5.4.4.) for the rapid purification of native human CD26/dipeptidyl peptidase IV (EC 3.4.14.5). *J. Immunol. Methods* **189,** 99–105.
24. Van Damme, J. and Billiau, A. (1981) Large-scale production of human fibroblast interferon. *Methods Enzymol.* **78(Pt. A),** 101–119.
25. De Ley, M., Van Damme, J., Claeys, H., et al. (1980) Interferon induced in human leukocytes by mitogens: production, partial purification and characterization. *Eur. J. Immunol.* **10,** 877–883.
26. Wuyts, A., Proost, P., Put, W., Lenaerts, J.-P., Paemen, L., and Van Damme, J. (1994) Leukocyte recruitment by monocyte chemotactic proteins (MCPs) secrected by human phagocytes. *J. Immunol. Methods* **174,** 237–247.
27. Van Damme, J., Proost, P., Put, W., et al. (1994) Induction of monocyte chemotactic proteins MCP-1 and MCP-2 in human fibroblasts and leukocytes by cytokines and cytokine inducers. *J. Immunol.* **152,** 5495–5502.
28. Durinx, C., Lambeir, A.-M., Bosmans, E., et al. (2000) Molecular characterization of dipeptidyl peptidase activity in serum: soluble CD26/dipeptidyl peptidase IV is responsible for the release of X-Pro dipeptides. *Eur. J. Biochem.* **367,** 5608–5613.
29. Lambeir, A.-M., Proost, P., Durinx, C., et al. (2001) Kinetic investigation of chemokine truncation by CD26/dipeptidyl peptidase IV reveals a striking selectivity within the chemokine family. *J. Biol. Chem.* **276,** 29,839–29,845.
30. Belyaev, A., Zhang, X., Augustyns, K., et al. (1999) Structure–activity relationship of diaryl phosphonate esters as potent irreversible dipeptidyl peptidase IV inhibitors. *J. Med. Chem.* **42,** 1041–1052.

4

Chemotactic Profiling of Lymphocyte Subpopulations

Lucia Colantonio, Andrea Iellem, and Daniele D'Ambrosio

1. Introduction

Among a variety of trafficking signals, chemokines and their receptors represent key regulators of lymphocyte trafficking and localization under homeostatic as well as inflammatory conditions ***(1,2)***. Novel subsets of lymphocytes have been identified on the basis of their profile of chemokine-receptor expression ***(3–6)***. The ability of a cell population to adhere and migrate in response to a chemokine can be tested making use of several established in vitro chemotaxis assays. Among them, the transwell chemotaxis assay is suitable to meet the needs required for a functional characterization of the migrated cells. In this chapter, we describe a transwell chemotaxis method that allows the phenotypic and functional characterization of the responding cell populations. In particular, we illustrate how chemotactic responsiveness can be combined to known cell surface markers to identify the chemotactic response profile of known subpopulations of $CD4^+$ T-cells. This method can, in principle, be applied for the same purpose to different cell populations isolated from different tissues or organs.

2. Materials

1. Ficoll-Paque (Amersham-Pharmacia Biotech).
2. $CD4^+$ T-cell isolation kit (Miltenyi Biotech, cat. no. 130-053-101).
3. Phosphate-buffered saline (PBS) without Mg^{2+} and Ca^{2+} (PBS, Gibco-BRL).
4. Bovine serum albumin (BSA Fraction V, Sigma cat. no. A3294).
5. Labeling buffer: 0.5% BSA, 2.5 m*M* EDTA in PBS.
6. LS MACS separation columns (Miltenyi Biotech, cat. no. 130-042-401).
7. RPMI-1640 (Gibco-BRL).
8. Migration medium: 0.5% BSA in RPMI-1640.
9. Transwell tissue-culture polycarbonate filter inserts/plates (6.5 m*M* in diameter, 5 μm pore size) (Corning Costar, cat. no. 3421) (*see* **Note 1**).

From: *Methods in Molecular Biology, vol. 239: Cell Migration in Inflammation and Immunity*
Edited by: D. D'Ambrosio and F. Sinigaglia © Humana Press Inc., Totowa, NJ

10. Chemokines (CCL1, CCL19, and CCL22 from Dictagene).
11. Polybead polystyrene 15-μm microspheres (1.35×10^7 particles/mL; Polyscience, cat. no. 18328).
12. Labeling buffer: 1% FetalClone (HyClone), 0.01% NaN_3 in PBS.
13. Phycoerythzin (PE)-labeled anti-CD27, Cy-Chrome-labeled anti-CD45RA (BD PharMingen).
14. LSR flow cytometer (Becton Dickinson).

3. Methods

The method used to delineate the chemotactic profile of effector/memory $CD4^+$ human T-lymphocyte subsets is described. $CD4^+$ T-lymphocytes are first isolated from human peripheral blood mononuclear cells (PBMCs) and subsequently subject to transwell chemotaxis assay in response to various chemokines. Migrated cells are then collected and quantified on the basis of specific phenotypic characteristics by FACS analysis. The aim of the experiment described in this chapter is the delineation of the chemotactic response profile of naive and effector/memory helper T-lymphocytes defined by expression of CD45RA and CD27.

Variations of this method would represent a useful approach to explore the migratory potential of small cell subsets, which can be identified within larger and heterogeneous populations isolated from different tissues and organs.

3.1. Purification of $CD4^+$ T-Cells

3.1.1. PBMC Isolation

1. Collect heparinized blood.
2. Dilute 1:2 with warm PBS and gently stratify 30 mL of blood–PBS mixture on 15 mL of Ficoll-Paque.
3. Centrifuge at 950*g* for 30 min at room temperature.
4. Harvest PBMCs from the ring at the interface with Ficoll-Paque. Wash cells three times with PBS at 200*g* for 10 min to remove remaining platelets (*see* **Note 2**).

3.1.2. Purification of $CD4^+$ T-Cells

Purification of $CD4^+$ T-cells from PBMCs was performed using the $CD4^+$ isolation kit from Miltenyi Biotech and following the directions indicated by the manufacturer.

3.2. Chemotaxis Assay

1. Count $CD4^+$ T-cells and resuspend them at 2.5×10^6 cell/mL in migration medium.
2. Incubate cells for 2 h at 37°C in 5% CO_2.
3. Set up the chemotaxis assay by first removing the transwells from the plate and setting them aside (taking care to avoid damaging the polycarbonate membrane).

Add 600 µL of the chemokine solution (*see* **Note 3**) to the wells of the 24-well plate (*see* **Note 4**). To have duplicates, two sets of three wells each are set up for every chemokine dilution. Twelve wells should be designated as negative controls and receive 600 µL of migration medium only. These wells are used to determine the background or "spontaneous" migration (*see* **Note 5**).

4. Dispense 100 µL of $CD4^+$ T-cells into the transwell insert and quickly but gently transfer them to their original position onto the 24-well plate. It is important to avoid trapping of air bubbles.
5. Four wells devoid of transwell inserts should be used for measuring the number of cells of the "input" populations. This is achieved by the addition of 100 µL of the $CD4^+$ T-cell suspension into 500 µL of migration medium.
6. Incubate the plates at 37°C, 5% CO_2, for 1 h (*see* **Note 6**).
7. After the incubation time, remove the transwell inserts from the wells.
8. Dilute Polybeads 1:40 in FACS buffer.
9. Add 20 µL of diluted Polybeads for each well. Only 10 µL of Polybeads should be added to the negative control wells (to keep constant the number of Polybeads after pulling). The Polybead suspension should be mixed before addition. Pool the contents of three wells in a single FACS tube for each condition. In the case of negative controls, the contents of six wells are pooled in a single FACS tube (*see* **Note 7**).

3.3. Labeling of the Cells

1. Centrifuge the sample and input cells.
2. One sample of the input population follows the staining procedure described in **step 3** and the others are single stained and used as stained sample controls for the appropriate setting of fluorescence compensation of the flow cytometer (*see also* **Note 8**).
3. Add labeled antibodies (PE-labeled anti-CD27, Cy-Chrome-labeled anti-CD45RA) and incubate on ice for 15 min.
4. Wash the cells with 1 mL of FACS buffer.
5. Resuspend the cells in 600 µL of FACS buffer.
6. Set flow cytometer acquisition parameters using single-stained controls.
7. Set side scatter (SSC) and forward scatter (FSC) parameters for detection of the Polybeads. With both physical parameters in a linear scale, the beads will be located in the upper side of the acquisition dot plot; with both parameters in a logarithmic scale, beads will be visible on the upper right corner of the acquisition dot plot (*see* **Fig. 1**).
8. Draw a region around cells (region 1, R1) and a region around Polybeads (R2) (*see* **Fig. 1**).
9. Set acquisition parameters to acquire 3×10^4 events in R2 and to store events of R1 plus R2.
10. Acquire samples with a sample flow rate of 200 µL/min.
11. Analyze the number of migrated cells within each region defined in the dot plots by different cell surface marker expression (CD45RA, CD27) using the Cell Quest software.

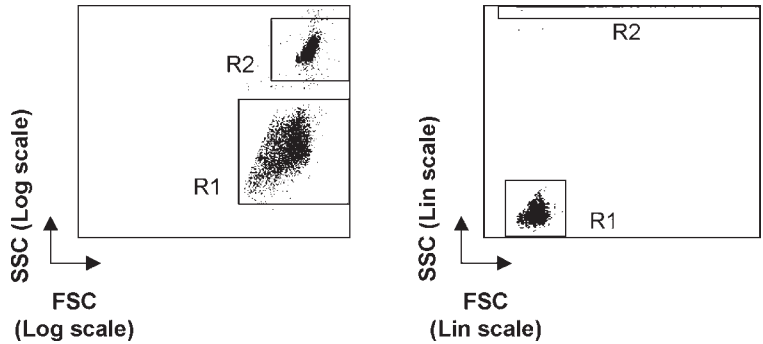

Fig. 1. Cells (R1) and polystyrene beads (R2) can be visualized on the basis of their different SSC versus FSC properties, in a logarithmic scale (log). When plotting in a linear scale (lin), polystyrene beads are scarcely visible, but can be easily gated by drawing a rectangular region in the upper side of the plot (R2).

3.4. Analysis of Transwell Cell Migration and Chemotactic Profiling of Human CD4⁺ T-Cells

There are various ways to express the results obtained from transwell migration experiments, which can provide different kinds of information regarding the experimental data. We usually express the migration data as a duplicate acquisition ± standard deviation, calculated according to statistical rules. We consider the following most suited for our analysis:

1. *Specific Cell Migration* (*Percentage*). This index provides a relative measurement of the contribution given by each specific cell subset within a heterogeneous population of cells to the overall migration in response to a given chemokine (specificity of action of the chemokine). Specificity of migration in response to a given chemokine can be calculated for the whole population by first defining the number of specifically migrated cells:

Fig. 2. (*opposite page*) $CD4^+$ T-cell migration assay in response to the chemokines CCL1, CCL19, or CCL22. Before (Input) and after migration, cells were stained for CD45RA and CD27. (**A**) Flow cytometer dot plots of the indicated samples. Gates indicate the subpopulations $CD4^+CD45RA^+CD27^+$ (R1) and $CD4^+CD45RA^-CD27^-$ (R2), which have been analyzed in (**B**), (**C**), and (**D**). The results of the transwell migration assay are presented in three different ways. The results of the transwell migration assay can be represented using three different kind of indexes: Chemotactic index (**B**), specific cell migration (**C**), and percentage of input (**D**). In the diagrams in which specific cell migra-tion (Percent) is expressed, the dashed horizontal lines indicate the percentage of $CD4^+CD45RA^+CD27^+$ or $CD4^+CD45RA^-CD27^-$ in the starting cell population.

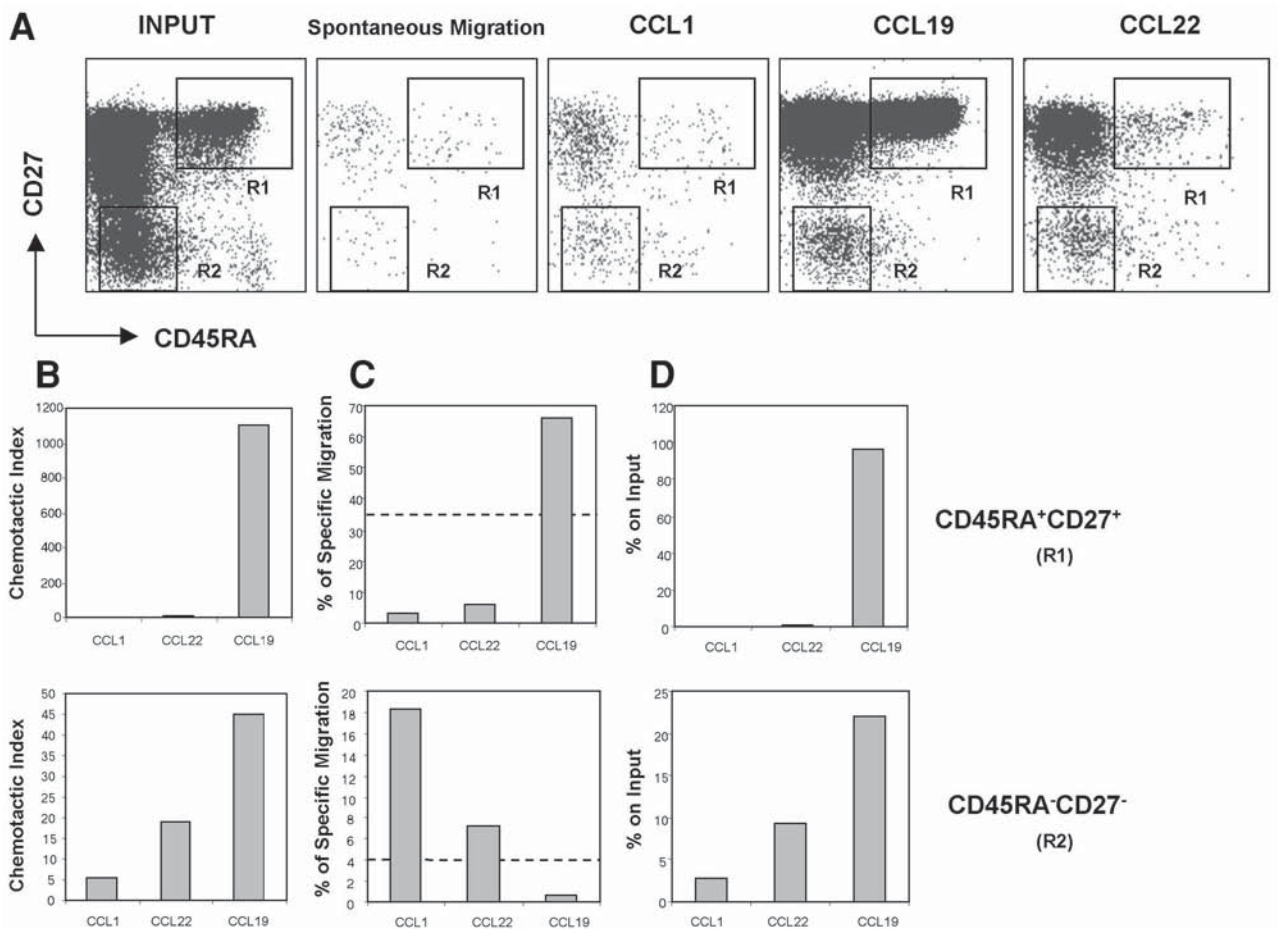
A
INPUT
Spontaneous Migration
CCL1
CCL19
CCL22
CD27
CD45RA
R1
R2
B
C
D
Chemotactic Index
% of Specific Migration
% on Input
CCL1
CCL22
CCL19
CD45RA+CD27+
(R1)
CD45RA-CD27-
(R2)

Specifically migrated cells = Number of chemokine migrated $CD4^+$ T-cells counted in a defined region (after 3×10^4 beads have been acquired) – Number of spontaneously migrated cells counted in the same region.

Migrated cells can be further characterized on the basis of their expression of the surface markers that have been used (in our case, CD45RA and CD27). In this case, we refer to the migrated cells as *specifically migrated subpopulation*.

Specifically migrated subpopulation = Number of specifically chemokine migrated cells belonging to a defined subpopulation (identified by specific cell surface marker expression and gated region) – Number of spontaneously migrated cells belonging to the same subpopulation (identified within the same gated region).

Specific cell migration (percentage) = 100 × (Specifically migrated subpopulation)/(Specifically migrated cells).

To evaluate the relative migratory capacity of each cell subset in response to a specific chemokine, it is useful to compare the frequency of that given subpopulation in the starting population (percentage of the input) with the percentage of specific migration for the same population.

2. *Chemotactic Index*. This index is a helpful indicator of the potency of a given chemokine toward a specific lymphocyte subset.

   Chemotactic Index = Number of chemokine migrated cells counted in a defined gated region identified by surface marker expression (after 3×10^4 microbeads have been acquired)/Number of spontaneously migrated cells acquired in the same gated region.

3. *Percentage of Input*. This index provides a good measure of the overall efficacy of a chemokine in attracting a specific cell subset.

   Percentage of input = 100 × [Number of chemokine migrated cells counted in a gated region]/ [Number of cells counted in the same region of the "input" population].

4. Notes

1. When choosing the transwell pore size, it is important to take into account that cells should not diffuse through the filter pores, but must actively transmigrate through them by changing their shape in a process similar to the diapedesis, which occurs in vivo. Filters with a pore size of 5 μm are used for human peripheral blood mononuclear cells.
2. Peripheral blood mononuclear cells can be stored overnight in labeling buffer and kept at 4°C before the isolation of $CD4^+$ T lymphocytes.
3. When the final aim of the experiment is establishing the chemotactic profile of a quite heterogeneous cell populations (like, in this case, effector/memory CD4+ T lymphocytes), it is useful to determine at which chemokine concentration a substantial migration of that specific cell subset is achieved. Thus, we suggest initially performing transwell migration assays for chemokine titration.

4. Our chemokine stock solutions are prepared by resuspending lyophilized powder in sterile migration medium at no less than 50 µg/mL and stored at –80°C until use. Once thawed, chemokine vials are stocked at 4°C for a few weeks. It is advised to refrigerate chemokine aliquots for no longer than 4–5 wk. For this reason, we stock the chemokine suspensions in small aliquots.
5. It is also important to dedicate a number of transwells for detection of nonspecific cell migration, which occurs in the absence of any chemotactic agents. When setting the controls of "spontaneous migration," the number of transwells that are included is usually doubled. Given the very low rate of nonspecific lymphocyte migration, a higher number of transwell inserts for the control gives the advantage of having a more accurate measurement of such spontaneous migration.
6. Another essential point of the assay is the incubation time during which directed cell migration occurs. In our hands, when working with human PBMCs, a chemotaxis assay of 1 h seems to be an optimal compromise between a low spontaneous migration and a relatively high chemotaxis. We suggest routinely setting up a pilot experiment when working with different types of cell, trying different time-points to optimize these parameters.
7. The importance of adding polystyrene microbeads to the plate wells after transwell removal relies on the necessity to have an internal standard. Indeed, it should be taken into account that although time-dependent acquisition of the events is a quite common method for counting migrated cells with a flow cytometer, fluctuations as a result of the setup of the equipment may occur. Such difficulty generates poor interexperimental reproducibility but may be overcome by the addition of a known number of inert particles followed by FACS analysis performed on the basis of an event-dependent acquisition. In our experience, a detectable amount of migrated cells can be stained and analyzed by pooling together the contents of three single wells ***(7)***. For this reason, we always suggest to set up at least two series of three transwells each, for every chemokine concentration.
8. In our experience, surface staining of the cells should not precede the transwell migration assay. Indeed, although such procedure works considerably well for the staining of markers like CD4 or CD8, for some other receptors, the fluorochrome staining intensity might undergo appreciable loss during the process of cell chemotaxis.

References

1. Campbell, J. J. and Butcher, E. C. (2000) Chemokines in tissue-specific and microenvironment-specific lymphocyte homing. *Curr. Opin. Immunol.* **12,** 336–341.
2. Butcher, E. C., Williams, M., Youngman, K., Rott, L., and Briskin, M. (1999) Lymphocyte trafficking and regional immunity. *Adv. Immunol.* **72,** 209–253.
3. Campbell, J. J., Haraldsen, G., Pan, J., et al. (1999) The chemokine receptor CCR4 in vascular recognition by cutaneous but not intestinal memory T cells. *Nature* **400,** 776–780.
4. Sallusto, F., Lenig, D., Forster, R., Lipp, M., and Lanzavecchia, A. (1999) Two subsets of memory T lymphocytes with distinct homing potentials and effector functions. *Nature* **401,** 708–712.

5. Schaerli, P., Willimann, K., Lang, A. B., Lipp, M., Loetscher, P., and Moser, B. (2000) CXC chemokine receptor 5 expression defines follicular homing T cells with B cell helper function. *J. Exp. Med.* **192,** 1553–1562.
6. Kim, C. H., Rott, L. S., Clark-Lewis, I., Campbell, D. J., Wu, L., and Butcher, E. C. (2001) Subspecialization of $CXCR5^+$ T cells: B helper activity is focused in a germinal center-localized subset of $CXCR5^+$ T cells. *J. Exp. Med.* **193,** 1373–1381.
7. Iellem, A., Mariani, M., Lang, R., et al. (2001) Unique chemotactic response profile and specific expression of chemokine receptors CCR4 and CCR8 by $CD4^+$ $CD25^+$ regulatory T cells. *J. Exp. Med.* **194,** 847–853.

5

Measurement of the Levels of Polymerized Actin (F-Actin) in Chemokine-Stimulated Lymphocytes and GFP-Coupled cDNA Transfected Lymphoid Cells by Flow Cytometry

Miguel Vicente-Manzanares, Mariano Vitón, and Francisco Sánchez-Madrid

1. Introduction

The development of both microscopic and flow cytometry techniques has allowed investigators to examine the individual behavior of migratory cells under many different conditions, such as inflammation, invasion and metastasis, normal recirculation of blood cells, and so forth. Cells belonging to the immune system provide a typical example of cells in which migration is a critical feature for them to exert their physiological function ***(1–3)***. Leukocyte migration requires the reorganization of the cytoskeleton of the cell to allow the transition from a medium of high flow stress, such as the blood, into the target tissues across narrow gaps provided by endothelial cell–cell junctions ***(4)***. Thus, cytoskeletal plasticity is a key requirement for leukocyte migration and its associated morphological changes ***(5)***. Such a property is provided by the actomyosin system, a flexible compartment of the cell cytoskeleton that is dynamically regulated by a number of signaling intermediates and adaptor molecules that ensure its proper polymerization/depolymerization and contractility ***(6–9)***. These molecules are regulated by extracellular cues, which function as molecular on/off devices, providing the cell with the appropriate signal that triggers changes in the cytoskeleton by the recruitment and/or activation of the adequate intracellular components. Chemoattractants are among the most widely studied of these signals. They can be simple molecules, such as fMLP, or complex polypeptides, such as chemokines. They guide the navigation of the cells of the immune system through the body, both during normal processes such

From: *Methods in Molecular Biology, vol. 239: Cell Migration in Inflammation and Immunity*
Edited by: D. D'Ambrosio and F. Sinigaglia © Humana Press Inc., Totowa, NJ

as maturation, recirculation, and so forth, and also during infection to achieve a correct and efficient response to avoid injury ***(10)***. They transmit their signals by binding to specific receptors expressed on the surface of target cells ***(11)***, which belong to the family of seven transmembrane domain, G-coupled receptors. Ligand occupancy of receptors triggers a cascade of intracellular events that are required for the migration of the cell. These include intracellular calcium mobilization, activation of protein and lipid kinases and/or phosphatases, and so forth ***(12,13)***. Another early event consists in a wave of actin polymerization, as detected by specific staining with the fungal toxin phalloidin, which binds with high affinity to the polymerized form of actin (filamentous actin or F-actin), whereas it binds free actin (G-actin) with a much lower affinity ***(14,15)***. The effect of the chemokine SDF-1α in actin polymerization in both peripheral blood lymphocytes and lymphoid T-cell lines will be employed to illustrate the procedure of quantitative measurement of the increase in the cell content of F-actin, a procedure that has been succesfully employed for monitoring the effect of triggering with exogenous ligands such as the SDF-1α chemokine ***(16,17)*** or the effect of gene deletion in the content of F-actin of selected subpopulations of cells, such as neutrophils ***(18)***. In addition, we also describe a method for monitoring the effect of an exogenously introduced signaling intermediate coupled to green fluorescent protein (GFP) in the levels of F-actin, illustrating this method with experimental data employing active mutants as well as dominant negative forms of the small GTPases Rac and Cdc42. These GTPases have been selected because of their well-known ability to regulate actin-related phenomena in different cell models, such as fibroblasts ***(19,20)*** or lymphocytes ***(21–23)***.

2. Materials

2.1. Chemokine-Induced F-Actin Measurement

1. Jurkat T-cell line (American Tissue Culture Collection, ATCC).
2. Freshly isolated peripheral blood lymphocytes (*see* below).
3. Ficoll-Hypaque high-density medium (Sigma Chemical Co., St. Louis, MO).
4. Standard culture medium (RPMI 1640 medium from Life Technologies [Flow Lab, Irvine, UK] supplemented with 100 U/mL penicillin 100 µg/mL streptomycin [Flow Lab], and 10% fetal bovine serum [FBS] [Flow Lab]).
5. SDF-1α, interleukin (IL)-8, and RANTES (R&D Systems, Minneapolis, MN).
6. *Bordetella pertussis* toxin (Calbiochem, La Jolla, CA).
7. Antibodies against CXCR4 (clone 44708.111 [IgG2a], from R&D Systems [Minneapolis, MN] and clone 12G5 [IgG1] from Pharmingen [Pennsylvania, PA]).
8. Antibodies against CCR5, CXCR1, and CXCR2 (R&D Systems).
9. Antibody P3X63 (described in **ref. *24***) or other relevant control.
10. A suitable fluorescein isothiocyanate (FITC)- or Alexa-488-conjugated anti-mouse antibody.

11. FITC-conjugated phalloidin (Molecular Probes, Eugene, OR).
12. Phosphate-buffered saline (PBS) containing 4% formaldehyde (alternatively, PBS containing 3% paraformaldehyde may be employed).
13. Tris buffer saline (TBS).
14. Triton X-100 (10% stock in distilled water).
15. Flow cytometer with two laser lines of excitation at 488 and 635 nm, respectively (e.g., FACScalibur®; Becton Dickinson, Mountain View, CA).
16. Data acquisition software (e.g., CellQuest® software; Becton Dickinson).

2.2. Measurement of the Effect of GFP-Tagged Proteinsin the Content of F-Actin

1. Expression plasmids (in the examples, pEGFP-C1 [Clontech Laboratories Inc., Palo Alto, CA], expressing GFP alone or fused to wild-type Rac1, V12Rac1, N17Rac1, wild-type Cdc42, V12Cdc42, and N17Cdc42).
2. Standard molecular-biology reagents and procedures for the generation of transfection-grade plasmid DNA.
3. Optimem® medium (Life Technologies, Paisley, UK).
4. Electroporator (e.g., GenePulser; Bio-Rad, Hercules, CA).
5. Alexa-647-conjugated phalloidin (Molecular Probes).
6. Commercial lysis buffer (Becton Dickinson).

3. Methods

The methods described in **Subheading 3.1.** comprise the obtainment of fresh peripheral blood lymphocytes and the maintenance in culture of Jurkat T-cells, the triggering of the cells with chemokines, both in a kinetics study and following a dose–response curve, the fixation, permeabilization, and staining of the cells, the measurement of the levels of F-actin by flow cytometry, and the treatment of the data. **Subheading 3.2.** deals with transient transfection of Jurkat T-cells, measurement of the transfection efficiency, and determination of the levels of F-actin in both the untransfected and transfected populations and generation of expression–response curves.

3.1. Measurement of Chemokine-Induced F-Actin Polymerizationin Nontransfected or Primary Cells

3.1.1. Culture of Jurkat T-Cells

Jurkat T-cells are a typical lymphoblastoid $CD3^+$ T-cell line. They are grown in RPMI 1640 medium supplemented with 10% FBS, 100 U/mL penicillin and 100 µg/mL streptomycin. Routine passage of the cells involves removal of the medium through centrifugation and substitution by fresh medium, the cells being at an optimal concentration of 5×10^5 cells/mL. This is achieved approximately every 48 h.

3.1.2. Obtainment of Fresh Peripheral Blood Lymphocytes

Peripheral blood lymphocytes are obtained through standard methods by Ficoll-Hypaque gradient centrifugation. Briefly, freshly collected blood is diluted 1:3 (blood:solvent) in saline solution and gently laid on 1:1 volume of lymphocyte separation medium (Ficoll). Centrifugation is then performed on a culture table centrifuge at 800*g* for 45 min. No braking should be employed in the centrifuge to avoid dispersion of the ring of mononuclear cells. After centrifugation, three phases are separated. Closer to the top, the yellow fraction is the cell-free serum, then a cloudy ring comprising mononuclear cells, and, finally, a pellet that includes both anucleate cells (such as red cells) and polymorphonuclear leukocytes (PMNs). Mononuclear cells are then collected with a glass or plastic thin pipet. Cells are washed twice with fresh saline solution and allowed to adhere to culture-treated plastic dishes. This method allows purification of monocytes, which actively bind to the plastic dish and can be further purified. To obtain lymphocytes of purity >90%, this procedure should be repeated at least twice. Finally, the cells are resuspended in RPMI 1640 medium supplemented as described in **Subheading 3.1.1.** However, it should be noted that there are other commercial procedures to isolate specific subpopulations of lymphocytes, such as nylon-column filtration, incubation of the cells with specific antibody-coated magnetic beads, and so forth. For further information, readers are directed to excellent technical sections in commercial catalogs from firms that distribute kits to isolate selected subpopulations of cells (e.g., Dynal, Oslo, Norway, or Miltenyi Biotech Inc., Auburn, CA).

3.1.3. Pretreatment of the Cells

Many different studies can be performed with this technique: the study of the effect of chemical inhibition of specific signaling cascades, blocking experiments with specific antibodies, dose–response curves, kinetics studies, and so forth. In this example, we will preincubate the cells with toxin from *Bordetella pertussis*, a well-characterized toxin that selectively blocks the uncoupling of α- and β/γ-subunits of heterotrimeric G_i proteins, which has been involved in many different cellular processes induced by chemokines ***(12,13)***. Treatment with this toxin, as well as with most of commercially available chemical inhibitors, should be performed at 37°C for 30 min with mild or occasional stirring at a cell concentration of $(1.5–3 \times 10^6$/mL. A typical concentration of this toxin selected for this example will be 0.5 µg/mL. If the inhibitor is dissolved in a vehicle other than distilled water, a vehicle-only control is strongly recommended.

For receptor antibody competition experiments, typical concentrations of range from 0.5 to 20 µg/mL, but a dose–response curve should be performed for each individual antibody. It is noteworthy that the antibody should not act

as an agonist, because this could mask or enhance the effect of the chemokine. Control antibodies employed in this assay should ideally recognize but not block the same receptor triggered by the chemokine. This situation will be illustrated in **Fig. 1**, with two specific anti-CXCR4 receptors: the 44708.11 antibody (R&D Systems), which blocks SDF-1α-induced responses, and the 12G5 antibody (Pharmingen), which does not ***(25)***.

3.1.4. Treatment with the Chemokines

There is no need to wash out the inhibitors or the antibodies unless specified by the manufacturer. The cells (control and toxin- or antibody-treated) must be transferred to clean flow cytometer tubes to a final volume of 100 µL/tube, which contains $(1.5–3) \times 10^5$ cells, and kept at 37°C. Triplicates or quadriplicates are highly recommended.

The cells should now be triggered with the adequate concentration of the chemokine (for dose–response curves) or for the indicated time with a selected concentration (for kinetics studies). A typical example can be found in **Table 1**. For each case, the chemokine should be prepared at a 50X or 100X dilution. Kinetics studies should be performed in a countdown fashion to be able to stop all of the points at the same time, which has provided to be critical for reproducibility.

3.1.5. Fixation, Permeabilization, and F-Actin Staining

Nontransfected cells allow a fast, convenient, and highly reproducible method to stop the effect of the chemokine on the cells, which consists of simultaneous fixation, permeabilization, and staining. To achieve this, a fixation–permeabilization–staining (FPS) buffer should be prepared, which should contain 8% formaldehyde (or 6% paraformaldehyde), 1% Triton X-100, and 150 n*M* FITC-conjugated phalloidin in PBS. The FPS buffer should be freshly prepared for each experiment and stored at 4°C in the dark. When the countdown of chemokine stimulation comes to the end, 100 µL of FPS buffer should be added over the cells for 10 min in the dark (*see* **Note 1**). After FPS incubation, 500 µL of TBS should be added and the cells centrifuged at 325*g* for 5 min. After discarding the supernatant, the cells should be resuspended in 500 µL of TBS. If it is not possible to measure the levels of F-actin immediately, the samples should be kept at 4°C until measurement (*see* **Note 2**).

3.1.6. Measurement of the Levels of F-Actin by Flow Cytometry

This step requires that the personnel be familiar with general flow cytometry procedures. First, a suitable acquisition screen comprising a forward scatter–side scatter (FSC-SSC) dot plot or density plot and a FL-1 histogram (for green fluorescence detection) screen should be prepared following CellQuest software manuals (*see* **Note 3**). Then, acquisition should be conducted. Settings should

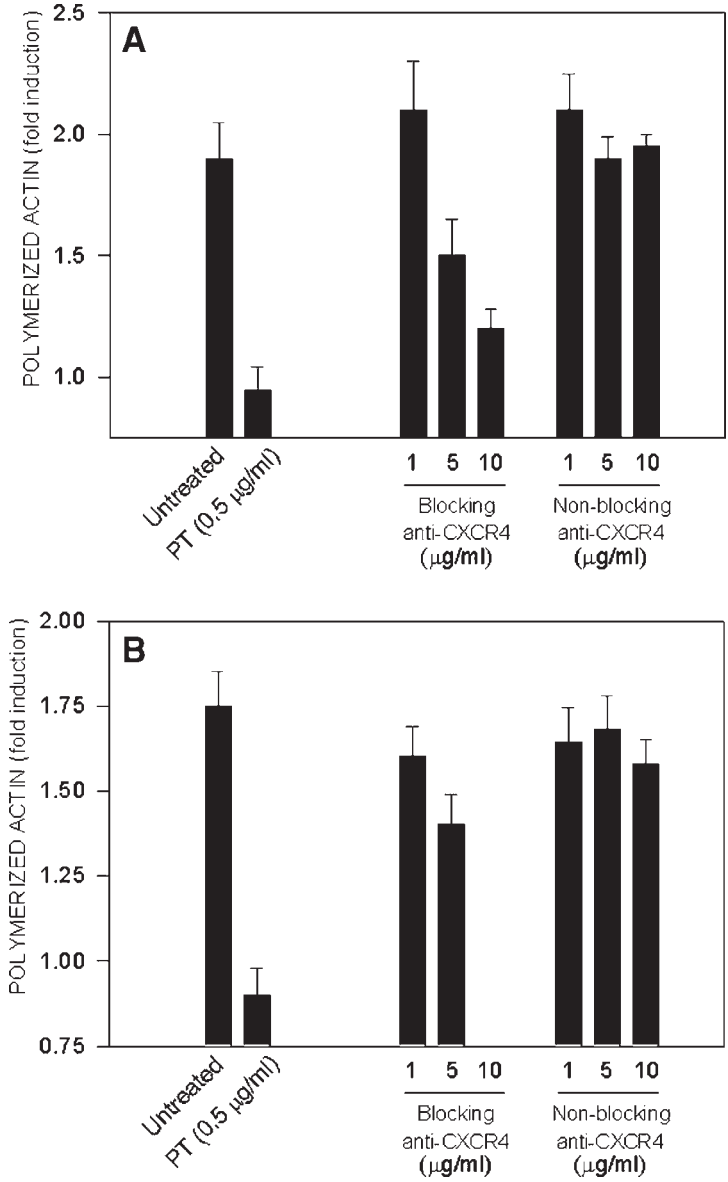

Fig. 1. Effect of different pretreatments in chemokine-induced actin polymerization in Jurkat T-cells and PBLs. (**A**) Jurkat T-cells were pretreated for 30 min with 0.5 µg/mL pertussis toxin (PT) or vehicle (untreated), or different concentrations of the blocking anti-CXCR4 antibody 44708.111 (IgG2a) and the nonblocking anti-CXCR4 antibody 12G5 (IgG1), then triggered with the chemokine SDF-1α and stained for F-actin as described earlier. Data represent the mean ± SD of three independent experiments performed by triplicate. (**B**) Same as (**A**) but employing freshly isolated PBLs.

Table 1
Dose–Response and Kinetics Studies of the Effect of the Chemokine SDF-1α in the Levels F-Actin of Jurkat T-Cells

Dose of chemokine (ng/mL) [n*M*]	0 [0]	0.1 [0.01]	0.5 [0.05]	1 [0.1]	**10 [1]**	**50 [5]**	**100 [10]**	250 [25]	500 [50]	1000 [100]
Time-points for kinetics experiment (s)	0		**15**	45		90		180	300	

Note: These tables provide an overview of the ranges in which it can be useful to test the effect of chemokines in actin polymerization. Points in bold underscore the ranges in which differences to basal levels (dose= 0, time= 0) may be maximal; however, note that these estimations are based on the results shown for SDF-1α and may not be applicable to other cell types or chemokines.

be adjusted for either Jurkat cells or peripheral blood lymphocytes (PBLs). At least 10,000 cells should be quantified. Finally, analysis of the samples should be performed on the collected population. Statis-tical analysis is then performed on the mean or GeoMean of FL-1 of the selected population (*see* **Note 4**). Data should be represented on two-dimensional (2D) Cartesian, linear plots for kinetics analysis and in 2D bar plots for dose–response curves including standard deviations. Examples are shown for dose–response and kinetics of the response of Jurkat cells (*see* **Fig. 2A,B**) and PBL (*see* **Fig. 3A,B**) to the chemokines SDF-1α, RANTES, and IL-8 (*see* **Note 5**). Other experiments, including blockade with either *B. pertussis* toxin or anti-CXCR4, are also shown (*see* **Fig. 1**).

3.2. Measurement of Chemokine-Induced F-Actin Polymerization in Transfected Jurkat T-Cells

3.2.1. Plasmid Constructs

The cDNAs employed in this experiment have been previously described *(23)*. Briefly, the cDNA of either wild-type, active mutants or dominant negative mutants of the small GTPases Rac1 and Cdc42 (kindly donated by Dr. Alan Hall, MRC-LMCB, University College, London, UK) were subcloned in the pEGFP-C1 plasmid (Clontech, Palo Alto, CA). Frame correlation between the GFP and the subcloned constructs was achieved by manual DNA sequencing with a commercial DNA sequencing kit (USB, Cleveland, OH) and standard electrophoresis. Transfection-grade DNA was produced by commercial MaxiPrep procedures (Qiagen, Hilden, Germany).

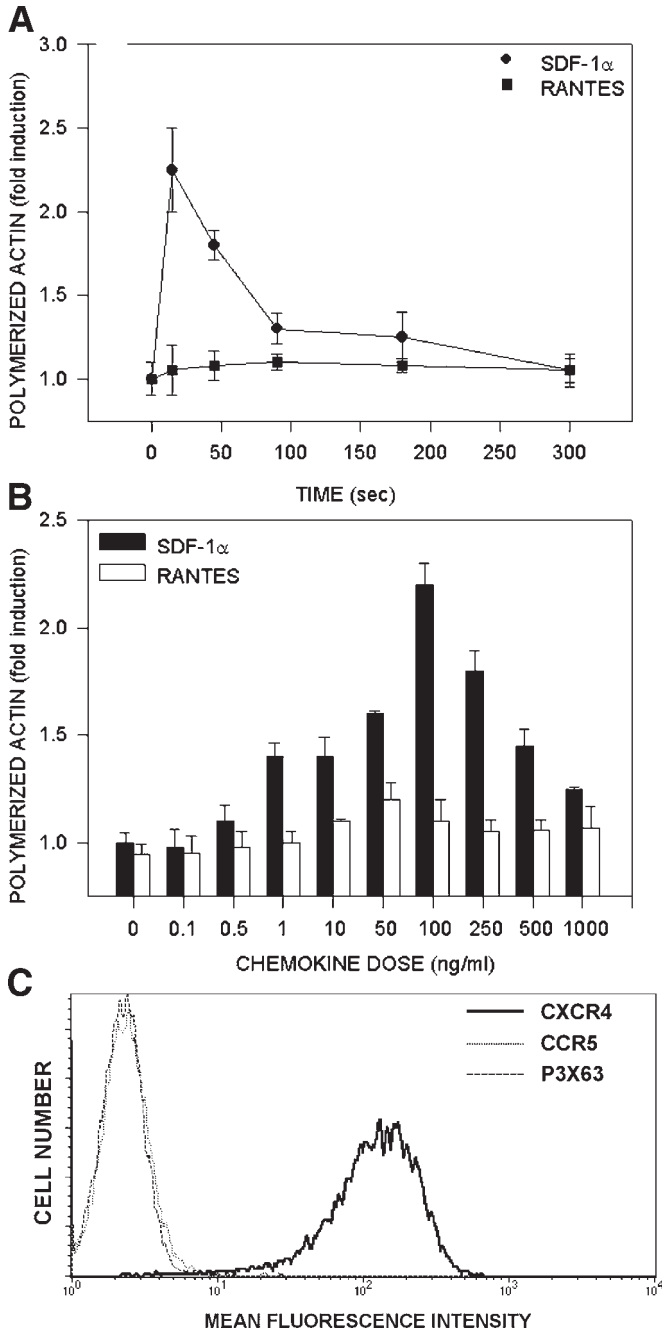
A
SDF-1α
RANTES
POLYMERIZED ACTIN (fold induction)
3.0
2.5
2.0
1.5
1.0
0
50
100
150
200
250
300
TIME (sec)
B
SDF-1α
RANTES
POLYMERIZED ACTIN (fold induction)
2.5
2.0
1.5
1.0
0
0.1
0.5
1
10
50
100
250
500
1000
CHEMOKINE DOSE (ng/ml)
C
CXCR4
CCR5
P3X63
CELL NUMBER
MEAN FLUORESCENCE INTENSITY

3.2.2. Transient Transfection of Jurkat T-Cells

Jurkat T-cells should be maintained according to the procedure described in **Subheading 3.1.1** (*see also* **Note 6**)**.** Cells can be transfected between 18 and 30 h after passage. First, cells should be washed thoroughly with chilled serum-free medium to remove traces of serum, which reduce the transfection efficiency by electroporation. Cells should then be counted and resuspended at 40×10^6 cells/mL in ice-cold serum-free Optimem medium.

Samples of 500 µL of resuspended cells (20×10^6 cells) are then distributed into 0.5-mm-wide electroporation cuvets and subjected to an electroporation pulse (280 V, 1200 µF), conditions that yield around 30 ms of pulse time in a GenePulser Biorad electroporator (other conditions are available for other electroporators, and conditions should be accordingly adjusted). After the pulse, the cells should be seeded in RPMI 1640 medium supplemented with 10% FCS and antibiotics. Then, 20–40 h after the pulse, the cells should be harvested, and actin polymerization can be analyzed. This may include chemokine treatments, triggering with antibodies or pretreatment with blockers, and so forth, as described in **Subheadings 3.1.3.** and **3.1.4.**).

3.2.3. Fixation, Permeabilization, and F-Actin Staining

The FPS buffer provides an excellent tool for achieving a complete stop of the actin polymerization machinery as well as simultaneous F-actin staining. However, FPS buffer results in extraction of the GFP tag of most signaling intermediates tested, thus impeding the following of transfected cells and comparison

---

Fig. 2. (*opposite page*) Kinetics profile and dose-dependent effect of the chemokines SDF-1α and RANTES in the induction of actin polymerization in Jurkat T-cells. (**A**) Kinetics study. The cells were treated for the indicated times with 100 ng/mL of SDF-1α or 10 ng/mL of RANTES, stained for F-actin, and the levels of F-actin were measured by flow cytometry as described in the text. Although a direct representation employing arbitrary fluorescence units may be used, this example shows a correction consisting of the division of each value by the mean of the fluorescence corresponding to untreated cells ($t = 0$); then, increments are represented as fold induction. Data represent the mean ± SD of three independent experiments performed by triplicate. (**B**) Dose–response study. Jurkat T-cells were treated for 15 s with the indicated dose of the chemokines SDF-1α and RANTES, fixed, and stained for F-actin as earlier. This example shows bar plots with the correction applied in (**A**). Data represent the mean ± SD of three independent experiments performed by triplicate. (**C**) Expression of the chemokine receptors CXCR4 and CCR5 on Jurkat T-cells. Staining of Jurkat cells was performed with monoclonal antibodies against CXCR4 (thick line), CCR5 (dotted line) and the levels of receptor expression determined by standard flow cytometry. The irrelevant antibody P3X63 (dashed line) was employed as a control.

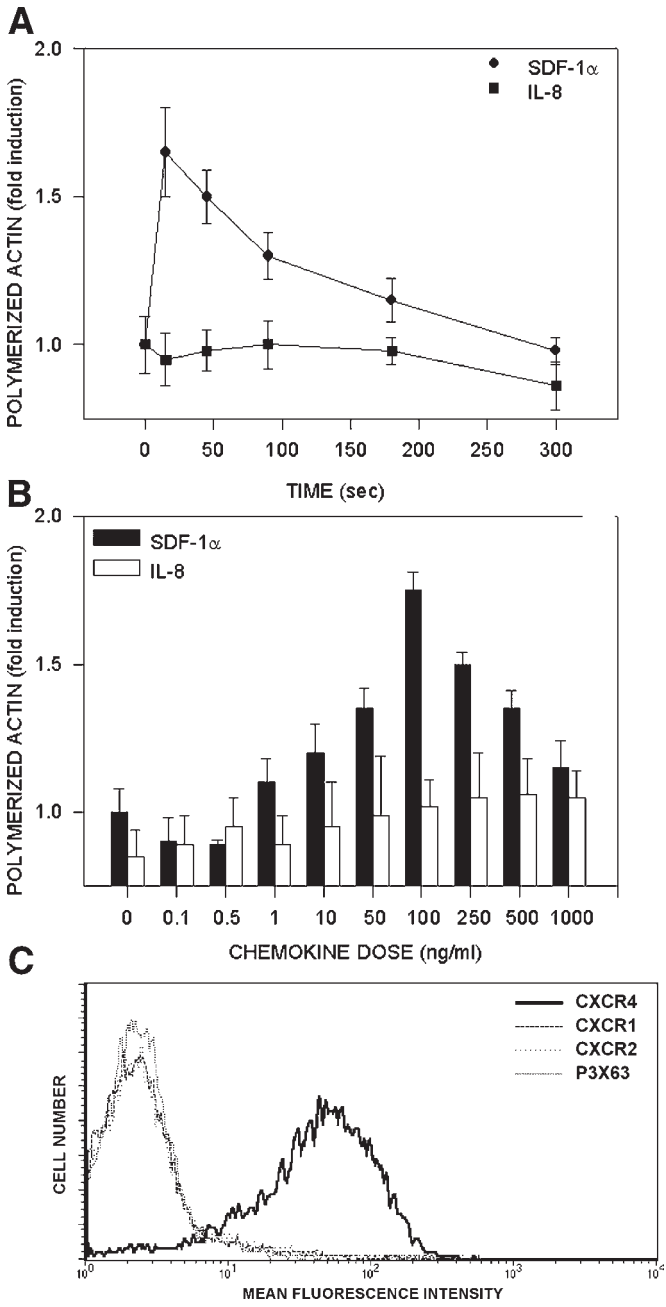
A
POLYMERIZED ACTIN (fold induction)
2.0
1.5
1.0
SDF-1α
IL-8
0
50
100
150
200
250
300
TIME (sec)
B
POLYMERIZED ACTIN (fold induction)
2.0
1.5
1.0
SDF-1α
IL-8
0
0.1
0.5
1
10
50
100
250
500
1000
CHEMOKINE DOSE (ng/ml)
C
CELL NUMBER
CXCR4
CXCR1
CXCR2
P3X63
MEAN FLUORESCENCE INTENSITY

with nontransfected cells. Therefore, when employing actin polymerization triggers such as chemokines, alternate protocols to bring actin polymerization to a halt at the desired moment must be employed. This includes ice chilling of the cells and fixation and permeabilization with specific buffers designed to protect the fluorescence of the cell, such as commercial lysis (CL) buffer from Becton Dickinson, which, although designed to lysate red blood cells, softly fixes and permeabilizes more resistant cells, such as lymphoid cells. Therefore, a suggested protocol consists of the addition of 200 µL of CL buffer to 100 µL of Jurkat cells and cooling of the tube with the cells in ice. The cells should be incubated for 15 min in ice with CL buffer and then washed with 500 µL of TBS. Then, F-actin staining should be performed by incubation for 30 min at 4°C with 150 n*M* Alexa-647-conjugated phalloidin in TBS (for FACScan® cytometers or other models not equipped with a second laser line, phycoerythrin–phalloidin may be employed, although compensations must be performed according to standard protocols). Final washout of the excess of staining should be performed with 500 µL of ice-cold TBS.

3.2.4. Measurement of the Levels of F-Actin by Flow Cytometry

Measurement of the levels of polymerized F-actin differs from the method described for nontransfected cells. First, a suitable acquisition screen comprising a forward scatter–side scatter (FSC-SSC) dot plot or density plot, a FL-1 histogram (for GFP detection) and a FL-4 histogram (for Alexa-647-phalloidin) should be prepared following CellQuest software manuals. If phycoerythrin is employed, the FL-4 screen should be replaced with a FL-2 histogram. Then, regions are selected, the first one a polygonal region in the FCS/SSC plot (R1), then subsequent regions in the FL-1 histogram according to the level of expression of the transfected protein, which usually bears a typical profile with a

---

Fig. 3. (*opposite page*) Kinetics profile and dose-dependent effect of the chemokines SDF-1α and IL-8 in the induction of actin polymerization in peripheral blood lymphocytes. Fresh human lymphocytes were isolated according to the text and the following assays were performed. (**A**) Kinetics study. The cells were treated for the indicated times with 100 ng/mL of SDF-1α or 10 ng/mL of IL-8, stained for F-actin, and the levels of F-actin were measured by flow cytometry as described in the text. Data represent the mean ± SD of three independent experiments performed by triplicate. (**B**) Dose–response study. Human PBL were treated for 15 s with the indicated dose of the chemokines SDF-1α and IL-8, fixed, and stained for F-actin as earlier. Data represent the mean ± SD of three independent experiments performed by triplicate. (**C**) Expression of the chemokine receptors CXCR4, CXCR1 and CXCR2 in PBLs. Staining of PBLs was performed with monoclonal antibodies against CXCR4 (thick line), CXCR1 (dashed line), and CXCR2 (spotted line) and the levels of receptor expression determined by standard flow cytometry. The irrelevant antibody P3X63 (dotted line) was employed as a control.

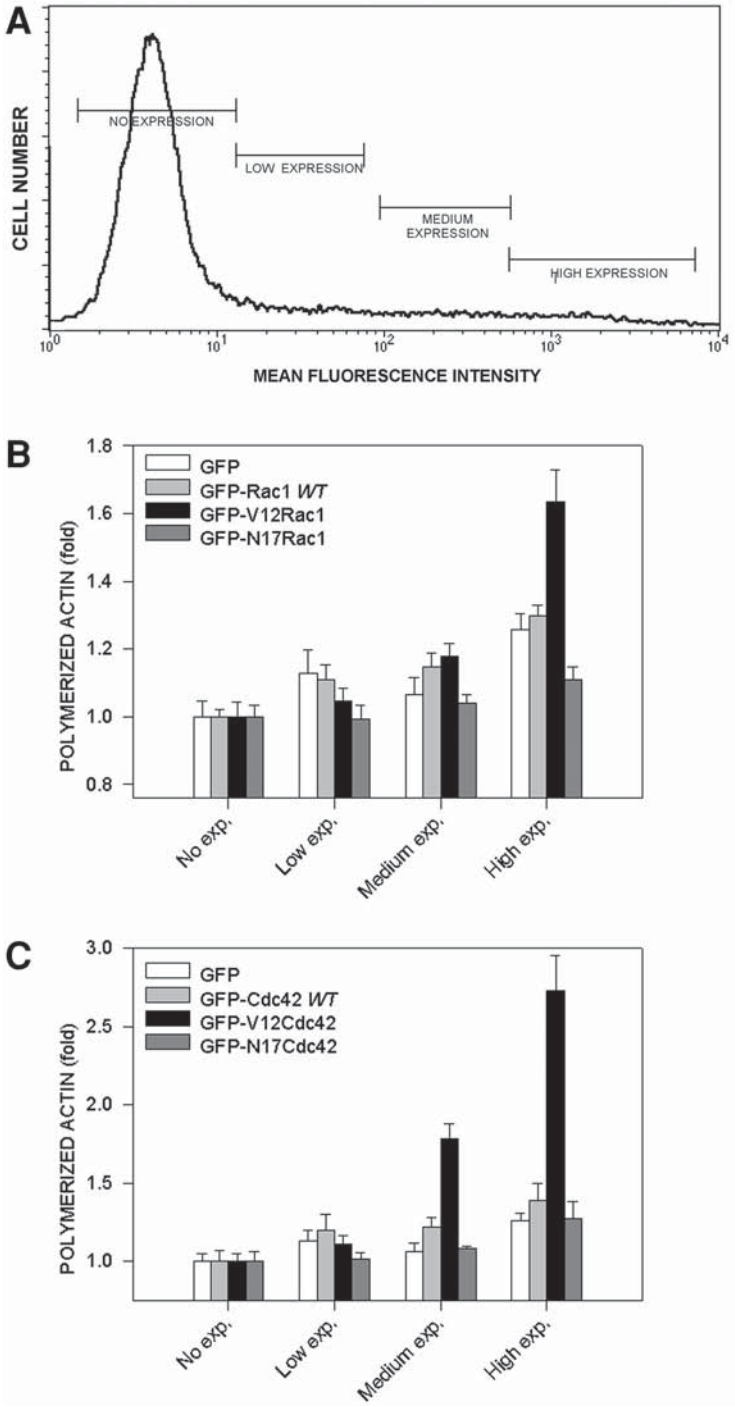
A
CELL NUMBER
NO EXPRESSION
LOW EXPRESSION
MEDIUM EXPRESSION
HIGH EXPRESSION
MEAN FLUORESCENCE INTENSITY
B
POLYMERIZED ACTIN (fold)
GFP
GFP-Rac1 WT
GFP-V12Rac1
GFP-N17Rac1
No exp.
Low exp.
Medium exp.
High exp.
C
POLYMERIZED ACTIN (fold)
GFP
GFP-Cdc42 WT
GFP-V12Cdc42
GFP-N17Cdc42
No exp.
Low exp.
Medium exp.
High exp.

large population of nontransfected cells with a long tail corresponding to increasing levels of expression of the GFP-tagged construct. A typical example is shown in **Fig. 4A**, in which four regions have been selected (R2–R5) corresponding to null (R2), low (R3), medium (R4), and high expression (R5). A minimum of 500 cells should be counted in each region for statistical significance.

Further analysis of the samples allows one to obtain means and GeoMeans for different levels of transfection in each case. Therefore, a semiquantitative correlation between expression of the GFP-tagged protein and the levels of polymerized actin can be established. To determine the levels of polymerized actin for a given level of GFP construct expression, analysis of FL-4 in an histogram plot is performed, in which the intersection between R1 and one of the regions selected in the FL-1 histogram plot are selected, which yields the level of polymerized F-actin corresponding to the analyzed degree of transfection (*see* **Note 7**). Data are usually represented in a bar plot with standard deviation, and common statistical analysis may be applied to these data (*see* **Note 8**).

4. Notes

1. Instead of FPS buffer, sequential fixation, permeabilization, and staining can be performed, but it is quite common to lose reproducibility in the duplicates because of manipulation of the tubes.
2. Because of the permeabilization procedure, it is not possible to examine the viability of the cells by propidium iodide in the same sample. Therefore, viability should be examined in separate, fresh samples of cells.
3. The procedure outlined in **Subheading 3.1.6.** employs CellQuest software in Becton Dickinson equipment; appropriate modifications should be performed for measurement in other hardware/software combinations.

Fig. 4. (*opposite page*) Effect of the overexpression of wild-type forms, activated and dominant negative mutants of the small GTPases Rac1 and Cdc42 coupled to GFP in the levels of F-actin in Jurkat T-cells. Jurkat T cells were transfected according to the protocol described in **Subheading 3.2.2.** and assayed for polymerized F-actin. Data represent the results of three independent experiments performed by triplicate. (**A**) FL-1 (green fluorescence) histogram representing the regions selected for analysis of polymerized F-actin. Regions corresponding to undetectable, low, medium, and high expression are shown. (**B**) Effect of GFP-Rac1 mutants in F-actin polymerization. GFP, green fluorescent protein; Rac1 WT, wild-type (non-mutated) form; V12Rac1, active mutant form; N17Rac1, dominant negative form. (**C**) Effect of GFP-Cdc42 mutants. GFP, green fluorescent protein; Cdc42 WT, wild-type (nonmutated) form; V12Cdc42, active mutant form; N17Cdc42, dominant negative form.

4. If the fluorescence bleaches during measurement in the flow cytometer, keep the cells at 4°C and in the dark JUST before acquisition. However, this step should not be necessary in normal laboratory conditions.
5. If an antibody against the specific receptor is available, it is quite interesting to show its levels in parallel to establish a correlation between the levels of chemokine receptor and the response. An example is shown in **Figs. 2C** and **3C**.
6. It is important to remember that other gene-transfer protocols, such as liposome-based protocols may be employed for the transfection of the cells with similar (although usually less) efficiency than electroporation.
7. As for transfected cells (*see* **Suhheading 3.2.4.**), it is possible to limit the measurement of actin polymerization to selected subpopulations by double staining with specific antibodies. This is quite useful when measuring actin polymerization in different subpopulations of peripheral blood lymphocytes. Typical subpopulations can be isolated by costaining with antibodies against CD3 (total T-lymphocytes), CD4 (helper T-lymphocytes), CD8 (cytotoxic T-lymphocytes), CD19 (B-lymphocytes), CD16 (natural killer [NK] cells), CD14 (monocytes), and so forth. Typical combinations of fluorochromes include phalloidin conjugated to FITC and antibodies to phycoerythrin or APC or vice versa. When performing these experiments, it should be taken into account that the FITC–phycoerythrin combination requires compensation between the FL-1 and FL-2 detectors, whereas the FITC–APC combination does not, although this procedure requires a second laser line (at 635 nm) and a FL-4 detector.
8. The main reason why these experiments are so precise and reproducible is because they include an excellent internal control that is provided by nonexpressing cells, which have been subjected exactly to the same conditions as the transfected, GFP-expressing cells. Therefore, it is strongly recommended to employ this system, which, in addition, employs mixed populations, to other theoretically more accurate systems, such as the employment of stable transfectants.

Acknowledgments

This work was supported by grants SAF99-0034-CO2-01 and 2FD97-0680-CO2-02 from the Ministerio de Ciencia y Tecnología, and QLTR-1999-01036 from the European Community to Dr. Sánchez-Madrid.

References

1. Butcher, E. C. and Picker, L. J. (1996) Lymphocyte homing and homeostasis. *Science* **272,** 60–66.
2. Ansel, K. M. and Cyster, J. G. (2001) Chemokines in lymphopoiesis and lymphoid organ development. *Curr. Opin. Immunol.* **13,** 172–179.
3. Von Andrian, U. H. and Mackay, C. R. (2000) T-Cell function and migration. Two sides of the same coin. *N. Engl. J. Med.* **343,** 1020–1034.
4. Worthylake, R. A. and Burridge, K. (2001) Leukocyte transendothelial migration: orchestrating the underlying molecular machinery. *Curr. Opin. Cell Biol.* **13,** 569–577.

5. Brown, M. J., Hallam, J. A., Colucci-Guyon, E., and Shaw, S. (2001) Rigidity of circulating lymphocytes is primarily conferred by vimentin intermediate filaments. *J. Immunol.* **166,** 6640–6646.
6. Bear, J. E., Krause, M., and Gertler, F. B. (2001) Regulating cellular actin assembly. *Curr. Opin. Cell Biol.* **13,** 158–166.
7. Cooper, J. and Schafer, D. (2000) Control of actin assembly and disassembly at filament ends. *Curr. Opin. Cell Biol.* **12,** 97–103.
8. Small, J. V., Rottner, K., and Kaverina, I. (1999) Functional design of the actin cytoskeleton. *Curr. Opin. Cell Biol.* **11,** 54–60.
9. Volkmann, N. and Hanein, D. (2000) Actomyosin: law and order in motility. *Curr. Opin. Cell Biol.* **12,** 26–34.
10. Moser, B. and Loetscher, P. (2001) Lymphocyte traffic control by chemokines. *Nat. Immunol.* **2,** 123–128.
11. Horuk, R. (2001) Chemokine receptors. *Cytokine Growth Factor Rev.* **12,** 313–335.
12. Thelen, M. (2001) Dancing to the tune of chemokines. *Nat. Immunol.* **2,** 129–134.
13. Mellado, M., Rodríguez-Frade, J. M., Mañes, S., and Martínez-A, C. (2001) Chemokine signaling and functional responses: the role of receptor dimerization and TK pathway activation. *Annu. Rev. Immunol.* **19,** 397–421.
14. Dancker, P., Low, I., Hasselbach, W., and Wieland, T. (1975) Interaction of actin with phalloidin: polymerization and stabilization of F-actin. *Biochim. Biophys. Acta* **400,** 407–414.
15. Vandekerckhove, J., Deboben, A., Nassal, M., and Wieland, T. (1985) The phalloidin binding site of F-actin. *EMBO J.* **4,** 2815–2818.
16. Bleul, C. C., Fuhlbrigge, R. C., Casasnovas, J. M., Aiuti, A., and Springer, T. A. (1996) A highly efficacious lymphocyte chemoattractant, stromal cell-derived factor 1 (SDF-1). *J. Exp. Med.* **184,** 1101–1109.
17. Vicente-Manzanares, M., Cabrero, J. R., Rey, M., Pérez-Martínez, M., Itoh, K., and Sánchez-Madrid, F. (2002) Activation of the Rho-Rho-kinase pathway by the chemokine SDF-1α: a role for p160ROCK in the maintenance of lymphocyte morphology and migration. *J. Immunol.* **168,** 400–410.
18. Roberts, A. W., Kim, C., Zhen, L., et al. (1999) Deficiency of the hematopoietic cell-specific Rho family GTPase Rac2 is characterized by abnormalities in neutrophil function and host defense. *Immunity* **10,** 183–196.
19. Ridley, A. J., Paterson, H. F., Johnston, D., Diekmann, D., and Hall, A. (1992) The small GTP-binding protein Rac regulates growth factor-induced membrane ruffling. *Cell* **70,** 401–410.
20. Nobes, C. and Hall, A. (1995) Rho, Rac and Cdc42 GTPases regulate the assembly of multimolecular focal complexes associated with actin stress fibers, lamellipodia and filopodia. *Cell* **81,** 52–62.
21. D'Souza-Schorey, C., Boettner, B., and Van Aelst, L. (1998) Rac regulates integrin-mediated spreading and increased adhesion of T lymphocytes. *Mol. Cell Biol.* **18,** 3936–3946.
22. Haddad, E., Zugaza, J. L., Louache, F., et al. (2001) The interaction between Cdc42 and WASP is required for SDF-1-induced T-lymphocyte chemotaxis. *Blood* **91,** 33–38.

23. del Pozo, M. A., Vicente-Manzanares, M., Tejedor, R., Serrador, J. M., and Sanchez-Madrid, F. (1999) Rho GTPases control migration and polarization of adhesion molecules and cytoskeletal ERM components in T lymphocytes. *Eur. J. Immunol.* **29,** 3609–3620.
24. Vicente-Manzanares, M., Montoya, M. C., Mellado, M., et al. (1998) The chemokine SDF-1alpha triggers a chemotactic response and induces cell polarization in human B lymphocytes. *Eur. J. Immunol.* **28,** 2197–2207.
25. Vicente-Manzanares, M., Rey, M., Jones, D., et al. (1999) Involvement of phosphatidylinositol 3-kinase in stromal-cell derived factor-1alpha-induced lymphocyte polarization and chemotaxis. *J. Immunol.* **163,** 4001–4012.

6

Evaluation of Rho Family Small G-Protein Activity Induced by Integrin Ligation on Human Leukocytes

Angela Gismondi, Fabrizio Mainiero, and Angela Santoni

1. Introduction

Integrin engagement by natural ligands or specific antibodies (Abs) initiates a series of intracellular signaling events that are important for regulating different cell functions, including migration, adhesion, proliferation, differentiation, apoptosis, and specific gene expression. A central role in the integrin-triggered signaling cascades is played by activation of the small GTP-binding proteins belonging to the Ras and Rho families ***(1–3)***.

The Rho family small GTP-binding proteins include Rho, Rac, and Cdc42 members that are implicated in a wide spectrum of cellular processes, including cytoskeletal organization, cell adhesion, cell polarity, cell motility, and transcriptional activation ***(4,5)***. Like members of the Ras family, Rho family GTPases cycle between a GDP-bound (inactive) state and a GTP (active) state. These GTPases in their active state are capable of connecting extracellular signals to a large number of downstream effectors. Recently, a biochemical assay to evaluate the activation state of Rho family small G-proteins has been described; this assay takes advantage of the ability of some downstream effectors to specifically bind to the GTP, but not to the GDP forms of Rho family members ***(6,7)***. Among the downstream effectors endowed with this capability, there are members of the p21-activated kinase (Pak) family and, in particular, p65Pak that binds to both active Rac and Cdc42, and rhotekin that specifically binds to active Rho. p65Pak is a serine–threonine kinase whose activity is strongly enhanced upon interaction of its Cdc42/Rac interactive binding (CRIB) motif with GTP-bound Rac or Cdc42. Different from p65Pak, rhotekin does not contain a catalytic domain and specifically binds to the GTP-bound form of Rho through its Rho-binding region, termed Rho effector motif class 1 (REM-1).

From: *Methods in Molecular Biology, vol. 239: Cell Migration in Inflammation and Immunity*
Edited by: D. D'Ambrosio and F. Sinigaglia © Humana Press Inc., Totowa, NJ

The main focus of this chapter is to describe the GST-fusion protein-mediated pull-down assay employed to evaluate Rho GTPase activity in leukocytes upon integrin stimulation with natural ligands or specific antibody.

2. Materials

2.1. Preparation of Ab-Coupled Beads

1. 2.5-μm-Diameter polystyrene latex beads (product no. 1-2400; Interfacial Dynamics Corp., Portland, OR).
2. Carbonate buffer: 30 m*M* Na_2CO_3, 70 m*M* $NaHCO_3$, pH 9.5.
3. Purified monoclonal antibody (mAb) against α- and/or β-integrin subunits or adhesive proteins (such as extracellular matrix [ECM] components and their proteolytic fragments, or ICAM-1 or VCAM-1) in carbonate buffer or in phosphate-buffered saline (PBS). Avoid the use of any buffer or medium containing serum or bovine serum albumin (BSA), as they interfere with the binding procedures.
4. Formaldehyde 0.01% in PBS.

2.2. Cell Stimulation and Lysate Preparation

1. Polystyrene latex beads precoated with Ab against α- and/or β-integrin subunits or with adhesive proteins.
2. Lysis buffer 1% [v/v] Triton X-100, 0.1% Na deoxycholate, 1 m*M* EDTA, 1 m*M* EGTA, 150 m*M* NaCl, 1 m*M* phenylmethylsulfonyl fluoride (PMSF), 2 μg/mL aprotinin, 2 μg/mL leupeptin, 100 m*M* NaF, 1 m*M* Na_3VO_4, 50 m*M* $Na_4P_2O_7$ in 50 m*M* Tris-HCl, pH 7.5. Protease inhibitors should be freshly added.

2.3. Preparation of GST-Fusion Protein and Pull-Down Assay

1. pGEX transformant encoding for the following GST-C21-fusion protein containing the Rho-binding region of rhotekin that binds to active Rho A and Rho B; GST-PAK-fusion protein specific for active Rac1 and Cdc42. These pGEX transformants have been kindly provided by Dr. J. G. Collard (The Netherlands Cancer Institute, Amsterdam, The Netherlands).
2. Luria–Bertani (LB) medium: Add 10 g Bacto tryptone (Difco Lab., Detroit, MI, USA), 5 g Bacto yeast extract (Difco Lab.), and 10 g NaCl to 950 mL of deionized H_2O, mix until dissolved, adjust pH to 7.0 with 5 *N* NaOH, adjust the volume to 1 L with deionized H_2O, and sterilize for 20 min in an autoclave pump.
3. LB/ampicillin medium (LB plus 100 μg/mL ampicillin).
4. 100 m*M* Isopropyl-1-thio-β-D-galactoside (IPTG) (Sigma-Aldrich, St. Louis, MO, USA).
5. Bacterial lysis buffer: 50 m*M* Tris-HCl, pH 7.5, 1 m*M* EDTA, 100 m*M* NaCl, 5% glycerol, 0.1% Triton X-100, 1 m*M* dithiothreitol (DTT), 1 m*M* PMSF, 2 μg/mL aprotinin, 2 μg/mL leupeptin.
6. Glutathione–agarose beads (Pharmacia BioTech AB, Uppsala, Sweden).
7. Cell lysates.
8. GST-fusion protein bound to glutathione-coupled Sepharose beads.

9. GST-fish buffer: 50 m*M* Tris-HCl, pH 7.4, 1% NP-40, 10% glycerol, 100 m*M* NaCl, 2 m*M* $MgCl_2$, 1 m*M* PMSF, 2 μg/mL aprotinin, 2 μg/mL leupeptin.
10. SDS sample buffer: 60 m*M* Tris-HCl, 2% sodium dodecyl sulfate (SDS), 20% glycerol, 0.05% of a bromophenol blue sature solution, 2% β-mercaptoethanol, pH 6.8.
11. Additional reagents and equipment for SDS–polyacrylamide gel electrophoresis (SDS-PAGE).

2.4. Western Blotting

1. Transfer buffer: 25 m*M* Tris, 192 m*M* glycine, 20% methanol.
2. 0.45 μm Nitrocellulose membrane filter (Schleicher & Schuell, Dassel, Germany).
3. Ponceau S solution (0.5 % Ponceau S/1% acetic acid in H_2O).
4. PBS-T (PBS plus 0.05% [v/v] Tween-20).
5. Blocking solution (1–3% BSA or 5% nonfat dry milk in PBS-T).
6. Anti-RhoA mAb (cat no. sc-418) from Santa Cruz Biotechnology Inc. (Santa Cruz, CA); anti-Rho rabbit antiserum (cat no. 06-770), anti-Rac mAb (cat no. 05-389), and anti-Cdc42 mAb (cat no. 17-299) were from Upstate Biotechnology Inc. (Lake Placid, NY).
7. Enhanced chemiluminescence (ECL) kit (Amersham Biosciences).
8. Photographic equipment.

3. Methods

3.1. Preparation of Ab- or Protein-Coupled Beads

1. Wash 300 μL of polystyrene latex beads twice with the carbonate buffer, and incubate the beads with 30–60 μg of purified mAb or proteins, in 300–500 μL of carbonate buffer, for 30–60 min at room temperature under continuous agitation (*see* **Note 1**). Washing the beads can be easily performed in a microcentrifuge, in the pulse operation mode (by allowing it to achieve top speed and stopping after a few seconds).
2. Wash beads three times with PBS and resuspend them in 100 μL of PBS. Ab- or protein-bound beads can be sterilized and stored for up to 1 yr at 4°C. For this purpose, conjugated beads are incubated for 30 min at 37°C in 0.01% formaldehyde (1 mL) and washed extensively in sterile PBS (*see* **Note 2**).

3.2. Cell Stimulation and Lysate Preparation

1. Cells are first washed in RPMI 1640, Hank's balanced salt solution (HBSS), or equivalent medium free of fetal calf serum (FCS), resuspended in HBSS and aliquoted in different Eppendorf tubes so that each tube will contain 30×10^6 cells, and then centrifuged for 5 min at 500*g*.
2. Add 100 μL/tube of stimulating beads precoated with Ab or ECM proteins or ICAM-1 or VCAM-1 and allow incubation to proceed for the desired time period (from 1 to 30 min) at 37°C.
3. Add ice-cold PBS to stop the stimulation and centrifuge the cells for 5 min at 500*g*.

4. Decant washing buffer, add 600 µL of ice-cold lysis buffer, incubate for 5 min at 4°C, and then centrifuge cell lysates at 15,000*g* for 15 min at 4°C to remove insoluble material.

3.3. Preparation of GST-Fusion Protein

1. Inoculate a colony of the pGEX transformant into 100 mL of LB medium supplemented with 100 µg/mL of ampicillin and allow to grow for 12 h at 37°C in a shaking incubator.
2. Dilute this culture 1:10 into 1 L of LB/ampicillin medium and grow (for 1–3 h) at 37°C in a shaking incubator until the optical density (OD_{600}) reaches a value of 0.6–0.8.
3. Add 0.1 m*M* IPTG and incubate for 2–7 h at 37°C in a shaking incubator (*see* **Note 3**).
4. Centrifuge cultures in 250-mL bottles for 10 min at 5000*g* (5500 rpm on a Beckman JA-10 rotor) at room temperature. Discard supernatant and resuspend pellets in 10–20 mL ice-cold PBS.
5. Immerse the tube in ice and lyse cells using a probe sonicator (*see* **Note 4**).
6. Add Triton X-100 to 1% final concentration and then add the following protease inhibitors: 2 µg/mL aprotinin, 5 µg/mL leupeptin, 1 m*M* PMSF (*see* **Note 5**).
7. Centrifuge for 5 min at 10,000*g* (9500 rpm in a Beckman JA-20 rotor), at 4°C, to remove insoluble material.
8. Collect supernatants and pool them.
9. Add supernatant to 2.5 mL of 50% (v/v) glutathione–agarose beads in PBS and incubate for 1 h at 4°C in continuous agitation (*see* **Note 6**).
10. Wash the beads three times by adding 50 mL ice-cold PBS, mixing, and centrifuging 5 min at 1500*g*.
11. Resuspend the beads in 1–2 mL of ice-cold PBS and transfer to a 1.5-mL microcentrifuge tube (*see* **Note 7**).

3.4. Pull-Down of Small G-Proteins Using GST-Fusion Proteins

1. Distribute 20 µL of GST-fusion protein bound to glutathione-coupled Sepharose beads in 1.5-mL Eppendorf tubes (*see* **Note 8**).
2. Wash 300 µL of glutathione-coupled Sepharose beads whith PBS, resuspend in 1 mL of PBS, and add 100 µL to the tubes containing the GST-fusion protein (*see* **Note 9**).
3. Wash once more with PBS.
4. Add cell lysate (500 µL containing at least 500 µg total proteins) and incubate for 1 h at 4°C in continuous agitation (*see* **Note 10**).
5. Wash three times with GST-fish buffer and resuspend the pellet in 40 µL of SDS sample buffer, boil for 5 min, and then centrifuge for 2 min.
6. Load the supernatant into a gel lane and separate proteins by 12% SDS-PAGE.
7. As the loading control of the small G-protein, run 20–30 µL of total cell lysate (20–30 µg proteins).

3.5. Western Blotting

1. Following electrophoresis, equilibrate the gel in transfer buffer for 10 min at room temperature and transfer the proteins from SDS-PAGE gel to nitrocellulose membrane at 500 mA for 2–3 h or at 150 mA overnight at 4°C (*see* **Note 11**).
2. Transferred proteins can be visualized by staining the membrane for 5 min with Ponceau S solution (*see* **Note 12**).
3. Rinse excess stain with PBS-T, and place the blot into blocking solution (1–3% BSA in PBS-T or 5% nonfat milk). Allow the blot to block for 1 h at room temperature or overnight at 4°C with agitation.
4. Decant the blocking solution and rinse the membrane using two changes of washing buffer (PBS-T). Then, wash once for 10 min and three times for 5 min with fresh changes of the washing buffer at room temperature with agitation.
5. Add the primary Ab appropriately diluted in PBS-T (i.e., anti-Rac mAb [1 : 1000], anti-Cdc42 [0.5–1 μg/mL], anti-Rho [2 μg/mL]). Incubate with agitation for at least 1 h at room temperature or overnight at 4°C (*see* **Note 13**).
6. Decant the primary Ab solution and wash the membrane as detailed in **step 5**.
7. Decant the washing buffer and add the enzyme- (i.e., horseradish peroxidase) conjugated anti-mouse or anti-rabbit Ig, appropriately diluted in PBS-T plus 1% BSA. Incubate with agitation for 45 min or 1 h at room temperature (*see* **Note 14**).
8. Decant the secondary Ab solution and wash the membrane as detailed in **step 5**.
9. Detect immunoreactivity using an enhanced chemiluminescence kit (i.e., Amersham Internetional plc, Amersham, UK) according to the instructions (*see* **Note 15**).
10. The blot can be stripped with 62.5 m*M* Tris-HCl (pH 6.8), 2% SDS, and 100 m*M* β-mercaptoethanol at 50°C for 30 min, washed three times with large amounts of PBS-T, blocked as described in **step 4**, and reprobed (*see* **Note 16**).

4. Notes

1. The exact incubation time and amount of Ab or protein needed for optimal bead conjugation can be varied between the limits cited. The amount of Ab bound to the beads can be monitored by fluorochrome-conjugated secondary Ab staining and flow cytometric analysis.
2. Natural ligands, such as extracellular matrix components, are preferably used shortly after conjugation to the beads.
3. To improve the yield of fusion protein, the growth condition can be optimized by delaying the addition of IPTG or altering the induction period. If the activity and stability of the fusion protein is not altered during the growth of the bacteria, the yield may be improved by increasing the induction period. By contrast, if the stability of the fusion protein is altered during the growth of the bacteria, the yield can be improved by adding IPTG when the culture is denser and/or by decreasing the induction times.
4. Because excessive sonication can result in contamination of purified fusion protein with bacterial proteins, cell lysis must occur in 30 s; sonication time can be adjusted by varying the frequency and intensity of sonication. Bacterial cell lysis

can be also monitored controlling the color of the cell suspension, which is brown when cells are intact, but changes to gray-brown when cells are lysed.

5. Detergent (Triton X-100) is generally added to the cell lysate to prevent the association of the fusion protein with bacterial proteins and, thus, to reduce the contamination of the fusion protein. Addition of protease inhibitors (i.e., aprotinin, PMSF, and leupeptin) to the lysis buffer may help to increase the stability of fusion protein and to reduce its degradation in small fragments capable of binding to glutathione beads, which can contaminate the fusion protein preparation.
6. One milliliter of glutathione–agarose beads can bind ≥8 mg of protein.
7. To control the amount and purity of the fusion protein obtained, aliquots corresponding to 5, 10, 25, 50, and 100 μL of the final fusion protein suspension and different doses of BSA (ranging from 2 to 20 μg used as standard) can be loaded in a 10% polyacrylamide gel. The gel can be fixed and stained with Comassie blue. The yield of the fusion protein can vary from 1 to 5 mg/L.
8. The amount of GST-fusion protein used for pull-down assay can vary depending on the cell type used; thus, the optimal working concentration should be determined for each particular system.
9. Unconjugated glutathione beads were added to increase the total volume of the pellets in order to facilitate manipulation.
10. Pull-down assay must be performed in a very short time to avoid inactivation of the small G-protein. However, to obtain good results, the incubation time of cell lysates with the GST-fusion protein should be determined, as it can vary depending on the cell system used.
11. Use gloves when manipulating filter papers, gels, and nitrocellulose because oil from hands blocks the transfer to the nitrocellulose paper. Transfer time is dependent on the thickness of the gel and the size of the protein being transferred. In general, small G-proteins are transferred within 1–6 h, but high-molecular-weight molecules may take longer. Overnight transfer is reliable and convenient.
12. If air bubbles are trapped between the filter and the gel, they will appear as clear white spots on the filter after blotting and staining. Take extra care to ensure that all bubbles are removed.
13. Dilution of primary Ab required to give optimal results will vary and should be determined for each Ab used.
14. Do not include sodium azide in any solution containing horseradish peroxidase-labeled reagents, as it can induce an irreversible inactivation of horseradish peroxidase.
15. The presence of multiple bands in the blot may be related to excessive amount of lysate, protein degradation, or nonspecific binding by the primary or secondary Ab. Excessive or diffuse signal may be related to too much protein on the gel, excess of primary Ab, or to overexposure. No signal or weak signal may be the result of inadequate transfer of proteins, horseradish peroxidase inactivation, or a low amount of protein.
16. Following stripping, incubate the membrane with ECL detection reagents and expose to the film to ensure removal of Ab.

References

1. Clark, E. A. and Brugge, J. S. (1995) Integrins and signal transduction pathways: the road taken. *Science* **268,** 233–239.
2. Giancotti, F. and Ruoslahti, E. (1999) Integrin signaling. *Science* **285,** 1028–1032.
3. Mainiero, F., Soriani, A., Strippoli, R., et al. (2000) Rac1/p38 MAPK signalling pathway controls β1 integrin-induced interleukin-8 production in human natural killer cells. *Immunity* **12,** 7–16.
4. Symons, M. and Settleman, J. (2000) Rho family GTPases: more than simple switches. *Trends Cell Biol.* **10,** 415–419.
5. Hall, A. (1998) Rho GTPase and the actin cytoskeleton. *Science* **279,** 509–514.
6. Sander, E. E., van Delft, A., ten Klooster, J. P., et al. (1998) Matrix-dependent Tiam1/rac signalling in epithelial cells promotes either cell–cell adhesion or cell migration and is regulated by phosphatidylinositol 3-kinase. *J. Cell Biol.* **143,** 1385–1398.
7. Reid, T., Bathoorn, A., Ahmadian, M. R., and Collard, J. G. (1999) Identification and characterization of hPEM-2, a guanine nucleotide exchange factor specific for Cdc42. *J. Cell Biol.* **274,** 33587–33593.

7

Reconstructing Leukocyte Migration in 3D Extracellular Matrix by Time-Lapse Videomicroscopy and Computer-Assisted Tracking

Peter Friedl and Eva-B. Bröcker

1. Introduction

The quantification of cell migration within three-dimensional (3D) extracellular matrix has become an important tool to investigate how cells integrate molecular events into higher-order adhesion and positioning within the tissue. Because most processes in vivo occur within 3D tissues rather than on two-dimensional (2D) surfaces, modern 3D tissue-based culture systems have been developed to mimick aspects of in vivo-like scaffolding and reconstruction of cell adhesion and motility, cell patterning, and cell–cell communication ***(1–4)***.

Three-dimensional extracellular matrix (ECM)-based cell culture models have been used to analyze the path structure of locomoting T-lymphocytes ***(5)*** for real-time analysis of effects exerted by activating factors, such as chemokines ***(6)***, as well as the invasive migration of tumor cells ***(7)***. Recently established more complex bicellular ECM culture systems have provided insights into basic aspects of immune cell interactions, such as T-cell contacts with antigen-presenting cells ***(8,9)***. Furthermore, combining 3D ECM culture systems with living tissue explants allows the reconstruction of multicellular dynamics involved in cancer cell invasion and motility ***(10)***, angiogenic sprouting, and wound healing.

Common to all of these applications is that the cells are incorporated within a transparent 3D extracellular matrix to be monitored by time-lapse videomicroscopy and quantitative real-time data assessment. This chapter will outline the procedures for the generation of 3D collagen matrix cultures and give an introduction

From: *Methods in Molecular Biology, vol. 239: Cell Migration in Inflammation and Immunity*
Edited by: D. D'Ambrosio and F. Sinigaglia

to time-lapse videomicroscopy and computer-assisted approaches to quantify cell motility, cellular morphodynamics, and cell–cell interaction. Here, we emphasize the analysis of leukocytes, such as T-lymphocytes, but will also comment on other cell types, such as tumor cells and fibroblasts.

2. Materials

1. Glass object slides and standard glass cover slips.
2. Paraffin (Tissue Prep; Fisher, Fair Lawn, NJ, USA).
3. Vaseline.
4. Dulbecco's modified Eagle's medium (DMEM) or other medium appropriate for a given cell type; may contain serum and antibiotics.
5. 10X Concentrated minimal essential Eagle's medium (MEM) (Flow Laboratories, McLean, USA) or other 10X concentrated medium.
6. 7.5% Sodium bicarbonate solution (Life Technologies).
7. Collagen stock solution, 3.0 mg/mL, acidified (e.g., bovine dermal collagen [Vitrogen, Nutacon BV, Leimniden, NL] or rat tail collagen [Becton Dickinson]).
8. Inverted tissue culture light microscope; for controlled experiments on primary cells, at least two independent microscopes are required.
9. CCD camera mounted onto the microscope.
10. A black container that includes an upper transparent window for microscopy and an open bottom side (*see* **Fig. 1D**). This container is placed onto the microscope stage on top of the migration chamber, providing stable temperature and lightning conditions.
11. One independent video recorder for each microscope unit; alternatively, computerized image acquisition via frame grabber and image grabbing software can be used.
12. Cell-tracking computer equipped with audiovisual (AV) input and frame grabber (video card) for video overlay to the tracking software; in the case of digital image acquisition, no additional hardware is required.
13. Cell-tracking software that allows the determination of *x*- and *y*-position of moving objects (cells) from step to step from computerized image sequences. Several commercial packages are available for cells on 2D surfaces. For cell populations moving within 3D collagen matrices, most reliable results will be obtained from semiautomated computer-assisted cell tracking (*see* **Notes 1** and **2**).

3. Methods

3.1. Construction of Migration Chamber

1. Wax consisting of equal amounts of vaseline and paraffin is melted on a heating plate (100°C).
2. Three lanes of melted wax are applied with a small brush onto the glass slide, forming an open rectangle (*see* **Fig 1A**). The height should be approx 350–800 µm. To standardize chamber dimensions, a flat plastic or metal template of defined height can be laid onto the glass side. The wax is then applied around the template. Wax exceeding the predefined template height is removed using a razor blade.

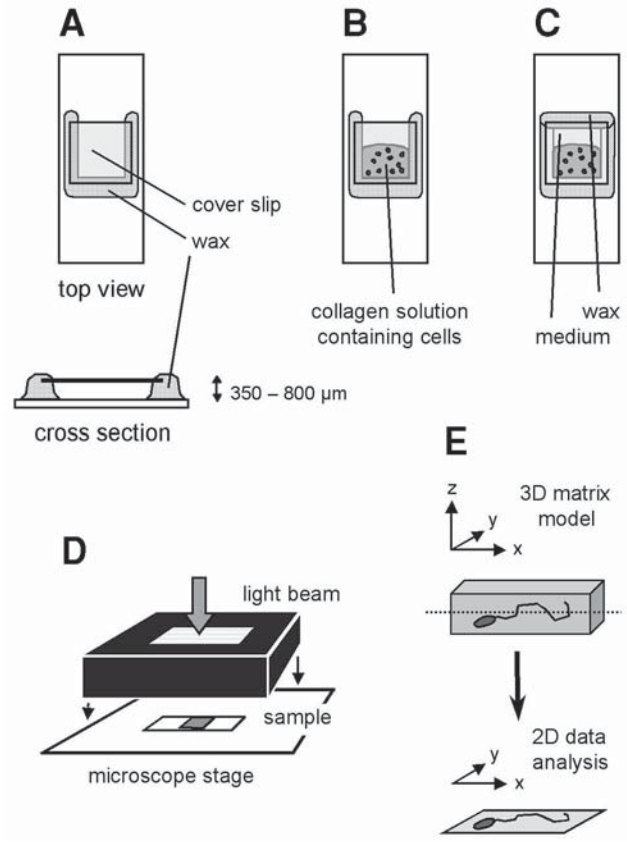

Fig. 1. Construction and positioning of migration chamber for time-lapse videomicroscopy: (**A–C**) construction and loading of the migration chamber for 3D collagen matrix culture; (**D**) position of migration chamber and container on the microscope stage; (**E**) extensions of the 3D matrix culture and data reduction by 2D cell tracking.

3. Overlay with glass cover slip and seal the top edge of the cover slip by one or two more layers of melted wax (*see* **Fig. 1A**). The migration chamber is open on one side (*see* **Note 3**).

3.2. Setup of 3D Collagen Cultures

1. Cells (e.g., 2×10^5) from suspension culture, such as T-lymphocytes and neutrophils, are collected, washed once or twice, and resuspended in 450 µL of medium used for ECM culture (*see* **Note 4**). Adherent cells, such as monocytes and many tumor cells, should be detached by EDTA (concentration at 2 m*M*, 2–5 min, 37°C), washed twice, and resuspended in medium (*see* **Note 5**).
2. Add 10X MEM (100 µL) to sodium bicarbonate (50 µL) in a small sterile tube. Indicator color changes from yellow (acidic) to purple (basic).

3. Add cell-free collagen stock solution (750 µL) and mix until homogenous slightly purple color is obtained. Avoid air bubbles while mixing (*see* **Note 6**).
4. Add cell suspension in medium (450 µL) and mix until homogenous bright pink color is reached. Again, avoid generating air bubbles. The pH should now be 8.0.
5. Hold the migration chamber in a vertical, upright position. Add the cell-containing collagen solution into the migration chamber until the chamber is one-third to two-thirds filled (*see* **Fig. 1B**).
6. Place the migration chamber in an upright position into the incubator (37°C, 5% CO_2, 15–30 min) for collagen polymerization and equilibration of the gas conditions (*see* **Note 7**). The final pH should be 7.4–7.5.
7. Fill the chamber with warm and previously equilibrated medium. This medium can contain chemokines or other factors, such as antibody or pharmacological inhibitors.
8. Seal the migration chamber by an additional lane of wax (*see* **Fig. 1C**). If a commercially available climatized incubator is used with the videomicroscope, **steps 1–6** can be modified for ECM culture in conventional Petri dishes or microtiter plates.

3.3. Time-Lapse Video or Digital Microscopy

1. The microscope stage should be warmed to 37°C for approx 30 min before the experiment. The temperature stage control can be a commercial chamber system provided by most microscope manufacturers. Alternatively, a remote temperature control including a flexible temperature sensor and heating device can be used.
2. Place the migration chamber containing the polymerized collagen in the horizontal position onto the microscope stage (*see* **Fig. 1D**). For controlled investigation and improved reproducibility of different parameters (e.g., plus/minus chemokine) in primary cells, the simultaneous setting up of at least two independent units (*see* **Fig. 2**) should be preferred to sequential imaging using a single unit. Alternatively, a motorized stage and image acquisition system can be used on a single microscope for multichannel recording using independent cultures in one micro-titer plate.
3. If a flexible temperature control sensor is used, position the sensor in direct proximity to the migration chamber and fix it with paraffin for reliable physical contact to the sample.
4. The black container is placed on the microscope stage and the transparent top surface is adjusted to the light beam of the microscope and sample position (*see* **Fig. 1D**).
5. Adjust the *z*-position of the stage by focusing through the sample from bottom to top and reverse (*see* **Note 8**). For recording, a *z*-position in the middle of the lattice should be used (*see* **Fig. 1E**). Cells in focus appear as small, sharp, gray objects. Cells below the in-focus level are large and dark and display a blurred boundary. Cells above the in-focus level are large and display a white center and a blurred black boundary (*see* **Figs. 2** and **3**).
6. Adjust the microscope condensor width (should be small) in order to detect as many cells as possible from different *z*-positions within the lattice. Ideally, at a small enough condensor width, all cells at different *z*-positions can be visualized (*see* **Fig. 3**).

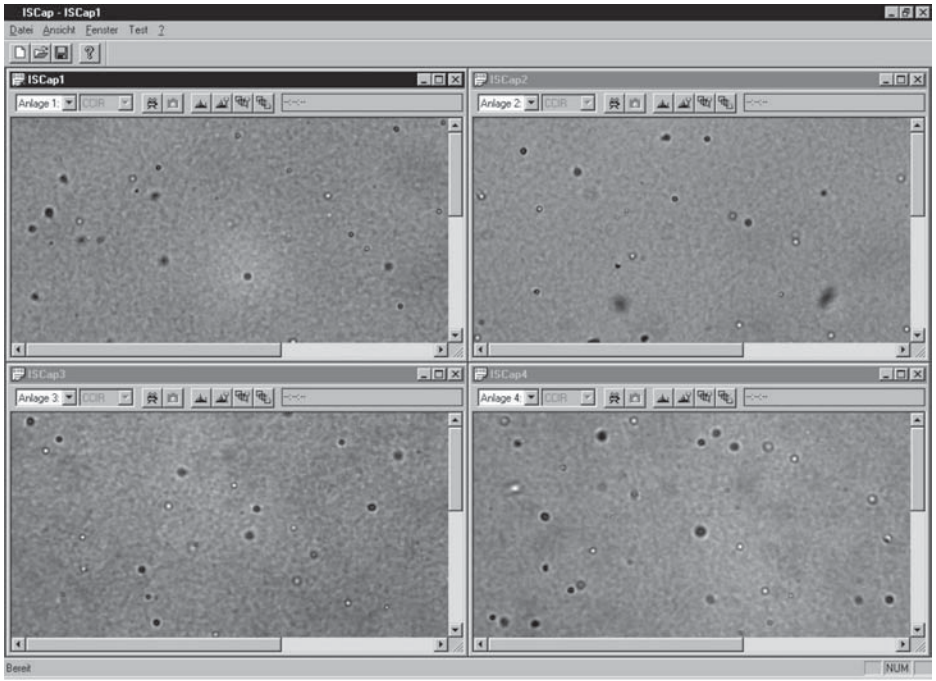

Fig. 2. Digital time-lapse microscopy by simultaneous image acquisition from up to four independent microscopes. The minimum frame rate for this setting is one per second. The example shows $CD4^+$ cells in 3D collagen cultures.

7. Preselect the time-lapse recording mode, depending on the migration speed of a given cell type (*see* **Table 1**) and start image acquisition. Alternatively, digital image acquisition using a frame grabber can simultaneously collect sequences from up to four independent microscopes (*see* **Fig. 2**).
8. The recommended duration for videomicroscopy varies depending on the cell type examined and the expected kinetics of the biological response (*see* **Note 9**). Leukocyte migration experiments on, for example, chemokine functions usually last from 30 to 240 min (*see* **Figs. 4** and **5**). Tumor cells may be monitored for 8–48 h ***(11)*** and explant cultures for up to 4 wk ***(12)***.
9. After the migration experiment, the extensions of the field of view (micrometers) relative to the resolution of the digital image (pixels) are calibrated. Record the inner quadrats of a cell-counting chamber (Neubauer) for some seconds at the same magnification used for the migration experiment (*see* **Subheading 3.4.**, **step 9**).

3.4. Computer-Assisted Cell Tracking

1. Load the video or digital recording into the cell-tracking computer.

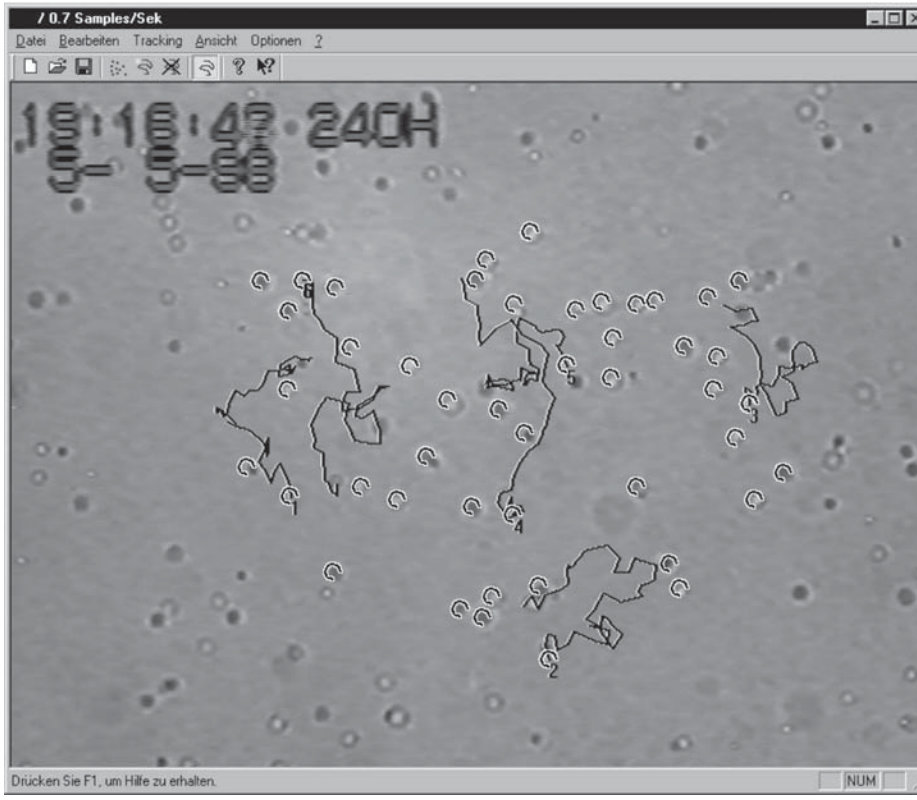

Fig. 3. Screen shot of cell tracking window containing $CD4^+$ T-cells in 3D collagen lattice. Cells were selected prior to tracking of the cell paths (open circles). Six paths are shown after semiautomated tracking (*see* **Notes 1, 2,** and **10**).

2. Load the first frame of the movie and preselect the cells to be analyzed (*see* **Fig. 3**, open circles). For a nonbiased assessment of cell migration, *all* cells within a representative field of view irrespective of their migration status, polarity, and *z*-position within the lattice should be analyzed (*see* **Note 11**). For statistical analysis, an average of 25–40 cells per experiment is sufficient.
3. Define the time interval from step to step in the "time window" of the tracking software, corresponding to the appropriate step interval in real time. This parameter depends on the acceleration factor of the time-lapse mode (*see* **Table 1**). To calculate the step interval, measure first the duration (in seconds) of time-lapse playback of 1 h in real time. Divide this value by 60, yielding the tracking interval (in seconds) for data collection from a step interval of 1 min real time. As an example, 1-h playback of a 240-h time-lapse video recording will last 45 s. After division by 60, a step interval of 0.75 s is obtained for automated *x*/*y* data acquisition at 1-min intervals.

Table 1
Time-Lapse Videomicroscopy and Time Interval for Cell Tracking of Different Cell Types

Cell type	Average velocity (μm/min)	Time-lapse mode: Video recording (mode)	Time-lapse mode: Digital recording[a] step interval
Fibroblast	0.1–0.2	960 h (+ 72 h)[b]	7 min
Tumor cell	0.2–0.5	960 h (+ 24 h)	5 min
Dendritic cell	1–4	480 h	1 min
T-Lymphocyte	4–18	240 h	15–20 s

[a]Play back at 10 frames/s.

[b]The 240-h or 960-h recording mode of a time-lapse videorecorder represents the duration a 3-h video tape can accommodate in time-lapse mode, corresponding to a respective 80- or 320-fold acceleration of movements compared to real time. For further acceleration of slow movements in fibroblasts and tumor cells, the time-lapse movie can be recorded a second time in time-lapse mode using a second video recorder.

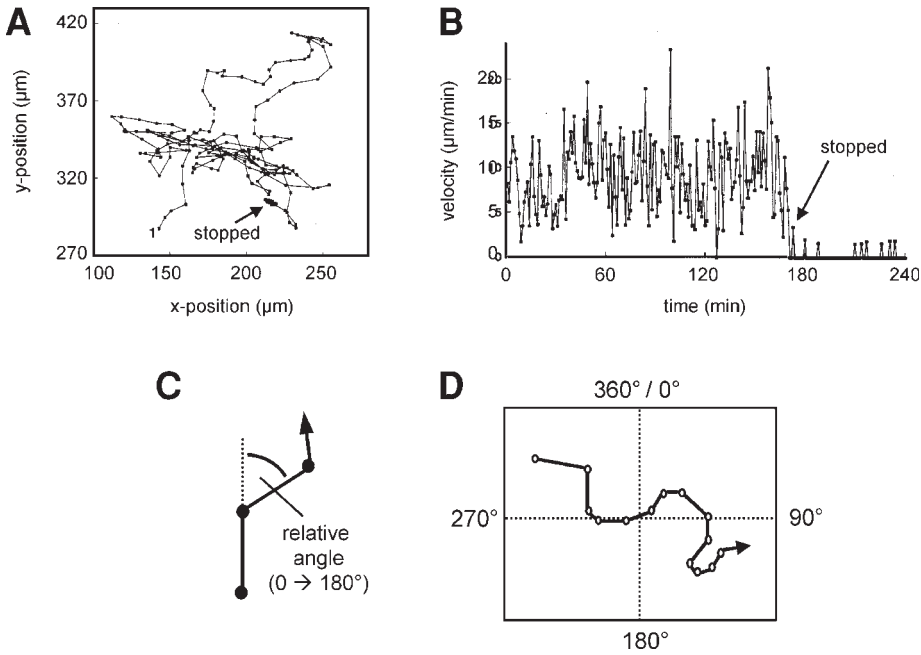

Fig. 4. Export function of data for reconstruction of migration path (**A**), time-dependent velocity (**B**), relative step angles (**C**), and absolute angles (directionality) (**D**).

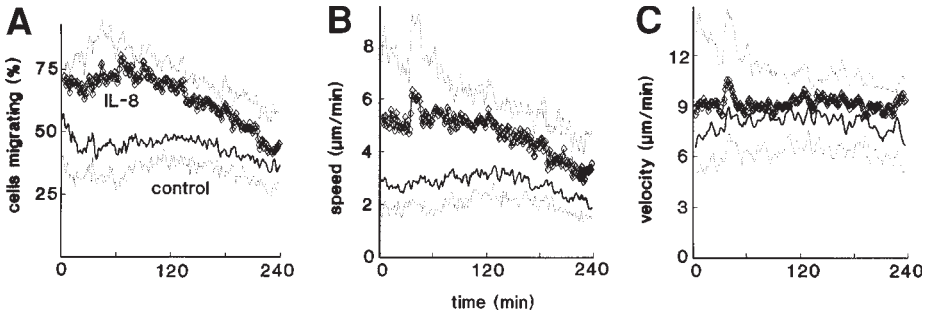

Fig. 5. Time-dependent representation of the number of migrating cells (**A**), the population speed (**B**) (containing stops), and velocity (**C**) (excluding stops, hence representing the actual step lengths upon migration). $CD4^+$ cells were monitored in the presence or absence of interleukin (IL)-8 (20 ng/mL). Data represent the means ± SD for three independent experiments (in total, 120 cells).

4. Start the movie playback a few frames before the onset of time-lapse recording and start the tracking routine at frame 1 with a mouse click.
5. Follow the center of the cell with the cursor via computer mouse or a track ball while the cell is moving (*see* **Notes 1** and **12**). In nonmoving cells yet oscillating cells ("running on the spot"), the cursor should not be moved. In the background, the computer automatically collects the respective *x*- and *y*-positions at the predefined step interval (*see* **step 3**).
6. The end of the track is determined by a second mouse click. The path can now be displayed (*see* **Fig. 3**).
7. Return the movie to the start and track cell number 2. Repeat **steps 4–6** for each cell.
8. After tracking of the predefined population, export the pixel data as an ASCII file for further data analysis by a spreadsheet (e.g., Microsoft Excel® or QuattroPro®). Different parameters can be extracted from the *x*/*y*-coordinates and exported:
   a. The *x*- and *y*-coordinates for display of the path structure (*see* **Fig. 4A**).
   b. Step length: distance migrated for each step (*see* **Fig. 4B**).
   c. Relative angles from step to step: linearity of paths representing cell polarity and directional persistence (*see* **Fig. 4C**).
   d. Absolute angles in the field of view: chemotaxis toward one side of the migration field versus random migration (*see* **Fig. 4D**).
   e. Stop–go pattern: sequence of gos and stops irrespective of step length.
9. To calculate the pixel size in micrometers, load the image displaying the calibration chamber (Neubauer). Collect the *x*- and *y*-coordinates using the tracking software for all four corners of one square usually representing 200 or 250 µm. For horizontal resolution, the measured amount of pixels along the horizontal line is divided by the distance (in µm), giving the pixel resolution factor. The same factor

Table 2
Quantification of Cell Migration from Cell Paths Using Spreadsheet Analysis

Step (min)	Cell (1)	Cell (2)	…	Cell (n)	Mean (1) (μm/min)
1	*a*(1)	*b*(1)	…	*n*(1)	*x*(1)
2	*a*(2)	*b*(2)	…	*n*(2)	*x*(2)
⋮	… ⋮	… ⋮	…	… ⋮	⋮
n	*a*(*n*)	*b*(*n*)	…	*n*(*n*)	*x*(*n*)
mean (2)	*y*(1)	*y*(2)	…	*y*(*n*)	

Note: Means (1) and (2) represent population and single cell parameters, respectively.

should be obtained by measuring the vertical pixel resolution. Slightly differing values in horizontal and vertical resolution (e.g., slight hardware-related optical image distortion) may be averaged to one common pixel resolution factor.

3.5. Data Analysis

1. Load the exported ASCII data file into the spreadsheet. Each cell is represented by vertical columns, and each step is represented by lines (*see* **Table 2**).
2. Define the absolute time from step to step (minutes or hours) in the first column as a formula that is copied using the scroll down routine of the spread sheet (*see* **Table 2**, first column).
3. For analysis of time-dependent parameters from step to step in cell populations, use horizontal lines [*see* **Table 2**, mean (1)]. Calculate the horizontal mean for all cells in the line using the spread sheet formula for mean values. Multiply the mean by the pixel resolution factor (*see* **Subheading 3.4.**, **step 9**), converting pixel values into micrometers. Divide the micrometer value by the predefined real-time step interval (minutes or hours), resulting in step *speed* (in μm/min or μm/h). Copy the formula along the column using the pull-down menu of the spread sheet software.
4. Display the graphics of the time-dependent velocity for a single cell (*see* **Fig. 4B**) or the calculated average for the population (*see* **Fig. 5**). If overlaid with the data from a control experiment, changes in real-time migration parameters within the population can be displayed (*see* **Fig. 5B**).
5. The time-dependent migration *velocity* (step lengths) for cell population represents the "true" speed of a cell while it is moving, hence excluding stopping intervals (whereas *speed* includes stops). Here, only numbers greater 0 are averaged by the formula in the horizontal.
6. The time-dependent *step frequency* (stop–go pattern) is calculated in the same manner. Count the amount of steps ≥1 pixel divided by the number of cells.
7. Single-cell analysis is obtained by averaging the values in the columns, representing the mean step length for each cell [*see* **Table 2**, mean (2)]. The fraction of time

an individual cell was actively migrating is calculated from the sum of steps ≥1 pixel divided by the total number of tracked steps. Single-cell parameters can be used to identify heterogeneity in migratory activity within the source population (*see* **Fig. 6A**). The single-cell parameters velocity, step frequency (representing the time migrated), and the resulting distance migrated can be combined for 3D-like representation of subset heterogeneity using commercially available statistics software (*see* **Fig. 6B**).

8. Kinetic information on cell–cell interactions ***(8)*** include contact duration (by frame-to-frame analysis), the migration velocity upon cell–cell contact (*see* **step 3**), and the stop–go pattern (*see* **step 6**).

4. Notes

1. To date, software packages for automated cell tracking are designed and optimized for cell movement on 2D substrata. However, such tracking algorithms have consistently failed to perform reliable object detection in 3D matrices. The reasons for such failure reside in the inhomogeneous opaque background structure of the matrix, heterogeneous and frequently blurry edges of the objects, changing gray scale characteristics upon change in the *z*-position, and a high frequency of cell–cell interactions and superimposition of paths leading to visual object fusion. Therefore, in our laboratory, a semiautomated manual tracking device is preferred over automated cell tracking.
2. The semiautomated tracking system described herein allows the convenient manual tracking of each cell sequentially at the computer-controlled step interval from video recordings or digital image sequences, allowing high-throughput digitization of cell paths and export of migration parameters.
3. For long-term culture in the self-constructed chamber, both glass slides are autoclaved before the chamber is constructed under sterile flow conditions.
4. The protocol describes a 1.7-mg/mL collagen preparation optimized for cell motility of different cell types, including leukocytes and tumor cells ***(13,14)***. Other collagen concentrations can be generated by varying the volume of the cell suspension (*see* **Subheading 3.2.**, **step 4**).
5. Detachment of adherent cells by trypsin should be avoided because cell surface receptors involved in adhesion and migration may be cleaved ***(15,16)***. Receptor cleavage potentially interferes with migration properties.
6. For optimized cell viability in long-term cultures, osmolarity of the medium is slightly hypertonic, taking into account the inner surface provided by the collagen fiber network, putatively adsorbing a certain fraction of ions and/or nutrients from the medium.
7. In the process of collagen polymerization, a substantial fraction of the cells will sink to the bottom of the glass-matrix before the gel is polymerized. To avoid cell accumulation to the bottom interphase, the migration chamber must be positioned in the upright, vertical position for collagen polymerization. In most cases, a simple 50-mL tube holder will be sufficient.

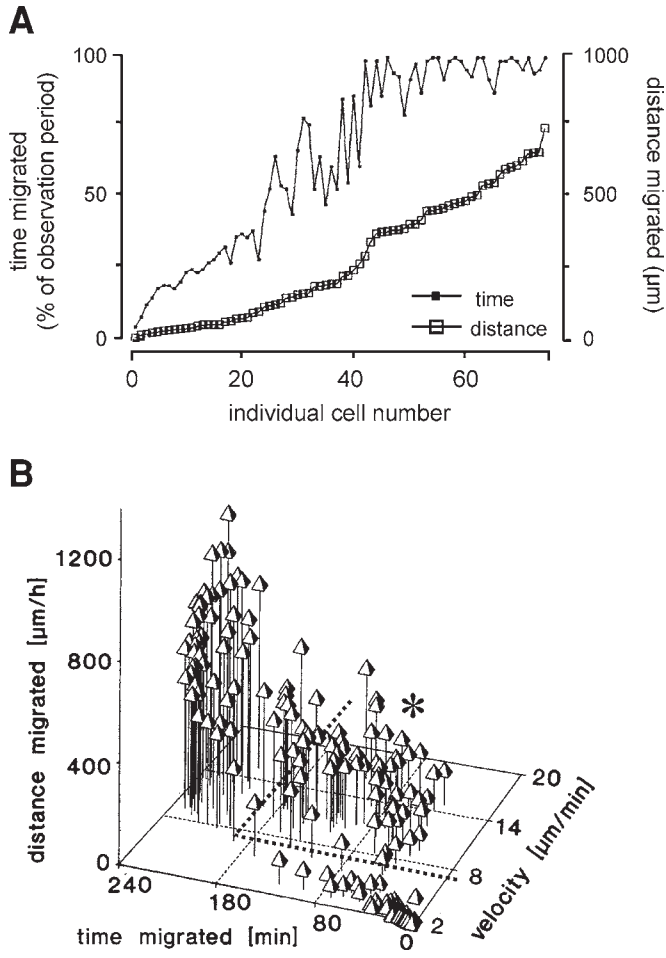

Fig. 6. Single-cell parameters. $CD8^+$ cells were stimulated by IL-8 (20 ng/mL) and monitored for 90 (**A**) or 240 min (**B**). (**A**) The total distance migrated for each cell after 90 min in increasing order and the corresponding time migrated. Combined data for two experiments are shown (77 cells). (**B**) Subset analysis combining velocity, time migrated, and the resulting distance migrated for each individual cell. Several functional subpopulations can be distinguished. A subset delineated by dashed line and asterisk was newly recruited by IL-8, showing high velocity yet temporarily limited migration.

8. By focusing up and down in the *z*-direction, you can avoid being simply "trapped" by the region of highest cell density (which will usually be the matrix-free lower liquid interphase toward the bottom of the chamber). To be sure that cells in focus are indeed *within* the matrix, an equal number of black (below focus) and white cells (above focus) should be visible.

9. The use of a closed migration chamber offers several advantages over open culture systems. The first is that the closed chamber favors long-term mechanical stability of the matrix. For certain, highly adherent cells such as fibroblasts and some tumor cells that show a tendency to remodel and contract the collagen matrix, physical shrinking of the lattice is delayed because top and bottom collagen interphases are simultaneously adsorbed to the glass template (*see* **Fig. 1A**). The second advantage is that sealed chambers maintain more stable medium and gas conditions for 24–48 h, depending on cell number and proliferation activity. For long-term cultures, the medium can be changed on the microscopy stage by carefully removing the wax from one side, loading the fresh medium, and resealing the chamber with liquid wax. The third advantage is that for experiments on the impact of matrix fibers on cell migration (contact guidance), alligned collagen lattices can be generated by gentle pulling (by a small hook) and orienting the fibers along the traction line, favoring migration along these aligned fiber stands ***(17)***.
10. Using transmission light videomicroscopy, motility is determined by the *x*- and *y*-positions of the cells, hence neglecting the *z*-position (movement up and down within the lattice) (*see* **Fig. 1E**). In our experience using a chamber height of 400 µm, most movements occur in the *x*- and *y*-directions, whereas a comparatively minor change in *z*-position is observed, based on changes in the cell gray scale and sharpness of the cell body in the course of migration. Flatter matrices allow preferential polymerization of collagen fibers in parallel to the template interphase along the top and bottom glass interphase, generating predominantly horizontally alligned fibrils, as shown by confocal reflection microscopy ***(7,18)***, and thereby increase the probability of cells to move along these fibrils in the *x*- and *y*-directions.
11. To generate representative and reproducible results, it is important to track a nonbiased selection of *all* cells within a given region, irrespective of whether the cell is migratory. The migratory activity then represents a dynamically oscillating average of migrating and nonmigrating cells within a population, allowing investigations on chemokine-mediated recruitment, antibody-blocking studies, and others.
12. Cell–cell interactions or crossing paths result in the optical fusion of both cell bodies into one object, frequently making both cells indistinguishable from each other. Such optical fusion is an inherent feature of 3D matrix cultures monitored at low magnification (*see* **Fig. 3**). After fusion and separation, it is frequently not possible to correctly devise the appropriate path for each cell. For population analysis, quantitative migration parameters are unaffected if the trajectories after separation are randomly defined. In contrast, single-cell analysis will yield incorrect "hybrid" paths.

Acknowledgments

Julian Storim and Martin Kretzschmar are acknowledged for critical reading of the manuscript and Jochen Moeller for generating digital screen shots. The Cell Migration Laboratory is supported by grants from the Wilhelm-Sander-Foundation, the Deutsche Forschungsgemeinschaft, and the Bundesministerium für Bildung und Forschung.

References

1. Friedl, P., Zanker, K. S., and Brocker, E.-B. (1998) Cell migration strategies in 3-D extracellular matrix: differences in morphology, cell matrix interactions, and integrin function. *Microsc. Res. Tech.* **43,** 369–378.
2. Friedl, P. and Brocker, E.-B. (2000) The biology of cell locomotion within three-dimensional extracellular matrix. *Cell. Mol. Life Sci.* **57,** 41–64.
3. Geiger, B. (2001) Cell biology. Encounters in space. *Science* **294,** 1661–1663.
4. Cukierman, E., Pankov, R., Stevens, D. R., and Yamada, K. M. (2001) Taking cell-matrix adhesions to the third dimension. *Science* **294,** 1708–1712.
5. Friedl, P., Noble, P. B., and Zanker, K. S. (1993) Lymphocyte locomotion in three-dimensional collagen gels. Comparison of three quantitative methods for analysing cell trajectories. *J. Immunol. Methods* **165,** 157–165.
6. Friedl, P., Noble, P. B., and Zanker, K. S. (1995) T Lymphocyte locomotion in a three-dimensional collagen matrix. Expression and function of cell adhesion molecules. *J. Immunol.* **154,** 4973–4985.
7. Friedl, P., Maaser, K., Klein, C. E., Niggemann, B., Krohne, G., and Zanker, K. S. (1997) Migration of highly aggressive MV3 melanoma cells in 3-dimensional collagen lattices results in local matrix reorganization and shedding of alpha2 and beta1 integrins and CD44. *Cancer Res.* **57,** 2061–2070.
8. Gunzer, M., Schafer, A., Borgmann, S., et al. (2000) Antigen presentation in three-dimensional extracellular matrix: interactions of T cells with dendritic cells are dynamic, short lived, and sequential. *Immunity* **13,** 323–332.
9. Friedl, P. and Gunzer, M. (2001) Interaction of T cells and antigen presenting cells: the serial encounter model. *Trends. Immunol.* **22,** 187–191.
10. Hegerfeldt, Y., Tusch, M., Brocker, E. B., and Friedl, P. (2002) Collective cell movement from primary melanoma explants: plasticity of cell–cell interactin, β1 integrin function, and migration. *Strat. Cancer Res.* **62,** 2125–2130.
11. Maaser, K., Wolf, K., Klein, C. E., et al. (1999) Functional hierarchy of simultaneously expressed adhesion receptors: integrin alpha2beta1 but not CD44 mediates MV3 melanoma cell migration and matrix reorganization within three-dimensional hyaluronan-containing collagen matrices. *Mol. Biol. Cell* **10,** 3067–3079.
12. Friedl, P., Noble, P. B., Walton, P. A., et al. (1995) Migration of coordinated cell clusters in mesenchymal and epithelial cancer explants in vitro. *Cancer Res.* **55,** 4557–4560.
13. Haston, W. S., Shields, J. M., and Wilkinson, P. C. (1982) Lymphocyte locomotion and attachment on two-dimensional surfaces and in three-dimensional matrices. *J. Cell Biol.* **92,** 747–752.
14. Schor, S. L., Allen, T. D., and Winn, B. (1983) Lymphocyte migration into three-dimensional collagen matrices: a quantitative study. *J. Cell Biol.* **96,** 1089–1096.
15. Blue, M. L., Davis, G., Conrad, P., and Kelley, K. (1993) Specific cleavage of the alpha 4 integrin associated with activation of peripheral T lymphocytes. *Immunology* **78,** 80–85.

16. Bishop, L. A., Rahman, D., Pappin, D. J., and Watt, F. M. (1995) Identification of an 80 kD protein associated with the alpha 3 beta 1 integrin as a proteolytic fragment of the alpha 3 subunit: studies with human keratinocytes. *Cell Adhes. Commun.* **3,** 243–255.
17. Gunzer, M., Friedl, P., Niggemann, B., et al. (2000) Migration of dendritic cells within 3-D collagen lattices is dependent on tissue origin, state of maturation, and matrix structure and is maintained by proinflammatory cytokines. *J. Leukocyte Biol.* **67,** 622–629.
18. Friedl, P. and Brocker, E. B. (2001) Biological confocal reflection microscopy: reconstruction of three-dimensional extracellular matrix, cell migration, and matrix reorganization, in *Image Analysis. Methods and Applications*, 2nd ed. (Hader, D. P., ed.), CRC, Boca Raton, FL, pp. 9–21.

8

Analyzing Chemotaxis Using *Dictyostelium discoideum* as a Model System

Mark A. Landree and Peter N. Devreotes

1. Introduction

Dictyostelium discoideum are simple eukaryotic amoebas that when starved of a food source have the remarkable ability to spontaneously aggregate and differentiate to form a cluster of spores on top of a stalk of vacuolated cells (*see* **Fig. 1** and **ref. *1***). The process of aggregation, although quite fascinating to simply observe, has proven extremely powerful for the molecular dissection of chemotaxis signaling pathways. Mechanisms of chemoattractant sensing discovered in *D. discoideum* have been tested in higher eukaryotic systems and were found to be strikingly similar ***(2)***. In particular, a paradigm for directional sensing has been derived from studies in *D. discoideum* ***(3)***.

The current model for directional sensing involves stimulation of heterotrimeric G-protein-linked transmembrane receptors by chemoattractant. A host of additional cellular responses occur concurrently, including actin polymerization, adenylyl cyclase activation (ACA), myosin phosphorylation, Ca^{2+} influx, and cell spreading (*see* **Fig. 2**). A key early response is the transient appearance of phosphoinositides [$PI(3,4)P_2$ and $PI(3,4,5)P_3$] on the inner face of the plasma membrane. In a gradient of chemoattractant, the phosphoinositides appear at the leading edge of the cell and persist even in the absence of a functional actin cytoskeleton or cell movement. Directional sensing is therefore achieved by temporally and spatially regulating phosphoinositide signaling activity ***(3)***.

This model is based on the following information. Cells express four heptahelical transmembrane cAMP receptors, designated cAR1–cAR4. Each receptor can mediate chemotaxis to cAMP, although the dose responses differ. cAR1–cAR4 are linked to Gα2, which associates with the unique Gβ- and Gγ-subunits

From: *Methods in Molecular Biology, vol. 239: Cell Migration in Inflammation and Immunity*
Edited by: D. D'Ambrosio and F. Sinigaglia © Humana Press Inc., Totowa, NJ

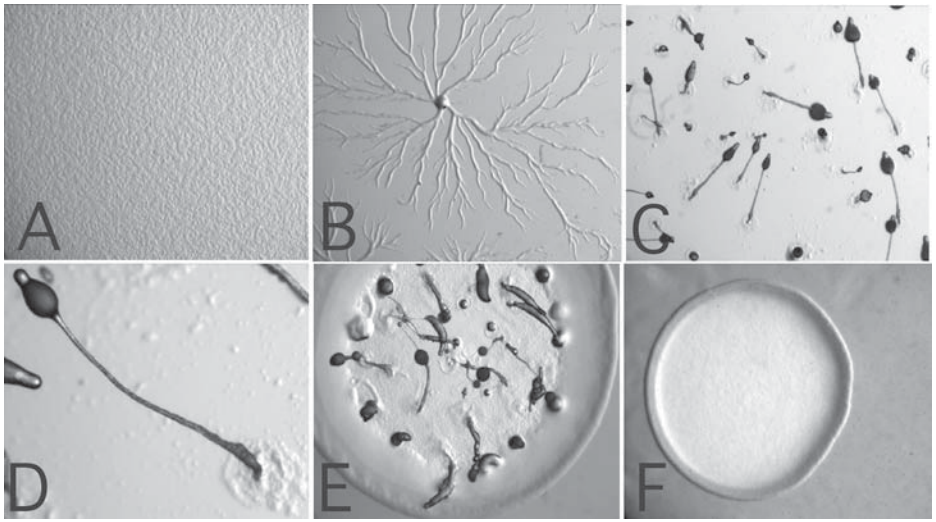

Fig. 1. *Dictyostelium discoideum* development. Development on development buffer (*see* **Subheading 3.2.1.**) agar at 0 h (**A**), 7 h (**B**), 24 h (**C**), and 24 h, 10 times higher magnification (**D**) after plating. Wild-type plaque (**E**) and aggregation-deficient plaque (**F**) on Sm/KA plates after 5 d.

and mediate aggregation to cAMP ***(1)***. Interestingly, chemotaxis to folic acid is mediated by Gα4 and the same unique βγ-subunits ***(4)***. cAR1 and the G-protein subunits are distributed evenly around the plasma membrane of a chemotaxing cell (*see* **Fig. 3A** and **refs. *5*** and ***6***). Therefore, the localization of the receptor–G-protein complex is not responsible for the asymmetric signal transduction confined to the leading edge of a cell in a gradient of chemoattractant. This uniform distribution of the receptor–G-protein complex does, however, explain the cell's ability to respond to stimulus at any point along the perimeter of the cell. An important tool for investigating the mechanism of asymmetry was introduced in 1995, when the cytosolic regulator of adenylyl cyclase (CRAC) was shown to transiently translocate to membranes upon stimulation with cAMP ***(7)***. A fusion protein of CRAC with green fluorescent protein (GFP) showed that CRAC not only translocates to the membrane upon receptor stimulation, but it also translocates to the front of a cell in a chemoattractant gradient (*see* **Fig. 3A** and **ref. *8***). It was also demonstrated that movement and directional sensing can be separated. When cells are treated with latrunculin A, an inhibitor of actin polymerization, CRAC–GFP still translocates to the side of the cell facing the highest concentration of chemoattractant ***(8)***. In fact, the pleckstrin homology (PH) domain of CRAC is sufficient for this translocation as demon-

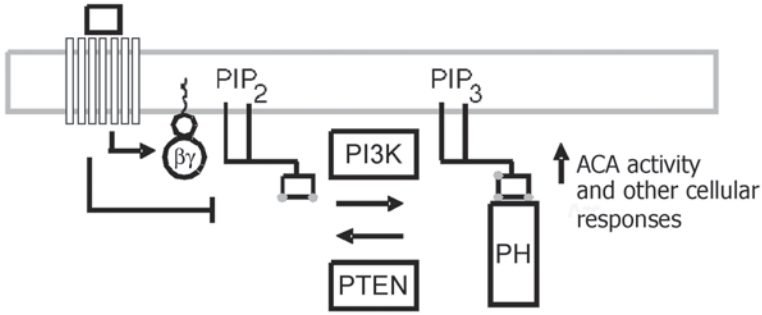

Fig. 2. Model for directional sensing. Upon ligand binding to the cAMP receptor, the G-protein is activated, which releases the βγ-subunit. PI3K is recruited to the plasma membrane and activated, converting PIP_2 to PIP_3. Pleckstrin homology (PH)-domain containing proteins, such as cytosolic regulator of adenylyl cyclase (CRAC), are recruited to the leading edge of the cell and the activity of ACA and other cellular responses is increased. PTEN is involved with turning this signaling off along with a ligand-dependent adaptation signal from the receptor itself.

strated by a PH_{CRAC}–GFP-fusion protein. Until recently, the identity of the PH-domain-binding sites at the inner face of the plasma membrane was not clear. It now seems rather certain that the binding sites are the phosphoinositides $PI(3,4)P_2$ and $PI(3,4,5)P_3$. These phospoinositides are generated by phosphoinositide 3-kinase (PI3K) and degraded by phosphoinositide 3-phosphatase (PTEN) in a stimulation-dependent manner ***(9,10)***. Cells lacking PI3K have a chemotaxis defect and the amount of PH–GFP that translocates to the leading edge of a cell is greatly reduced ***(10)***. Conversely, in PTEN deficient cells, the translocation of PH–GFP persists upon stimulation, such that the transient nature of the response is greatly elongated (*see* **Fig. 3B** and **ref. *9***). These two critical pieces of data strongly suggest that phosphoinositides are the binding site for PH-domain-containing proteins at the leading edge of a chemotaxing cell.

The overall picture of chemotactic signaling in *D. discoideum* and neutrophils is essentially the same, with the exception of a few salient features. Neutrophils and *D. discoideum* have G-protein-coupled chemoattractant receptors that are uniformly distributed around the cell's periphery and PH-domain-con-taining proteins asymmetrically localize to the fronts of chemotaxing cells in a phosphoinositide-dependent manner ***(3,11)***. Neutrophils, however, become polarized and move rapidly in a uniform concentration of attractant ***(12)***, whereas in *D. discoideum*, polarization and random motility do not seem to require exogenous chemoattractant. Another difference seems to be centered around the observation of a feedback loop in the neutrophil system ***(13)***, which has not been observed

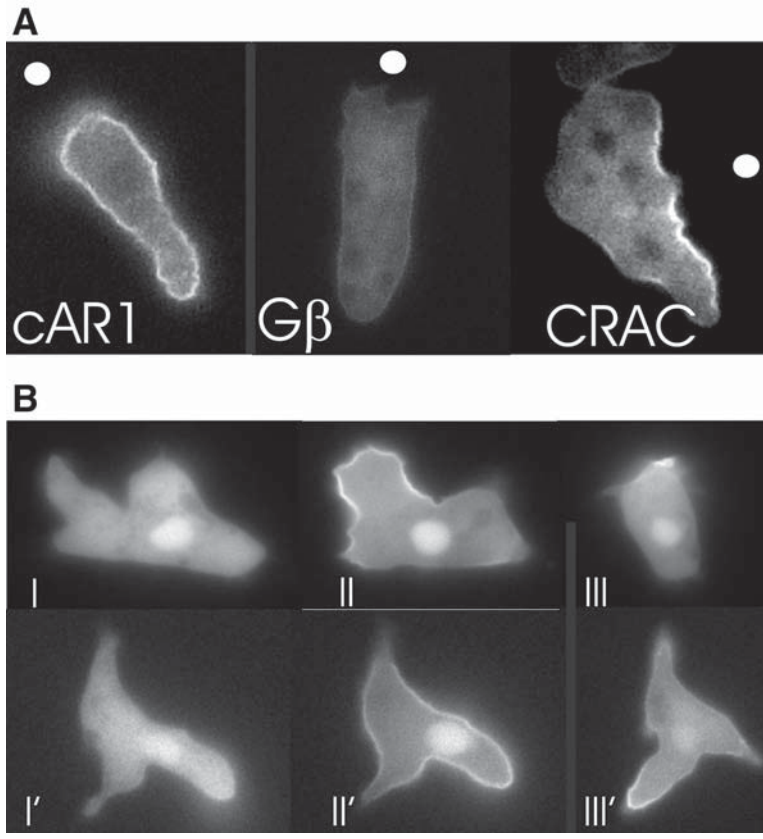

Fig. 3. Localization of key signaling components during chemotaxis. (**A**) Localization of the receptor, G-protein, and CRAC in a gradient of cAMP. The highest point of the gradient is marked by the white dot. (**B**) Dynamic response of CRAC–GFP in wild-type (I to III) and in PTEN null (I' to III') cells at time 0 (I and I'), 20 s (II and II'), and 2 min (III and III') after adding cAMP.

in *D. discoideum*. $PI(3,4,5)P_3$ seems to positively regulate the generation of more $PI(3,4,5)P_3$ in a Rac/actin-dependent manner. Further analysis is currently underway to understand these differences.

1.1. Advantages of D. discoideum *as a Model System*

Dictyostelium discoideum grow rapidly to high density, either in a Petri dish or in shaking culture. They are amenable to most modern molecular genetic,

cell biological, and biochemical techniques. Tools exist for insertional mutagenesis ***(14)***, library complementation ***(15)***, and protein localization ***(5,6,8)***, and the cells move at a rate that is easily observed using time-lapse microscopy.

One of the many strengths of this model system is the ability to easily perform phenotypic screens for the loss of aggregation. When cells are starved, they undergo a developmental program that upregulates the machinery required for aggregation (i.e., cAR1 and Gα2), they aggregate, and they ultimately form a sorus on top of a stalk of vacuolated cells. If the cells do not aggregate, they do not form fruiting bodies. Therefore, when individual cells are plated on agar with bacteria, wild-type clones will digest the bacteria, forming a plaque devoid of nutrients, and enter the developmental pathway. Mutant clones defective for aggregation will not form fruiting bodies, resulting in a smooth plaque (*see* **Fig. 1** and **refs.** ***1*** and ***16***).

Another strength is that growth and development of *D. discoideum* are two distinct phases of its life cycle. This suggests that disruption of a gene involved in development or aggregation is not likely to have deleterious growth defects ***(1)***. Therefore, maintenance of a strain that does not develop is simple and straightforward.

2. Materials

1. HL5 medium: To make 1 L, solubilize the following in H_2O: 20 g maltose or 10 g dextrose, 10 g proteose peptone, 5 g yeast extract, 0.51 g Na_2HPO_4, 0.485 g KH_2PO_4. Before use, add 0.03 g streptomycin.
2. Sm agar: For 1 L of plates, solubilize the following in H_2O: 10 g glucose, 10 g bactopeptone, 1 g yeast extract, 1.9 g KH_2PO_4, 0.6 g K_2HPO_4, 4 mL of 1 *M* $MgSO_4$. Add 20 g agar and autoclave 25 min.
3. DB: To make 4 L, solubilize the following in H_2O: 5.36 g $Na_2HPO_4 \cdot 7H_2O$, 2.72 g KH_2PO_4, 4 mL 2 *M* $MgSO_4$, 0.8 mL 1 *M* $CaCl_2$.
4. RLB: To make 500 mL, solubilize the following in H_2O: 54.8 g sucrose, 0.508 g $MgCl_2 \cdot 6H_2O$, 5 mL 1 *M* Tris-HCl pH 7.5, 5 mL Triton X-100.
5. Buffer A: To make 100 mL: mix 1.0 mL 1 *M* Tris-HCl pH 7.5, 2.0 mL 0.5 *M* EDTA, and 97 mL H_2O.
6. Buffer B: To make 100 mL: mix 1.0 mL 1 *M* Tris-HCl pH 7.5, 3.5 mL 20% SDS, and 95.5 mL H_2O.

3. Methods

The methods described in this section outline how to (1) disrupt a gene (*see* **Subheading 3.1.**), (2) analyze a mutant for defects in chemotaxis (*see* **Subheading 3.2.**), and (3) rescue the mutant's morphological defect with the wild-type (WT) allele of the disrupted gene while localizing the protein in the cell (*see* **Subheading 3.3.**).

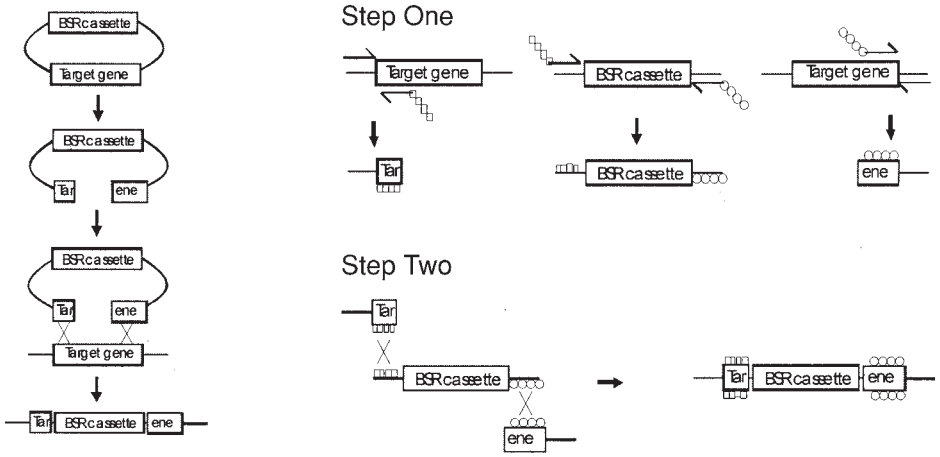

Fig. 4. Disruption vectors for targeted disruption: (**A**) conventional disruption vector diagram for homologous disruption of a gene; (**B**) construction of a linear targeting vector using PCR.

3.1. Targeted Disruption of a Gene of Interest

This section describes how to (1) identify a *D. discoideum* homolog and design a targeting construct (*see* **Subheading 3.1.1.**), (2) transform the targeting construct (*see* **Subheading 3.1.2.**), (3) clone individual isolates based on the aggregation phenotype (*see* **Subheading 3.1.3.**), and (4) screen for a targeted disruptant (*see* **Subheading 3.1.4.**). If a clear homolog is found and the gene is easily disrupted, one can expect to complete these four methods and have an initial determination of the chemotactic phenotype in as little as 4–10 wk.

3.1.1. Constructing a Targeting Vector

1. In order to disrupt a gene, identify a *D. discoideum* homolog by database mining. Rather than searching with the full-length mammalian sequence, it is usually beneficial to search with blocks of conserved sequence. The link www.dicty.sdsc.edu directs you to the *D. discoideum* database, where you can perform a Blast search of genomic DNA to identify the gene and flanking sequence. Another site that is useful is the Japanese cDNA project URL is www.csm.biol.tsukuba.ac.jp/cDNAproject.html. Links to these websites, information about *D. discoideum*, and a list of laboratories that use this model system can be found at www.dictybase.org.
2. Once the homologous gene and its flanking sequence have been identified, either clone it into a disruption vector (commonly containing blasticidin S resistance gene ***[17]***) or generate a linear fragment of DNA for disruption via polymerase chain reaction (PCR) (*see* **Fig. 4** and **ref.** ***18***). The length of the flanking region required for efficient homologous recombination is 0.5–1.0 kbp, but flanking regions as

small as 100 bp have been successfully used. Additionally, an inducible expression system has been described ***(19)***.
3. Linearize the vector, deleting a major portion of gene but leaving the ends and flanking sequence intact or gel purify PCR product. This DNA is used to transform cells.

3.1.2. Transformation

This transformation protocol is used to introduce plasmid DNA into *D. discoideum*. Typically, circular DNA is transformed for an expression vector and linear DNA for a disruption vector. Ten to 1000 foci per plate are observed in 1–4 wk and expanded to shaking cultures 1–2 wk after foci are observed.

1. Grow cells to 5×10^6 cells per milliliter (avoid exceeding 1×10^7 cells/mL). Use 1×10^7 cells per transformation.
2. Spin down cells at 1000*g* for 4 min at 4°C.
3. Resuspend cells at 2.5×10^7 cells/mL in electroporation (E) buffer (10 m*M* Na/K phosphate buffer, pH 6.1, 50 m*M* sucrose).
4. Transfer 0.4 mL of cells to an ice-cold tube containing 10–15 µg DNA, mix with a Pasteur pipet, and incubate on ice for 5 min.
5. Transfer cells and DNA to an ice-cold 0.2-cm gap electroporation cuvet.
6. Set up electroporator (Bio-Rad Gene Pulser): Voltage at 1.2 kV, capacitance at 3.0 µFd; use a 5-Ω resistor in series with the sample chamber.
7. Immediately electroporate cells. A successful electroporation results in a time constant between 0.6 and 0.9, usually 0.6.
8. Incubate cuvet on ice for 15 min.
9. Set up cell culture plate (100 × 20 mm, sterile) with 2 µL healing solution (100 m*M* $CaCl_2$, 100 m*M* $MgCl_2$) in the middle of the plate.
10. Add cells to the healing solution dropwise and incubate 10–15 min at 22°C.
11. Add HL5 media (without drug) and incubate overnight at 22°C.
12. After 18–24 h, remove media and replace with media containing the appropriate drug selection (i.e., blasticidin S at 5 µg/mL or G418 at 20 µg/mL; *see* **Note 1**).
13. If clones are desired, plate into 96-well plates at an average density of one cell per well.
14. Foci are readily apparent after approx 1–4 wk. Once the plate is confluent, remove the cells by gentle disruption using a 10-mL pipet and add all the cells to a 125-mL flask containing 50 mL of HL5 with drug selection. Shake the flask at 200 rpm at 22°C for approx 2 d.
15. Allow cells to grow to a density of 5×10^6 cells/mL. Dilute cells to 1×10^5 cells/mL to carry.

3.1.3. Isolation of Individual Clones by Plaque Formation on Bacterial Lawns

Once the transformation has been performed, a population of cells with independent targeting events exists. In order to assess the developmental phenotype

and simultaneously isolate individual clones, the cells are plated with bacteria. Individual clones will form a plaque on the bacterial lawn, which can be easily isolated. Clonal isolation allows Southern analysis to determine whether the gene of interest was targeted correctly. In addition, the cells in the center of the plaque will starve, sending the signal to develop. If the cells are wild type, they will fruit and the plaque will have a "rough" appearance. If the cells are aggregation deficient, however, the cells will not fruit and the plaque will remain "smooth" (*see* **Fig. 1**).

1. Dilute cells to 5×10^3 cells/mL using HL5 without streptomycin.
2. Add one loop of *Klebsiella aerogenes* (KA) bacteria from an Sm plate grown at 22°C to 1 mL of HL5 without streptomycin and disperse bacterial cells by vortexing briefly. Alternatively, 100 mL of HL5 without streptomycin can be innoculated with KA and left at room temperature without shaking overnight. It is important not to shake the bacteria at 37°C, as this inhibits subsequent *D. discoideum* development.
3. Plate 450 µL of KA and 10 µL (50 cells) of diluted *D. discoideum* on a 100-mm Sm agar Petri dish. It is important that the Sm plates be less than 2 wk old. If the plates become dehydrated, the efficiency of plaque formation decreases significantly.
4. Allow plate to dry and invert.
5. Put plates in container with a lid and a moist paper towel at 22°C for 4–5 d.
6. Observe morphological phenotype, typically on d 5.
7. Pick individual plaques with a sterile loop and add the cells to 1 well of a 24-well plate containing HL5 plus drug for selection.
8. Once the 24-well plate well is confluent, transfer the cells to a 100-mm dish and add more media to the 24-well plate. This serves as a convenient backup stock of cells.
9. Once the 100-mm dish is confluent, transfer cells to a flask as described in **Subheading 3.1.2., step 14** and add more media to the dish.

3.1.4. Screen for Targeted Disruptant

Because homologous recombination only occurs in a fraction of the cells (the other fraction being random insertion), one must design a screen based on PCR or Southern hybridization to be sure the clone has the desired mutation. The PCR or Southern strategy should utilize a probe that will detect the targeted gene and not detect the targeting vector. Clones are isolated as described in **Subheading 3.1.3.**, keeping in mind that a targeted disruption may result in an aggregation-deficient plaque morphology. Therefore, it is wise to pick plaques of varying morphologies for southern analysis. A protocol to isolated genomic DNA for this analysis is listed in **Subheading 3.1.5.** Identifying the appropriate disruption takes approx 2 wk for a typical gene.

Some genes prove more difficult to disrupt. If a phenotypic defect is not observed on Sm/KA plates (outlined above) but Southern analysis demonstrates

that the gene has been disrupted, gene redundancy is a possibility. However, if Southern analysis does not show a targeted disruption, the gene may be essential for growth or inherently difficult to disrupt. To distinguish between these two possibilities, one can cotransform the targeting vector with an expression vector that is maintained extrachromosomally. If this allows efficient disruption, the gene is probably lethal. If the gene is not targeted efficiently, it may be inherently difficult to disrupt because of size, location, or sequence composition, such that additional rounds of targeting should be attempted.

3.1.5. Isolation of Genomic DNA

1. Spin down 10 mL of suspension cells (5×10^6 cells/mL) or all cells from a confluent 10-cm plate at 1000*g* for 4 min.
2. Wash the cell pellet with developmental buffer (DB: 5 m*M* Na_2HPO_4, 5 m*M* NaH_2PO_4, 2 m*M* $MgSO_4$, 200 µ*M* $CaCl_2$, pH 6.1).
3. Resuspend the cell pellet in 0.5 mL of ice cold real lysis buffer (RLB: 0.32 *M* sucrose, 10 m*M* Tris-HCl, pH 7.5, 5 m*M* $MgCl_2$, 1% Trition X-100).
4. Spin down the nuclei at 12,000*g* for 10 min and remove the supernatant. **Caution**: The pellet is loose.
5. Resuspend the nuclei very gently in 200 µL of buffer A (10 m*M* Tris-HCl, pH 7.5, 10 m*M* EDTA).
6. Add 220 mL of buffer B (10 m*M* Tris-HCl, pH 7.5, 0.7% sodium dodecyl sulfate [SDS]) and mix gently.
7. Add 3 µL of 10 mg/mL RNaseA and incubate at 37°C for 1 hour.
8. Add 15 µL of 20 mg/mL Proteinase K and incubate at 55°C for 1 h with gentle mixing every 15 min.
9. Extract with 0.5 mL phenol/chloroform/isoamyl alcohol and then extract with 0.5 mL chloroform.
10. Add 16 µL of 5 *M* NaCl and 1 mL room-temperature 100% ethanol to precipitate the DNA.
11. Wash pellet with 70% ethanol.
12. Resuspend pellet in 50 µL TE (10 m*M* Tris-HCl, pH 7.5, 1 m*M* EDTA).
13. Perform PCR or Southern screen; 1–5 µg genomic DNA is typically used for Southern analysis (approx 5 µL from this preparation) and 100 ng genomic DNA for PCR analysis.

3.2. Analyze Null Mutant

This section is designed to outline the methods to follow if an aggregation defect was observed when the mutant cells were plated with bacteria, as detailed in **Subheading 3.1.3.** Cells are first plated on nonnutrient (DB) agar plates (*see* **Subheading 3.2.1.**). Wild-type cells make cell shape changes induced by pulsatile waves of cAMP at 5 h, observable; they aggregate to the mound stage at 10 h and form fruiting bodies by 24 h. If cells do not make cAMP waves, they

can be pulsed with exogenous cAMP (*see* **Subheading 3.2.2.**) for 5 h and then plated on nonnutrient agar. Cells that have a cAMP regulation defect but are aggregation competent will form fruiting bodies if pulsed with exogenous cAMP. If they have an aggregation defect (other than in the regulation of cAMP), exogenous cAMP will not rescue development. Cells should also be observed in a chemoattractant gradient. Using bright-field microscopy and a microinjector to establish a cAMP gradient, chemotaxis can be directly monitored independent of the other requirements for fruiting body formation (*see* **Subheading 3.2.3.**).

3.2.1. DB Agar Development Assay

This assay is used to confirm/extend the aggregation phenotype of a mutant strain found on Sm/KA plates. The cells are plated on non-nutrient agar such that starvation ensues, allowing the cells to attempt to aggregate and develop (*see* **Fig. 1**). Most of the genes identified to date in this signaling pathway have an aggregation defective phenotype in this assay.

This assay analyzes aggregation and development. If the cells do not develop (i.e., upregulate the genes required for aggregation such as cAR1), then the cells will not aggregate. To determine whether the cells have developed, one can perform Western blot analysis on clones to check for the upregulation of cAR1, Gα2, gp80, and ACA. These genes are not expressed in the vegetative state (fed) but are expressed after approx 5 h of starvation. If these genes are not upregulated, the cells can be pulsed with exogenous cAMP, which may rescue gene expression such that the aggregation phenotype can be determined on DB agar. This allows one to distinguish the difference between the regulation of the cAMP relay and the regulation of aggregation.

1. Grow the cells in HL5 to a density of 5×10^6 cells/mL, shaking at 200 rpm, 22°C.
2. Plate 3 mL melted DB agar (DB + 1.5% agar) in a 35 × 10-mm sterile Petri dish. Allow to harden.
3. Spin down 1×10^7 cells per plate.
4. Wash cells once with DB.
5. Resuspend cells in DB at concentration of 1×10^7 cells/mL.
6. Pipet 1 mL of cells onto the DB agar plate and let the cells settle and spread onto the agar for 15 min. Check this on a light microscope.
7. Remove the media by aspiration.
8. Tip the plates by resting one edge of the dish on the lid such that an approx 30° angle is achieved for approx 5 min, at which time the agarose turns from a shiny surface to a matte finish.
9. Aspirate the last bit of liquid, as it inhibits aggregation.
10. Allow the cells to develop at 22°C, placing the Petri dish upside down.

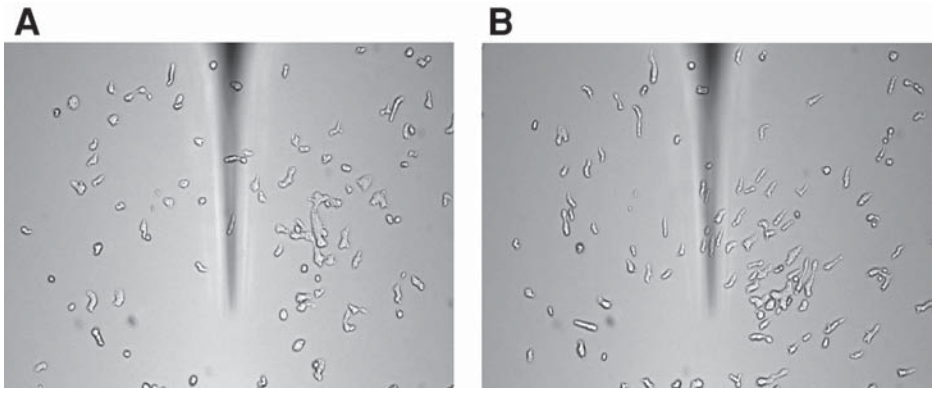

Fig. 5. Visualizing chemotaxis. Cells are developed for 5 h and put in a gradient of cAMP emanating from the needle (dark shadow). Pictures are taken at time 0 (**A**) and 20 min (**B**) after the needle is positioned.

11. Observe development using a low-power dissection microscope over the course of 24 h. Alternatively, plates can be analyzed and cAMP waves can be observed using videomicroscopy for the first 5–10 h.

3.2.2. Preparation of Cells by Development in Suspension with Exogenous cAMP Addition

This method is performed when one wants to bypass the cells requirement to make cAMP waves. This is typically performed to prepare cells for microscopy or when cells have a cAMP production problem.

1. Grow cells to a density of 5×10^6 cells/mL.
2. Spin down 50–100 mL of cells at 1000*g* for 4 min.
3. Wash once with DB.
4. Resuspend cells at a density of 2×10^7 cells/mL in DB. Ten milliliters of culture should be shaken in a 50-mL flask.
5. Shake cells at 110 rpm for 1 h at 22°C.
6. Pulse the cells with 50 n*M* cAMP at 6-min intervals while shaking at 110 rpm for at least another 4 h. A timer (ChronTrol model XT) can be used to control a peristaltic pump for delivery of the cAMP.

3.2.3. Chemotaxis in a Gradient Generated Using a Needle

This assay is used to observe the movement of individual cells in a gradient of chemoattractant (*see* **Fig. 5**). The gradient is established using a microinjector with a cAMP filled micropipet tip. Wild-type *D. discoideum* cells that have been developed for 5 h move approx 15 µm/min toward cAMP.

1. Prepare *D. discoideum* cells for chemotaxis as described in **Subheading 3.2.2.**
2. Wash cells once with DB.
3. Dilute cells to 2×10^5 cells/mL, vortex to disperse cells, and spot 20 µL on the chamber cover glass, wait for 10 min for the cells to adhere, and then fill chamber with DB buffer.
4. Load a femtotip (Eppendorf) microinjection needle with 100 µ*M* cAMP and lower the needle to just above the cover glass. This is accomplished by watching the needle come into focus.
5. Take a short video of 30 frames at 5- to 30-s intervals. The typical exposure time is milliseconds. A large field of cells is usually obtained using a ×10 phase objective or the detail of pseudopod extension can be observed with a ×100 oil lens.

3.3. Localization of the Protein in the Cell and in the Signaling Pathway

Once a mutant is created by targeted disruption and an aggregation phenotype has been observed, the localization of the protein in the cell is analyzed (*see* **Subheading 3.3.1.**). The disruption strain allows one to complement the mutation with an extrachromosomal copy of either the wild-type cDNA or a GFP fusion. The power of this system is the ease of determining protein localization while rescuing the morphological phenotype with the same strain. If the morphological phenotype is rescued with the GFP-fusion construct, the localization studies can be interpreted as being a direct reflection of where the protein is normally localized in the cell. The wild-type cDNA should be compared to the GFP fusion for morphological complementation. Once the protein has been localized in the cell, the disrupted gene should be placed in the signaling pathway (*see* **Subheading 3.3.2.**).

3.3.1. Localization of the Protein in Living Cells

Protein localization may be developmentally regulated in a stimulation-dependent manner. Therefore, one should analyze the GFP fusion in vegetative and developed cells in the absence and presence of stimulation with cAMP. Two modes of stimulus application should be used: uniform stimulation and gradient stimulation. One can also use latrunculin A to distinguish a proteins role in movement from directional sensing, because latrunculin A is an actin polymerization inhibitor that prevents movement without disturbing directional sensing. Cells are pulsed with cAMP as in **Subheading 3.2.2.** and viewed under the microscope as in **Subheading 3.2.3.**, except that fluorescence mode is used (*see* **Note 2**).

3.3.2. Localize the Protein in the Signaling Pathway

As mentioned in **Subheading 1**, a prominent asymmetric signal that has been found in this pathway is involved in the maintenance of the 3' phosphoinositide

lipids at the front of the cell. In order to determine whether the targeted disruption is upstream, downstream, or in a different pathway, transform the disrupted strain with an expression plasmid encoding the PH domain of either CRAC or PKB fused to GFP. If the gene is involved upstream of the phosphoinositide, stimulation-dependent localization of PH–GFP to the front of the cell will not be observed. However, if the gene acts downstream, then the fusion protein should transiently translocate to the front of the cell in a stimulation-dependent manner, which can be monitored by time-lapse microscopy as described earlier.

4. Notes

1. The following selectable markers are available for gene disruption: neomycin (G418), blasticidin, uracil, thymidine, and hygromycin.
2. Cells that are developed in DB for a couple of hours show less autofluorescence because the cells feed by phagocytosis and the standard growth media (HL5) is autofluorescent. It must be kept in mind, however, that starving cells in DB has biological consequences (the cells develop).

Acknowledgments

This work was supported by NIH grants GM28007 and 34933 to P.N.D. M.A.L. is supported by Postdoctoral Fellowship grant PF-02-109-01-DDC from the American Cancer Society. The authors wish to thank Hongbo Luo, Carol Manahan, and James Silverman for critical evaluation of this manuscript and Miho Iijima for sharing unpublished data.

References

1. Parent, C. A. and Devreotes, P. N. (1996) Molecular genetics of signal transduction in Dictyostelium. *Annu. Rev. Biochem.* **65,** 411–440.
2. Devreotes, P. N. and Zigmond, S. H. (1988) Chemotaxis in eukaryotic cells: a focus on leukocytes and *Dictyostelium*. *Annu. Rev. Cell Biol.* **4,** 649–686.
3. Parent, C. A. and Devreotes, P. N. (1999) A cell's sense of direction. *Science* **284,** 765–770.
4. Hadwiger, J. A., Lee, S., and Firtel, R. A. (1994) The G alpha subunit G alpha 4 couples to pterin receptors and identifies a signaling pathway that is essential for multicellular development in *Dictyostelium*. *Proc. Natl. Acad. Sci. USA* **91,** 10,566–10,570.
5. Xiao, Z., Zhang, N., Murphy, D. B., and Devreotes, P. N. (1997) Dynamic distribution of chemoattractant receptors in living cells during chemotaxis and persistent stimulation. *J. Cell Biol.* **139,** 365–374.
6. Jin, T., Zhang, N., Long, Y., Parent, C. A., and Devreotes, P. N. (2000) Localization of the G protein betagamma complex in living cells during chemotaxis. *Science* **287,** 1034–1036.

7. Lilly, P. J. and Devreotes, P. N. (1995) Chemoattractant and GTP gamma S-mediated stimulation of adenylyl cyclase in *Dictyostelium* requires translocation of CRAC to membranes. *J. Cell Biol.* **129,** 1659–1665.
8. Parent, C. A., Blacklock, B. J., Froehlich, W. M., Murphy, D. B., and Devreotes, P. N. (1998) G Protein signaling events are activated at the leading edge of chemotactic cells. *Cell* **95,** 81–91.
9. Iijima, M. and Devreotes, P. (2002) Tumor suppressor PTEN mediates sensing of chemoattractant gradients. *Cell* **109,** 599–610.
10. Funamoto, S., Meili, R., Lee, S., Parry, L., and Firtel, R. A. (2002) Spatial and temporal regulation of 3-phosphoinositides by PI 3-kinase and PTEN mediates chemotaxis. *Cell* **109,** 611–623.
11. Rickert, P., Weiner, O. D., Wang, F., Bourne, H. R., and Servant, G. (2000) Leukocytes navigate by compass: roles of PI3Kgamma and its lipid products. *Trends Cell Biol.* **10,** 466–473.
12. Wang, F., Herzmark, P., Weiner, O. D., Srinivasan, S., Servant, G., and Bourne, H. R. (2002) Lipid products of PI(3)Ks maintain persistent cell polarity and directed motility in neutrophils. *Nat. Cell Biol.* **4,** 513–518.
13. Weiner, O. D., Neilsen, P. O., Prestwich, G. D., Kirschner, M. W., Cantley, L. C., and Bourne, H. R. (2002) A PtdInsP(3)- and Rho GTPase-mediated positive feedback loop regulates neutrophil polarity. *Nat. Cell Biol.* **4,** 509–513.
14. Kuspa, A. and Loomis, W. F. (1992) Tagging developmental genes in Dictyostelium by restriction enzyme- mediated integration of plasmid DNA. *Proc. Natl. Acad. Sci. USA* **89,** 8803–8807.
15. Robinson, D. N. and Spudich, J. A. (2000) Dynacortin, a genetic link between equatorial contractility and global shape control discovered by library complementation of a *Dictyostelium discoideum* cytokinesis mutant. *J. Cell Biol.* **150,** 823–838.
16. van Es, S. and Devreotes, P. N. (1999) Molecular basis of localized responses during chemotaxis in amoebae and leukocytes. *Cell. Mol. Life Sci.* **55,** 1341–1351.
17. Sutoh, K. (1993) A transformation vector for *Dictyostelium discoideum* with a new selectable marker bsr. *Plasmid* **30,** 150–154.
18. Kuwayama, H., Obara, S., Morio, T., Katoh, M., Urushihara, H., and Tanaka, Y. (2002) PCR-mediated generation of a gene disruption construct without the use of DNA ligase and plasmid vectors. *Nucleic Acids Res.* **30,** E2.
19. Blaauw, M., Linskens, M. H., and van Haastert, P. J. (2000) Efficient control of gene expression by a tetracycline-dependent transactivator in single *Dictyostelium discoideum* cells. *Gene* **252,** 71–82.

9

Conditional Transgenic Models to Study Chemokine Biology

Sergio A. Lira, Borna Mehrad, Shu-Cheng Chen, Petronio Zalamea, David J. Kinsley, Maria T. Wiekowski, Elizabeth Coronel, Galya Vassileva, Denise Manfra, and Kristian K. Jensen

1. Introduction

Leukocyte migration is a crucial component of defense against many infections and in the pathogenesis of multiple inflammatory disorders. Therefore, the elucidation of the mechanisms responsible for leukocyte recruitment is critical for the development of novel therapeutic approaches for these conditions. Among the molecules implicated in regulating leukocyte trafficking are the chemokines, low-molecular-weight secreted molecules that interact with G-protein-coupled receptors. Evidence supporting an important role for chemokines in leukocyte migration derives from studies employing (1) in vitro chemotaxis assays ***(1–4)***, (2) in vivo chemotaxis assays involving administration of exogenous recombinant mediators into a body cavity ***(5)***, (3) animal models of disease ***(6–10)***, and (4) transgenic models ***(11)***. Although critical to our understanding of these processes, both in vitro and in vivo chemotaxis assays are limited because they do not fully reproduce the complex environment of healthy or diseased tissues. On the other hand, the myriad perturbations in the biochemical and physical microenvironment of diseased tissue, including the expression of multiple mediators, changes in the characteristics of resident cells, and the influx of inflammatory cells, make it difficult to discern the role of a single mediator. In this context, studies on genetically engineered mice are uniquely positioned to examine the biology of both ligands and receptors in the environment of the relevant tissue without the confounding influence of coexisting disease.

From: *Methods in Molecular Biology, vol. 239: Cell Migration in Inflammation and Immunity*
Edited by: D. D'Ambrosio and F. Sinigaglia

Genetically engineered mice have helped to delineate an important role for chemokines in guiding leukocyte migration and homing (reviewed in **ref. *11***). Homing and inflammatory trafficking of specific leukocyte subsets are severely disrupted in mice lacking chemokines or chemokine receptors (loss-of-function mutants, or knockout mice) ***(12–19)***. Mice overexpressing chemokines (transgenic mice) have also been generated and proven to be important in defining the biological roles of some chemokines. For instance, tissue-specific expression of the murine chemokines KC and JE (mMCP-1) induces recruitment of neutrophils and monocytes, respectively, to the expressing tissues ***(20–25)***. These results show that these chemokines are sufficient to trigger the mechanisms responsible for tissue infiltration of these two leukocyte subsets.

Despite significant contributions to our understanding of chemokine biology, the genetic approaches used so far are not perfect because, in many cases, they do not allow for a dynamic analysis of chemokine biology. Chemokines and chemokine receptors show a significant diversity in their spatial and temporal patterns of expression. Some chemokines are constitutively expressed at high levels in some tissues. For instance, the chemokine CCL21 (SLC, 6Ckine) is highly expressed in lymphoid tissues and the chemokine (CX3CL1) fractalkine is highly expressed in the brain. Chemokines, such as the murine chemokines KC and JE, are expressed at low or negligible levels, but can be highly induced by inflammatory stimuli. Other chemokines, such as CCL20 (MIP-3a), are constitutively expressed in some tissues (Peyer's patches and spinal cord), but can be induced in other tissues (lymph nodes) by inflammatory mediators such as lipopolysaccharide (LPS) ***(26)***. Chemokine receptors are also expressed in a complex manner. A given leukocyte subset can express different sets of receptors depending on developmental and environmental cues. A program for chemokine-receptor expression has been well documented for T-cells and dendritic cells ***(27)***. The exquisite pattern of expression of chemokines and their receptors suggests that the ability of these molecules to exert their biological effects may be highly context dependent.

The ability to reproduce or to subvert the patterns of chemokine expression in a living organism may offer unique insights into the biology of the chemokine system. In this chapter, we will describe novel genetic technologies to study the chemokine system in vivo. These technologies will provide for better control of chemokine or chemokine-receptor expression in vivo and for a better understanding of how the chemokine system works.

2. Conditional Systems for Expression of Transgenes

Conventional transgenic approaches have proven to be useful in defining the functional role of chemokines and chemokine receptors ***(11)***. However, constitutive overexpression of chemokines does not mimic the physiological nature

of chemokine expression, which is characterized by tightly controlled spatial and temporal expression. In recent years, conditional genetic systems have been developed for conditional ablation or expression of particular genes. In this chapter, we will review the approaches for conditional expression of chemokines using transgenesis.

The earliest attempts to develop systems for conditional transgenic expression utilized the inherent responsiveness of certain promoters to various stimuli, such as heat shock, heavy metals, and steroid hormones, but these systems generally suffered from pleiotropic effects of the stimuli and high basal levels of activity ***(28)***. Prokaryotic organisms have evolved the ability to respond to changes in the molecular composition of the environment by linking transcriptional activity of specific genomic elements to the presence of specific nutrient or toxins, the *lac* operon of *Escherichia coli* being the classical example. Bujard and Gossen used regulatory elements of the *E. coli* tetracycline-resistance system to generate an eukaryotic conditional expression system, which has since revolutionized conditional transgenic expression ***(29)***.

In the *E. coli* tetracycline-resistance system, the tetracycline repressor protein (tetR) negatively regulates transcription of resistance-mediating genes ***(29)***. Tetracycline binds to tetR, which is then released from the tetracycline operator (tetO), allowing transcription of these genes. By fusing tetR and the herpes simplex virus-encoded transcription factor VP16 and combining a cytomegalovirus (CMV)-derived minimal promoter and the tetO sequence (*see* **Fig. 1A**), Bujard and Gossen elegantly transformed a prokaryotic repressor system into an eukaryotic tetracycline-controlled activator system ***(29)***. The functionality of this system in eukaryotic cells was demonstrated using HeLa cells stably expressing the tetR/VP16-fusion protein (termed the tetracycline-controlled transactivator, tTA) ***(29)***. These cells were transfected with a plasmid containing the luciferase-encoding gene downstream of the tetO/minimal CMV promoter element (the tet-responsive element, TRE). In the presence of tetracycline, the luciferase activity was low or undetectable. However, upon tetracycline withdrawal, luciferase activity was enhanced more than 100,000-fold. Furthermore, luciferase activity could be regulated over five orders of magnitude, depending on the tetracycline concentration.

Recently, the tetracycline-inducible system was made more versatile by the development of the reverse tetracycline-controlled transactivator (rtTA). A novel transactivator, capable of tetracycline binding to the tetO sequences, was developed. This activator differs from tTA by only four amino acids. This novel system is conventionally referred to as the "tet-on" system (*see* **Fig. 1B**) ***(30)***. An advantage of the "tet-on" system is the faster induction of target gene expression compared to tTA-driven "tet-off" system, which requires clearance of tetracycline before full induction is achieved.

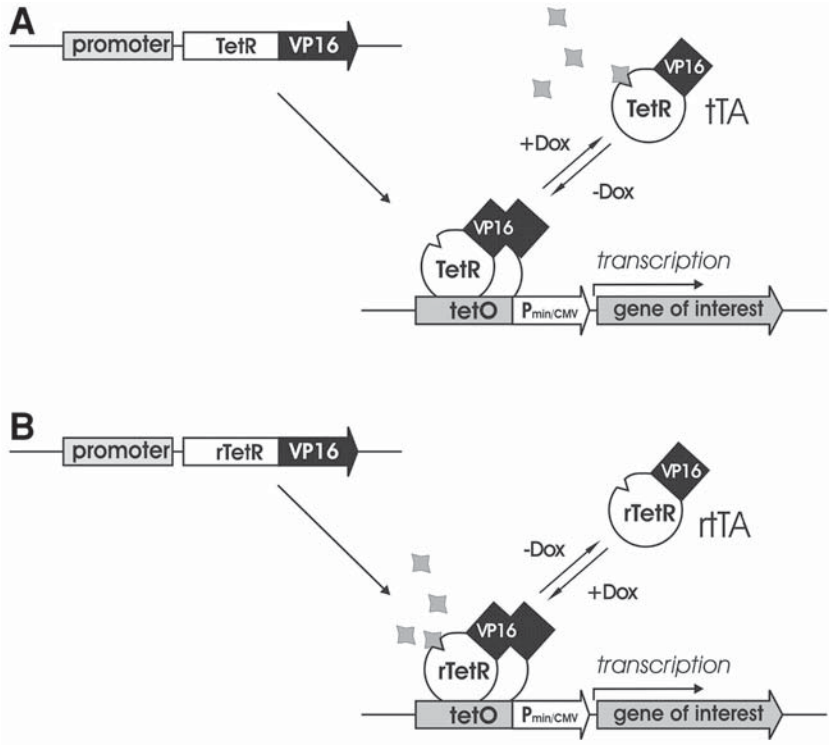

Fig. 1. The tetracycline-dependent system for gene expression in eukaryotic cells. (**A**) Tetracycline inducibility is based on two regulatory elements derived from the *E. coli* tetracycline-resistance operon: the Tet repressor protein (tetR) and the tetracycline operator DNA sequence (tetO). tetR contains binding sites for tetO and tetracycline. Tetracycline binding induces conformational changes in tetR, releasing it from tetO. tTA is a fusion of tetR and the viral transcription factor VP16. In the absence of tetracycline or its derivative doxycycline (dox), tTA binds tetO and promotes transcription via VP16 and the minimal promoter. In the presence of dox, the tetR/VP16 fusion protein (tTA) is released and transcription is stopped. (**B**) Four amino acid changes to TetR alter its ability to bind tetO and create the reverse TetR (rTetR). The VP16 fusion protein (rtTA) activates transcription from the minimal promoter only in the presence of dox.

The use of the tetracycline-inducible system in mice requires a binary transgenic mouse system. Traditionally, two independent transgenic strains are generated, one carrying the tTA or rtTA, often called the activator line, and the gene of interest under control of the tet-responsive element, usually referred to as the reporter line (*see* **Fig. 2**). Crossing of the two lines generates double transgenic mice, in which transgene expression can be controlled by tetracycline

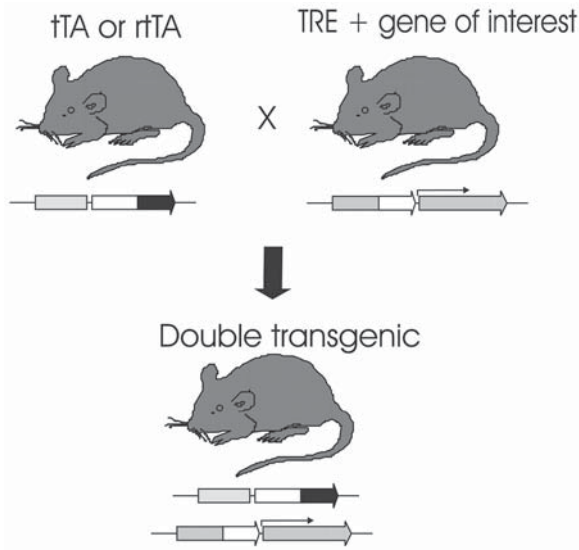

Fig. 2. Transgenic application of the tetracycline-dependent expression system. Two independent transgenic strains are generated: One is carrying the tTA or rtTA under transcriptional control of a promoter of choice, and the other is carrying the gene of interest under control of the tet-responsive element (TRE). Crossing the two lines generates double transgenic mice, in which transgene expression can be controlled by the administration of tetracycline or its derivatives.

administration. Initial studies in mice transgenic for tTA or rtTA crossed with luciferase reporter mice demonstrated the power of the tetracycline-inducible system in controlling transgenic expression in mice ***(31,32)***. In selected lines, expression could be induced up to 100,000-fold in certain tissues by administrating doxycycline, a tetracycline analog more effective in regulating tTA- and rtTA-binding properties. Furthermore, when using rtTA as an inducer, kinetic studies showed significant induction within hours of doxycycline administration. However, these studies also revealed some drawbacks to the system. In many lines, significant background levels of luciferase activity could be observed, indicating leakiness in the system.

Recently, a second generation of tetracycline-controlled transactivators with lower basal activity and codon optimization for mammalian expression has been reported ***(33)***. These novel transactivators carry different mutations compared to rtTA, but retain doxycycline dependency for binding to tetO. These modified versions of rtTA show tighter regulation of gene expression and enhanced sensitivity to doxycycline both in vitro and in vivo ***(33)***, but their usefulness has not yet been evaluated in transgenic mice.

3. Development of a Ubiquitous Conditional System for Chemokine Expression

To better understand the mechanisms regulating leukocyte recruitment in vivo, we have applied conditional transgenesis to study the function of the murine CXC chemokine KC. KC is a murine immediate early gene ***(34,35)***, whose expression is low or undetectable in most tissues ***(5,35,36)***. KC expression is highly upregulated in vitro and in vivo by a variety of factors, such as LPS, platelet-derived growth factor (PDGF), and bombesin ***(5,35,37–40)***. Similar to its human relatives Gro/MGSA (CXCL1) and interleukin (IL)-8 (CXCL8), KC is a potent inducer of neutrophil migration in vitro and in vivo ***(5)***. In humans, these molecules promote neutrophil chemotaxis via their interaction with the receptors CXCR1 and CXCR2, but only one such receptor, CXCR2, has been identified thus far in the mouse ***(38,39,41,42)***. We have previously developed transgenic animals expressing KC in the skin, thymus, lung, and brain and shown that its expression is sufficient to promote neutrophil recruitment to these tissues ***(24,25,43)***. However, the nonphysiological, high constitutive expression of this ligand since early fetal life represented an important shortcoming of these models. In fact, the nonphysiological expression of KC over a prolonged period was associated with a decrease in the number of recruited neutrophils in mice expressing KC specifically in the lung and thymus ***(43)***. Thus, chronic transgenic expression of KC apparently attenuated the mechanisms involved in the recruitment of neutrophils, precluding an assessment of its physiological role. These findings clearly defined the need for transgenic models that more closely mimicked the physiologic expression of KC, in particular, and of other inducible chemokines, in general.

To generate transgenic mice in which expression of KC could be induced conditionally, we used the "tet-on" tetracycline-dependent gene expression system described by Bujard ***(29)*** and discussed earlier. The activator transgene was driven by the CMV enhancer/β-actin promoter (*see* **Fig. 3**), which promotes expression of transgenes in multiple tissues ***(44,45)***. All lines generated expressed the activator transgene. One line was selected for expansion ***(36)***. In this selected line, the activator transgene was expressed at high levels in skeletal muscle and heart, at lower levels in skin, kidney, thymus, and lung, and at low levels in spleen and liver.

Four independent lines of transgenic mice were generated carrying the reporter transgene. This transgene contained the tet-responsive element (TRE) and two genes in opposite direction, KC and β-galactosidase (β-gal) (*see* **Fig. 3**). Because this transgene carried only minimal promoter sequences, it should not be expressed significantly. Indeed, analysis of multiple tissues (bladder, bone, brain, esophagus, heart, kidney, liver, lung, muscle, pancreas, skin, spleen, stomach, thymus,

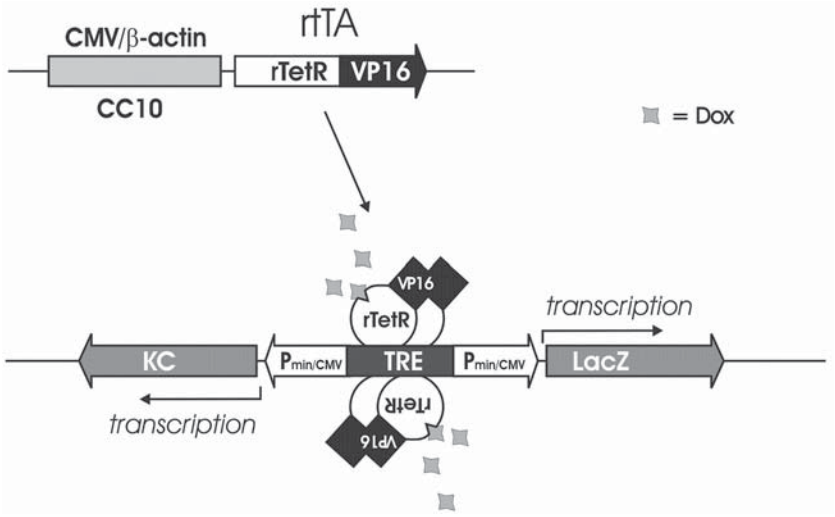

Fig. 3. Activator and reporter transgenes used for tetracycline-dependent expression of KC and β-galactosidase (LacZ). Combining tetO with two identical cytomegalovirus-derived minimal promoters in opposite directions creates a bidirectional, tetracycline-dependent expression system. Here, we describe the use of two activator transgenes: One utilizes the CMV/β-actin promoter targeting expression of rtTA to multiple tissues and the other contains the lung-specific CC10 promoter. Transgenic mice carrying either of the activator transgenes were crossed to a reporter line carrying both KC and β-galactosidase genes.

and trachea) from these animals showed that most tissues did not express β-galactosidase ***(36)***. Few positive cells were detected in the intestine and stomach of the transgenic mice, but similar staining was also detected in wild-type mice. The only site where β-gal staining was specific in these transgenic mice was the brain. The staining, however, was of very low intensity and restricted to a few scattered cells. These results suggested that, at least in these transgenic lines, there was no significant "leakage" in the expression of the "reporter" transgene. Reporter and activator lines were intercrossed and double transgenic mice were obtained.

Treatment of the double transgenic mice with increasing doses of doxycycline (dox) caused a significant increase in the blood levels of KC. The highest levels of KC were detected in circulation 24 after an ip injection of 500 μg of dox. Using this dose, we performed a kinetic analysis of the response and found that within 2 h of injection, the average concentration KC in the serum was 10-

fold higher than baseline (from 0.1 ± 0.01 to 1.1 ± 0.71 ng/mL). After 24 h of treatment, the serum KC levels were extremely elevated (approx 2000-fold over baseline). After this time, the concentration of KC declined steadily, reaching baseline levels 7 d after treatment. Thus, injection of a single dose of doxycycline resulted in a rapid, strong and reversible induction of KC gene expression.

We mapped the expression of the reporter transgene at the tissue and cellular level by examining β-gal activity in tissues from doxycycline-treated and untreated transgenic mice. β-gal activity was not detected in the majority of the rtTa expressing tissues in the absence of doxycycline (*see* **Table 1**). In contrast, β-gal activity was easily detected in 27 out of the 32 tissues tested 24 h after dox treatment (500 μg intraperitoneally). The highest expressing tissues were skeletal muscle, pancreas, prostate, liver, and seminal vesicles (*see* **Table 1**). In some organs, β-gal expression was restricted to morphologically defined areas such as the cortex of the kidney, the exocrine pancreas, the epithelial lining of the stomach, and the epithelium of the small and large intestines. In tissues like skeletal muscle, tongue, and heart, a mosaic pattern of transgene expression could be clearly appreciated. In the thymus, spleen, bone marrow, and brain (not shown), β-gal activity was low or absent, despite expression of the activator transgene. β-gal expression was thus detected in most of the transgenic tissues expressing the activator transgene after, but not before, doxycycline treatment. However, β-gal was not expressed in all tissues in which the activator transgene was expressed. For instance, β-gal expression was minimal or not detected in lymphoid tissues, in lung, or in the brain, tissues where low but detectable expression of the activator transgene was demonstrated. The lack of β-gal expression in these settings could have been caused by low levels of rtTa protein or by other tissue-specific transcriptional requirements. As expected, there was very good concordance between β-gal and KC expression. Both genes were found to be expressed at high levels in skeletal muscle, liver, heart, kidney, and skin, expressed at low levels in thymus and lung, and not expressed in the spleen.

The most interesting finding of this study was that despite high KC expression in many tissues and increased numbers of neutrophils in circulation, no neutrophil infiltration could be detected in any of the expressing tissues ***(36)***. This finding suggested that neutrophil migration from the bloodstream into tissue parenchyma was impaired. This could be caused by a general deficit in neutrophil function or by the production of a biologically defective KC. To investigate whether the KC produced in the transgenic tissues was biologically active, we performed skin-grafting experiments. We used β-gal expression to mark the grafted cells because we had previously shown that it was expressed in skin upon doxycycline treatment. After the grafts had healed, the host animals were treated with doxycycline, and 48 h later, biopsies were taken encompassing

Table 1
Expression of β-Gal in Tissues of Wild-Type and Transgenic Mice in the Presence or Absence of dox

Tissue	WT + dox	CMTKC – dox	CMTKC + dox
Adrenal gland	–	–	++
Aorta	–	–	+
Bone, marrow (femur)	–	–	–
Bone, marrow (sternum)	–	–	–
Brain	–	+/–	+
Cervix	–	+	+
Eye	–	–	–
Gallbladder	–	–	++
Heart	–	–	++/+++
Intestine (large)	+	+	++
Intestine (small)	–	–	++
Kidney	–	–	+++
Lymph node	–	–	–
Liver	–	–	+++
Lung	–	–	+
Muscle	–	–	+++/++++
Ovary	–	–	+
Pancreas	–	–	+++
Pituitary	–	–	+
Prostate	–	–	+++
Salivary gland	–	–	+
Seminal vesicle	–	–	+++
Skin	–	–	++
Spleen	N/A	N/A	+/–
Spine	–	–	–
Stomach	+/–	+/–	++
Testes	–	–	+
Thymus	N/A	N/A	+
Thyroid	–	–	–
Tongue	–	–	++/+++
Trachea	–	–	+
Uterus	–	–	–
Vagina	–	–	+

Key: –: negative or only a couple of faintly stained cells; +: lightly or punctate staining or a few strongly stained cells; ++: light overall staining or moderate to strong staining in restricted area of the tissue; +++: moderate to strong overall staining or very strong staining in restricted area of the tissue; ++++: very strong overall staining as seen in pancreas.

the graft and surrounding tissue. β-gal expression was visualized in the grafted transgenic skin, but not in the surrounding host skin. Interestingly, neutrophils readily accumulated within the grafted, but not the adjacent host skin. This process was specific to the grafted skin from double transgenic mice and was not observed in grafted control skin (derived from ROSA mice) expressing β-gal. These results indicated that the KC produced by the transgenic tissues was biologically active and confirmed previous studies showing that tissue-specific, local production of this chemokine leads to neutrophil infiltration.

The paradoxical absence of neutrophil infiltration in mice expressing KC in multiple tissues could be the result of a general defect in the ability of the transgenic neutrophils to migrate. To test this hypothesis, we promoted expression of neutrophil chemoatractants by injection of LPS in a subcutaneous air pouch in transgenic mice with or without doxycycline treatment. LPS is by itself a potent inducer of neutrophil migration and also induces other neutrophil chemoattractants such as C5a ***(46)***. There was no difference in the number of neutrophils recruited in the pouch, suggesting that the overall capacity of neutrophils to respond to chemoattractants had been preserved, even in the presence of high systemic levels of KC. There was, however, a significant impairment in the response of neutrophils to KC after, but not before, doxycycline treatment. These results indicated again that the transgenic neutrophils were essentially normal before treatment and suggested that they became less capable to migrate toward a localized source of KC after doxycycline treatment. We hypothesized that the high systemic levels of KC were directly causative of the abnormal neutrophil response. In vivo, high levels of circulating chemokines inhibit leukocyte infiltration into tissues. High systemic levels of IL-8 attenuate pro-inflammatory effects of locally administered IL-8 ***(47,48)***, or neutrophilia induced by LPS in the lung ***(49)***. Furthermore, high constitutive expression of MCP-1 or IL-8 in transgenic mice does not result in leukocyte infiltration into the expressing organ or any other organ ***(50,51)***. Moreover, tissue-specific constitutive transgenic expression of KC results over time in the attenuation of neutrophil recruitment ***(43)*** and monocyte recruitment induced by tissue-specific expression of MCP-1 can be abrogated in the presence of high systemic levels of MCP-1 ***(21)***. The reduced ability of leukocytes to migrate from the blood into tissue in these circumstances has been attributed to a number of factors such as shedding of L-selectin, the absence of a chemoattractant gradient, or desensitization of the cognate chemokine receptor ***(21,50,51)***.

We ruled out shedding of L-selectin as a factor contributing to the lack of neutrophil migration in our system, because we found that surface expression of L-selectin on transgenic neutrophils remained constant even after prolonged doxycycline treatment. To further investigate the nature of the defective migration, we examined the possibility that the constitutively high levels of serum

KC had desensitized its receptor, CXCR2, a G-protein-coupled seven-transmembrane receptor ***(39,52)***. Like other GPCRs, the murine CXCR2 receptor induces calcium mobilization and cell migration in response to agonist binding ***(53)***. Freshly isolated transgenic white blood cells were tested for calcium mobilization in response to recombinant KC by calcium fluorometry. The response was greatly reduced in white blood cells derived from doxycycline-treated mice, indicating that the functionality of the CXCR2 receptor was affected by high concentrations of KC. Indeed, induction of transgene expression in multiple tissues resulted in a rapid increase in the levels of circulating KC reaching maximal levels of about 224 ng/mL 24 h after doxycycline injection. In vitro, similar concentrations of neutrophil chemoattracting molecules arrest neutrophil movement ***(53)***. Thus, the neutrophil migration deficit seen in our model could be the result of an uncoupling of the receptor in response to KC binding, leading to desensitization or to increased internalization of the receptor.

4. Development of a Tissue-Specific System for Conditional Chemokine Expression

The lung, the intestine, and the skin are the surfaces of contact with the environment. Many inflammatory processes have been modeled in the lung and a great deal of information is now available about the role of chemokines in lung homeostasis and disease (reviewed in **refs. *54–56***). To better understand the role of chemokines in lung disease, we have recently developed a lung-specific conditional transgenic system ***(57)***. In this set of experiments, the rtTA gene was placed under the control of the CC10 promoter (*see* **Fig. 3**), targeting its expression to a nonciliated subset of airway epithelial cells, known as Clara cells. Previous studies using this promoter have shown the transgene expression to be restricted to the airway epithelium ***(43,58,59)***. We generated eight founder animals carrying the activator transgene and mated them to mice of a reporter line containing the bidirectional transgene encoding β-gal and KC to generate double transgenic mice.

Double transgenic mice were found to have a normal phenotype and longevity. To determine whether transgene expression could be induced in the lung, the transgenic mice were injected intraperitoneally with either doxycycline or saline. After 24 h, animals were sacrificed; the lungs and tracheas were removed and tested for β-gal activity. Macroscopically, lungs and tracheas from doxycycline-treated animals showed strong blue staining when exposed to X-gal, whereas no staining could be detected in organs from saline-treated animals. To test whether doxycycline treatment induced expression of KC, lungs and tracheas of double transgenic animals were removed 24 h after doxycycline injection and homogenized to determine KC concentrations. High concentrations of KC (> 600 ± 100 pg/mg protein and approx 100 ± 10 pg/mg protein, respectively)

were detected in lungs and tracheas of doxycycline-treated double transgenic animals, whereas no KC could be detected in lungs or tracheas of wild-type animals. The highest responder line was selected for additional studies.

To define the kinetics of transgene expression after doxycycline treatment, we determined KC concentrations in the bronchoalveolar lavage (BAL) of double transgenic animals. BAL fluid was collected from wild-type and double transgenic animals before and at 24, 48, and 72 h following a single doxycycline injection (500 µg intraperitoneally). Prior to doxycycline injection, the levels of KC in the BAL of double transgenic animals were equal to those of wild-type controls, but within 24 h of doxycycline injection, KC concentrations in the BAL increased 58-fold over baseline. Thereafter, KC concentrations declined steadily over the subsequent 2 d. These changes in KC expression were not caused by doxycycline alone, because KC could not be detected in the lungs of wild-type mice after doxycycline treatment.

To investigate whether the transgenically expressed KC observed after acute administration of doxycycline was biologically active, we determined the number of neutrophils in the BAL after administration of doxycycline. The number of neutrophils in the BAL of the double transgenic animals increased about eightfold 24 h after doxycycline injection and declined thereafter, closely following the changes in KC expression, thereby demonstrating that doxycycline-induced transgenic KC expression in the lung resulted in an accumulation of KC protein and neutrophils in the lung air space.

To determine the effects of chronic administration of doxycycline, double transgenic animals were fed for 28 d with drinking water containing 2 mg/mL doxycycline. In response to this treatment, the KC concentrations in the BAL increased nearly 200-fold and the number of neutrophils was about 100-fold higher than in untreated controls. Thus, administration of doxycycline in a single injection or through drinking water over a prolonged time resulted in induction of KC expression and neutrophil accumulation in the lung.

The biological result of the conditional expression of KC in the lung was assessed by comparing the lung histology before and after administration of doxycycline. Lungs appeared histologically normal in nontreated double transgenic animals, but showed a marked accumulation of neutrophils around bronchi and bronchioles 24 h after administration of doxycycline. Interestingly, despite the marked accumulation of neutrophils, there was no damage to bronchial and alveolar structures in animals treated with either a single dose or a prolonged course of doxycycline.

5. Discussion

We have now expanded the transgenic approaches used to investigate the biology of chemokines to include the tetracycline-inducible system. Here, we

have given examples of the use of this system to study the biology of KC, a mouse chemokine. Using this system, we have learned that both timing and expression levels are important determinants of the biological activity of this chemokine. We have also been able to verify that KC's primary activity is to recruit neutrophils to the sites where it is produced.

The ubiquitous conditional expressing system has provided us with a tool to investigate the mechanisms underlying inhibition of neutrophil migration associated with high systemic expression of KC. Multiple tissues were shown to express KC, which resulted in high serum levels of this chemokine. Grafting of tissues conditionally expressing KC into Rag1 –/– mice established that the KC was biologically active to promote neutrophil recruitment into the grafts, confirming previous studies ***(24,25)***. In the presence of high systemic levels of KC, we found an impaired neutrophil response to KC and identified desensitization of CXCR2 as a mechanism to explain the migration defect. It is likely that high expression of KC or other CXCR2 ligands will attenuate or reduce neutrophil infiltration during pathological situations and profoundly impact host responses. Thus, by conditionally promoting the expression of KC in several tissues and by inducing its expression in a localized graft, we were able to demonstrate that KC's biological properties depend on the way in which it is produced. The ability to regulate gene expression in multiple, transplantable tissues will likely facilitate the analysis of the biological role of KC and other chemokines.

An important and novel feature of the transgenic system described here is the simultaneous expression of β-gal and a specific chemokine (in this case, KC). This provided a rapid, convenient, and highly sensitive screening method to test reporter lines for transgene expression in the absence of rtTA or doxycycline. This reporter line carrying KC and β-gal can be crossed to other transgenic activator lines, and the biological activity of KC can be studied in different tissue contexts. As demonstrated here, crossing of this reporter line with a line expressing the activator specifically in the lung resulted in mice expressing KC conditionally in the lung. Upon doxycycline treatment, β-gal expression was detected in cells lining the airways. Conditional expression of KC specifically in lung resulted in accumulation of neutrophils in the interstitium and the air space. Despite the accumulation of neutrophils in these tissues, we failed to detect tissue damage. Similarly, in transgenic models, KC had been constitutively expressed because early fetal life tissue damage was absent despite the accumulation of neutrophils ***(24,43)***. However, under those circumstances, neutrophil migration and activation could have been affected by continuous exposure to KC. Using the conditional system described in this chapter, we now confirm that KC functions primarily as a neutrophil-attracting chemokine that by itself does not activate neutrophils. These transgenic studies are in contrast to others where administration of recombinant KC or its functional human analog

IL-8 caused neutrophil activation, characterized by the induction of a respiratory burst and release of storage enzymes damaging the surrounding tissue ***(60)***. However, under these conditions, other inflammatory factors could have been produced in response to the trauma caused by the injection itself, contributing to the activation of the recruited neutrophils. This highlights the final and perhaps most important advantage of the transgenic approach: The conditional system is minimally invasive, allowing for reduction in the number of variables associated with classical injection approaches.

In summary, we generated bigenic conditional systems for expression of chemokines ubiquitously and in a lung-specific fashion. These systems are modular and allow for expression of any chemokine or cytokine upon administration of doxycycline. Using these conditional systems, we established that the CXC chemokine KC primarily chemoattracts, but not activates, neutrophils and that its high, systemic expression inhibits neutrophil mobilization. The development of these different conditional models should greatly facilitate the analysis of the mechanisms by which KC affects neutrophil migration in vivo.

References

1. Baggiolini, M., Walz, A., and Kunkel, S. L. (1989) Neutrophil-activating peptide-1/interleukin 8, a novel cytokine that activates neutrophils. *J. Clin. Invest.* **84,** 1045–1049.
2. Richardson, M. D. and Patel, M. (1995) Stimulation of neutrophil phagocytosis of *Aspergillus fumigatus conidia* by interleukin-8 and *N*-formylmethionyl-leucyl-phenylalanine. *J. Med. Vet. Mycol.* **33,** 99–104.
3. Thelen, M., Peveri, P., Kernen, P., von Tscharner, V., Walz, A., and Baggiolini, M. (1988) Mechanism of neutrophil activation by NAF, a novel monocyte-derived peptide agonist. *FASEB J.* **2,** 2702–2706.
4. Wolpe, S. D., Sherry, B., Juers, D., Davatelis, G., Yurt, R. W., and Cerami, A. (1989) Identification and characterization of macrophage inflammatory protein 2. *Proc. Natl. Acad. Sci. USA* **86,** 612–616.
5. Bozic, C. R., Kolakowski, L. F. Jr., Gerard, N. P., et al. (1995) Expression and biologic characterization of the murine chemokine KC. *J. Immunol.* **154,** 6048–6057.
6. Broaddus, V. C., Boylan, A. M., Hoeffel, J. M., et al. (1994) Neutralization of IL-8 inhibits neutrophil influx in a rabbit model of endotoxin-induced pleurisy. *J. Immunol.* **152,** 2960–2967.
7. Greenberger, M. J., Strieter, R. M., Kunkel, S. L., et al. (1996) Neutralization of macrophage inflammatory protein-2 attenuates neutrophil recruitment and bacterial clearance in murine Klebsiella pneumonia. *J. Infect. Dis.* **173,** 159–165.
8. Huang, S., Paulauskis, J. D., Godleski, J. J., and Kobzik, L. (1992) Expression of macrophage inflammatory protein-2 and KC mRNA in pulmonary inflammation. *Am. J. Pathol.* **141,** 981–988.

9. Kooguchi, K., Hashimoto, S., Kobayashi, A., et al. (1998) Role of alveolar macrophages in initiation and regulation of inflammation in *Pseudomonas aeruginosa* pneumonia. *Infect. Immun.* **66,** 3164–3169.
10. Sekido, N., Mukaida, N., Harada, A., Nakanishi, I., Watanabe, Y., and Matsushima, K. (1993) Prevention of lung reperfusion injury in rabbits by a monoclonal antibody against interleukin-8. *Nature* **365,** 654–657.
11. Lira, S. A. (1999) Lessons from gene modified mice. *Forum (Genova)* **9,** 286–298.
12. Boring, L., Gosling, J., Chensue, S. W., et al. (1997) Impaired monocyte migration and reduced type 1 (Th1) cytokine responses in C–C chemokine receptor 2 knockout mice. *J. Clin. Invest.* **100,** 2552–2561.
13. Boring, L., Gosling, J., Cleary, M., and Charo, I. F. (1998) Decreased lesion formation in CCR2–/– mice reveals a role for chemokines in the initiation of atherosclerosis. *Nature* **394,** 894–897.
14. Cook, D. N., Prosser, D. M., Forster, R., et al. (2000) CCR6 mediates dendritic cell localization, lymphocyte homeostasis, and immune responses in mucosal tissue. *Immunity* **12,** 495–503.
15. Forster, R., Mattis, A. E., Kremmer, E., Wolf, E., Brem, G., and Lipp, M. (1996) A putative chemokine receptor, BLR1, directs B cell migration to defined lymphoid organs and specific anatomic compartments of the spleen. *Cell* **87,** 1037–1047.
16. Forster, R., Schubel, A., Breitfeld, D., et al. (1999) CCR7 coordinates the primary immune response by establishing functional microenvironments in secondary lymphoid organs. *Cell* **99,** 23–33.
17. Gao, J. L., Wynn, T. A., Chang, Y., et al. (1997) Impaired host defense, hematopoiesis, granulomatous inflammation and type 1–type 2 cytokine balance in mice lacking CC chemokine receptor 1. *J. Exp. Med.* **185,** 1959–1968.
18. Gosling, J., Slaymaker, S., Gu, L., et al. (1999) MCP-1 deficiency reduces susceptibility to atherosclerosis in mice that overexpress human apolipoprotein B. *J. Clin. Invest.* **103,** 773–778.
19. Gu, L., Okada, Y., Clinton, S. K., et al. (1998) Absence of monocyte chemoattractant protein-1 reduces atherosclerosis in low density lipoprotein receptor-deficient mice. *Mol. Cell* **2,** 275–281.
20. Fuentes, M. E., Durham, S. K., Swerdel, M. R., et al. (1995) Controlled recruitment of monocytes and macrophages to specific organs through transgenic expression of monocyte chemoattractant protein-1. *J. Immunol.* **155,** 5769–5776.
21. Grewal, I. S., Rutledge, B. J., Fiorillo, J. A., et al. (1997) Transgenic monocyte chemoattractant protein-1 (MCP-1) in pancreatic islets produces monocyte-rich insulitis without diabetes: abrogation by a second transgene expressing systemic MCP-1. *J. Immunol.* **159,** 401–408.
22. Gunn, M. D., Nelken, N. A., Liao, X., and Williams, L. T. (1997) Monocyte chemoattractant protein-1 is sufficient for the chemotaxis of monocytes and lymphocytes in transgenic mice but requires an additional stimulus for inflammatory activation. *J. Immunol.* **158,** 376–383.

23. Kolattukudy, P. E., Quach, T., Bergese, S., et al. (1998) Myocarditis induced by targeted expression of the MCP-1 gene in murine cardiac muscle. *Am. J. Pathol.* **152,** 101–111.
24. Lira, S. A., Zalamea, P., Heinrich, J. N., et al. (1994) Expression of the chemokine N51/KC in the thymus and epidermis of transgenic mice results in marked infiltration of a single class of inflammatory cells. *J. Exp. Med.* **180,** 2039–2048.
25. Tani, M., Fuentes, M. E., Peterson, J. W., et al. (1996) Neutrophil infiltration, glial reaction, and neurological disease in transgenic mice expressing the chemokine N51/KC in oligodendrocytes. *J. Clin. Invest.* **98,** 529–539.
26. Tanaka, Y., Imai, T., Baba, M., et al. (1999) Selective expression of liver and activation-regulated chemokine (LARC) in intestinal epithelium in mice and humans. *Eur. J. Immunol.* **29,** 633–642.
27. D'Ambrosio, D., Iellem, A., Bonecchi, R., et al. (1998) Selective up-regulation of chemokine receptors CCR4 and CCR8 upon activation of polarized human type 2 Th cells. *J. Immunol.* **161,** 5111–5115.
28. Gossen, M., Bonin, A. L., and Bujard, H. (1993) Control of gene activity in higher eukaryotic cells by prokaryotic regulatory elements. *Trends Biochem. Sci.* **18,** 471–475.
29. Gossen, M. and Bujard, H. (1992) Tight control of gene expression in mammalian cells by tetracycline-responsive promoters. *Proc. Natl. Acad. Sci. USA* **89,** 5547–5551.
30. Gossen, M., Freundlieb, S., Bender, G., Muller, G., Hillen, W., and Bujard, H. (1995) Transcriptional activation by tetracyclines in mammalian cells. *Science* **268,** 1766–1769.
31. Furth, P. A., St. Onge, L., Boger, H., et al. (1994) Temporal control of gene expression in transgenic mice by a tetracycline-responsive promoter. *Proc. Natl. Acad. Sci. USA* **91,** 9302–9306.
32. Kistner, A., Gossen, M., Zimmermann, F., et al. (1996) Doxycycline-mediated quantitative and tissue-specific control of gene expression in transgenic mice. *Proc. Natl. Acad. Sci. USA* **93,** 10,933–10,938.
33. Urlinger, S., Baron, U., Thellmann, M., Hasan, M. T., Bujard, H., and Hillen, W. (2000) Exploring the sequence space for tetracycline-dependent transcriptional activators: novel mutations yield expanded range and sensitivity. *Proc. Natl. Acad. Sci. USA* **97,** 7963–7968.
34. Oquendo, P., Alberta, J., Wen, D. Z., Graycar, J. L., Derynck, R., and Stiles, C. D. (1989) The platelet-derived growth factor-inducible KC gene encodes a secretory protein related to platelet alpha-granule proteins. *J. Biol. Chem.* **264,** 4133–4137.
35. Ryseck, R. P., MacDonald-Bravo, H., Mattei, M. G., and Bravo, R. (1989) Cloning and sequence of a secretory protein induced by growth factors in mouse fibroblasts. *Exp. Cell Res.* **180,** 266–275.
36. Wiekowski, M. T., Chen, S. C., Zalamea, P., et al. (2001) Disruption of neutrophil migration in a conditional transgenic model: evidence for CXCR2 desensitization in vivo. *J. Immunol.* **167,** 7102–7110.

37. Zullo, J. N., Cochran, B. H., Huang, A. S., and Stiles, C. D. (1985) Platelet-derived growth factor and double-stranded ribonucleic acids stimulate expression of the same genes in 3T3 cells. *Cell* **43,** 793–800.
38. Suzuki, H., Prado, G. N., Wilkinson, N., and Navarro, J. (1994) The N terminus of interleukin-8 (IL-8) receptor confers high affinity binding to human IL-8. *J. Biol. Chem.* **269,** 18,263–18,268.
39. Lee, J., Cacalano, G., Camerato, T., Toy, K., Moore, M. W., and Wood, W. I. (1995) Chemokine binding and activities mediated by the mouse IL-8 receptor. *J. Immunol.* **155,** 2158–2164.
40. Cochran, B. H., Reffel, A. C., and Stiles, C. D. (1983) Molecular cloning of gene sequences regulated by platelet-derived growth factor. *Cell* **33,** 939–947.
41. Harada, A., Kuno, K., Nomura, H., Mukaida, N., Murakami, S., and Matsushima, K. (1994) Cloning of a cDNA encoding a mouse homolog of the interleukin-8 receptor. *Gene* **142,** 297–300.
42. Bozic, C. R., Gerard, N. P., von Uexkull-Guldenband, C., et al. (1994) The murine interleukin 8 type B receptor homologue and its ligands. Expression and biological characterization. *J. Biol. Chem.* **269,** 29,355–29,358.
43. Lira, S. A., Fuentes, M. E., Strieter, R. M., and Durham, S. K. (1997) Transgenic methods to study chemokine function in lung and central nervous system. *Methods Enzymol.* **287,** 304–318.
44. Okabe, M., Ikawa, M., Kominami, K., Nakanishi, T., and Nishimune, Y. (1997) "Green mice" as a source of ubiquitous green cells. *FEBS Lett.* **407,** 313–319.
45. Manfra, D. J., Chen, S. C., Yang, T. Y., et al. (2001) Leukocytes expressing green fluorescent protein as novel reagents for adoptive cell transfer and bone marrow transplantation studies. *Am. J. Pathol.* **158,** 41–47.
46. Kalmar, J. R. and Van Dyke, T. E. (1994) Effect of bacterial products on neutrophil chemotaxis. *Methods Enzymol.* **236,** 58–87.
47. Van Zee, K. J., Fischer, E., Hawes, A. S., et al. (1992) Effects of intravenous IL-8 administration in nonhuman primates. *J. Immunol.* **148,** 1746–1752.
48. Hechtman, D. H., Cybulsky, M. I., Fuchs, H. J., Baker, J. B., and Gimbrone, M. A. Jr. (1991) Intravascular IL-8. Inhibitor of polymorphonuclear leukocyte accumulation at sites of acute inflammation. *J. Immunol.* **147,** 883–892.
49. Blackwell, T. S., Lancaster, L. H., Blackwell, T. R., Venkatakrishnan, A., and Christman, J. (1999) Chemotactic gradients predict neutrophilic alveolitis in endotoxin-treated rats. *Am. J. Respir. Crit. Care Med.* **159,** 1644–1652.
50. Simonet, W., Hughes, T., Nguyen, H., Trebasky, L., Danilenko, D., and Medlock, E. (1994) Long-term impaired neutrophil migration in mice overexpressing human interleuklin-8. *J. Clin. Invest.* **94,** 1310–1319.
51. Rutledge, B. J., Rayburn, H., Rosenberg, R., et al. (1995) High level monocyte chemoattractant protein-1 expression in transgenic mice increases their susceptibility to intracellular pathogens. *J. Immunol.* **155,** 4838–4843.
52. Cacalano, G., Lee, J., Kikly, K., et al. (1994) Neutrophil and B cell expansion in mice that lack the murine IL-8 receptor homolog. *Science* **265,** 682–684.

53. McColl, S. R. and Clark-Lewis, I. (1999) Inhibition of murine neutrophil recruitment in vivo by CXC chemokine receptor antagonists. *J. Immunol.* **163,** 2829–2835.
54. Lukacs, N. W., Strieter, R. M., Chensue, S. W., and Kunkel, S. L. (1996) Activation and regulation of chemokines in allergic airway inflammation. *J. Leukocyte Biol.* **59,** 13–17.
55. Standiford, T. J. (1997) Cytokines and pulmonary host defenses. *Curr. Opin. Pulm. Med.* **3,** 81–88.
56. Griffiths-Johnson, D. A., Collins, P. D., Jose, P. J., and Williams, T. J. (1997) Animal models of asthma: role of chemokines. *Methods Enzymol.* **288,** 241–266.
57. Mehrad, B., Wiekowski, B. E., Morrison, S. C., et al. (2002) Transient lung-specific expression of the chemokine KC improves outcome in invasive aspergillosis. *Am. J. Respir. Crit. Care Med.* **166,** 1263–1268.
58. Stripp, B. R., Sawaya, P. L., Luse, D. S., et al. (1992) Cis-acting elements that confer lung epithelial cell expression of the CC10 gene. *J. Biol. Chem.* **267,** 14,703–14,712.
59. Sawaya, P. L., Stripp, B. R., Whitsett, J. A., and Luse, D. S. (1993) The lung-specific CC10 gene is regulated by transcription factors from the AP-1, octamer, and hepatocyte nuclear factor 3 families. *Mol. Cell. Biol.* **13,** 3860–3871.
60. Frevert, C. W., Huang, S., Danaee, H., Paulauskis, J. D., and Kobzik, L. (1995) Functional characterization of the rat chemokine KC and its importance in neutrophil recruitment in a rat model of pulmonary inflammation. *J. Immunol.* **154,** 335–344.

10

Intravital Microscopy as a Tool for Studying Recruitment and Chemotaxis

Denise C. Cara and Paul Kubes

1. Introduction

Leukocyte recruitment is a hallmark feature of the inflammatory response, which involves a sequential series of molecular interaction between the leukocyte and endothelial cells. First, leukocytes in the mainstream of blood flow come into contact with the endothelium and they roll along the endothelial surface via a group of molecules termed the selectins ***(1)***. Next, rolling leukocytes are activated by pro-inflammatory molecules presented on the endothelial surface to firmly adhere to the endothelium via integrins. Once adherent, leukocytes emigrate out of the vasculature and respond to directional (chemotactic) stimuli that guide them to the inflammatory source ***(2)***.

Most experiments are done using simple leukocyte recruitment assays where a stimulus is added to a tissue like the peritoneal cavity, and at some delayed time, the number of cells are counted. Although this "black-box-type" experiment provides information regarding whether leukocytes can be recruited, it provides no meaningful insight as to the step at which leukocyte recruitment is impaired. This prompted scientists to begin to use intravital microscopy as a means of visualizing the process of leukocyte recruitment from the mainstream of blood to the vessel wall, out of the vasculature, and through the interstitial space. These types of experiment were extremely useful to help identify, for example, that the selectins were important in rolling, β_2-integrins were important in adhesion, and α_4-integrins (β_1 or β_7) could mediate both rolling and adhesion. However, most of these experiments were performed in tissues that could be easily transilluminated, including the mesentery and cremaster muscle. Although very useful, these tissues may not reflect what may occur in organs like the liver, lung, heart, skin, intestine, and brain. With the availability of

From: *Methods in Molecular Biology, vol. 239: Cell Migration in Inflammation and Immunity*
Edited by: D. D'Ambrosio and F. Sinigaglia

fluorescence microscopy, examination of these other tissues has revealed that they do not behave like the mesentery or cremaster muscle and clearly require examination to provide information in those specific microvascular beds.

Finally, much work has been done on the motility and chemotaxis of leukocytes in vitro, but chemotaxis and migration in tissues has received very little attention. Transillumination of transluscent tissues combined with time-lapse photography can be visualized by intravital microscopy, which allows observations of chemotaxis in vivo. In intravital microscopy experiments, chemoattractants have been used in different ways, including superfusion ***(3–6)***, interstitial microinjection ***(7,8)***, or intravenous injection ***(9)***, although these methods do not generate a gradient of concentration as occurs in natural conditions. A new technique where an agarose gel containing chemoattractant is placed 350 μm from a post-capillary venule can be used. The chemoattractant is released slowly from the gel and establishes a unidirectional chemotactic gradient within the cremaster muscle. This method allows the visualization of directed movement of the cells toward the source of the chemoattractant in vivo. These different intravital microscopy techniques are outlined in this chapter.

2. Materials

1. Ketamine (200 mg/kg).
2. Xylazine (10 mg/kg).
3. Bicarbonate-buffered saline (131.9 m*M* NaCl, 4.7 m*M* KCl, 1.2 m*M* $MgSO_4$, 20 m*M* $NaHCO_3$, pH 7.4).
4. P10 canule.
5. Board with an optically clear viewing pedestal for cremaster preparation.
6. Surgery tools.
7. Cautery.
8. 4-0 Suture thread.
9. Intravital microscope set (microscope with ×25 objective lens and ×10 eyepiece; video camera; TV monitor and time-lapse videocassette recorder).
10. Agarose.
11. Chemokine.
12. Hank's balanced salt solution (HBSS) without fenol red and sodium bicarbonate.

3. Methods

The methods described outline (1) the mouse preparation for intravital microscopy, (2) the surgery for cremaster preparation, (3) preparation of the liver, (4) and the study of chemotaxis using the gel preparation.

3.1. Mouse Preparation for Intravital Microscopy

Male mice are used for intravital observations for the cremaster preparation. The animal is anesthetized with an intraperitoneal injection of a mixture of xyla-

zine and ketamine hydrochloride. Although other anesthetics may be used, this approach generates very steady hemodynamic parameters that are absolutely necessary to avoid blood flow effects on leukocyte recruitment. For all protocols, the left jugular vein is cannulated to administer additional anesthetic or drug if necessary.

3.2. Intravital Microscopy of Cremaster Muscle

It is absolutely essential that the investigator attempt to minimize preparation-induced inflammation. Although it is extremely difficult to eliminate basal rolling at least in part because of the result of surgery, basal adhesion and emigration should be near zero values (*see* **Note 1**). The anesthetized mouse is placed on a board that has circulating warm water running through a milled internal cavity (*see* **Fig. 1**). An incision is made in the scrotal skin to expose the left cremaster muscle, which is then carefully removed from the associated fascia. A lengthwise incision is made on the ventral surface of the cremaster muscle using a cautery. The testicle and the epididymis are separated from the underlying muscle and moved into the abdominal cavity. The muscle is then spread out over an optically clear viewing pedestal and secured along the edges with threads. The exposed tissue is superfused with warm bicarbonate-buffered saline.

3.3. Intravital Microscopy of the Liver

Unlike the cremaster muscle, which has high shear rates in blood vessels, the liver preparation is a portal circulation with lower shear and much more extensive capillary (sinusoid) network. Leukocytes localize not only in the postcapillary venules but also in the sinusoids.

The preparation is similar to that described for the cremaster muscle with respect to the anesthetic. However, the abdomen is opened via a midline incision, the skin and peritoneum are removed close to the costal margin, and the hepatoform ligament is carefully released from the gallbladder. Mice are then placed in a left lateral position on the board and the left lobe of the liver is gently flipped out onto the stage. The liver can be covered with Saran Wrap and the intestines are kept close to the abdomen in their anatomic position and covered with saline-soaked gauze (*see* **Note 2**). Animals are kept warm with a heat lamp. Once the liver is under the intravital microscope, a single postsinusoidal venule with 8–10 μm accompanying sinusoids is located and observed.

Although fluorescence microscopy can be used by adding Rhodamine 6G (0.3 mg/kg), as this dye is taken up almost exclusively by leukocytes, the hepatocytes do have a propensity to take up this dye as well. Although the leukocytes can be distinguished from the hepatocytes, more recently we have used conventional illumination, but used oblique lighting provided by a fiber-optic source

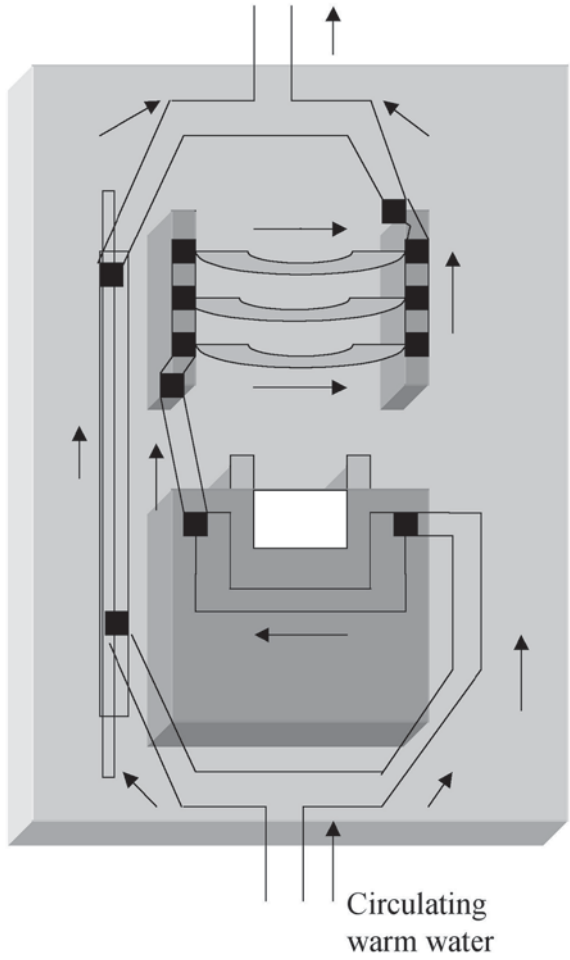

Fig. 1. Design of the board for murine cremaster preparation with circulating warm water.

positioned at about 45° to the optical axis. No fluorescence is required, and the image of the liver microcirculation is much clearer.

3.4. Preparation of Chemokine in Agarose Gel to Induce Chemotaxis

1. Micropipet the chemokine in a desired concentration (e.g., 0.5 µg Keratinocyte-derived Cytokine-KC into a lid of Eppendorf tube).
2. Add a very small amount (approx 2 µL) of Indian ink to enable visualization of the gel on the cremaster muscle.
3. Pipet 10 mL of 2X HBSS into a 50-mL conical tube.
4. Pipet 10 mL of distilled water into a second 50-mL conical tube.

5. Add 0.4 g of agarose powder to distilled water.
6. Heat a beaker of water, until boiling, in a microwave oven.
7. Put HBSS tube into beaker (just to warm up).
8. With the lid loosely screwed on, heat the distilled water with agarose, until boiling (approx 1 min, 10 s), in a microwave oven.
9. Add HBSS to the agarose solution (4% in 10 mL distilled water). Swirl while keeping warm in a beaker.
10. Micropipet 100 µL of solution into the Eppendorf lid (cut very end of the 20- to 200-µL tip).
11. Mix the agarose with the chemokine and dye. Gently, make circles around the lid using a 0.5- to 10-µL tip.
12. Refrigerate.

3.5. Placing the Gel on Cremaster Preparation

A single unbranched cremasteric venule (25–40 µm in diameter) is selected to be observed throughout the experiment. The videocamera is adjusted to allow the visualization of the venule in a vertical position at the extreme left or right side of the TV screen. A 1-mm^3 piece of agarose with chemokine is punched out using the tip of a Pasteur pipet (*see* **Note 3**). A piece of gel is carefully placed on the surface of the cremaster, 350 µm (two monitor screens wide) from this venule, in a preselected avascular area, visualized at the end of the second screen (**Figs. 2** and **3**). The gel is held in place using a cover slip, and the tissue is superfused with buffer beneath the cover slip. The flux of superfusion buffer is placed on the side of the gel distal to the venule and the suction on the side of the venule distal to gel to allow the flux of fluid and chemokine to flow from the gel to the vessel. The perfusion rate is 0.7 mL/min.

3.6. Evaluation of the Leukocyte Recruitment Parameters

The number of rolling, adherent, and emigrated leukocytes is determined off-line during video playback analysis. Rolling leukocytes are defined as those cells moving at a velocity less than that of erythrocytes within a given vessel. The flux of rolling cells is measured as the number of rolling cells passing by a given point in the venule per minute. A leukocyte is considered to be adherent if it remained stationary for at least 30 s, and total leukocyte adhesion is quantified as the number of adherent cells within a 100-µm length of venule. Leukocyte emigration is defined as the number of cells in the extravascular space within a 200 × 300 µm area. Only cells adjacent to and clearly outside the vessel under study were counted as emigrated. The chemotaxis is evaluated counting the number of cells in each 25 µm of grid from the venule to the gel. If cells are allowed to move for 1 h, there is a decreasing number of leukocytes the further one moves away from the vessel. If cells are allowed to move for 2 h,

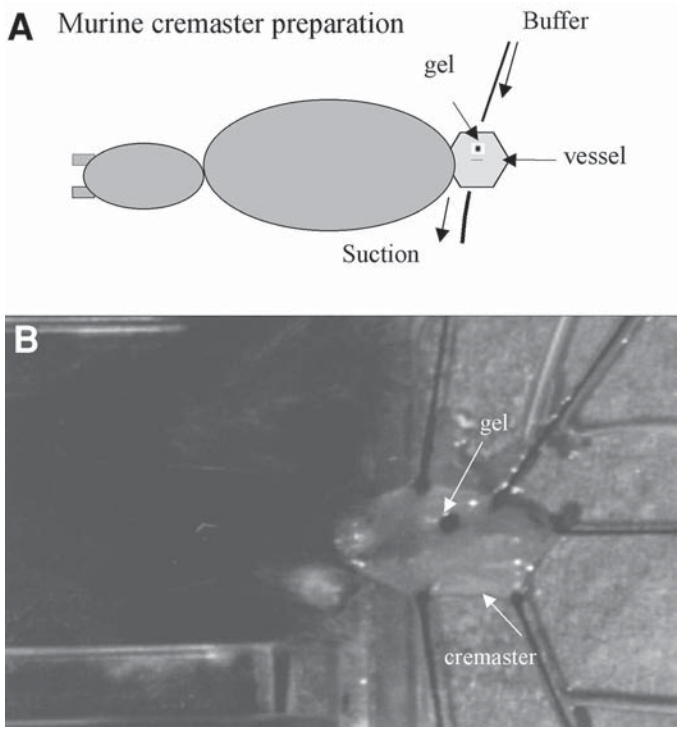

Fig. 2. Design (**A**) and photograph (**B**) showing the cremaster preparation with the gel (black dot).

there are many cells in all grids. The experiment is videotaped using time-lapse photography and plotted as a function of distance moved towards the chemotactic source (*see* **Fig. 4**).

4. Notes

1. The largest hurdle to overcome is minimizing the preparation-induced leukocyte recruitment. In the first instance, it takes much practice to establish any of the techniques to avoid significant preparation artifact. We have accepted the fact that reducing basal rolling is almost impossible without pharmacological intervention. However, to ensure that activation of the preparation is minimal, control animals (without any stimulus) should have certain rolling characteristics over time. First, the rolling flux should either decrease or remain the same. The adhesion velocity should increase or stay the same. A decrease in rolling velocity or increase

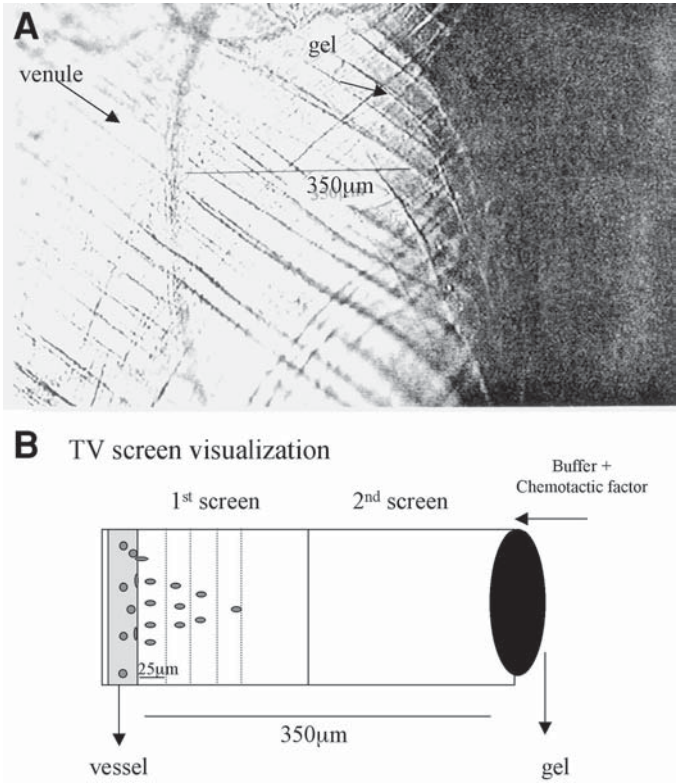

Fig. 3. (**A**) Photograph of the mouse cremaster with the gel placed 350 µm from the vessel (magnification: ×100). (**B**) Design showing the emigration and chemotaxis visualized on a TV screen.

in rolling suggests some activation of the preparation. Finally, rolling should remain below 5 cells/100-µm length venule and emigration should be essentially nonexistent. An increase in either of these parameters in untreated animals suggests an unacceptable preparation. Similar rules apply in both the liver and the cremaster preparation.

2. General issues regarding the preparations include no bleeding and a minimal amount of movement (primarily related to breathing). Breathing can move exteriorized tissue and this makes analysis of leukocyte parameters impossible. In the case of the liver preparation, the animal is placed on its left side to minimize any movement (the right side is far more difficult). The Saran Wrap often helps to minimize movement; if the animal is placed correctly on its side, the Saran Wrap is not necessary.
3. When studying various stimuli, there are certain issues that need to be kept in mind. First, one requires adequate blood flow through blood vessels to study leuko-

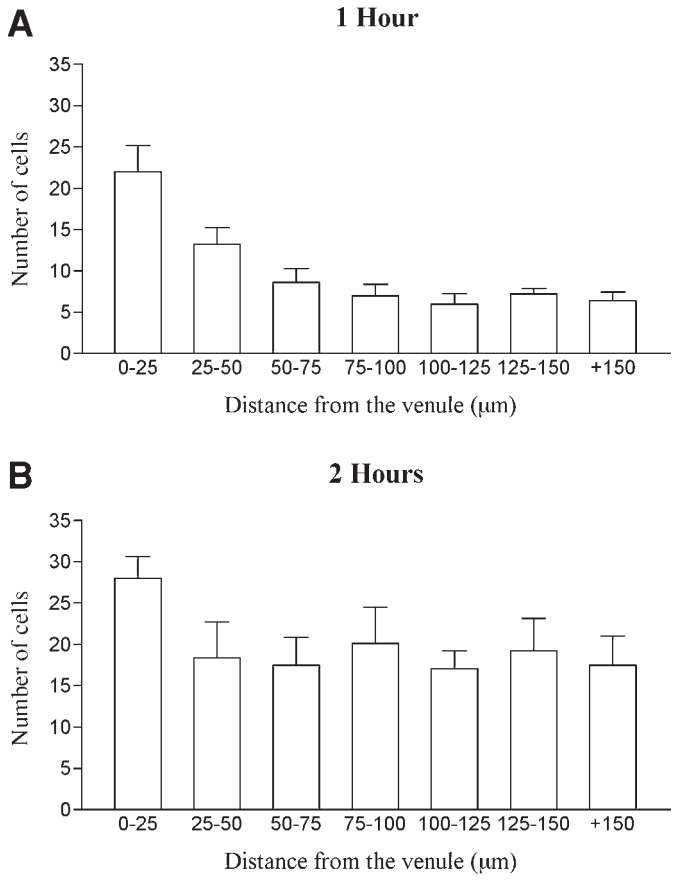

Fig. 4. Neutrophil emigration and chemotaxis in the murine cremaster muscle 1 h (**A**) and 2 h (**B**) after the directional release of KC toward a blood vessel.

cyte recruitment. Very high levels of a stimulus can often severely affect hemodynamic parameters such that changes in blood flow may dictate changes in leukocyte parameters. Although this likely occurs during the inflammatory response, total cessation of blood flow is unlikely reflective of true inflammation and almost certainly related to a poor preparation.

References

1. Springer, T. A. (1994) Traffic signals of lymphocyte recirculation and leukocyte emigration: the multistep paradigm. *Cell* **76,** 301–314.
2. Foxman, E. F., Campbell, J. J., and Butcher, E. C. (1997) Multistep navigation and the combinatorial control of leukocytes chemotaxis. *J. Cell. Biol.* **139,** 1349–1360.

3. Björk, J., Hedqvist, P., and Arfors, K.-E. (1982) Increase in vascular permeability induced by leukotriene B4 and the role of polymorphonuclear leukocytes. *Inflammation* **6,** 189–200.
4. House, S. D. and Lipowsky, H. H. (1987) Leukocyte–endothelium adhesion: microhemodynamics in mesentery of the cat. *Microvasc. Res.* **34,** 363–379.
5. Bienvenu, K., Harris, N., and Granger, N. (1994) Modulation of leukocyte migration in mesenteric interstitium. *Am. J. Physiol.* **267(4 Pt. 2),** H1573–H1577.
6. Hickey, M. J., Forster, M., Mitchell, D., Kaur, J., De Caigny, C., and Kubes, P. (2000) L-Selectin facilitates emigration and extravascular locomotion of leukocytes during acute inflammatory responses In vivo. *J. Immunol.* **165(12),** 7164–7170.
7. Morgan, S. J., Moore, M. W., Cacalano, G., and Ley, K. (1997) Reduced leukocyte adhesion response and absence of slow leukocyte rolling in interleukin-8 (IL-8) receptor deficient mice. *Microvasc. Res.* **54,** 188–191.
8. Zhang, X. W., Liu, Q., Wang, Y., and Thorlacius, H. (2001) CXC chemokines, MIP-2 and KC, induce P-selectin-dependent neutrophil rolling and extravascular migration in vivo. *Br. J. Pharmacol.* **133(3),** 413–421.
9. Ley, K., Baker, J. B., Cybulsky, M. I., Gimbrone, M. A. Jr., and Luscinskas, F. W. (1993) Intravenous interleukin-8 inhibits granulocyte emigration from rabbit mesenteric venules without altering L-selectin expression or leukocyte rolling. *J. Immunol.* **151,** 6347–6357.

11

Tracking Antigen-Specific Lymphocytes In Vivo

Claire L. Adams, Catherine M. Rush, Karen M. Smith, and Paul Garside

1. Introduction

With the development of antigen-specific T-cell-receptor (TcR) and B-cell-receptor (BcR) transgenic (Tg) mice, it is now feasible to track single, antigen-specific lymphocyte populations throughout the course of an immune response. Adoptive transfer of the transgenic cell populations into naïve recipients with the same genetic background increases precursor frequency sufficiently to allow researchers to locate and functionally assess lymphocytes, in the physiological context of a normal animal, early after antigen exposure ***(1–4)***. Prior to the availability of such transgenic mice, it was extremely difficult to track lymphocytes in vivo during the early phases of an immune response before significant clonal expansion, because of the low precursor frequency of antigen-specific B- and T-cells. The following methods will illustrate some of the techniques now available for the tracking of antigen specific B- and T-cell populations in vivo.

2. Materials

1. Incomplete medium: RPMI 1640 (Gibco-BRL, Paisley, UK).
2. Complete media: RPMI 1640 supplemented with 10% fetal calf serum (FCS), 2 m*M* L-glutamine, 100 U/mL penicillin, 100 µg/mL streptomycin, 1.25 µg/mL fungizone (all from Gibco-BRL).
3. Hanks balanced salt solution (Gibco-BRL).
4. Plasticware: 24- and 96-well plates and Immulon-4 plate (Costar UK Ltd, High Wycombe, UK).
5. Nitex (Cadisch Precision Meshes, London, UK).
6. Chicken ovalbumin (Fraction V [Sigma, Dorset, UK]).
7. Hen egg lysozyme (Biozyme, Gwent, UK).
8. Glutaraldehyde, 25% aqueous solution (Sigma).
9. Complete and incomplete Freund's adjuvant (CFA/IFA) (Sigma).

From: *Methods in Molecular Biology, vol. 239: Cell Migration in Inflammation and Immunity*
Edited by: D. D'Ambrosio and F. Sinigaglia

10. CFSE: Carboxyfluorescein diacetate, succinimidyl ester (5 [and 6]-CFDA, SE) (Molecular Probes Inc., USA).
11. FcR blocking buffer: Anti-CD16/32 hybridoma supernatant (Clone 2.4G2), 10% mouse serum (Diagnostic Scotland, Edinburgh, UK) and 0.1% sodium azide (Sigma).
12. Biotin KJ1-26 (produced from orginal hydridoma[5] and biotinylated using EZ-Link™ [Sulfo-NHS-Biotin, Pierce, Rockford, IL]).
13. Phycoerythrin (PE) anti-mouse CD4, peridinin chlorophyll (PerCP) anti-mouse CD4, FITC anti-mouse CD69, and fluorescein isothiocyanate (FITC) hamster IgG, Group 1, λ isotype standard (BD PharMingen, Oxford, UK).
14. FACS buffer: Phosphate-buffered saline (PBS) 1X, 2% FCS, and 0.05% sodium azide.
15. Phycoerytherin-conjugated streptavidin (BD, PharMingen).
16. Fluorescein streptavidin (Vector, Burlingame, CA).
17. Monoclonal antibodies: Anti-CD19, anti-CD11c, and anti-CD8 (Serotec, Oxford, UK).
18. Goat anti-IgG microbeads and CS cell separation column (Miltenyi Biotech, Alburn, CA, USA).
19. Polarization reagents: Interleukin (IL)-12, IL-4, anti-IL-4 monoclonal antibody (mAb) (Clone 11B11), anti IL-12 and anti-interferon (IFN)-γ (R & D Systems, Oxon, UK).
20. Peptide, $OVA_{323-339}$ (Genosys, Cambridgeshire, UK).
21. Cryomolds (Miles, Elkhart, IN).
22. O.C.T. embedding media (Bayer, Berkshire, UK).
23. Avidin–biotin blocking kit (Vector).
24. Biotin anti-mouse B220, Thy1.2 and IgM^a (BD PharMingen, Oxford, UK).
25. TNT buffer: 0.1 *M* Tris-HCl, 0.15 *M* NaCl, 0.05% Tween-20.
26. Tyramide Signal Amplification (TSA™) biotin system (NEN Life Science, Boston, MA).
27. 3,3'-diaminobenzidine (DAB) substrate kit (Vector).
28. DAB enhancing solution (Vector).
29. Hematoxylin (Vector).
30. Histoclear (BS & S Ltd, Edinburgh, UK).
31. Histomount (BS & S Ltd).
32. ABC-peroxidase (Vector).
33. ABC-alkaline phosphatase (Vector).
34. 5-Bromo-4-chloro-3-indolyl phosphate/nitroblue tetrazolium (BCIP/NBT) substrate kit (Vector).
35. Levamisole solution (Vector).

3. Methods

3.1. Adoptive Transfer of Transgenic Lymphocytes

We have described an adoptive transfer technique using OVA-specific DO11.10 TcR $CD4^+$ T-cells and HEL-specific MD4 B-cells to allow us to identify and track specific T- and B-cell interactions in vivo.

Adoptive transfer of ovalbumin-specific DO11.10 $CD4^+$ T-cells has been widely used to study a range of immune responses in vivo, including the activation and development of T-cell phenotypes following the induction of immunity, autoimmunity, allergy, and tolerance and the trafficking of effector lymphocyte populations ***(2,5–9)***. Other antigen-specific Tg lymphocytes, including (1) OVA-specific OT-I $CD8^+$ T-cells ***(10–15)***, (2) viral peptide-specific $CD8^+$ T-cells [e.g., LCMV gp33 ***(16)***], (3) myelin basic protein (MBP)-specific $CD4^+$ T-cells ***(17,18)***, and (4) pigeon cytochrome *c*-specific $CD4^+$ T-cells ***(19)***, have also been tracked in vivo using techniques similar to those described here.

3.1.1. Animals

3.1.1.1. MD4 B-Cell Transgenic Mice

Hen egg lysozyme (HEL)-specific MD4 B-cell-receptor transgenic mice were originally made ***(20)*** using the variable regions of the HEL-specific monoclonal antibody, HyHEL-10 ***(21)***. They contain four copies of both the heavy (μ and δ regions) and κ light immunoglobulin transgenes randomly integrated into the murine genome ***(22)***. The MD4 B-cells can be identified using an antibody specific for the IgM^a allotype. Transgenic B-cell mice (MD4) on the C57 BL/6 ($H\text{-}2^{b/b}$, $IgM^{b/b}$) background were crossed to Balb/c ($H\text{-}2^{d/d}$, IgM^a) mice, and offspring ($H\text{-}2^{d/b}$, $IgM^{a/b}$) from this cross were screened for the expression of the HyHEL-10 transgenes by flow cytometry (**Subheading 3.2.1.**); positives were used as Tg B-cell donors.

3.1.1.2. DO11.10 T-Cell Transgenic Mice

The $CD4^+$ T cells of the DO11.10 T-cell antigen receptor TcR Tg mice are specific for a chicken ovalbumin (cOVA) peptide (amino acid residues 323–339), in the context of the major histocompatibility complex (MHC) class II molecule $I\text{-}A^d$ ***(23,24)***. The TcR-DO11.10 transgenic mice were made with the rearranged Vβ8.1 and Vα13 T-cell-receptor genes from the OVA-specific T-cell hybridoma, DO11.10. The founder line has two copies of the Vα13 gene and four copies of the Vβ8.1 gene. In our laboratory, mice homozygous for the cOVA $peptide_{323–339}$/$I\text{-}A^d$-specific DO11.10 TcR transgenes (detected using the clonotypic mAb KJ1-26 ***[24]***) on the Balb/c background were crossed to C57 BL/6 mice to produce animals heterozygous for the DO11.10 transgenes on an F1 background (these were used as Tg T-cell donors).

3.1.1.3. Recipient Mice

IgH^b Balb/c ($H\text{-}2^{d/d}$, IgM^b) × C57 BL6 ($H\text{-}2^{b/b}$, $IgM^{b/b}$) F1 mice were used as recipients in the experiments described in this chapter to allow us to distinguish between the endogenous (IgM^b allotype) and transgenic (IgM^a allotype) B-cell

populations. All animals were specified pathogen-free and were maintained under standard animal house conditions with free access to both water and standard rodent pellets in accordance with UK Home Office regulations.

3.1.2. Preparation of Cell Suspensions for Adoptive Transfer

1. Harvest peripheral lymph nodes (PLN) [axillary, inguinal, brachial, and cervical] mesenteric lymph nodes (MLN) and spleens from DO11.10 Balb/c × C57BL/6 F1 mice and MD4 F1 mice into an excess volume (at least 30 mL) of sterile incomplete medium.
2. Force pooled tissues through sterile (autoclaved) Nitex in the base of a sterile Petri dish using a sterile syringe plunger. Collect cells into a sterile 50-mL tube.
3. Pellet cells by centrifuging at 450*g* for 5 min. Pour off supernatant into another tube and recentrifuge at 450*g* for 5 min. Resuspend cell pellets in a total volume of at least 30 mL of sterile incomplete media. Count cells using a hemocytometer.
4. Calculate the percentage of $CD4^+KJ1\text{-}26^+$ DO11.10 T-cells in these suspensions by flow cytometric analysis as described in **Subheading 3.2.1.**
5. Dilute cells in incomplete RPMI to give $1\text{–}6 \times 10^6$ Tg T-cells per 0.2 mL. Immediately prior to intravenous injection, pass the cells through sterile Nitex to remove any cell clumps.
6. Inject 0.2 mL of cells into the tail vein of age- and sex-matched $IgH^b \times$ C57 BL/6 F1 or Balb/c × C57 BL/6 F1 recipients (*see* **Note 1**).
7. For T- and B-cell cotransfers, calculate the percentage of $CD4^+KJ1\text{-}26^+$ DO11.10 T-cells and HEL-binding IgM^{a+} B-cells in the cell suspensions by flow cytometric analysis (*see* **Subheading 3.2.1.**). Mix the two suspensions to give $1\text{–}6 \times 10^6$ Tg T-cells and $(1\text{–}6) \times 10^6$ Tg B-cells and inject as described in **step 6**.
8. For adoptive transfer experiments using polarized T-cells, prepare Th1 and Th2 cells as described in **Subheading 3.1.4.** and transfer as described.

3.1.3. CFSE Labeling of Transgenic Lymphocytes

Carboxyfluorescein diacetate (CFSE) segregates equally between daughter cells upon division, resulting in sequential halving of fluorescence intensity with each generation (*see* **Fig. 1**). This technique allows us to follow the proliferative history of individual cells.

1. Prepare single-cell suspensions and count as described in **Subheading 3.1.2.** Wash twice in sterile Hank's balanced salt solution (HBSS) by centrifuging the cell suspension at 450*g* for 5 min, followed by resuspension in at least 30 mL HBSS. Repeat. Resuspend in HBSS to give 5×10^7 lymphocytes/mL.
2. Add CFSE (5- [and-6-] carboxyfluorescein diacetate, succinimidyl ester) to cells diluted as in **step 1** to give a final concentration of 5 μ*M* and incubate at 37°C for 10 min. Mix gently by inversion once during the incubation period.
3. Wash cells once in HBSS and once in complete medium by centrifugation as described in **step 1** and resuspend in incomplete medium to give $(2\text{–}5) \times 10^6$ Tg cells/0.2 mL for adoptive transfer as described in **Subheading 3.1.2.**

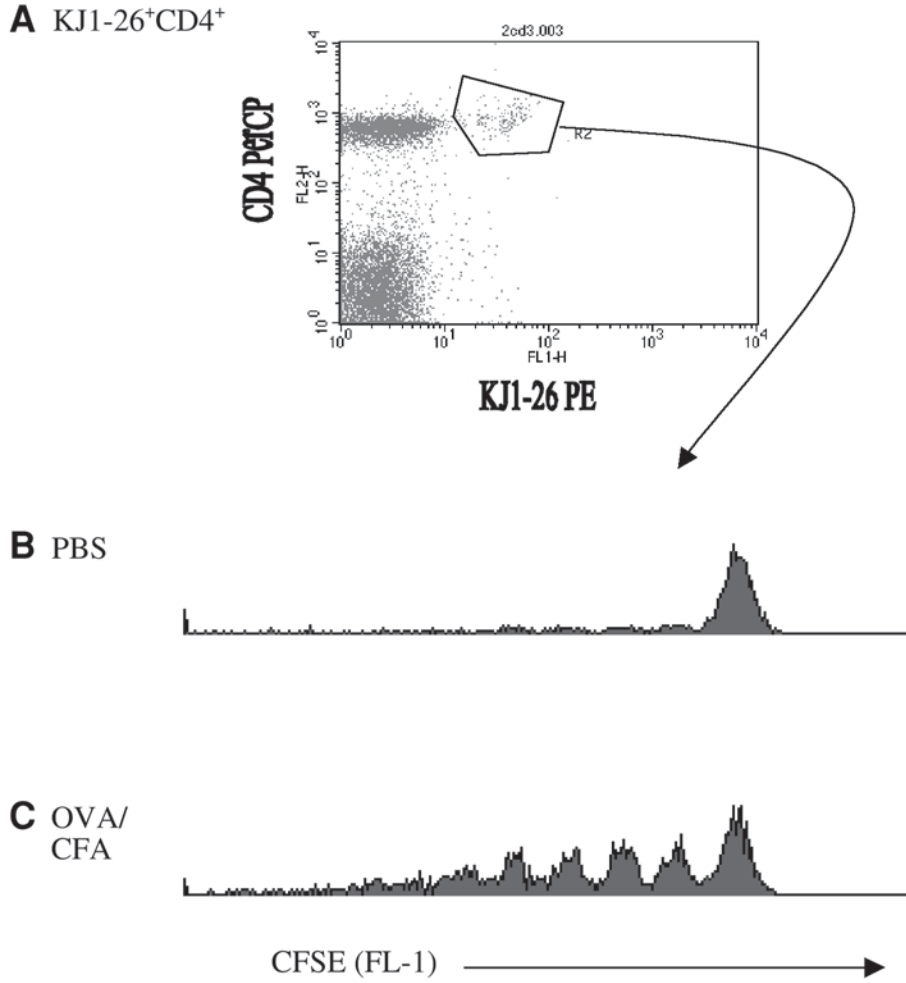

Fig. 1. Tracking cell divsions of antigen-specific lymphocytes using CFSE labeling and flow cytometry. Cell divisions of $CD4^+$, KJ1.26$^+$ Tg T-cells were detected by gating around CD4-PerCP/KJ1-26-PE positive cells (**A**) and viewing the CFSE fluorescence using the FITC channel (FL1). CFSE-labeled DO11.10 $CD4^+$KJ1-26$^+$Tg T-cells in the peripheral lymph nodes, d3 after antigen exposure: (**B**) PBS control and (**C**) OVA/CFA.

3.1.4. Purification of Transgenic T-Cells and Polarization of Th1/Th2 T-Cells

Described in this subsection are the steps that can be utilized to obtain a purified DO11.10 Tg T-cell population by negative selection and cell differentiation to a Th1/Th2 phenotype ***(4)***.

3.1.4.1. Purification of a Lymphocyte Population

1. Make a single-cell population (described in **Subheading 3.1.2.**) from the pooled lymph nodes and spleens of DO11.10 Balb/c × C57 BL/6 F1 mice (*see* **Note 2**).
2. Remove B-cells, monocytes, and $CD8^+$ T-cells by incubating the cell suspension with anti-CD19 (70 µg/mL), anti-CD11b (50 µg/mL), and anti-CD8 (25 µg/mL) monoclonal antibodies, respectively, together with anti-CD16/32 (120 µg/mL) to block FcR, for 20 min on ice.
3. Add the correct amount of goat anti-mouse IgG microbeads to the appropriate amount of cells and remove the unwanted cells by using a CS cell separation column (according to the Miltenyi Biotech manufacturer's instructions).
4. Check the purity of your T-cell population by two-color flow cytometry (*see* **Subheading 3.2.1.**).

3.1.4.2. T-Cell Differentiation

1. Make antigen-presenting cells by irradiating 2–5 × 10^8 murine spleen cells (in 5 mL incomplete media) at 2000 rads for 15 min.
2. Induce T-cell differentiation by culturing 2 × 10^5/mL $CD4^+$ T-cells with 2 × 10^6/mL APC and 0.3 µ*M* $OVA_{323–339}$.
3. To the Th1-cell cultures, add 5 ng/mL IL-12 and 10 µg/mL anti-IL-4 mAb.
4. Incorporate 5 ng/mL IL-4, 10 µg/mL anti-IL-12, and 5 µg/mL anti-IFN-γ serum into the Th2-cell cultures.
5. Incubate for 3 d at 37°C, in 5% CO_2.
6. Wash cells in incomplete medium (450*g*, 5 min) and use for adoptive transfer (*see* **Subheading 3.1.2.**).

3.1.5. Preparation of Antigen

Because the TcR Tg and BcR Tg lymphocytes used recognize different antigens, it is necessary to chemically couple these proteins to facilitate cognate interactions between the T- and B-cells. Hen egg lysozyme and chicken ovalbumin are chemically linked to allow HEL presentation from the DO11.10 Tg T-cells (cOVA-specific) to the MD4 Tg B-cells (HEL-specific) at the early stages of germinal center formation. The following protocol outlines the HEL–cOVA chemical coupling procedure.

3.1.5.1. Chemical Coupling of HEL–cOVA and Antigen Administration

1. Prepare a 0.5-m*M* solution of both HEL and cOVA in phosphate buffer, pH. 7.5 (60 mL of 65 m*M* NaH_2PO_4 plus 300 mL of 65 m*M* Na_2HPO_4).
2. Combine equimolar amounts of HEL and cOVA and centrifuge (450*g*, 5 min) to remove the insoluble protein.
3. Dilute glutaraldehyde to a final concentration of 0.0825% in phosphate buffer, pH 7.5 and add to the OVA/HEL mixture at a ratio of 1:2.5 (glutaraldehyde:protein mixture).

4. Stir for 1 h at room temperature, repeat the centrifugation step, and discard precipitate.
5. Dialyze the resulting OVA/HEL solution against PBS, filter-sterilize (0.2 μm), and store at 4°C.
6. Check the formation of the HEL–cOVA conjugate by sodium dodecyl sulfate (SDS)–polyacrylamide gel electrophoresis (SDS-PAGE).
7. Inject IgH^b Balb/c × C57 BL6 recipients, which previously have received $2–5 \times 10^6$ Tg cells (*see* **Subheading 3.1.2.**), with 130 μg of HEL–cOVA in 50% complete Freund's adjuvant (CFA) subcutaneously in the scruff of the neck.

3.2. Tracking of Transgenic Lymphocytes

The availability of anticlonotypic antibodies to various transgenic B- and T-cells has enabled researchers to track the location, expansion, and phenotypic changes of antigen-specific lymphocyte populations using techniques such as flow cytometry (*see* **Fig. 2**) and immunohistochemistry (*see* **Fig. 3**).

3.2.1. Flow Cytometry

The anticlonotypic antibody KJ1-26 can be used to label the cOVA-specific DO11.10 Tg T-cells. The detection of helper ($CD4^+KJ1\text{-}26^+$) and early-activated ($CD4^+KJ1\text{-}26^+CD69^+$) T-cells by flow cytometry are described in **Subheadings 3.2.1.1.** and **3.2.1.2.**, respectively. The same protocols can be followed to determine the expression of the marker of choice in the lymphoid tissue of interest. Futhermore, with minor modification, they can be employed to assess the functional status of lymphocytes (e.g., intracellular cytokine staining) ***(25)***.

3.2.1.1. Two-Color Flow Cytometry

1. Harvest the relevant secondary lymphoid organs at the appropriate days after antigen exposure.
2. Prepare single-cell suspensions as described in **Subheading 3.1.2.**
3. Incubate approximately $10^6–10^7$ cells (in a volume of 50–100 μL) with 50 to 100 μL FcR blocking buffer for 10 min at 4°C to prevent binding of antibody to cells via their Fc regions. This can be done directly in FACS tubes.
4. For detection of $CD4^+$ DO11.10 T-cells, add phycoerythrin (PE)-conjugated anti-CD4 and biotinylated clonotypic anti-TcR antibody KJ1-26 to the cell suspension and incubate for 40 min at 4°C. When staining numerous cell suspensions, prepare a large volume of master mix of antibodies diluted appropriately in FACS buffer and aliquot 50 μL per tube.
5. Wash the cell suspensions by the addition of 3- to 4-mL FACS buffer and centrifuge at 450*g* for 5 min. Pour off supernatant and add FITC-conjugated streptavidin (SA-FITC) for 40 min at 4°C. For multiple samples, add 50 μL of SA-FITC diluted 1/50 in FACS buffer per tube.
6. Carry out a final wash in FACS buffer and resuspend the stained cells in FACS flow (*see* **Note 3**).

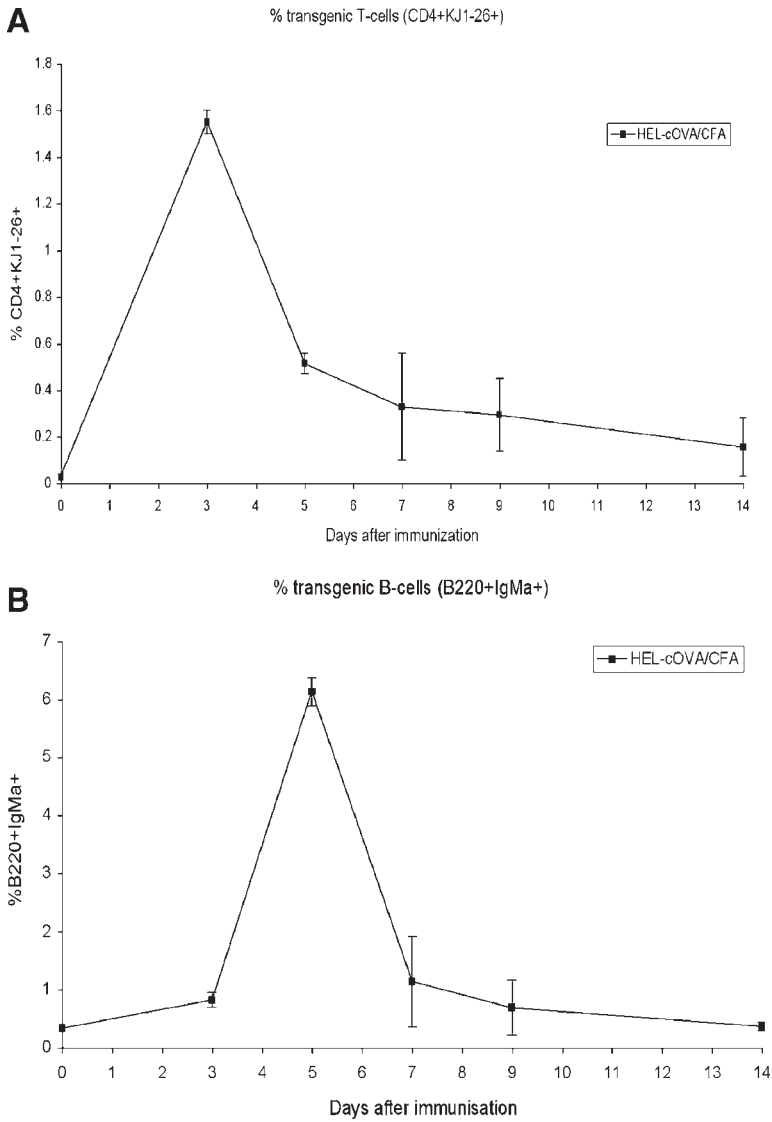

Fig. 2. Clonal expansion of DO11.10 Tg T-cells (**A**) and MD4 Tg B-cells (**B**) after immunization with HEL–cOVA/CFA (determined by two-color flow cytometry).

3.2.1.2. Three-Color Flow Cytometry

1. Prepare a single-cell suspension as described in **steps 1–3** of **Subheading 3.2.1.1.**
2. For detection of $CD4^+$ $KJ1\text{-}26^+$ $CD69^+$ cells, incubate the cell suspensions with PerCP-conjugated anti-CD4, biotinylated KJ1-26, and FITC-conjugated isotype control or anti-CD69 for 40 min at 4°C as described above.

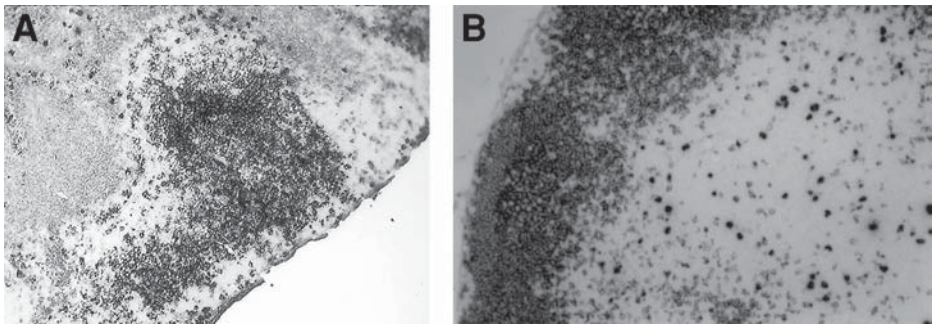

Fig. 3. Location of MD4 Tg B-cells and DO11.10 Tg T-cells using immunohistochemistry. (**A**) Peripheral lymph node, d 9 after immunization with HEL–cOVA/CFA. MD4 Tg B-cells are stained in blue (anti-IgM^a, shows as dark staining) and the endogenous T-cell zone is shown in brown (anti-Thy1.2 shows as pale staining). (**B**) Mesentric lymph node, d 3 after immunization with HEL–cOVA/CFA. DO11.10 Tg T-cells are stained in brown (anti-KJ1-26 shows as dark spots in the paracortex) and the B-cell area (anti-B220 shows as darkly stained follicles) is visualized in blue.

3. Wash the cells in FACS buffer and incubate with PE-conjugated streptavidin for 40 min at 4°C.
4. Carry out a final wash in FACS buffer and resuspend the stained cells in FACS flow (*see* **Note 3**).

3.2.2. Analysis of Lymphocyte Division History Using CFSE

1. Remove draining PLNs and MLNs at various times after antigen administration for flow cytometric analysis and prepare single-cell suspensions as described in **Subheading 3.1.2.**
2. Use three-color flow cytometry to demonstrate CFSE-labeled DO11.10 T-cells by staining with PerCP-conjugated anti-CD4 and biotinylated KJ1-26 followed by PE-conjugated streptavidin as described in **Subheading 3.2.1.2.**
3. Measure the CFSE fluorescence of 1000–2000 CD4$^+$, KJ1-26$^+$ events using the FITC channel (FL1). Labeled undivided cells are characterized by $CFSE_{high}$ staining, as can be seen in **Fig. 1**. However, following HEL–cOVA administration, Tg cells have divided in vivo.

3.2.3. Assessment of Lymphocyte Function

Lymphocyte effector function can be assessed in vivo, ex vivo, and in vitro using standard techniques. Standard protocols for measuring cOVA-specific delayed-type hypersensitivity (DTH) responses and in vitro restimulation assays

to measure T-cell proliferation and cytokine production have been described previously ***(4,26)***. The anti-HEL IgM^a antibodies produced by the transgenic B-cells can be detected using a standard enzyme-linked immunosorbent assay (ELISA) protocol (*see* **Note 4**).

3.2.4. Immunohistochemistry

1. Harvest the relevant secondary lymphoid organs at the appropriate days after antigen exposure.
2. Place organs carefully in cryomolds with O.C.T embedding medium filling the well. Snap-freeze in liquid nitrogen and store at –70°C.
3. Cut 6- to 10-µm tissue sections on a cryostat, allow to air-dry, and store at –20°C.
4. Bring sections to room temperature, fix for 10 min in acetone, and air-dry.
5. Mark areas to be stained with a wax pen and rehydrate sections with PBS/2% goat serum for 15 min. Keep slides in a humidified chamber from this stage of the protocol (*see* **Note 5**).

3.2.4.1. Single Staining for the DO11.10 TcR Using the Tyramide Signal Amplification System

1. Cover the rehydrated slides in 0.1% azide/3% H_2O_2 for 45 min, changing the solution three times, to block endogenous peroxidase.
2. Wash slides twice in PBS.
3. Use the avidin–biotin blocking kit according to the manufacturer's instructions to block unmasked endogenous biotin and excess avidin. Add the avidin solution for 15 min, wash twice in PBS, incubate slides with the biotin solution for 15 min, and repeat washes.
4. Incubate tissue with Fc block for 30 min and wash twice with PBS.
5. Add the primary biotinylated antibody (in our case, KJ1-26 [10 µg/mL]) diluted in TNB buffer for 30 min and wash twice in TNT buffer.
6. Dilute streptavidin–horseradish peroxidase at a ratio of 1:100 with TNB buffer, incubate for 30 min, and wash twice in TNT buffer.
7. After washing, add biotinyl–tyramide (1/50 in TNB) for 10 min and wash twice in TNT buffer.
8. Repeat **step 6**.
9. Detect enzymatic activity with 3,3'-diaminobenzidine substrate (DAB), leave for up to 10 min, wash in H_2O, incubate slides with DAB enhancing solution for approx 10 s, and repeat wash.
10. Counterstain sections with hematoxylin for 30 s, rinse in tap water followed by acid alcohol, tap water, 0.1 *M* sodium bicarbonate solution, and, finally, tap water.
11. Mount sections by subsequently exposing the slides to 70% ethanol, followed by 95% ethanol, 95% ethanol, then 100% ethanol, clear in Histoclear, and immediately mount in Histomount.
12. Seal slides with nail varnish and store at room temperature.

3.2.4.2. Double Staining for Tg B- and T-Cell Areas or Tg T- and B-Cell Areas

1. Incubate the rehydrated slides with either biotinylated KJ1-26 or biotinylated anti-IgM^a diluted appropriately in PBS/2% goat serum for 30 min to detect Tg T- or B-cells, respectively.
2. Wash sections three times in PBS.
3. Add ABC-alkaline phosphatase for 30 min and repeat washes.
4. Detect alkaline phosphatase activity by using the BCIP/NBT substrate kit (including levamisole to block endogenous alkaline phosphatase) for up to 45 min in the dark.
5. Counterstain the B- and T-cell areas of the tissue by using biotinylated B220 or Thy1.2 (diluted 1:500 in PBS/2% goat serum), respectively, for 30 min and wash sections three times in PBS.
6. Add ABC-peroxidase for 30 min and repeat washes.
7. Detect enzymatic activity with the DAB substrate kit, leave for up to 10 min, wash in H_2O, incubate slides with DAB enhancing solution for approx 10 s, and repeat H_2O wash.
8. Mount sections by subsequently exposing the slides to 70% ethanol, followed by 95% ethanol, 95% ethanol, then 100% ethanol, clear in Histoclear, and immediately mount in Histomount.
9. Seal slides with nail varnish and store at room temperature.

4. Notes

1. It is important that cell suspensions prepared for adoptive transfer are injected as soon as possible into recipient mice. This is particularly important following CFSE staining, as CFSE at the concentration used here is slightly toxic to cells. The concentration of CFSE can be decreased; however, we find that cell divisions are more easily discriminated if a higher starting fluorescence is used. We usually check the fluorescence intensity of CFSE-labeled cells prior to transfer and this should be extremely high (at least 10^4 on the FITC FL1 channel). For intravenous transfer, mice should be warmed prior to cell transfer.
2. Complete media is used to maintain cell populations throughout all manipulations unless stated otherwise. All cell cultures are incubated at 37°C in 5% CO^2. Routinely, to obtain the same number of Th1/Th2 cells at the end of the culture period, one-third of the purified T-cell population is utilized in the Th2 culture and the remainder is treated under Th1 conditions.
3. Antibodies are used at a dilution of 1 µg per 10^6 cells for flow cytometry. Normally, 20000 total events are collected for two-color FACS analysis with FACScan and CELLQuest software (BD PharMingen). The percentage of transgenic B-cells is calculated using PE-conjugated anti-B220 (RA3-6B2) and biotinylated anti-IgM^a (Igh-6a, DS-1) monoclonal antibodies followed by FITC-labeled streptavidin. For three-color FACS analysis, approx 1000–2000 double-positive $CD4^+KJ1\text{-}26^+$ events are used to assess the activation of the T-cells via the CD69 early T-cell

activation marker. The most prominent cell markers such as CD4 or B220 are chosen to be PerCP-conjugated antibodies in the three-color FACS experiments. Isotype controls are run in conjunction with experiments to ensure specific staining is observed; that is, the isotype control, FITC hamster IgG, Group 1, γ isotype standard is used when detecting T-cell activation using FITC-conjugated anti-mouse CD69. Immediately before cell preparations are analyzed by flow cytometry, they are filtered through Nitex to remove cell aggregates.

4. The anti-HEL IgM^a antibodies produced by the transgenic B-cells are detected using a standard ELISA protocol. Briefly, the ELISA plate is coated in 20 µg/mL of hen egg lysozyme, serially diluted serum samples are added, and IgM^a levels are determined using 2 µg/mL biotinylated anti-IgM^a (Igh-6a) followed by Extravidin perioxidase ***(4)***.
5. For immunohistochemistry, all slides were washed for 5 min in a Coplin jar, unless stated otherwise. Antibodies are normally used at a concentration of 1- to 10-µg/mL. To ensure the correct intensity of color, watch the development of the BCIP/NBT (blue) and DAB (brown) substrates at appropriate intervals throughout the procedure. Always carry out a no-primary-antibody control on each of the slides to ensure that the observed staining is specific.

References

1. Kearney, E., Pape, K., Loh, D., and Jenkins, M. (1994) Visualization of peptide-specific T cell immunity and peripheral tolerance induction in vivo. *Immunity* **1,** 327–339.
2. Pape, K., Kearney, E., Khoruts, A., et al. (1997) Use of adoptive transfer of T-cell antigen-receptor-transgenic T cell for the study of T-cell activation in vivo. *Immunol. Rev.* **156,** 67–78.
3. Garside, P., Ingulli, E., Merica, R. R., Johnson, J. G., Noelle, R. J., and Jenkins, M. K. (1998). Visualisation of specific B and T lymphocyte interactions in the lymph node. *Science* **281,** 96–99.
4. Smith, K. M., Pottage, L., Thomas, E. R., et al. (2000) Th1 and Th2 CD4+ T cells provide help for B cell expansion and antibody synthesis in a similar manner in vivo. *J. Immunol.* **165,** 3136–3144.
5. Pape, K., Merica, R., Mondino, A., Khourts, A., and Jenkins, M. K. (1998) Direct evidence that functionally impaired CD4+ T cells persist in vivo following induction of peripheral tolerance. *J. Immunol.* **160,** 4719–4722.
6. Saparov, A., Kraus, L. A., Cong, Y., et al. (1999) Memory/effector T cells in TCR transgenic mice develop via recognition of enteric antigens by a second, endogenous TCR. *Int. Immunol.* **118,** 1253–1264.
7. Walter, D. M., McIntire, J. J., Berry, G., et al. (2001) Critical role for IL-13 in the development of allergen-induced airway hyperreactivity. *J. Immunol.* **167,** 4668–4675.
8. Chen, Z. M. and Jenkins, M. K. (1998) Revealing the in vivo behaviour of CD4+ T cells specific for an antigen expressed in *Escherichia coli*. *J. Immunol.* **160,** 3462–3470.

9. Iqbal, N., Oliver, J. R., Wagner, F. H., Lazenby, A. S., Elson, C. O., and Weaver, C. T. (2002) T Helper 1 and T helper 2 cells are pathogenic in an antigen-specific model of colitis. *J. Exp. Med.* **195,** 71–84.
10. Kurts, C., Heath, W. R., Carbone, F. R., Allison, J., Miller, J. F., and Kosaka, H. (1996) Constitutive class I-restricted exogenous presentation of self antigens *in vivo*. *J. Exp. Med.* **184,** 923–926.
11. Kurts, C., Kosaka, H., Carbone, F. R., Miller, J. F., and Heath, W. R. (1997) Class I-restricted cross-presentation of exogenous self-antigens leads to deletion of autoreactive CD8+ T cells. *J. Exp. Med.* **186,** 239–243.
12. Kim, S. K., Reed, D. S., Heath, W. R., Carbone, F. R., and Lefrancois, L. (1997) Activation and migration of CD8 T cells in the intestinal mucosa. *J. Immunol.* **159,** 4295–4306.
13. Lefrancois, L., Parker, C. M., Olson, S., et al. (1999) The role of beta7 integrins in CD8 T cell trafficking during an antiviral immune response. *J. Exp. Med.* **189,** 1631–1638.
14. Pope, C., Kim, S.-K., Marzo, A., Williams, K., Jiang, J., Shen, H., and Lefrancois, L. J. (2001) Organ-specific regulation of the CD8 T cell response to Listeria monocytogenes infection. *J. Immunol.* **166,** 3402–3409.
15. Topham, D. J., Castrucci, M. R., Wingo, F. S., Belz, G. T., and Doherty, P. C. (2001) The role of antigen in the localisation of naïve, acutely activated and memory CD8+ T cells to the lung during influenza pneumonia. *J. Immunol.* **167,** 6983–6990.
16. Zimmerman, C., Brduscha-Riem, K., Blaser, C., Zinkernagel, R. M., and Pircher, H. (1996) Visualization, characterization, and turnover of CD8+ memory T cells in virus-infected hosts. *J. Exp. Med.* **183,** 1367–1375.
17. Meyer, A. L., Benson, J., Song, F., et al. (2001) Rapid depletion of peripheral antigen-specific T cells in TCR-transgenic mice after oral administration of myelin basic protein. *J. Immunol.* **166,** 5773–5781.
18. Goverma, J. (1999) Tolerance and autoimmunity in TCR transgenic mice specific for myelin basic protein. *Immunol. Rev.* **169,** 147–159.
19. Collazo, C. M., Miller, C., Yap, G., et al. (2000) Host resistance and immune deviation in pigeon cytochrome c T-cell receptor transgenic mice infected with *Toxoplasma gondii*. *Infect. Immun.* **68,** 2713–2719.
20. Goodnow, C. C., Crosbie, J., Adelstein, S., et al. (1988) Altered immunoglobulin expression and functional silencing of self-reactive B lymphocytes in transgenic mice. *Nature* **334,** 676–682.
21. Smith-Gill, S. J., Mainhart, C. R., Lavoie, T. B., Feldmann, R. J., Drohan, W., and Brooks, B. R. (1987) A three dimensional model of an anti-lysozyme antibody. *J. Mol. Biol.* **194,** 713–724.
22. Goodnow, C. C. (1992) Transgenic mice and analysis of B-cell tolerance. *Annu. Rev. Immunol.* **10,** 489–518.
23. Haskins, K., Kubo, R., White, J., Pigeon, M., Kappler, J., and Marrack, P. (1983) The major histocompatibility complex-restricted antigen receptor on T-cells. 1. Isolation with a monoclonal antibody. *J. Exp. Med.* **157,** 1149–1169.

24. Murphy, K. M., Heimberger, A. B., and Loh, D. Y. (1990) Induction by antigen of intrathymic apoptosis of CD4+CD8+ TCRlo thymocytes in vivo. *Science* **250,** 1718–1721.
25. Zell, T., Khoruts, A., Ingulli, E., Bonnevier, J. L., Mueller, D. L., and Jenkins, M. K. (2001) Single-cell analysis of signal transduction in CD4 T cells stimulated by antigen *in vivo*. *PNAS* **98,** 10,805–10,810.
26. Leishman, A., Garside, P., and Mowat, A. (2000) Induction of oral tolerance in the primed immune system: influence of antigen persistence and adjuvant form. *Cell Immunol.* **202,** 71–78.

12

Analysis of Homing-Receptor Expression on Infiltrating Leukocytes in Disease States

Margherita Mariani and Paola Panina-Bordignon

1. Introduction

Chemokines regulate a wide array of physiological and pathological processes, including physiological trafficking, inflammation, hematopoiesis, angiogenesis, tumor growth, and human immunodeficiency virus (HIV) infection ***(1,2)***. All of these functions are mediated by signaling through seven-transmembrane domain G-protein-coupled receptors expressed on the target cell membrane. The coordinated expression of chemokines and their receptors define patterns of leukocyte trafficking during physiological immune surveillance and inflammation. Discrete tissue-committed subpopulations of circulating naive and memory T-cells can be distinguished, in part, by their expression of chemokine receptors. Whereas physiological trafficking is characterized by the homing of such receptor expressing cells to those tissues where cognate ligands are constitutively produced, the situation during local inflammation is intricate. A series of in vitro studies has demonstrated that Th1 and Th2 cells express distinct sets of chemokine receptors that might regulate the recruitment and localization of these cells to inflammatory sites ***(3,4)***. CXCR3 and CCR5 have been associated with the Th1 cytokine profile ***(5,6)***, whereas CCR3, CCR4, and CCR8 have been associated with the Th2 phenotype ***(7–10)***. Selective recruitment of subsets of $CD4^+$ effector T-cells into sites of inflammation may contribute to the development of different pathological conditions ***(11,12)***. It is still a matter of speculation whether the infiltration of tissues by T-cells is contingent on the function of inflammatory chemokine receptors or whether the expression of such receptors is upregulated during tissue infiltration, therefore supporting the retention of T-cells in the tissue.

From: *Methods in Molecular Biology, vol. 239: Cell Migration in Inflammation and Immunity*
Edited by: D. D'Ambrosio and F. Sinigaglia © Humana Press Inc., Totowa, NJ

During the complex development of an inflammatory response, chemokines produced by the recruited T-cells can amplify Th1 or Th2 responses by further attracting polarized cells through their preferential expression of distinct chemokine receptors. The coordinated production of specific chemokines and the expression of distinct receptors on different leukocyte subsets are likely to dictate the type and severity of inflammatory responses, making chemokine receptors ideal targets for therapeutic intervention.

Various techniques can be utilized for the analysis of patterns of chemokine receptors expressed by inflammatory T-cells invading specific tissues. In the case where no specific antibody is available, *in situ* hybridization provides information on the level of specific messenger RNA. Immunohistochemistry in association with double immunofluorescence represents the most accurate analysis providing information on both the tissue morphology and the coexpression of distinct cell-specific markers.

2. Materials

2.1. *Radioactive* In Situ *Hybridization*

1. Developer D19 (Kodak Italia, Milan, Italy; cat. no. A00021242).
2. Fixer Kodak 3000 (Kodak Italia, Milan, Italy; cat. no. A00020394).
3. Autoradiography emulsion type NTB-2 (Kodak Italia, Milan, Italy; cat. no. 654433).
4. 4% paraformaldehyde (PFA)/1X PBS: To prepare 200 mL of solution, warm at 60°C 180 mL of diethyl pyrocarbonate (DEPC)-treated water. Add 100 µL of 1 *M* NaOH. Add 8 g of paraformaldehyde (PFA) and mix well on a stirrer. When all of the PFA has completely dissolved, recover the neutral pH of the solution adding 100 µL of 1 *M* HCl. Finally, add 20 mL of 10X phosphate-buffered saline (PBS).
5. FSM: 50% Deionized formamide, 2X SSC, 20 m*M* β-mercaptoethanol, added immediately before use.
6. STE: 4X sodium chloride–sodium citrate (SSC) buffer, 20 m*M* Tris-HCl, pH 7.6, 1 m*M* EDTA.
7. STEM: STE + 20 m*M* β-mercaptoethanol, added immediately before use.
8. 10X High salt: 3 *M* NaCl, 100 m*M* Tris-HCl, pH 8.0, 100 m*M* NaH_2PO_4, 50 m*M* EDTA, 2% Ficoll 400, 2% polyvinyl pirrolidone in DEPC water.
9. Canada balsam: 5 g Canada balsam in 10 mL methylsalicilate.

2.2. *Nonradioactive* In Situ *Hybridization*

1. Digoxigenin 11-UTP (Roche Diagnostics S.p.A. Monza, Milan, Italy; cat. no. 1209256).
2. Dig RNA-labeling kit (SP6-T7) (Roche Diagnostics S.p.A. Monza, Milan, Italy; cat. no. 1175025).
3. AntiDIG AP FAB fragment (Roche Diagnostics S.p.A. Monza, Milan, Italy; cat. no. 1093274).
4. Dig control teststrips (Roche Diagnostics S.p.A. Monza, Milan, Italy; cat. no. 1669966).

5. Denhardt's solution 50X.
6. Yeast tRNA: Reconstitute the lyophilized powder in DEPC water, make 200 µL aliquots, and store at –20°C.
7. Salmon sperm DNA: It is solid and usually comes in one piece, so it is better to dissolve all of the quantitative of the bottle at once. Add the genomic DNA into the right quantity of DEPC water to make a 10-mg/mL stock solution in a sterile glass bottle. The DNA does not dissolve immediately in water. Autoclave it for 10 min at 120°C and then let it reach room temperature. During this step, the genomic DNA is destroyed in smaller pieces and dissolves in the water. Control the average size of the DNA by loading 1 µg on 1% agarose gel. If the denaturation occurred, the DNA appears as a smear less than 1 kb of size. If the size is very large or too small, this can lead to a high background. Make aliquots of the prepared solutions and store them at –20°C.
8. NTE: 0.5 *M* NaCl, 10 m*M* Tris-HCl, pH 8, 5 m*M* EDTA, pH 8.
9. NTM: 100 m*M* NaCl, 100 m*M* Tris-HCl, pH 9.5, 50 m*M* $MgCl_2$.
10. Tris buffered saline (TBS): 100 m*M* Tris-HCl, pH 7.5, 150 m*M* NaCl.
11. Blocking solution: 10% Sheep serum in TBS.
12. Staining solution with AP substrates: Dilute 4.5 µL of NBT, nitrotetrazolium blue chloride (stock 75 mg/mL in 75% dimethylformamide), and 3.5 µL of BCIP (5-bromo-4-chloro-3-indolyl phosphate) (50 mg/mL in 75% dimethylformamide) in 1 mL of NTM.

2.3. Immunohistochemistry

Vectastain elite ABC kit (Vector Laboratories, Burlingame, CA, USA; cat. no. PK 6100).

2.4. Immunohistochemistry and Nonradioactive In Situ *Hybridization*

All of the reagents and solutions listed in **Subheadings 2.2.** and **2.3.**

2.5. Double Immunofluorescence

1. Blocking solution: To prepare 10 mL of solution, use the following:
   a. 3 mL Normal serum (fetal bovine serum [FBS] works well with the majority of antibodies; alternatively, you can block with normal serum from the same species in which the secondary antibody has been made);
   b. 600 µL of 10% (v/v) Triton X-100 in water.
   c. 1.6 mL P buffer.
   d. 1.8 mL of 5 *M* NaCl.
   e. H_2O to 10 mL.
   Dilute this solution 1:1 in water to use it as dilution buffer for both primary and secondary antibodies.
2. Wash buffer: To prepare 1 L, use the following:
   a. 90 mL of 5 *M* NaCl.
   b. 30 mL of 10% (v/v) Triton X-100 in water.

c. 83 mL of P buffer.
d. Water to 1 L.
3. P buffer: 19 mL of 0.24 *M* NaH_2PO_4 +81 mL of 0.24 *M* Na_2HPO_4 in 200 mL of H_2O.

3. Methods

3.1. Radioactive In Situ *Hybridization*

3.1.1. Preparation of Paraffin-Embedded Tissue

Paraffin sections are recommended for *in situ* hybridization because of better conservation of tissue morphology. Also, frozen sections can be used with good results.

1. Fix the tissues in cold 4% paraformaldehyde/PBS overnight (O/N) at 4°C.
2. Rinse twice in 1X PBS.
3. Dehydrate through 50%, 70%, 85%, and 95% ethanol for 30 min each passage and then twice in 100% ethanol for 30 min at 4°C.
4. Clear in xylene twice for 30 min at room temperature.
5. Infiltrate tissues with xylene/wax 1:1, twice for 30 min at 60°C and then O/N.
6. Position the tissue with hot forceps and then let the wax solidify at room temperature. Blocks can be stored indefinitely at 4°C.
7. Cut ribbon of 5-µm sections with a microtome.
8. Place two to four sections onto polylysine-coated slides covered by a thin layer of DEPC water.
9. Let the slides dry on a slide warmer at 42°C.
10. When the water layer is completely dried, put the slides at 37°C O/N.
11. Store the slides in a sealed box with desiccant at 4°C for no more than 1 yr.

3.1.2. Synthesis of Riboprobe

The template for transcription of the riboprobe should be cDNA cloned into a plasmid, which has promoter elements for T3 or Sp6 and T7 polymerase flanking the polylinker (*see* **Note 1**). Both the antisense probe, to detect the specific mRNA of interest, and the sense probe, as a negative control, must be transcribed. The plasmid must be completely linearized with two restriction enzymes, cutting at the 5' end to transcribe the antisense probe and at the 3' end for sense probe (*see* **Notes 2** and **3**). Purify the linearized DNA and resuspend at a final concentration of 1 µg/mL.

1. Prepare the mix at room temperature (the transcription buffer precipitates on ice).

10X transcription buffer	2.5 µL
Linearized plasmid (1 µg/µL)	1 µL
10m*M* ATP	1 µL
10m*M* GTP	1 µL

10m*M* CTP	1 µL
0.2 *M* dithiothreitol (DTT)	3.75 µL (30 m*M* final concentration)
RNAse inhibitor	20 U
S^{35}-UTP	5 µL (100 µCi)
RNA polymerase	10 U
DEPC H_2O	to 25 µL

2. Incubate for 2 h at 37°C.
3. Add 1 µL of RNA polymerase after the first hour of transcription.
4. Digest the DNA template. Follow **step 5**.
5. Add the following to the transcription mix:
   17 µL of DEPC-treated water;
   2 µL of 10X transcription buffer;
   1 µL of DNase (2 U).
6. Incubate for 15 min at 37°C.
7. Precipitate riboprobe by adding the following:
   100 µL of DEPC-treated water;
   100 µL of yeast RNA, 1 mg/mL;
   250 µL of 4 *M* ammonium acetate;
   1 mL of 100% Et-OH.
8. Mix well and put on ice for 1 h.
9. Spin for 15 min at 11,000*g* at 4°C, discard supernatant, and air-dry the RNA pellet.
10. Resuspend in 200 µL of DEPC water.
11. Vortex well and add the following:
    200 µL of 4 *M* ammonium acetate;
    1 mL of 100% Et-OH.
12. 1 h on ice.
13. Spin for 15 min at 11,000*g* at 4°C and discard the supernatant.
14. Wash with 1 mL of 70% Et-OH and perfectly dry the pellet under a hood before resuspension.
15. Resuspend in 50 µL of 10 m*M* DTT.
16. Count 1 µL of riboprobe in 2 mL of liquid scintillation fluid with the β-counter. The activity should be approx 3×10^6 counts per minute (cpm)/µL. Store at –80°C.
17. Check transcribed riboprobe, loading 1 µL on a denaturing 5–6% polyacrylamide gel.

3.1.3. Prehybridization Treatment of Tissue

Dewax and rehydrate tissues through a series of 10-min washes at room temperature:

1. Xilene twice.
2. 100% Ethanol twice.
3. 95% Ethanol twice.

4. 70% Ethanol twice.
5. Ethanol 100% and NaCl 0.9%, 1:1.
6. 0.9% NaCl.
7. Acid treatment: 0.2 *N* HCl, 15 min at room temperature.
8. Three washes in 1X PBS for 1 min at room temperature.
9. Protein digestion: 20 µg/mL proteinase K in 50 m*M* Tris-HCl, pH 7.6, 5 m*M* EDTA for 5–15 min. The time depends on the thickness of the sections and the type of tissue. Titrate the optimal digestion time. For bronchial biopsies, 5 min is sufficient. After this step and until postfixation, the sections are particularly fragile.
10. Block proteinase K acitivity with the following:
    Two washes in 0.4% glycine in 1X PBS for 2 min at room temperature;
    Two washes in 0.9% NaCl for 2 min at room temperature.
11. Postfixation: Fix sections with cold 4% paraformaldehyde/PBS, 15 min at room temperature.
12. Rinse twice in 1X PBS.
13. Two minutes in 0.9% NaCl.
14. Acetylation of amino groups of positively charged amino acids to reduce background as a result of nonspecific electrostating binding: immediately before use, add 0.5 mL of acetic anhydride in 200 mL of 0.2 *M* triethanolamine–HCl, pH 8.0, 5 min at room temperature and repeat the step.
15. Rinse twice in DEPC water for 1 min and let the slides completely dry at room temperature on a paper towel.
16. Store the slides in a sealed box with desiccant for several days.

3.1.4. Hybridization

1. Prepare 150 µL of hybridization mix per slide (because of the high viscosity of the solution, count 1 extra slide for every 20):
   1X High salt.
   50 m*M* DTT.
   500 µg/mL polyribo A.
   50 µg/mL yeast tRNA.
   10% (w/v) Dextran sulfate.
   50% (v/v) Formamide.
   DEPC water to final volume.
   The hybridization mix can be frozen at –80°C.
2. Add 1 µL (3×10^6 cpm) of riboprobe to 150 µL of hyb mix, denaturate at 65°C for 10 min, and then put at room temperature.
3. Immediately put the mix in one drop on the sections and spread it on the slide.
4. Cover the sections with a piece of Parafilm (5 × 2 cm). Avoid forming bubbles during this operation and make sure that there are no bubbles on the sections.
5. Incubate slides O/N in a humidified chamber at 55–65°C. Hybridization temperature depends on the probe length and it has to be titrated in your experiment (generally, 60°C is a good starting point).

3.1.5. Washing

Prepare 200 mL of each washing solution per step and prewarm solutions for at least 1 h. For FSM washing, use the same temperature that has been used for the hybridization.

1. With forceps, carefully remove the parafilm from the slides, dipping the slide in a Petri dish with 10 mL of prewarmed FSM solution to let the parafilm detach from sections without forcing.
2. Put the slides in a 20-slides carrier and perform washing **steps a–h** in a staining dish.
   a. FSM, 30 min at 55–65°C, twice.
   b. STE, 10 min at 37°C, twice.
   c. 10 µg/mL RNAse type II-A in STE, 30 min at 37°C.
   d. STEM, 10 min at 37°C.
   e. FSM, 45 min at 55–65°C, twice.
   f. 2X SSC, 10 min at 37°C.
   g. H_2O, 2 min at room temperature.
   h. Put the slides face up on a paper towel and let them air-dry for 1–2 h.

3.1.6. Visualization of Signal

To have a very preliminary idea of your results, the air-dried slides can be exposed on an X-ray film (Kodak Biomax) for 3 d at room temperature. Slides that show a good signal-to-noise ratio are then dipped into photographic emulsion. All of the following steps have to be conducted under safelight conditions. Use Kodak red safelight #2 filter and keep the slides at least 0.5 m away from direct light and put black tape on all indicator lights of the instruments you are using. Prepare Kodak NTB-2 emulsion.

1. Warm the emulsion (118 mL) at 42°C for 30–60 min and then dilute it with 200 mL of prewarmed deionized water. Mix very gently to avoid bubbles formation.
2. Make 40-mL aliquots in Falcon tubes or glass vials, wrapped with aluminum, and store them in the dark at 4°C in a Plexiglas box to avoid emulsion damage by radiations. Alternatively, you can directly aliquot prewarmed emulsion and dilute one aliquot with 1 volume of deionized water, immediately before use.
3. Put an aliquot of emulsion into the dipping chamber immersed in a 42°C water bath.
4. Warm the solution for 30 min. In the meantime, prepare a slide carrier, some paper towels and a black box with its slide rack.
5. Dip each slide for 5 s in the emulsion, drain the excess in a vertical position, and then clean the back of the slide with a paper towel.
6. Put the slide face up in the mailer. About 40 slides can be dipped using one emulsion aliquot.
7. Dry the sections for 5 h in the dark.

8. Put the slides in a rack, in the vertical position in a plastic black box with silica gel as the desiccant. You can place the box in a black plastic bag (normally used for autoradiography film exposure) and then in a Plexiglas box.
9. Slides are exposed to emulsion for 7–30 d, depending on the target mRNA abundance in the tissue. Usually, a 15-d exposure is sufficient for most probes; too short an exposure can lead to low detectable signal because of small silver granule precipitation, whereas overexposure gives too high a background (*see* **Note 4**). After exposure, silver granules are developed as in **steps 11–17**.
10. Remove Plexiglas box containing slides from 4°C at least 1 h prior, to equilibrate to room temperature. Temperature differences can lead to emulsion cracking.
11. Open the black box under the safelight and develop slides in Kodak D-19 developer for exactly 2 min.
12. Rinse in deionized water for 12 s.
13. Fix slides in Kodak fixer solutions for 15 min.
14. Wash slides for 15 min in deionized water with gentle agitation.
15. Dry sections overnight, keeping them away from dust.
16. Mount cover slips with Canada balsam or another nonaqueous mounting medium.
17. Examine and photograph slides with a dark-field-equipped microscope; under these conditions, silver grains of an *in situ* signal appear white. Use Kodak T-max 100 film to record images.

3.1.7. Counterstaining

To better visualize tissues, after the last rinse in water before mounting the slides, you can stain them with hematoxylin or with a lighter nuclei stain such as methyl green. Alternatively, you can counterstain sections with Hoechst-33258 (5 µg/mL) and simultaneously visualize nuclei and an *in situ* signal with ultraviolet (UV) fluorescence.

3.2. *Nonradioactive* In Situ *Hybridization*

3.2.1. Preparation of Tissue

Both paraffin-embedded and liquid-nitrogen frozen tissues work well in nonradioactive *in situ* hybridization. Follow the protocol of radioactive *in situ* hybridization for prehybridization treatment of paraffin-embedded tissue. For snap-frozen tissues, 5- to 7-µm cryostat cut sections are treated according the following protocol in **Subheading 3.2.2.**

3.2.2. Synthesis of Probe

General considerations on probe transcription reported for radioactive *in situ* hybridization are valid also for nonradioactive *in situ* hybridization. Instead of radioactive UTP to label the probe, insertion of digoxigenin-conjugated UTP is used. The hybridized probe is then revealed with a monoclonal antibody against digoxigenin.

1. Prepare the linearized plasmids as for radioactive *in situ* hybridization and transcribe the riboprobe with the Roche kit or alternatively as follows:

10X Transcription buffer	2 µL
Linearized plasmid (1µg/µL)	1 µL
10 m*M* ATP	µL
10 m*M* GTP	2 µL
10 m*M* CTP	2 µL
10 m*M* UTP	1.2 µL
0.2 *M* DTT	1 µL (10 m*M* final concentration)
RNAse inhibitor	20 U
10m*M* Digoxigenin-11-UTP	0.8 µL
RNA polymerase	10 U
DEPC H_2O	to 20 µL

2. Incubate for 2 h 37°C.
3. Add 1 µL of RNA polymerase after the first hour of transcription.
4. Digest the DNA template. Follow **step 5**.
5. Add the following to the transcription mix:
   17 µL of DEPC-treated water;
   2 µL of 10X transcription buffer;
   1 µL of DNase (2 U).
6. Incubate for 15 min at 37°C and then put on ice.
7. Precipitate riboprobe by adding the following:
   5 µL of 4 *M* LiCl;
   155 µL of 100% Et-OH.
8. Let the riboprobe precipitate O/N at –20°C.
9. Spin for 20 min at 11,000*g* at 4°C, discard supernatant, and air-dry the RNA pellet.
10. Resuspend in 22.5 µL of DEPC water.
11. Vortex well and add the following:
    2.5 µL of 4 *M* LiCl;
    75 µL of 100% Et-OH.
12. 2 h at –20°C.
13. Spin for 20 min at 11,000*g* at 4°C and discard supernatant.
14. Wash with 1 mL of 70% Et-OH and perfectly dry the pellet under a hood before resuspension.
15. Resuspend in 50 µL of DEPC water.
16. Load 1 µL of riboprobe on a formaldheyde gel. Concentration of riboprobe is usually 100–150 ng/µL. Alternatively, you can accurately check the quantity of transcribed probe with the Roche kit DIG Control Test Strips.
17. Store at no less that –20°C.

3.2.3. Prehybridization Treatment of Tissue

With paraffin-embedded tissues, follow the protocol for radioactive *in situ* hybridization. Alternatively, if you have frozen sections work according to the following protocol.

1. Take the slides from –80°C and let them dry for few minutes. All of the following steps are at room temperature.
2. Fix with cold 4% PFA/1X PBS for 20 min.
3. Wash twice in 1X PBS for 5 min.
4. Wash in 0.9% NaCl for 2 min.
5. Immediately before use, add 0.5 mL of acetic anhydride in 200 mL of 0.2 *M* triethanolamine-HCl, pH 8.0, 5 min at room temperature and repeat the step.
6. Rinse twice in 2X SSC for 1 min.
7. Store the slides at this step in a sealed box with desiccant for a few days.
8. Dehydrate sections through a series of 5-min washes at room temperature:
   30% Ethanol.
   50% Ethanol.
   70% Ethanol.
   95% Ethanol.
   100% Ethanol, twice.
   Chloroform, 10 min.
   100% Ethanol, 2 min twice.
   95% Ethanol, 2 min.
9. Air-dry sections for 2 h at room temperature, keeping the slides away from dust.

3.2.4. Hybridization

1. Prepare the hybridization mix immediately before use, 150 µL per slide (because of the high viscosity of the solution, count 1 extra slide for every 20):
   50% Deionized formamide.
   1X Denhardt's solution.
   3X SSC.
   10% (w/v) Dextransulfate (stock 50% [w/v] in DEPC water).
   500 µg/mL yeast tRNA (stock 10 mg/mL in DEPC water).
   500 µg/mL Salmon sperm DNA denatured for 5 min at 95°C (stock 10 mg/mL in DEPC water).
2. Denature digoxigenin-labeled riboprobe to a final concentration of 1 µg/mL (denature riboprobe heating it at 65°C for 10 min and put immediately on ice).
3. Warm the hybridization mix for 10 min at 50°C and add the denatured riboprobe.
4. Cover each slide with 150 µL of the prepared mix and cover with a piece of Parafilm, avoiding bubble formation, especially on the tissues.
5. Incubate slides in the horizontal position in a humidified chamber at 55–65°C O/N. Hybridization temperature depends on the probe length and it has to be titrated in each experiment (generally, 60°C is a good starting point).

3.2.5. Posthybridization Washings

1. Eliminate the pieces of Parafilm from the slides, dipping them in a Petri dish with 10 mL of prewarmed wash solution. Let the Parafilm gently detach from the tissues without forcing or stretching.

2. Put the slides in a vertical rack and wash them as in **steps 3–7**.
3. 50% Formamide–2X SSC for 30 min at 55–65°C, twice.
4. NTE for 15 min at 37°C, twice.
5. 20 µg/mL RNAseA type II-A in NTE for 30 min at 37°C, to digest the single-strand RNA that remained nonhybridized.
6. NTE for 15 min at 37°C.
7. 50% Formamide–1X SSC for 30 min at 55–65°C, twice.
8. 2X SSC for 10 min at room temperature.
9. Go directly to the immunostaining step (*see* **Subheading 3.2.6.**) and do not let the slides air-dry between each step.

3.2.6. Immunostaining

1. Wash the slides twice in TBS for 15 min at room temperature.
2. Take the slides and drain the excess liquid; put them in the horizontal position in a humidified chamber.
3. Cover the tissues with 1 mL of blocking solution and incubate at room temperature for 1 h.
4. Discard the blocking solution and replace with the AP-conjugated anti-digoxigenin monoclonal antibody diluted 1:1000 to 1:2000 in 1% sheep serum in TBS.
5. Incubate O/N at 4°C in the humidified chamber.

3.2.7. Washing

1. Put the slides in a vertical rack and wash them at room temperature with 200 mL of each solution of **steps 2** and **3**.
2. TBS for 15 min, twice.
3. NTM for 10 min, twice.

3.2.8. Visualization of Signal

1. Drain the excess of washing solution from the slides with a paper towel. Put the slides in horizontal position and cover the tissues with the staining solution prepared almost 15 min before use.
2. Keep the slides in the dark, because the AP substrates are light sensitive. Check the developing of the staining under a bright-field microscope. NBT/BCIP gives a purple staining. Alternatively, you can use BM purple from Roche that gives a blue staining.
3. When a sufficient staining has developed, block the reaction by repetitively washing the slides in 1X PBS for 10 min (*see* **Note 5**).

3.2.9. Nuclei Counterstaining

When using NBT/BCIP as AP substrates, counterstain the nuclei to better visualize the morphology of the tissue with hematoxylin. Alternatively, different counterstaining procedures routinely used for immunohistochemistry, such as methyl green, can be used. *See* **Subheading 3.3.**

1. Dip the slides for 30–60 s in hematoxylin.
2. Wash them in water until the blue color has disappear from the water.
3. Mount the slides with an aqueous mounting medium and observe results under a bright-field microscope.

3.3. Immunohistochemistry

3.3.1. Preparation of Tissue

In general, snap-frozen tissues work better in immunohistochemistry than paraffin sections, because of the high temperature used for paraffin inclusion and the long time of fixation in PFA that tend to alter the conformation of antigens. However, many antibodies work well also on paraffin sections without any specific treatment. In some cases, it is useful to pretreat sections with antigen unmasking solutions, such as trypsin, citrate acid, or other protocols (i.e., boiling sections in a microwave oven) that induce a change in the protein conformation and facilitate access of the antibody to its specific antigen (*see* **Note 6**).

Another advantage of liquid-nitrogen frozen tissues is that sections can be cut without fixing the tissues and so one can choose between different fixation methods and select the one that works better with each specific primary antibody.

1. Air-dry sections for 10–15 min at room temperature.
2. Fix with cold PFA 4%/1X PBS for 15 min at room temperature.
3. Rinse twice with 1X PBS for 2 min at room temperature.
4. If a horseradish peroxidase (HRP)-conjugated system is used to detect signal, quencing of endogenous peroxidase activity is required, by incubating the sections in 0.3% H_2O_2/1X PBS for 30 min at room temperature. Otherwise, when an alkaline phosphatase-conjugated system is used, this step is not necessary because all of the AP substrates already contain levamisole, an inhibitor of endogenous phosphatases.
5. Rinse twice with 1X PBS for 2 min at room temperature.

3.3.2. Blocking

1. Blocking in 10% normal serum (normal serum from the species in which the secondary antibody is made) 1X PBS/0.1% Triton X-100 for 1 h at room temperature in a humidified chamber.
2. Apply a sufficient volume on the slide to cover the entire section and do not let the sections dry. Generally, 100–150 µL per slide is sufficient.

3.3.3. Incubation of Primary Antibody

1. Blot the excess of serum on a paper towel and replace blocking with the primary antibody, diluted in the same blocking solution. Add 100 µL per slide (*see* **Note 7**).
2. Incubate the sections alternatively for 1 h at 37°C and 2 h at room temperature or O/N at 4°C, in a humidified chamber.

3. Wash with 1X PBS for 10 min at room temperature four to five times with gentle shaking.

3.3.4. Incubation of Secondary Antibody

1. Incubate sections with biotinylated secondary antibody diluted 1:400 in 1X PBS/10% normal serum for 1 h at room temperature in a humidified chamber.
2. Wash with 1X PBS for 10 min at room temperature four to five times with gentle shaking.

3.3.5. Avidin–Biotin Amplification of Signal

1. Prepare the avidin–biotin complex as follows: Add 10 µL of avidin to 1 mL of 1X PBS, mix well, and then add 10 µL of biotinylated HRP or AP and mix immediately.
2. Allow the reagent to stand for about 30 min before use.
3. Incubate sections for 1 h at room temperature.
4. Wash with 1X PBS for 10 min at room temperature four to five times with gentle shaking (*see* **Notes 8** and **9**).

3.3.6. Visualization of Signal and Nuclei Counterstaining

1. Incubate sections with the corresponding enzyme substrate solution (*see* **Notes 10** and **11**) for about 10 min and follow the tissue staining under a microscope.
2. When the specific staining is dark enough and before the background has reached too high a level, stop the staining by immerging the slides in 1X PBS.
3. Rinse sections several times with 1X PBS, before counterstaining the nuclei (*see* **Note 12**).
4. Dehydrate sections with ethanol series (50%, 70%, 95%, 100%, 10 min each) and permanently mount with nonaqueous mounting medium.

3.4. Immunohistochemistry and Nonradioactive In Situ *Hybridization*

This combination of two different techniques on the same slide allows the simultaneous detection of an antigen with a specific antibody and the mRNA coding for a protein for which a specific antibody is not available. Alternatively, it can be useful to detect both mRNA and the corresponding translated protein on the same cell. This protocol works well especially for membrane or nuclear protein, because in this case, the immunohistochemistry signal does not overlap with the cytoplasmic staining of *in situ* hybridization.

Unfortunately, the protein digestion step with proteinase K, necessary to permeabilize tissue and to let the *in situ* probe reach the corresponding mRNA, disrupts all of the protein epitopes. Thus, immunohistochemistry must precede nonradioactive *in situ* hybridization, although this second protocol has more critical points because of the RNase-free conditions required.

1. The tissues are to be prepared as for nonradioactive *in situ* hybridization. Keep all of the reagents and instruments used RNase-free.

2. First perform the immunohistochemistry following the standard protocols but using RNase-free solutions (*see* **Note 13**).
3. Immediately after the staining has developed, block the reaction according to the protocol of the substrate used and wash the slides three times in DEPC water.
4. Start with the *in situ* hybridization protocol: Fix the tissue with cold 4% PFA in 1X PBS for 10 min at room temperature.
5. Wash twice in 1X PBS for 2 min at room temperature.
6. Digest protein with 1 µg/mL of proteinase K in 20 m*M* Tris-HCl, 1 m*M* EDTA, pH 7.2, for 15 min at room temperature.
7. Wash twice in 1X PBS for 2 min at room temperature.
8. Fix the tissues again with cold 4% PFA in 1X PBS for 5 min at room temperature.
9. Wash twice in 1X PBS for 2 min at room temperature.
10. Air-dry the sections and perform hybridization following the steps in **Subheading 3.2.**

3.5. Double Immunofluorescence

3.5.1. Preparation of Tissue

This protocol was developed for frozen tissues, but it works well on paraffin-embedded sections also, provided that the primary antibody works on them. For further details, see preparation of tissue in **Subheading 3.3.**

Some tissues with large amounts of fibrillar or naturally pigmented components can be autofluorescent, so check if this is the case by observing a non-stained section under the microscope. Sometimes, the tissue autofluorescence is higher when the sections is excited with a particular wavelength and not with others, so choose a wavelength that is out of the range of natural autofluorescence (in our experience, green dyes such as FITC give more problems of autofluorescence of connettival tissue of the bronchi mucosa than red dyes such as Texas red).

When staining snap-frozen sections, fix tissues for 15 min in 4% PFA/1X PBS before the blocking step. For paraffin-embedded tissues, follow the protocol for the prehybridization treatment of tissue described in **Subheading 3.1.3.** to rehydrate the sections.

3.5.2. Blocking

1. Wash slides once in 1X PBS, drain the excess of solution, and put them in the horizontal position.
2. Block with 0.1 *M* Gly/1X PBS, pH 7.4, for 10 min at room temperature, twice.
3. Block with blocking solution for 15 min at room temperature, twice.

3.5.3. Incubation with Primary Antibody

1. Drain the excess blocking solution.

2. Incubate with the two primary antibodies diluted in blocking solution/water 1:1 in a humidified chamber. The incubation with primary antibodies is 2 h at room temperature or O/N at 4°C. In the last case, cover the slides with Parafilm to avoid excessive evaporation. The selection of the pair of primary antibodies to be used is made on the basis of the animal species in which the two antibodies are produced. Select antibodies made in different species (i.e., mouse monoclonal antibody against human CD3 and goat polyclonal antibody against human CCR4) or at least of different isotypes (i.e., IgG1 and IgM or IgG2a) to avoid risk of cross-reaction of the secondary antibodies. Otherwise, if you have two antibodies from the same species, you can perform sequential staining, starting with the antibody against the more abundant antigen. In this case, remember to perform the second staining protocol completely in dark boxes to protect slides from photo bleaching of the first dye used (*see* **Note 14**).

3.5.4. Washing

Wash the slides five times, 10 min each, in washing solution and then put them in the humidified box in the horizontal position.

3.5.5. Incubation of Secondary Antibody

1. Dilute the conjugated secondary antibodies as for primary ones (usually commercially available antibodies work at 1:100 dilution).
2. Use about 150 µL per slide and incubate in a black box, avoiding excessive light exposure of the slides, for 1 h at room temperature.

Choose secondary antibodies that are cross-adsorbed (one antibody is adsorbed with proteins from the species in which the other one has been made); otherwise, you will have nonspecific double-positive staining. Usually, antibodies made in the donkey have less problems of crossreaction with other species.

3.5.6. Washing

1. Wash the slides five times, 10 min each, in washing solution and then twice in 1X PBS.
2. Mount the slides using 90% glycerol/1X PBS and seal the edges of the slides with transparent enamel. Alternatively, several aqueous mounting media suitable for immunofluorescence are commercially available.

3.5.7. Visualization of Signal

The fluorescent signal can be visualized either with a classic incident light fluorescent microscope equipped with a 50-W mercury lamp and filter blocks for fluorescein and rhodamine or, even better, with a confocal microscope. This last option gives better results, because the confocal microscope analyzes

a single optical section of the specimen corresponding to one focal plane. This reduces the background resulting from overlapping of different focal sections and gives higher-quality images with more distinct fluorescent details. In double-fluorescence confocal analysis, the sample is scanned sequentially with two different excitation laser lines allowing detection of the two different fluorescent markers. After image acquisition, single fluorescent images are then digitally merged. Regions of coexpression of the two markers will appear as yellow pixels.

Because this kind of analysis is limited by the optical resolution of the system, it is necessary to remember that colocalization does not imply molecular interaction between the two molecules that are detected with this system, but only that the two molecules are expressed by the same cell, in the same subcellular compartment, and that they are very close to each other. Other more sophisticated techniques such as FRET (fluorescence resonance energy transfer) have been developed for this purpose.

4. Notes

1. All of the solutions and equipment (slide dishes, slide carriers) used before the hybridization step must be Rnase-free, so prepare the solutions in DEPC water, with perfectly clean instruments and powders. It is better to have chemical powders dedicated to *in situ* only. All of the solutions must be autoclaved. Always wear gloves when preparing the solutions and performing all the steps of the protocol until hybridization. After this step, the RNA probe–mRNA duplex is resistant to RNAse.
2. To avoid cross-hybridization with homologous genes, the best choice is to design the probe spanning the 5' or 3' untranslated region of the gene of interest, which are the less conserved. The 200- to 600-bp probe usually works well. Smaller probes are not so specific and have insufficient specific activity. Longer probes must be alkali hydrolyzed before use.
3. If you can choose, clone the cDNA in a way that you can trascribe the antisense probe with the T7 polymerase that is the most efficient of the three. Do not linearize cDNA with an enzyme which leaves 5' protruding ends, because this may cause the start of the transcription in the wrong direction and a consequently low transcription level.
4. The emulsion is light, temperature, and stress sensitive, so keep it in a dry and fresh place, in a Plexiglas box, and try to avoid any mechanical stress during manipulation. You can control the integrity of the emulsion by dipping a control slide. Let it dry for 1 h and then develop it. If the emulsion is good, the slide appears completely clear.
5. Depending on the abundance of the target RNA and the length and quantity of probe used, the staining procedure can take from 30 min to several hours. If, after 3–4 h, no staining is visible under the microscope and if the background is not too high, continue the staining until the next day. Place the slides at 4°C in horizontal

position in a humidified chamber and completely cover the tissue with staining solution. Cover the slides with Parafilm to avoid evaporation of the solution. On the following morning, replace the staining solution with fresh one and continue the staining at room temperature.

6. There are several commercially available antigen-retrieval solutions that you can use. Alternatively, you can try the following two protocols:
   - Dip deparaffinated and dehydrated slides in a 10-m*M* citric acid solution. Set the microwave oven at maximal power and incubate slides for 5 min from the boiling point of the solution. Remove from the microwave oven and let the slides stand for 2 min at room temperature. Refill the evaporated solution to completely cover the slides and repeat the step in the microwave oven twice. Let the slides stand at room temperature until they are completely cold. Wash twice in 1X PBS and follow the standard protocol.
   - Prepare the trypsin solution (0.1% trypsine, 0.1% CaCl) and warm at 37°C. Prepare one dish with water at the same temperature and one at room temperature. Incubate deparaffinated and dehydrated sections in warm water for 10 min and then in the trypsin solution for 15 min before use. Stop the reaction by dipping the slides into cold water. Wash twice in 1X PBS and follow the standard protocol.
7. Set a control omitting the primary antibody or, in the case that the primary antibody is a monoclonal one, use the same quantity of an isotype matched antibody to control the specificity of the staining. If the background is too high, first titrate down the quantity of the secondary antibody and eventually also of the primary antibody.
8. Do not add serum in the preparation of the avidin–biotin solution, because serum biotin can inhibit the formation of the complex with the enzyme-conjugated biotin.
9. It is useful to set a control slide incubated only with the avidin–biotin complex to monitor the nonspecific binding of the complex to the tissue you are staining. If a high background is present, you can try to eliminate it by adding 0.3–0.5 *M* NaCl during the preparation of the avidin–biotin complex to decrease nonspecific ionic interactions. Alternatively, you can introduce an additional blocking step, after the blocking with serum, with an avidin–biotin blocking kit.
10. Some tissues have a high level of endogenous peroxidase activity that gives a high background in immunohistochemistry; check if this is the case by processing one slide omitting all the antibodies and incubating it only with the substrate. To minimize this effect, one can increase the incubation in H_2O_2 or, better, switch to an AP-conjugated system, which is less efficient but is less problematic than nonspecific staining.
11. As a substrate for peroxidase, you can choose among the SG-substrate, which gives a dark blue staining, DAB (brown), nickel-enhanced DAB (gray), or AEC (red), all from Vector. Remember that for naturally pigmented tissues, such as skin biopsies, red staining is desirable. For AP conjugated, you can choose between BCIP/NBT (Sigma), which gives a blue-violet staining, and Fucsin (Sigma). There are also other substrates both for AP and HRP sold by Vector that allows several different combinations of colors for multiple staining of the same tissue.

12. For nuclear counterstaining, use a system that gives a good contrast with the staining substrate chosen. If SG or nickel-enhanced DAB is used, a good contrast is obtained by staining the nuclei in red with Vector nuclear fast red. For DAB staining, methyl green is preferable, whereas AEC can be used with hematoxylin. Some substrates such as AEC are ethanol soluble, so sections must not be dehydrated and the slides can be mounted with an aqueous mounting medium.
13. Wear gloves and prepare all the buffers with DEPC water. Add 100 U/mL of RNase inhibitor to the normal serum used in the immunohistochemistry protocol.
14. One protocol we have used is as follows. Briefly, after the first single staining, sections were incubated with 15% normal serum to saturate any open antigen-binding site on the Cy2-conjugated secondary antibody, so that binding of the other primary antibody was prevented. The slides were then incubated with an excess of unconjugated Fab secondary antibody to block any nonspecific binding site. The second single staining was performed using a Rhodamine Red-X-conjugated secondary antibody.

Control stainings were performed as follows:

1. A single primary antibody with both secondary antibodies.
2. Negative control, omitting one or both primary antibodies.

Once mounted, slides were analyzed with a confocal microscope (MRC-1024, BioRad Laboratories) equipped with a 15-mW krypton/argon laser emitting at 488 nm and 647 nm, mounted on a Nikon Eclipse E600 microscope. Images were acquired and analyzed with Laser Sharp 3.2 software.

References

1. Gerard, C. and Rollins, B. J. (2001) Chemokines and disease. *Nat. Immunol.* **2,** 108–115.
2. Baggiolini, M. and Loetscher, P. (2000) Chemokines in inflammation and immunity. *Immunol. Today* **21,** 418–420.
3. Bonecchi, R., Bianchi, G., Panina-Bordignon, P., et al. (1998) Differential expression of chemokine receptors and chemotactic responsiveness of type 1 T helper cells (Th1s) and Th2s. *J. Exp. Med.* **187,** 129–134.
4. Sallusto, F., Lenig, D., Mackay, C. R., and Lanzavecchia, A. (1998) Flexible programs of chemokine receptor expression on human polarized T helper 1 and 2 lymphocytes. *J. Exp. Med.* **187,** 875–883.
5. Loetscher, P., Uguccioni, M., Bordoli, L., et al. (1998) CCR5 is characteristic of Th1 lymphocytes. *Nature* **391,** 344–345.
6. Qin, S., Rottman, J. B., Myers, P., et al. (1998) The chemokine receptor CXCR3 and CCR5 mark subsets of T cell associated with certain inflammatory reactions. *J. Clin. Invest.* **101,** 746–754.
7. Sallusto, F., Mackay, C., and Lanzavecchia, A. (1997) Selective expression of the eotaxin receptor CCR3 by human T helper 2 cells. *Science* **277,** 2005–2007.

8. Gerber, B. O., Zanni, M. P., Uguccioni, M., et al. (1997) Functional expression of the eotaxin receptor CCR3 in T lymphocytes co-localizing with eosinophils. *Curr. Biol.* **7,** 836–843.
9. Imai, T., Nagira, M., Takagi, S., et al. (1999) Selective recruitment of CCR4-bering Th2 cells toward antigen presenting cells by the CC chemokine thymus and activation regulated chemokine and macrophage-derived chemokine. *Int. Immunol.* **11,** 81–88.
10. Zingoni, A., Soto, H., Hedrick, J. A., et al. (1998) The chemokine receptor CCR8 is preferentially expressed in Th2 but not Th1 cells. *J. Immunol.* **161,** 547–551.
11. Panina-Bordignon, P., Papi, A., Mariani, M., et al. (2001) The C–C chemokine receptors CCR4 and CCR8 identify airway T cells of allergen-challenged atopic asthmatics. *J. Clin. Invest.* **107,** 1357–1364.
12. Saetta M., Mariani, M., Panina-Bordignon, P., et al. (2002) Increased expression of the chemokine receptor CXCR3 and its ligand CXCL10 in peripheral airways of smokers with chronic obstructive pulmonary disease. *Am. J. Respir. Crit. Care Med.* **165,** 1404–1409.

13

Interaction of Viral Chemokine Inhibitors with Chemokines

Antonio Alcami

1. Introduction

Viruses modulate the chemokine network by encoding homologs of chemokines and chemokine receptors and secreted proteins that bind chemokines ***(1–3)***. These mechanisms have been identified in large DNA viruses such as herpesviruses and poxviruses. The exceptions are the chemokinelike activity of the human immunodeficiency virus (HIV) Tat protein and the mimicry of fractalkine by the glycoprotein G of respiratory syncytial virus.

Virus-encoded chemokine homologs function as agonists, binding the cellular receptors and transducing signals, or antagonists, preventing the activity of chemokines by occupying chemokine receptors. Viral seven-transmembrane-domain chemokine receptors are expressed at the surface of infected cells and may transduce signals, sometimes in the absence of a ligand. Three viral chemokine-binding proteins (vCKBPs) have been identified to date ***(4)***. These vCKBPs are secreted in large amounts from infected cells and, despite the lack of sequence similarity to cellular chemokine receptors, bind chemokines and neutralize their activity. The myxoma virus M-T7 protein (vCKBP-1) has been proposed to inhibit chemokine activity by preventing the interaction of chemokines with glycolaminoglycans and disrupting the chemokine gradient ***(5)***. The vaccinia virus (VV) 35-kDa protein and myxoma virus M-T1 (vCKBP-2) bind CC chemokines with high affinity and neutralize their activity by preventing interaction with cellular chemokine receptors ***(6–8)***. The protein M3 encoded by murine gammaherpesvirus 68 (vCKBP-3) binds a broad range of chemokines, including CC, CXC, C, and CX_3C chemokines, and neutralizes their activity ***(9,10)***.

The methods used to study the binding properties and biological activity of viral chemokines and chemokine receptors are similar to those utilized to characterize

From: *Methods in Molecular Biology, vol. 239: Cell Migration in Inflammation and Immunity*
Edited by: D. D'Ambrosio and F. Sinigaglia © Humana Press Inc., Totowa, NJ

the cellular homologs and are described elsewhere in this volume. This chapter will focus on methods that have been specifically used to identify and characterize secreted virus-encoded proteins that bind chemokines (vCKBPs). A chemokine-binding assay to cells that can also be used to characterize the binding properties of the viral chemokine and chemokine-receptor homologs is described. The ability of vCKBPs to neutralize the biological activity of chemokines can be determined in standard chemokine-induced cell migration and calcium mobilization assays.

2. Materials

1. Serum-free tissue culture medium.
2. Phosphate-buffered saline (PBS).
3. Trioxsalen (4,5',8-trimethylpsoralen; Sigma). Freshly prepare 100X trioxsalen solution by disolving 1 mg in 1 mL of dimethyl sulfoxide (DMSO) at 37°C for 3 h and dilute to a final concentration of 200 µg/mL in DMSO. Trioxsalen is a potential carcinogen.
4. Ultraviolet (UV) crosslinker.
5. Centriprep spin protein concentrators (AMICON) of 3000 molecular-weight (MW) cutoff.
6. Micro-ProDiCon (Bio-Molecular Dynamics) with dialysis membrane (MWCO 25,000), available from Pierce.
7. 1 *M* HEPES, pH 7.4.
8. Binding medium: RPMI containing 20 m*M* HEPES, pH 7.5, and 0.1% bovine serum albumin (BSA).
9. Radioiodinated chemokines (2200 Ci/mmol), available from Perkin-Elmer Life Sciences and Amersham Biosciences.
10. EDC [1-ethyl-3(3-dimethylaminopropyl) carbodiimide] (Sigma). Final concentration in the assay is 40 m*M*. Prepare 10X stock solution at 400 m*M* (76 mg/mL) in water and store at –20°C.
11. EGS (ethylene glycol-bis-succinamidylsuccinate) (Sigma). Final concentration in the assay is 1 mg/mL. Prepare 10X stock solution at 10 mg/mL in DMSO, which should be prepared fresh for each experiment.
12. BS^3 [bis(sulfosuccinimidyl) suberate] from Pierce. Final concentration in the assay is 5 m*M*. Prepare 10X stock solution at 50 m*M* in 5 m*M* sodium citrate, pH 5, which should be prepared fresh every time.
13. 1 *M* Tris-HCl, pH 7.5.
14. Sodium dodecyl sulfate–polyacrylamide gel electrophoresis (SDS-PAGE) solutions and equipment.
15. Nitrocellulose membrane.
16. Electrophoretic transfer apparatus.
17. Blocking solution for ligand blot: 3% Nonfat skimmed milk powder in 10 m*M* Tris-HCl, pH 7.4, 140 m*M* NaCl, 0.02% NaN_3.
18. 0.5 *M* EDTA in PBS.

19. Phthalate oil mix: 1.5 Parts of dibutyl phthalate (Sigma) and 1 part of dioctyl phathlate [bis(2ethylhexyl)phthalate] (Aldrich).
20. Gamma-counter.
21. Binding buffer for scintillation proximity assay (SPA) and FlashPlate®, 0.1% BSA in PBS.
22. Protein A–fluoromicrosphere scintillant-embedded beads (SPA beads; Amersham Biosciences). Reconstitute with binding medium as recommended by the manufacturer. The SPA beads can be stored at 4°C for up to 7 d or at –20°C for extended periods.
23. β-scintillation counter.
24. Nickel chelate FlashPlate (Perkin-Elmer Life Sciences).
25. Packard TopCount™ microplate scintillation and luminiscent counter.
26. Microscint (Packard), a special scintillant design for the Packard TopCount microplate scintillation and luminiscent counter.

3. Methods

3.1. Generation of Secreted Proteins from Virus-Infected Cell Cultures

Initial screenings for the presence of vCKBPs are carried out with crude supernatants from cell cultures infected with relevant viruses ***(11,12)***. The supernatants may be concentrated to maximize the possibilities of finding vCKBPs. Although removal of virus particles by centrifugation may greatly reduce virus titers, additional methods should be used to ensure inactivation of infectious virus, such as treatment with trioxsalen and UV light ***(13)*** (*see* **Note 1**). Inactivation of infectious virus particles will render infected cell supernatants safe to handle on the open bench.

1. Infect cell monolayers with virus at high multiplicity of infection (5–10 plaque-forming units per cell) in a small volume of serum-containing tissue culture medium (i.e., 10 mL in a 175-cm^2 flask). Prepare supernatants from mock-infected cells as a control.
2. After an adsorption period of 1–2 h at 37°C, wash monolayers three times with serum-free tissue culture medium or PBS to remove any remaining virus or residual serum.
3. Follow the infection in a small volume of serum-free medium (i.e., 15–20 mL for a 175-cm^2 flask) for 24–48 h to ensure maximal expression of viral proteins.
4. Collect the supernatants and centrifuge at 4°C for 15 min at 3300*g* to remove cellular debris. Add HEPES, pH 7.4, to a final concentration of 20 m*M* to stabilize the pH of the supernatants.
5. Virus particles present in supernatants may be removed by ultracentrifugation (i.e., 33,000*g* for 1 h at 4°C).
6. Inactivate infectious virus by treatment with trioxsalen and UV light. Add 10 µL trioxsalen stock per milliliter of supernatant to give a final concentration of 2 µg/mL. Incubate for 10 min at room temperature. Transfer 3-mL aliquots of the supernatant

to six-well tissue culture plates. Remove the lid of the six-well plate and expose to UV in a crosslinker for 5 min (*see* **Note 2**). Test the inactivation by titration on cell monolayers.
7. Concentrate supernatant 5- to 10-fold using a Centriprep concentrator by centrifugation at 4°C. Alternatively, supernatants can be concentrated and dialyzed against PBS using a Micro-ProDicon.
8. Store the concentrated supernatants at –80°C.

3.2. Crosslinking of Radiolabeled Chemokines to Soluble vCKBPs

This method has been successfully used to identify all the vCKBPs described to date ***(5–7,9,10)***. After incubation of radioiodinated chemokines with samples that potentially contain vCKBPs, the interaction of chemokines with binding proteins is visualized by inducing covalent crosslinking between interacting proteins and analysis by SDS-PAGE (*see* **Fig. 1**). As an alternative, nonradioactive chemokines can be crosslinked and the complexes visualized by Western blot with specific antibodies ***(5,10)***. Once a vCKBP has been identified by using radioiodinated chemokines, the crosslinking may be repeated in the presence of increasing doses of unlabeled chemokines to determine the ability of other chemokines to bind the vCKBP (*see* **Fig. 1**). This method is very sensitive and will identify low-affinity interactions. It is critical that chemokine activity assays are also performed to confirm whether the vCKBP neutralizes the activity of specific chemokines.

1. Incubate 10–20 µL supernatants from uninfected or infected cells with 1–2 µL of ^{125}I-chemokine (0.4–0.8 n*M*) in 25 µL final volume for 2 h at room temperature. Add 100- to 1000-fold excess of unlabeled chemokine to demonstrate specificity of the interaction, or other unlabeled chemokines to determine chemokine-binding specificity.
2. Add 2.5 µL of the crosslinker EDC, EGS, or BS^3 and incubate for 15 min at room temperature (*see* **Note 3**).
3. Add 2.5 µL of 1 *M* Tris-HCl, pH 7.5, to quench the reaction.
4. Centrifuge the sample in a microfuge (15,000*g*) for 15 min (*see* **Note 4**).
5. Transfer 20 µL of the supernatant to a tube containing 20 µL of 2X Laemmli buffer with mercaptoethanol. Boil for 3 min.
6. Load 10–15 µL in a 12% polyacrylamide gel to separate chemokines from complexes by electrophoresis.
7. Fix and dry the gel, and expose to autoradiography film with two intensifying screens at –80°C. An overnight exposure may be sufficient to detect the presence of chemokine–vCKBP complexes.

3.3. Ligand Blot Assay

The ligand blot assay has been successfully used to identify the interaction of a variety of cytokines with their receptors and with viral proteins ***(11,14)***.

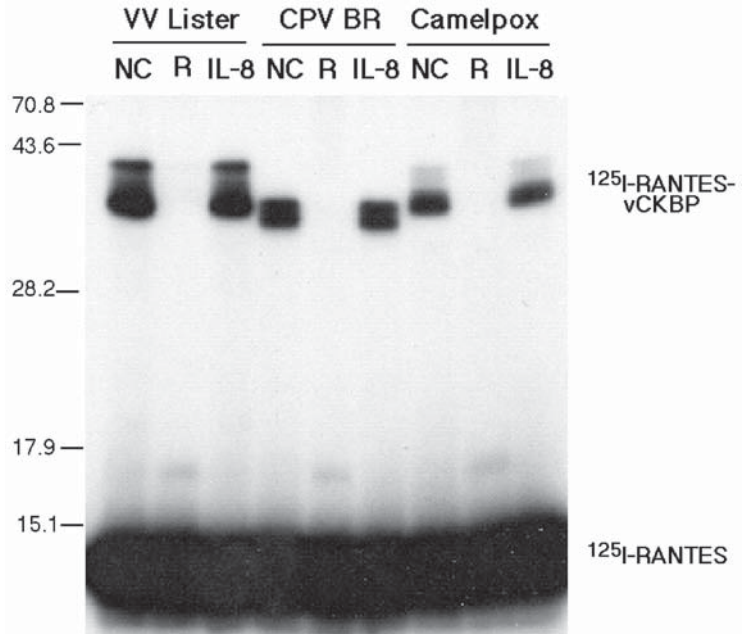

Fig. 1. Identification of vCKBPs by chemokine crosslinking assay. Media from cultures infected with VV strain Lister (VV Lister), cowpox virus strain Brighton Red (CPV BR), or camelpox virus were incubated with ^{125}I-RANTES and treated with the crosslinker EDC. The incubation was performed in the absence of unlabeled competitor (NC) or in the presence of a 500-fold excess of unlabeled RANTES (R) or interleukin-8 (IL-8). An autoradiograph of the SDS-PAGE analysis, with molecular masses in kilodaltons, is shown. The position of RANTES and RANTES–vCKBP complexes are indicated. The addition of unlabeled chemokines illustrates the binding specificity of the vCKBPs for CC chemokines (RANTES) but not CXC chemokines (IL-8).

Proteins are resolved by SDS-PAGE in the absence of reducing agents, tranferred to a nitrocellulose membrane, and incubated with radioiodinated chemokines. The major limitation of this method is that insufficient protein renaturation after immobilization onto the membrane support may limit the detection of chemokine–protein interactions.

1. Resolve 10–20 µL of concentrated serum-free virus-infected and mock-infected supernatants under nonreducing conditions by SDS-PAGE.
2. Transfer the proteins onto a nitrocellulose membrane using an electrophoretic transfer apparatus under standard conditions.
3. Incubate the nitrocellulose membrane with blocking solution overnight at 4°C on a shaker.

4. Incubate the nitrocellulose membrane with 2–10 n*M* ^{125}I-chemokine in blocking solution for 4 h at room temperature. Binding specificity should be demonstrated in the presence of a 100- to 1000-fold excess unlabeled chemokine.
5. Wash the nitrocellulose membrane with bocking solution three times for 30 min.
6. Air-dry the nitrocellulose membrane on filter paper for 10 min.
7. Place the membrane between layers of Saran Wrap and expose to autoradiography film with two intensifying screens at –80°C. Expose overnight or for longer periods as necessary.

3.4. Chemokine Binding to Cells

This method will test whether binding of chemokines to the vCKBP prevents the interaction of chemokines with specific cellular receptors (*see* **Fig. 2**) ***(6,9)***. It can also be used to study the binding of virus-encoded chemokines to cells expressing chemokine receptors or to test the ability of virus-infected cells or transfected cells expressing viral chemokine receptors to bind chemokines. The first step of the method should be ignored in studying viral chemokines and chemokine receptors.

The affinity of cellular chemokine receptors for chemokines can be determined from saturation curves. Once the affinity is known, the ability of purified vCKBPs to inhibit binding of ^{125}I-chemokines to cellular receptors will give us an indirect indication of the binding affinity of the vCKBP–chemokine interaction.

1. Incubate various doses of supernatant containing vCKBP or purified vCKBP with ^{125}I-chemokine (final concentration 100–300 p*M*) in 100 µL of binding medium for 1 h at 4°C.
2. Prepare cells expressing chemokine receptors. Cells growing in suspension, such as U937 and THP-1 cells, are washed twice with binding medium by centrifugation. Cells growing in a monolayer can be detached from the substrate by incubation with 0.5 m*M* EDTA in PBS for 10–15 min. Cells must be washed twice with binding

---

Fig. 2. (*opposite page*) Inhibition of chemokine binding to cellular receptors by vCKBPs. This assay can be used to demonstrate that some vCKBPs inhibit chemokine activity by blocking the interaction of chemokines with specific cellular receptors (**A**). Binding assay of 100 p*M* ^{125}I-MIP-1α and ^{125}I-GRO-α to U937 cells in the presence of purified VV 35-kDa vCKBP (**B**), supernatants from cultures infected with poxviruses or recombinant baculoviruses, or 100-fold excess unlabeled chemokines (**C**). Supernatants were prepared from cultures infected with VV Lister, VV Lister lacking the 35-kDa protein (ListerΔ35K), cowpox virus, or recombinant baculovirus expressing the VV Lister 35 kDa protein or the VV B8R protein. The dose of supernatant corresponding to a number of cells (cell equivalents) is indicated. Means (±SEM) from duplicate samples are expressed as the percentage of counts binding in the absence of competitor. [Panels (**B**) and (**C**) are reproduced from ref. ***6*** with permission.]

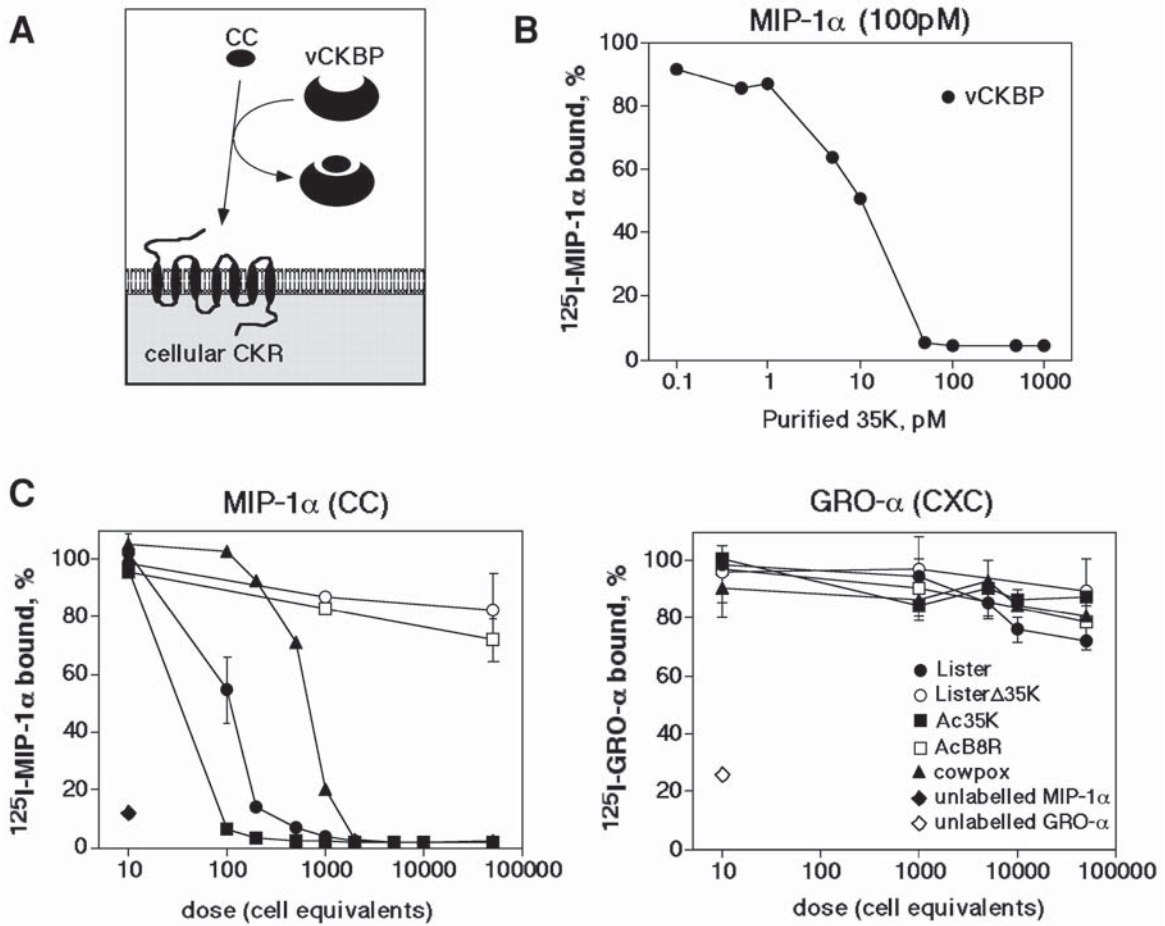
A
CC
vCKBP
cellular CKR
B
MIP-1α (100pM)
vCKBP
125I-MIP-1α bound, %
Purified 35K, pM
C
MIP-1α (CC)
125I-MIP-1α bound, %
dose (cell equivalents)
GRO-α (CXC)
125I-GRO-α bound, %
Lister
ListerΔ35K
Ac35K
AcB8R
cowpox
unlabelled MIP-1α
unlabelled GRO-α
dose (cell equivalents)

medium by centrifugation. After the washings, cells are resuspended to a concentration of 2.5×10^6 cells in 50 µL (*see* **Note 5**).
3. Add 2.5×10^6 cells in suspension in 50 µL and incubate for 2 h at 4°C with occasional shaking.
4. Centrifuge (microfuge 30 s) 125 µL of the cell suspension through 200 µL of the phthalate oil mix in 0.5-mL Eppendorf tubes. Aspirate the supernatant and cut with scissors the tip of the tube containing the pellet ***(15)***.
5. Transfer the tip of the Eppendorf tube to a suitable tube to count the radioactivity in a gamma-counter.

3.5. Scintillation Proximity Assay

Scintillation proximity assay (SPA) is a powerful quantitative binding method ***(16)***. This technology is available from Amersham Biosciences as microspheres embedded with scintillant. Different SPA bead formats are available with antibodies or proteins bound to the surface of the beads. In the protocol described here, protein A-coated beads are used to characterize the interaction of chemokines with vCKBPs fused to the Fc portion of IgG1 ***(6)***. The vCKBP-Fc protein binds to the surface of protein A-coated fluomicrospheres. In order to generate a signal, the radioligand must bind to the receptor to be in close proximity to the fluomicrospheres to excite the scintillant (*see* **Fig. 3**). The unbound radioligand does not activate the scintillant and eliminates the need to separate bound from free and to carry out extensive washings and manipulations. Therefore, this method consists of mixing all the reagents and counting the radioactivity bound.

It is important to determine experimentally the amount of purified vCKBP-Fc to be used in the assay, which will normally be 1–100 ng. High concentrations of vCKBP-Fc will saturate the binding capacity of the protein A–SPA beads and the excess vCKBP-Fc in solution will prevent binding of the radiolabeled chemokine to vCKBP-Fc-coated beads (*see* **Note 6**). The specific binding may be

---

Fig. 3. (*opposite page*) SPA to study the interaction of vCKBPs with chemokines. (**A**) Illustration of SPA using protein A fluoromicrospheres containing scintillant (SPA Prot.A) to detect the interaction of ^{125}I-MIP-1α with the VV Lister 35-kDa vCKBP fused to the Fc portion of human IgG1 (35K-Fc). (**B**) Saturation curve and Scatchard analysis of ^{125}I-MIP-1α binding to VV 35K-Fc. The mean (±SEM) specific binding of triplicate samples is shown. (**C**) Competitive inhibition with various doses of CC chemokines. Purified VV 35K-Fc protein was incubated in triplicate with 50 p*M* ^{125}I-MIP-1α in the presence of increasing doses of unlabeled human CC chemokines. The percentage of specific binding (mean ± SEM) refers to binding in the absence of competitor. The K_D values calculated from the data are indicated. (Panels [**B**] and [**C**] are reproduced from ref. ***6*** with permission.)

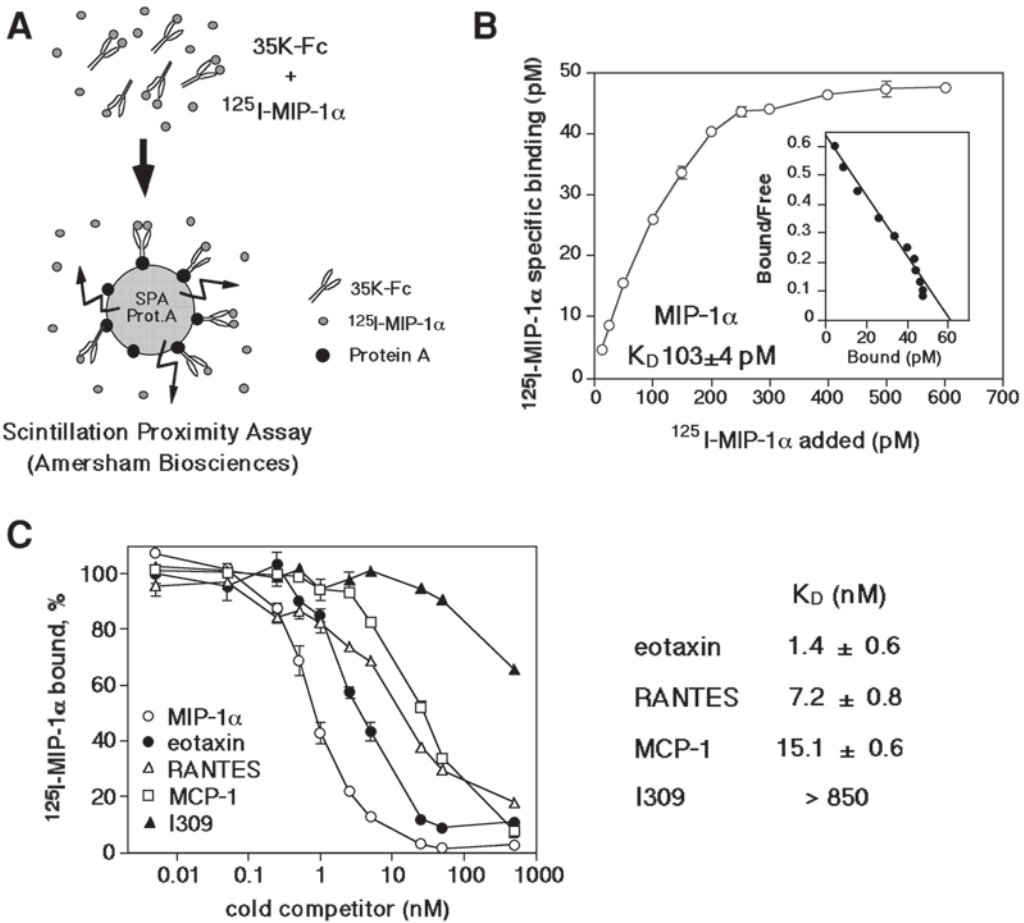

	K_D (nM)
eotaxin	1.4 ± 0.6
RANTES	7.2 ± 0.8
MCP-1	15.1 ± 0.6
I309	> 850

determined as the binding in the presence of an excess of unlabeled chemokines or as the binding in the presence of a control Fc-fusion protein or human IgG1.

This method can be used to determine chemokine specificity by either direct binding to a number of radioiodinated chemokines or by addition of unlabeled chemokines that may inhibit the interaction of a ^{125}I-chemokine known to bind to the vCKBP (*see* **Fig. 3**). This method is more quantitative than the crosslinking assay and will enable determination of the binding affinity of the vCKBP–chemokine interaction. This can be achieved by performing saturation curves with increasing doses of ^{125}I-chemokine followed by Scatchard analysis of the binding data. Alternatively, the affinity of vCKBP for chemokines can be indirectly calculated by determining the binding of a ^{125}I-chemokine of known binding affinity to vCKBP in the presence of increasing doses of unlabeled chemokines (*see* **Fig. 3**).

1. Incubate radiolabeled chemokines (200–400 p*M*) with 1–100 ng of purified vCKBP-Fc in 100 µL of binding buffer for 2 h at room temperature. Unlabeled chemokines can be added as necessary (*see* **Note 7**).
2. Add 50 µL of protein A–SPA beads and incubate for 2 h at room temperature (*see* **Note 8**).
3. Determine the radioactivity bound to vCKBP-Fc by counting in a β-scintillation counter (*see* **Note 9**).
4. The total radioactivity added must be determined in a β-scintillation counter after addition of a standard scintillant to a relevant amount of ^{125}I-chemokine.

3.6. FlashPlate Assay

The principle of the FlashPlate (Perkin-Elmer Life Sciences) is the same as that of SPA, but, in this case, the assay has been designed in a plate format. FlashPlate is a 96-well microplate designed for binding assays with radiolabeled ligands ***(17)***. The interior of each well is coated with a thin layer of polystyrene-based scintillant. In order to generate a signal, the radioisotope must be in close proximity to the surface of the well to excite the scintillant (*see* **Fig. 4**). Unbound radioligand does not activate the scintillant and, thus, there is no need to carry out

Fig. 4. (*opposite page*) FlashPlate assay to characterize the interaction of vCKBPs with chemokines. (**A**) Illustration of FlashPlate assay to determine the interaction of radiolabeled chemokines with purified vCKBP expressed with a C-terminal 6xhis tag (vCKBP-his) in nickel chelate FlashPlate. (**B**) Binding of 200 p*M* ^{125}I-IL-8 to increasing doses of purified murine herpesvirus 68 M3 protein fused to a C-terminal 6xhis tag. The M3 protein, expressed in the baculovirus system ***(9)*** and purified by metal-affinity chromatography, was provided by Campbell Bunce (Xenova, Cambridge, UK). The mean (±SD) specific binding of triplicate samples is shown. (**C**) Saturation curve of ^{125}I-IL-8 binding to purified M3 (1 ng). The mean (±SD) specific binding of triplicate samples is shown.

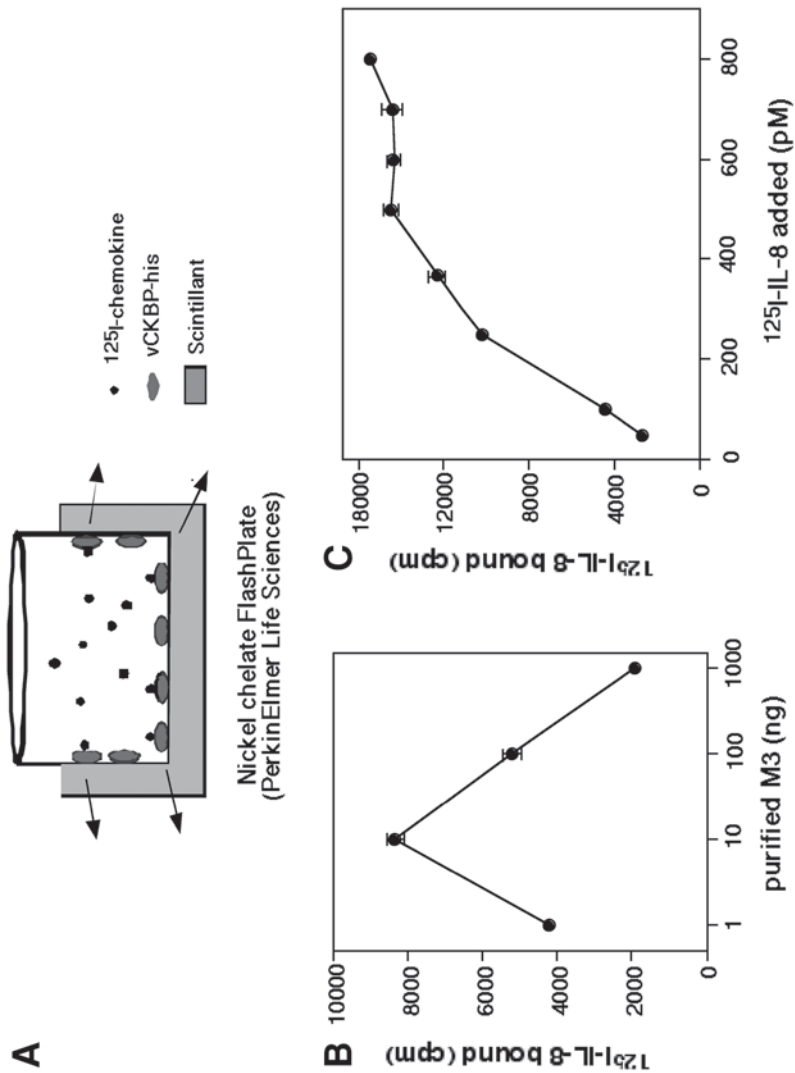
A
125I-chemokine
vCKBP-his
Scintillant
Nickel chelate FlashPlate
(PerkinElmer Life Sciences)
B
125I-IL-8 bound (cpm)
purified M3 (ng)
C
125I-IL-8 bound (cpm)
125I-IL-8 added (pM)

extensive washings. FlashPlate was designed for use with the Packard TopCount microplate scintillation and luminiscent counter, but the Wallac MicroBeta PLUS can also be used.

Different PlashPlate formats are available that have secondary antibodies or other proteins precoated into the wells. In the protocol described here, a nickel chelate FlashPlate format is used to study the interaction of chemokines with vCKBPs fused to a C-terminal 6xhis tag (vCKBP-his). The protein A-coated FlashPlate can also be used when the vCKBP or other receptors are expressed fused to the Fc portion of human IgG1 ***(18)***.

As for the SPA beads from Amersham Biosciences, the concentration of vCKBP-his used in the assay will need to be determined experimentally, which will normally be 1–100 ng. A typical experiment is shown in **Fig. 4**, which illustrates how the addition of an excess of vCKBP-his may reduce the signal (*see* **Note 6**). As indicated for SPA, the FlashPlate platform can be used to determine chemokine specificity, by either direct binding to ^{125}I-chemokines or by competitive inhibition with unlabeled chemokines, and for determination of the binding affinity of the vCKBP–chemokine interaction, from saturation curves or competitive inhibition assays with increasing doses of unlabeled chemokines (*see* **Fig. 4**).

One of the advantages of FlashPlate versus SPA beads is that the use of a microplate format reduces even further the manipulations of the samples and simplifies the process of counting.

1. Add radiolabeled chemokines (200–400 p*M*) and 1–100 ng of purified vCKBP-his in 100 µL of binding buffer to the wells of a nickel chelate FlashPlate. Unlabeled chemokines can be added as necessary (*see* **Note 7**).
2. Incubate for 4–6 h at room temperature or for longer periods at 4°C (*see* **Note 8**).
3. Count the FlashPlate at different times of incubation in a Packard TopCount microplate scintillation and luminiscent counter (*see* **Note 9**).
4. The total radioactivity added can be determined by addition of Microscint, a scintillant designed for this counter, to control wells.

4. Notes

1. Trioxalen is a photochemical DNA crosslinker that will efficiently inactivate virus infectivity. Treatment with UV light in the absence of trioxsalen will reduce virus infectivity but may not completely inactivate the infectivity.
2. The conditions of UV treatment must be determined by exposing the sample to different times and titration in standard virus plaque assays.
3. A variety of chemical crosslinkers with different functional group specificity and length of the spacer are available. Those listed here have been successfully used for this type of interaction. However, it is important to consider that not all protein–

protein interactions may be crosslinked efficiently with a particular crosslinker, and thus the use of a number of them is recommended.
4. This step can be avoided but it will be necessary if high background levels are observed.
5. Binding assays can be performed on cell monolayers, but the radioactivity bound may be low if the number of receptors per cell is not very high. Binding in suspension is more sensitive because higher cell densities can be achieved.
6. When large amounts of vCKBP-Fc protein are needed, the protein A–SPA beads or FlashPlate may be precoated with purified viral protein and the excess of protein removed by washing the beads or wells, before addition of the radiolabeled chemokines.
7. PBS containing 0.1% BSA instead of tissue culture medium is recommended in the binding buffer for SPA and FlashPlate to avoid possible quenching when counting radioactivity resulting from phenol red present in the medium. If tissue culture medium is used, phenol red-free medium should be used in these assays.
8. Affinity constants must be calculated at equilibrium. The time of incubation necessary to reach maximum binding should be detemined experimentally.
9. Because the complete mix is counted and no washings is necessary, the same set of tubes containing SPA beads or the same FlashPlate can be counted several times to determine the kinetics of interaction of chemokines with the viral protein.

Acknowledgment

The work in the author's laboratory is funded by the Wellcome Trust.

References

1. Murphy, P. M. (2001) Viral exploitation and subversion of the immune system through chemokine mimicry. *Nat. Immunol.* **2,** 116–122.
2. Lalani, A. S., Barrett, J. W., and McFadden, G. (2000) Modulating chemokines: more lessons from viruses. *Immunol. Today* **21,** 100–106.
3. Alcami, A. and Koszinowski, U. H. (2000) Viral mechanisms of immune evasion. *Immunol. Today* **21,** 447–455.
4. Smith, P. V., Bryant, N. A., and Alcami, A. (2002) Soluble chemokine binding proteins encoded by viruses, in *Chemokines and Viral Infections* (Mahalingam, S., ed.), Landes Bioscience, Austin, TX.
5. Lalani, A. S., Graham, K., Mossman, K., et al. (1997) The purified myxoma virus gamma interferon receptor homolog M-T7 interacts with the heparin-binding domains of chemokines. *J. Virol.* **71,** 4356–4363.
6. Alcami, A., Symons, J. A., Collins, P. D., Williams, T. J., and Smith, G. L. (1998) Blockade of chemokine activity by a soluble chemokine binding protein from vaccinia virus. *J. Immunol.* **160,** 624–633.
7. Graham, K. A., Lalani, A. S., Macen, J. L., et al. (1997) The T1/35kDa family of poxvirus-secreted proteins bind chemokines and modulate leukocyte influx into virus-infected tissues. *Virology* **229,** 12–24.

8. Smith, C. A., Smith, T. D., Smolak, P. J., et al. (1997) Poxvirus genomes encode a secreted, soluble protein that preferentially inhibits beta chemokine activity yet lacks sequence homology to known chemokine receptors. *Virology* **236,** 316–327.
9. Parry, C. M., Simas, J. P., Smith, V. P., et al. (2000) A broad spectrum secreted chemokine binding protein encoded by a herpesvirus. *J. Exp. Med.* **191,** 573–578.
10. van Berkel, V., Barrett, J., Tiffany, H. L., et al. (2000) Identification of a gammaherpesvirus selective chemokine binding protein that inhibits chemokine action. *J. Virol.* **74,** 6741–6747.
11. Symons, J. A., Alcamí, A., and Smith, G. L. (1995) Vaccinia virus encodes a soluble type I interferon receptor of novel structure and broad species specificity. *Cell* **81,** 551–560.
12. Alcami, A. and Smith, G. L. (1992) A soluble receptor for interleukin-1β encoded by vaccinia virus: a novel mechanism of virus modulation of the host response to infection. *Cell* **71,** 153–167.
13. Tsung, K., Yim, J. H., Marti, W., Buller, R. M. L., and Norton, J. A. (1996) Gene expression and cytopathic effect of vaccinia virus inactivated by psoralen and long-wave UV light. *J. Virol.* **70,** 165–171.
14. Spriggs, M. K., Hruby, D. E., Maliszewski, C. R., et al. (1992) Vaccinia and cowpox viruses encode a novel secreted interleukin-1-binding protein. *Cell* **71,** 145–152.
15. Dower, S. K., Kronheim, S. R., March, C. J., et al. (1985) Detection and characterization of high affinity plasma membrane receptors for human interleukin-1. *J. Exp. Med.* **162,** 501–515.
16. Bosworth, N. and Towers, P. (1989) Scintillation proximity assay. *Nature* **314,** 167–168.
17. Brown, B. A., Cain, M., Broadbent, J., et al. (1997) FlashPlate technology, in *High Throughput Screening: The Discovery of Bioactive Substances* (Devlin, J. P., ed.), Marcel Dekker, New York, pp. 317–328.
18. Komesli, S., Vivien, D., and Dutartre, P. (1998) Chimeric extracellular domain of type II transforming growth factor (TGF)-beta receptor fused to the Fc region of human immunoglobulin as a TGF-beta antagonist. *Eur. J. Biochem.* **254,** 505–513.

14

Discovery of Small-Molecule Antagonists of Chemokine Receptors

Screening Strategy and Assays

Maria Elena Fuentes

1. Introduction

Among the most important regulators of leukocyte migration are chemokines, a group of low-molecular-weight cytokines (8–10 kDa) that regulate cell infiltration and trafficking. They are responsible for the recruitment of leukocytes to sites of injury and inflammation and, more recently, have also been identified as major players in the homeostatic trafficking of cells to lymphoid tissues. They exert their action through seven-transmembrane G-protein-coupled receptors and trigger a cascade of signaling events including activation of phospholipase C and phosphoinositol 3 kinase γ and calcium mobilization ***(1)***.

Many reports indicated that chemokines played important roles in human diseases. Probably the best validated chemokine receptor in the clinic is CCR5 for its function as one of the two coreceptors for the human immunodeficiency virus (HIV). Strong genetic evidence supports an important role for this receptor in HIV pathogenesis. A deletion in the receptor (Δ32) correlates with the lack of surface expression of the receptor and resistance to HIV infection ***(2)***. Many companies are developing small molecules capable of blocking the binding of HIV virus to CCR5.

Other critical immune system diseases for which chemokine receptors play an important role include inflammatory diseases like rheumatoid arthritis (RA), inflammatory bowel diseases, psoriasis, asthma, and multiple sclerosis.

CCL3 (MIP-1α), a ligand for CCR1, has been found highly concentrated in the synovial fluid of rheumatoid arthritis patients and in the cerebrospinal fluid of patients with multiple sclerosis (MS) ***(3,4)***. Animal models of these diseases

From: *Methods in Molecular Biology, vol. 239: Cell Migration in Inflammation and Immunity*
Edited by: D. D'Ambrosio and F. Sinigaglia

have also shown a potential role for CCR1 in the development and/or maintenance of the inflammation in these diseases ***(5,6)***. In addition, strong evidence suggesting a role for CCR1 in transplant rejection has been obtained using knockout mice ***(7)***. All of these results have prompted pharmaceutical companies to develop small-molecule antagonists for CCR1. Several companies have reported the discovery of such antagonists and some of them are currently in the clinic.

Other receptors of significant interest for therapeutic use of antagonists include CCR3. This receptor is expressed mainly on eosinophils, basophils, mast cells, and T helper type 2 (Th2) cells ***(8–10)***. An important role in the development of allergic diseases has been suggested for all of these cell types. Thus, blocking CCR3 could have great potential for blocking allergic inflammation in diseases like asthma and allergic rhinitis. Animal models support this rationale.

Several other chemokine receptors have the potential for being good points of intervention for many diseases.

The chemokine system is highly redundant, with many chemokines hitting one receptor and, at the same time, several receptors responding to the same chemokine. There are a few exceptions to this rule where there is an exclusive 1:1 interaction for ligand and receptor. Some examples are CCR6 and its ligand CCL20 (MIP-3α), CXCR4 and CXCL12 (SDF-1), and CXCR5 and CXCL13 (BCA-1, BLC) ***(11)***. One question that remains unanswered is whether blocking one chemokine receptor would be sufficient to achieve clinical efficacy as a result of the redundancy of the system or whether it will be necessary to hit several receptors to achieve this goal. A final answer to this question awaits clinical trial results.

1.1. Screening Strategy

Several options exist for screening chemokine receptors in order to find small-molecule antagonists. **Figure 1** shows one possible strategy that we have used for the past few years. It involves a functional assay of receptor-activated Ca^{2+} signaling (FLIPR) (*see* **Subheading 3.1.**) as the primary high-throughput screening assay, binding and chemotaxis measurements as secondary assays, and final testing of efficacy in an animal model. Compounds that show consistent inhibition of Ca^{2+} of 50% or more in the functional test move to the next set of assays. Depending on the quality of the library being screened, it is always advisable to have chemistry input on the compounds that should move forward. In general, compounds that show low nanomolar inhibitory concentrations 50 (IC_{50}s) in the secondary assays move to the in vivo efficacy. Before testing in animal models, it is important to verify the activity of the compounds in the same species utilized in the model. Many reports have shown important

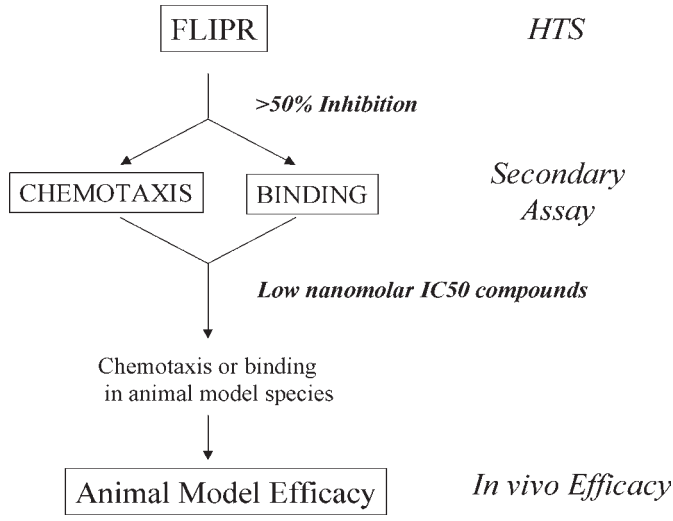

Fig. 1. Screening paradigm. Schematic representation of the screening strategy presented. HTS: high-throughput screening; FLIPR: fluorometric imaging plate reader.

species differences for potency of chemokine-receptor antagonists. One extreme example is the CCR1 antagonist. Although one selective inhibitor was able to displace the radiolabeled ligand from the human receptor with a K_i of 40 n*M*, the same molecule was unable to displace the ligand from the mouse receptor ***(12)***. Other molecules, however, show similar potencies against human and mouse CCR1 receptors ***(13)***. It is also very important to perform pharmacokinetic studies before moving into in vivo models.

2. Materials

2.1. High-Throughput Screening

1. Fluorometric imaging plate reader (Molecular Devices, Sunnyvale, CA).
2. Chinese hamster ovary cells expressing Gα16.
3. Purified chemokine (usually from R&D Systems).
4. Fluo-3 (TEFLABS, Austin, TX).

2.2. Binding Assay

1. Radiolabeled ligand (Amersham or NEN).
2. Cells expressing significant number of receptors.
3. Filters GF/B or GF/C (Perkin-Elmer Life Sciences).
4. Topcount (Packard, Meriden, CT).
5. Micro Lab® AT2 (Hamilton Instruments).
6. Harvester Filtermate 196 (Packard, Meriden, CT).

2.3. Chemotaxis

1. A 96-well chemotaxis plate (Neuroprobe #116-5 with 5-µm pores).
2. Chemotaxis medium: RPMI containing 0.1% bovine serum albumin (BSA), 10 m*M* HEPES.
3. Lysis bufer: 0.1% Triton X-100, 5 µ*M* propidium iodide, 2 m*M* Tris-HCl, pH 7.2.
4. Cells: L1.2 cells expressing hCCR3 receptor. (*See* **Note 1.)**
5. Eotaxin (R&D Systems) used at 2 n*M* final concentration in the assay.
6. Optional: Automatic pipetting station (Hamilton MICRO LAB® AT 2).

3. Methods

3.1. High-Throughput Screening

For high-throughput screening (HTS), probably the most heavily used technique in the G-protein coupled reactor (GPCR) field is the fluorometric imaging plate reader (FLIPR®; Molecular Devices, Sunnyvale, CA). It measures agonist-induced calcium mobilization in cells expressing the receptor endogenously or in cells that have been transfected with the receptor of interest. In order to increase the calcium signal, we usually use Chinese hamster ovary (CHO) cells that also express the G-protein Gα16 ***(14)***. We routinely use transfected cells expressing 50,000–200,000 receptors/cell in a 384-well format. In our experience, the average throughput for this assay is 20,000–30,000 compounds per day. The most widely used fluorophor is Fluo-3. Protocols for calcium mobilization measurements using the FLIPR have been described previously ***(15)***. The primary advantage of using a FLIPR-based functional assay is that it allows for the identification of antagonist activity quite quickly. Other advantages include consistently robust detection of responses and ease of adapting to different receptor–cell systems. Although one disadvantages is that the receptor need to be coupled to calcium, this seems not to be a problem with chemokine receptors. So far, all receptors we have tested respond in the Gα16 system. These include CCR3, CCR4, CCR6, CCR7, and CCR8. Disadvantages of the FLIPR are that a relatively high number of nonspecific inhibitors are usually identified. Anything that interferes with the signaling pathway downstream of receptor function will have an effect on the response. To filter true chemokine-receptor antagonists from other nonspecific compounds, it is necessary to establish good secondary assays (*see* **Subheading 3.2.**). It is also helpful to build a database with frequent hitters in this assay. Fluorescent compounds sometimes present challenges in this system as well.

One alternative assay to FLIPR for HTS is blocking direct binding of fluorescent-labeled ligand using the fluorometric microvolume assay technology (FMAT) ***(16)***.

3.2. Secondary Assays

As mentioned in **Subheading 3.1.**, to identify true antagonists it is imperative to follow up FLIPR hits with robust secondary assays. We usually use two types of secondary assay: inhibition of ligand binding to the receptor and inhibition of ligand-induced cell migration (chemotaxis assay).

3.2.1. Binding Assay

Binding assays are important because they allow the determination of direct receptor interaction for the hits identified in the HTS. Determinations of IC_{50}s in this assay also allow us to determine the relative potency of the compounds. Typically, we use ^{125}I-radiolabeled ligands (from Amersham or NEN) and transfected cells expressing large numbers of receptors. Detailed protocols for radioactive binding of chemokine receptors have been described ***(17)***. We typically obtain better signals with whole cells than with membrane preparations, although many chemokine receptors work well in the latter system. To avoid problems with receptor internalization, we use sodium azide in the binding buffer. Under these conditions, binding at room temperature and binding at 4°C have been shown to be comparable, suggesting no receptor internalization in the presence of sodium azide. The conditions need to be set up in such a way that only 5–10% of the total counts bind to the receptor. We routinely run this assay in a 96-well format, and all dilutions are done in an automatic pipetting station (e.g., Hamilton MICRO LAB® AT 2). Incubation is for 60–90 min at room temperature.

3.2.2. Chemotaxis Assay

The general strategy for finding a chemokine-receptor antagonist usually includes chemotaxis or cell migration assays. We use a 96-well format and either recombinant cells expressing the receptor or cells expressing the receptor endogenously. Instead of counting cells at the end of the experiment, we indirectly quantitate the number of cells that migrate using propidium iodide staining. **Figure 2A** shows a curve indicating the linear relationship between fluorescence units and number of cells. A linear curve is obtained to approx 62,000 cells/well. After that point, the curve loses linearity and tends to plateou even if the number of cells keep increasing. A detailed protocol of the chemotaxis assay is described in **Subheading 3.2.3**.

3.2.3. CCR3 Chemotaxis Assay in 96-Well Format

1. L1.2 cells transfected with hCCR3 are induced with 2 m*M* *n*-butyric acid overnight (*see* **Note 2**). An automatic pipetting station can be use for the dilutions and additions.

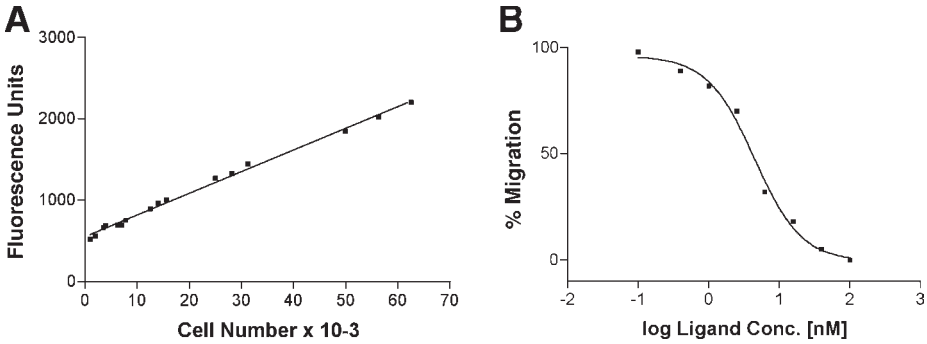

Fig. 2. (**A**) Relationship between fluorescence units and cell number. A fixed number of cells were incubated with chemotaxis lysis buffer and read as described in the protocol; r^2= 0.995. (**B**) Inhibition of migration of L1.2 cells transfected with CCR3 by a CCR3 antagonist. Migration was performed as described in the protocol.

2. Prepare 350 µL of each compound at 10X higher concentration than the desired highest final concentration to be tested in assay (usually 1 m*M* of compound because the highest concentration in the curve will be 100 µ*M* for low-potency compounds).
3. Place 250 µL of diluted drug in Costar assay plates #3365 in position 2.
4. Use the pipetting station to perform a serial dilution of the compounds. You will need 20 mL/plate of chemotaxis buffer in reservoir 1. Dilute the compounds serially 1:2.5 across the plate in wells 2–9 of each row and add media alone to wells in columns 1, 10, 11, and 12. Column 10 will be the 100% migration control. Column 11 will be the nonspecific migration control. Columns 1 and 12 are not used in analysis because of an edge effect.
5. Add 30 µL of diluted drugs or buffer alone to the chemotaxis plate (3 rows/drug) and 270 µL of 2 n*M* human eotaxin to colums 2–10. Add medium alone to column 11 for nonspecific control (*see* **Note 3**).
6. Right after dilutions are completed carefully attached Neuroprobe filters to the top of the plate.
7. Place the covers over the filters to protect them.
8. Spin hCCR3L1.2 cells and resuspend at 5×10^6 cells/mL in chemotaxis buffer.
9. Mix 180 µL of cells and 22 µL of previously diluted drug (enough for three rows). Add 50 µL to the chemotaxis plate. The mixing and the addition to the chemotaxis plate can also be done in an automatic pipet station.
10. Cover the plates and incubate for 3 h at 37°C.
11. After incubation is completed, wipe the drops from the filters. Spin the plates for 10 min at 650*g*.
12. Remove 150 µL of supernatant and add 100 µL of lysis solution and mix.
13. Cover with a plate sealer and read at excitation at 530 nm and emission at 590 nm in a fluorescence plate reader (*see* **Note 4**).

An example of inhibition of CCR3-L1.2 chemotaxis by a CCR3 antagonist is shown in **Fig. 2B**.

4. Notes

1. Isolated eosinophils can be used instead of CCR3 transfectants in this assay. Our standard procedure for eosinophil isolation involves a dextran sedimentation followed by Ficoll-Hypaque gradient. The final step is a negative selection using CD16 MicroBeads from Miltenyi Biotech.
2. Induction of L1.2 cells with butyric acid: To get optimal expression of the chemokine receptor on the surface of L1.2 cells, add 5 m*M* butyric acid (Sigma, cat. no. B-5687) to cells that are 8×10^5/mL for 16–24 h before they are used. Usually, we use cell populations containing an average of 50,000–100,000 receptors/cell after induction. However, the assay works also with cells expressing the receptor endogenously, in which case the number of receptors/per cell is usually much smaller.
3. Each compound is run in a 10-point curve in triplicate. Because columns 1 and 12 and rows A and H are not used because of "edge" effects, it is possible to run two compounds per plate.
4. Plates are usually read after overnight incubation at room temperature protected from light. It is also possible to read after 1 h incubation or even less. Just be sure that all cells are lysed.

References

1. Thelen, M. (2001) Dancing to the tunes of chemokines. *Nature Immunol.* **2,** 129–134.
2. Berger, E. A., Murphy, P. M., and Farber, J. M. (1999) Chemokine receptors as HIV-1 coreceptors: roles in viral entry, tropism and disease. *Annu. Rev. Immunol.* **17,** 657–700.
3. Kunkel, S. L., Lukacs, N., Kasama, T., and Strieter, R. M. (1996) The role of chemokines in inflammatory joint disease. *J. Leukocyte Biol.* **59,** 6–12.
4. Miyagishi, R., Kikuchi, S., Fukazawa, T., and Tashiro, K. (1995) Macrophage inflammatory protein-1 alpha in the cerebrospinal fluid of patients with multiple sclerosis and other inflammatory neurological diseases. *J. Neurol. Sci.* **129,** 223–227.
5. Karpus, W. J., Lukacs, N. W., McRae, B. L., Strieter, R. M., Kunkel, S. L., and Miller, S. D. (1995) An important role for the chemokine macrophage inflammatory protein-1 alpha in the pathogenesis of the T cell-mediated autoimmune disease, experimental autoimmune encephalomyelitis. *J. Immunol.* **155,** 5003–5010.
6. Szekanecz, Z., Halloran, M. M., Volin, M. V., et al. (2000) Temporal expression of inflammatory cytokines and chemokines in rat adjuvant-induced arthritis. *Arthritis Rheum.* **43,** 1266–1277.
7. Gao, W., Topham, P. S., King, J. A., et al. (2000) Targeting of the chemokine receptor CCR1 suppresses development of acute and chronic cardiac allograft rejection. *J. Clin. Invest.* **105,** 35–44.

8. Heath, H., Qin, S., Rao, P., et al. (1997) Chemokine receptor usage by human eosinophils. The importance of CCR3 demonstrated using an antagonistic monoclonal antibody. *J. Clin. Invest.* **99,** 178–184.
9. Uguccioni, M., Mackay, C. R., Ochensberger, B., et al. (1997) High expression of the chemokine receptor CCR3 in human blood basophils. Role in activation by eotaxin, MCP-4, and other chemokines. *J. Clin. Invest.* **100,** 1137–1143.
10. Sallusto, F. C., Mackay, C. R., and Lanzavecchia, A. (1997) Selective expression of the eotaxin receptor CCR3 by human T helper 2 cells. *Science* **277,** 2005–2007.
11. Murphy, P. M., Baggiolini, M., Charo, I. F., et al. (2000) International Union of Pharmacology. XXII. Nomenclature for chemokine receptors. *Pharmacol. Rev.* **52,** 145–176.
12. Liang, M., Rosser, M., Ng, H. P., et al. (2000) Species selectivity of a small molecule antangonist for the CCR1 chemokine receptor. *Eur. J. Pharmacol.* **389,** 41–49.
13. Naya, A., Sagara, Y., Ohwaki, K., et al. (2001) Design, synthesis, and discovery of a novel CCR1 antagonist. *J. Med. Chem.* **44,** 1429–1435.
14. Coward, P., Chan, S. D., Wada, H. G., Humphries, G. M., and Conklin, B. R. (1999) Chimeric G-proteins allow a high-throughput signaling assay of Gi-coupled receptors. *Anal. Biochem.* **270,** 242–248.
15. Sullivan, E., Tucker, E. M., and Dale, I. L. (1999) Measurement of [Ca^{+2}] using the Fluorometric Imaging Plate Reader (FLIPR) in *Calcium Signaling Protocols* (Lambert, D. G., ed.), Humana, Totowa, NJ, pp. 125–133.
16. Miraglia, S., Swartzman, E. E., Mellentin-Michelotti, J., et al. (1999) Homogeneous cell- and bead-based assays for high throughput screening using fluorometric microvolume assay technology. *J. Biomol. Screen.* **4,** 193–204.
17. Daugherty, B. L., Siciliano, S. J., and Spronger, M. S. (2000) Radiolabeled chemokine binding assay in *Chemokine Protocols* (Proudfoot, A. E. L., Wells, T. N. C., and Power, C. A., eds.), Humana, Totowa, NJ, pp. 129–134.

15

Visualization and Analysis of Adhesive Events in Brain Microvessels by Using Intravital Microscopy

Gabriela Constantin

1. Introduction

Leukocyte migration into the brain represents a critical step in the inflammatory pathologies of the central nervous system (CNS). Leukocytes extravasate through the blood–brain barrier (BBB) during cerebrovascular diseases, infections, autoimmune diseases, traumas, tumoral, and degenerative processes ***(1–5)***. All intravital microscopy studies employed up to now determine the interactions between blood leukocytes and brain endothelium carried out by performing a cranial window into the skull using a drill. Animals needed to be artificially ventilated while bleeding and tissue overheating from cautery occur. In this chapter, we describe a novel intravital microscopy model allowing visualization of cerebral vessels through the skull and analysis of the interactions between different leukocyte subpopulations and the endothelium in brain superficial microvasculature of mice.

Stroke and multiple sclerosis (MS) are classical pathologies characterized by leukocyte migration through the BBB. Polymorphonuclear leukocytes cross the BBB during reperfusion injury and are major culprits of parenchimal damage in ischemic brain injury ***(1)***. Multiple sclerosis and its animal model, experimental autoimmune encephalomyelitis (EAE), are autoimmune diseases characterized by perivascular inflammatory infiltrates, which mainly consists of lymphocytes and monocytes ***(6–8)***. In both stroke and multiple sclerosis, cerebral superficial vessels are involved in the inflammatory process ***(9–11)***. For instance, cortical lesions are common in MS and correlate with cortical atrophy. They can represent a significant proportion of total lesions and can now be efficiently detected by techniques such as fluid-attenuated inversion recovery magnetic resonance imaging (FLAIR MRI) during life ***(10,11)***. Growing evidence shows that the pattern of lesion topography in EAE reflects the dominant

From: *Methods in Molecular Biology, vol. 239: Cell Migration in Inflammation and Immunity*
Edited by: D. D'Ambrosio and F. Sinigaglia © Humana Press Inc., Totowa, NJ

autoimmune reaction against different CNS components, but not differences between spinal cord and medulla versus brain endothelium. For instance, when antigens that are recognized are in the compact myelin (myelin basic protein and proteolipid protein), the highest incidence of lesions is present in the spinal cord and brainstem ***(12)***. Controversly, when antigen is localized exclusively on the myelin surface such as myelin-oligodendrocyte glycoprotein (MOG) or myelin-associated glycoprotein (MAG), the inflammation affects the brain ***(12)***. When S100β protein and glial fibrillary acidic protein (GFAP), which are highly expressed in the gray matter, are targeted by autoimmune cells, high incidence of inflammatory lesions is present in the cerebral cortex ***(13)***. Finally, it was recently shown that in a new EAE model induced by autoreactive CD8+ T-cells, cerebral superficial vessels are involved ***(14,15)***. Thus, the model described here represents a useful tool for studying the mechanisms controlling leukocyte recruitment into the brain. The model may be exploited to study the molecular mechanisms of blood cell recruitment in normal, acute, subacute, and chronically inflamed brain vessels. Moreover, one can take advantage of the fact that human adhesion molecules expressed by leukocytes are able to efficiently interact with their endothelial counterligands expressed by mouse endothelium in the intravital microscopy setting ***(16–18)***.

2. Materials

2.1. Mice

Young females (8–12 wk old).

2.2. Materials

1. Phosphate-buffered saline (PBS).
2. Dulbecco modified Eagle's medium (DMEM) without sodium bicarbonate (Sigma).
3. HEPES.
4. Green CMFDA (5-chloromethylfluorescein diacetate) (Molecular Probes, Eugene, OR).
5. Orange CMTMR [5-(and-6)-(((chloromethyl)benzoyl)amino)tetramethylrhodamine] (Molecular Probes, Eugene, OR).
6. Fluorescein isothiocyanate dextran (molecular weight [MW] 150 kDa) (Sigma).
7. Tetramethyl-rhodamine isothiocyanate dextran (MW 160 kDa) (Sigma).
8. High-vacuum grease (Dow Corning GmbH, Wiesbaden, Germany).
9. Plastic Pasteur pipets, 3 mL.
10. Schwabs, rounded cotton tip (Amarillo, TX).
11. Silk surgical suture 6-0 and 5-0 (Denkel, MA).
12. PE-10 Polyethylene tube; inner diameter = 0.28 mm; outer diameter = 0.61 mm (Clay Adams/Becton Dickinson, MD).

13. Ketamine (Sigma).
14. Xylazine hydrochloride (Sigma).
15. Halothane (Sigma).
16. Square cover glasses, 24 × 24 mm.
17. Heparin grade I-A (Sigma).
18. Rhodamine 6G chloride (Sigma).
19. Lipopolysaccaride (LPS) *Escherichia coli* 026:B6 (Sigma).
20. Sterile syringes, 1 mL.
21. Alexa 568/488 protein labeling kit.
22. Rubber O-rings, inner diameter = 11 mm.

2.3. Instruments

2.3.1. Microsurgery

1. Fiber-optic light source.
2. Dissection microscope.
3. Forceps: Biologie tip 0.05 mm × 0.02 mm, 11-cm length; forceps: 45°, 0.10 mm × 0.06 mm, 11-cm length; eye-dressing forceps serrated, tip width = 0.8–0.5 mm.
4. Scissors: Fine iris scissors with large finger loops; extrafine spring scissors for incising vessel walls for catheter insertion.
5. Retractor, maximum spread 1.5 cm, 3–4 cm in length.
6. Vascular clamps: Microserrefines with delicate, atraumatic serrations and 2-mm spring width, 4-mm length, 0.75-mm width, pressure 125 g.
7. Forcep-type clip applicator.

2.3.2. Videomicroscopy

1. Silicon-intensified target videocamera (VE-1000 SIT, Dage MTI, Michigan, IL).
2. Epifluorescence microscope with large stage adapted for intravital microscopy studies (Olympus BX50WI).
3. Microscope objectives: ×10 (water immersion, focal distance 3.3, N.A. 0.3 ∞); ×20 (water immersion, focal distance 3.3 mm, N.A. 0.5 ∞), ×40 (water immersion, focal distance 3.3 mm, N.A. 0.8 ∞).
4. Monitor (Sony SSM-125CE).
5. Digital VCR (Panasonic NV-DV10000).
6. SP100*i* digital syringe pump (WPI, Sarasota, FL).

2.3.3. Data Analysis

1. Computer with a LG-3 frame grabber (Psion Corporation, Frederick, MD).
2. NIH Image 1.61 software.

3. Methods

3.1. Activation of Brain Endothelium

Mice must be kept in pathogen-free conditions (*see* **Note 1**). Young females receive no treatment if the study implies a normal brain endothelium or they

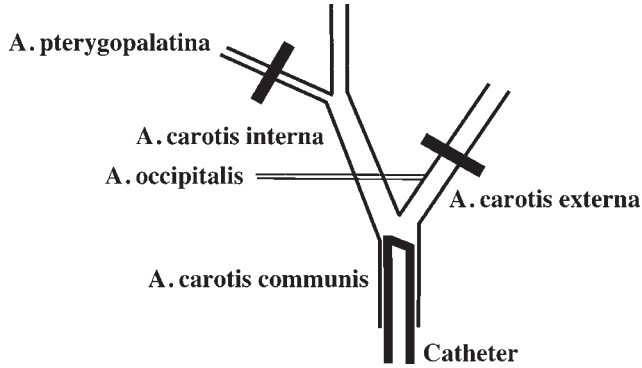

Fig. 1. Microsurgery for the exclusion of noncerebral vessels. A catheter is inserted into the right common carotid artery for the injection of fluorescent cells. In order to visualize the cells only in cerebral vessels and to exclude the noncerebral vessels, the right external carotid and right pterygopalatine artery are ligated.

are injected intraperitoneally with 15 µg LPS (*E. coli* 026:B6; Sigma) or with 1 µg tumor necrosis factor-α (TNF-α), 5–6 h or 3–4 h, respectively, before starting the intravital experiment ***(19)***.

3.2. Preparation of the Cells To Be Injected Through the Carotid

Lymphocyes are suspended at a concentration of 5×10^6/mL in DMEM without sodium bicarbonate supplemented with 20 m*M* HEPES, 5% fetal calf serum (FCS), pH 7.1, and are labeled with green CMFDA (Molecular Probes) or orange CMTMR (Molecular Probes) for 20–25 min at 37°C.

3.3. Ligation of the External Carotid and Pterygopalatine Arteries

Animals are anesthetized by intraperitoneal injection (10 mL/kg) of physiologic saline containing ketamine (5 mg/mL) and xylazine (1 mg/mL). The recipient is maintained at 37°C by a stage-mounted strip heater (Linkam CO102 [Olympus]). A heparinated PE-10 polyethylene catheter is inserted into the right common carotid artery toward the brain for the injection of fluorescent cells. In order to exclude from the analysis the noncerebral vessels (bone, bone marrow, and meningeal vessels), the right external carotid artery and pterigopalatin artery, a branch from the internal carotid, need to be ligated (*see* **Note 2**) (*see* **Fig. 1**) ***(19)***.

3.4. Preparation of the Skull

The scalp is reflected and the connective tissue adhered to the bone is carefully scraped away (*see* **Note 3**). The skull needs to be bathed with sterile phys-

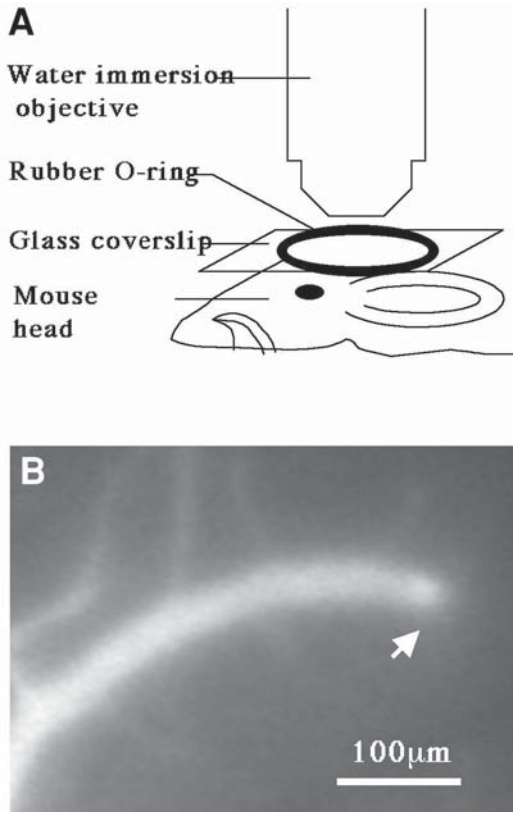

Fig. 2. Visualization of brain vessels. (**A**) The scalp is reflected and the connective tissue adhered to the bone is carefully scraped away. The skull needs to be bathed with sterile physiologic saline and a 24-mm × 24 mm coverslip is then applied and fixed with silicon grease. A round chamber of 11 mm internal diameter is attached on the cover slip and filled with water. The preparation is placed on a microscope with epi-fluorescence equipped with large-stage and water-immersion objectives. (**B**) Cerebral vessels were visualized by using fluorescent dextrans. Branches of superficial cerebral venules are easily recognized by their convex origin resulting from the emergence on the brain surface from the more profound layers (arrow).

iologic saline and a 24-mm × 24-mm cover slip is then applied and fixed with silicon grease. A round chamber of 11 mm internal diameter is attached on the cover slip and filled with water (*see* **Fig. 2A**).

3.5. Visualization of the Cerebral Superficial Vessels

The preparation is placed on a microscope with epifluorescence equipped with large-stage and waterimmersion objectives (*see* **Fig. 3**). Blood vessels are

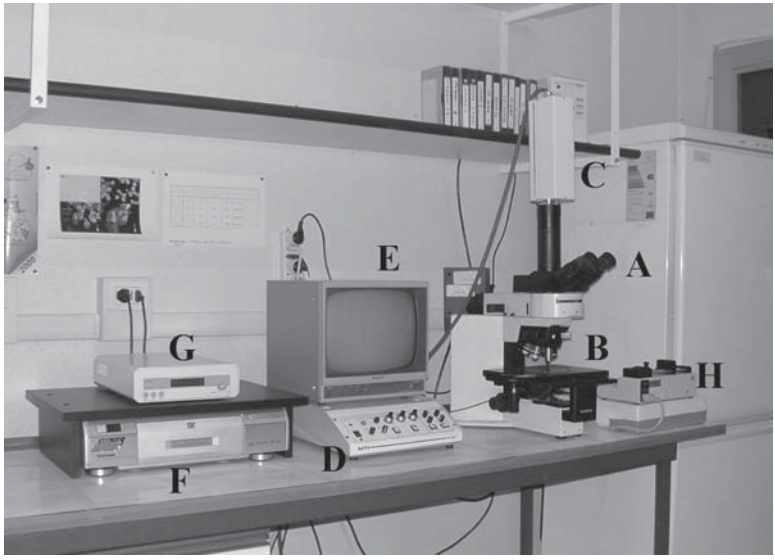

Fig. 3. Intravital microscopy equipment; *A*, epifluorescence microscope; *B*, water-immersion objective; *C*, SIT videocamera (DAGE MTI VE1000); *D*, control board of the videocamera; *E*, monitor; *F*, digital VCR; *G*, stage heater; *H*, digital pump for the injection of fluorescent cells.

visualized through the skull by using fluorescent dextrans: 5 mg of fluorescein isothiocyanate (FITC) dextran (148 kDa; Sigma) and/or 8 mg of tetramethylrhodamine isothiocyanate (TRITC) dextran (155 kDa; Sigma) are diluted in 0.5 mL sterile physiologic saline and centrifuged for 5 min at 14,000*g* (each mouse received 0.05 mL supernatant) (*see* **Fig. 2B**) (*see* **Note 4**). 2.5×10^6 fluorescent-labeled cells in 0.3 mL DMEM are slowly injected into the carotid artery for each condition (control cells and treated cells/endothelium by a digital pump [SP100; World Precision Instruments, UK] at a flow rate of 0.13–1 µL/s. The images are visualized by using a high-performance silicon-intensified target videocamera (VE-1000 SIT; Dage MTI, Michigan, IL) and a Sony SSM-125CE monitor. Recordings are digitalized and stored on videotapes employing a digital VCR (Panasonic NV-DV10000).

3.6. Analysis of the Interactions Between Leukocytes and Brain Endothelium

Video analysis is performed by playback of digital videotapes in real time or at reduced speed, and frame by frame ***(20)***. The vessel diameter (*D*), hemo-

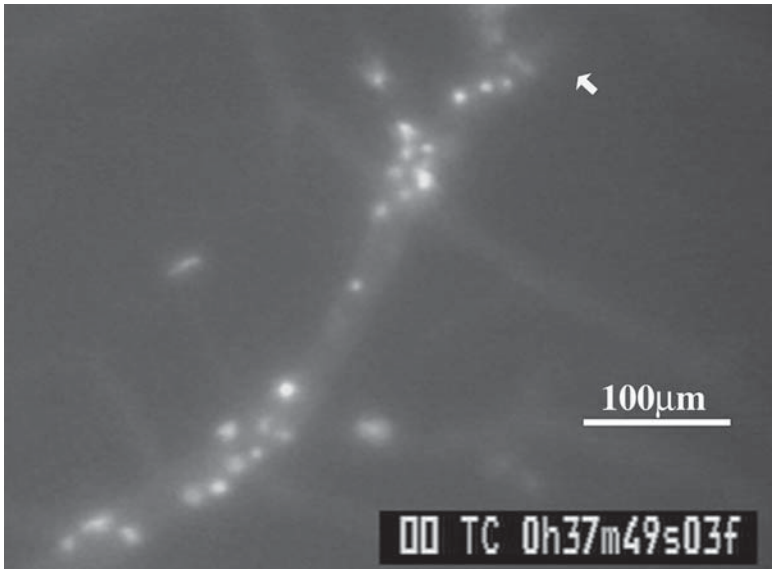

Fig. 4. Lymphocytes arrested in inflamed brain venules. Micrograph showing fluorescently labeled CD8+ T-cells (bright intravascular dots) isolated from patients with acute multiple sclerosis that arrested in mouse inflamed brain venules. Mice were treated with LPS 5–6 h before starting the intravital microscopy experiments. Animal received a low dose of fluorescent dextran. Note the "interrupted" shape of the vessel (arrow).

dinamic parameters, and the velocities of rolling are determined by using a PC-based system, including a LG-3 frame grabber (Psion Corporation, Frederick, MD), and the NIH Image 1.61 software. The velocities of ≥ 20 consecutive freely flowing cells/venule are calculated, and from the velocity of the fastest cell in each venule (V_{fast}), the mean blood flow velocities (V_m) is calculated: $V_m = V_{fast}/(2 - \varepsilon^2)$, where ε is the ratio of the lymphocyte diameter to vessel diameter. The wall shear rate (γ) is calculated from $\gamma = 8V_m/D$ (s^{-1}), and the shear stress (τ) acting on rolling cells is approximated by $\gamma \times 0.025$ (dyn/cm^2), assuming a blood viscosity of 0.025 ***(19)***. Lymphocytes are considered as rolling if they traveled at velocities below V_{crit} [$V_{crit} = V_m \times \varepsilon \times (2-\varepsilon)$] ***(19)***. Lymphocytes that remain stationary on the venular wall for ≥ 30 s are considered adherent (*see* **Fig. 4**). Transient tethering, "stop-and-go" very brief interactions with static binding, are interactions of ≤ 1 s. At least 100 consecutive cells/venule need to be examined (*see* **Note 5**). Rolling and firm arrest fractions are determined as the percentage of cells that rolled or firmly arrested within a given venule in the total number of cells that enter that venule during the same period ***(19)***.

3.7. In Vivo Staining of Endothelial Adhesion Molecules

Monoclonal antibody (MAb) antiadhesion molecules expressed by the endothelium (E-, and P-selectin, anti-VCAM-1, anti-ICAM-1, etc.) are fluoresceinated using the Alexa Fluor 488 labeling kit (Molecular probes). Control mAbs may be rhodaminated using the Alexa Fluor 566 kit (Molecular probes). Fifty micrograms of fluorescently labeled mAb are injected intravenously. Twenty minutes later, the animal is anesthesized, the vena cava is cut, and the mouse is perfused through the left ventricle and through a catheter inserted into the right common artery with cold PBS to remove the unbound mAbs. The skull and meninges are removed and cerebral vessels are visualized using the intravital microscopy setting ***(19)***.

3.8. Statistics

Statistical analysis of the results is performed by using SPSS 10.0 software. A two-tailed Student's *t*-test may be employed for statistical comparison of two samples. Multiple comparisons are performed employing the Kruskall–Wallis test with the Bonferroni correction of p. Velocity histograms are compared using Mann–Whitney *U*-test and Kolmogorov–Smirnov test. Linear regressions are analyzed employing the Spearman rank correlation test. Differences were regarded as significant with a value of $p < 0.05$.

4. Notes

1. Brain endothelium from mice that are not kept in pathogen-free conditions and that are chronically exposed to infections mediates interactions with leukocytes.
2. Different arterial variants may be encountered. The occipital artery may lack and its territory may be vascularized by a branch from the internal carotid. The pterygopalatine artery may branch at the origin. As a common rule, the internal carotid branch that is not ligated follows the direction of the common carotid toward the base of the skull.
3. Young females are used because they have a more transparent bone. Males have a thicker bone and the visualization of cerebral superficial vessels is less clear.
4. Often, branches of superficial cerebral venules are easily recognized by their "interrupted" shape and convex origin as a result of the emergence on the brain surface from the more profound layers. Meningeal venules are clearly distinguished, as they are longer and thinner than cerebral venules and their branches are visualized from the origin. Bone marrow vessels are in a more superficial focal plane and are encountered at bone sutures. They create a rich honeycomb net at the coronal suture ***(21)***.
5. The model allows the analysis of the interactions between the endothelium and different cell types: leukocytes, dendritic cells, tumor cells, staminal cells, and so forth.

References

1. Connolly, E. S. Jr, Winfree, C. J., Springer, T. A., et al. (1996) Cerebral protection in homozygous null ICAM-1 mice after middle cerebral artery occlusion. Role of neutrophil adhesion in the pathogenesis of stroke. *J. Clin. Invest.* **97,** 209–216.
2. Hafle, D. A. (1999) The distinction blurs between an autoimmune versus microbial hypothesis in multiple sclerosis. *J. Clin. Invest.* **104,** 527–530.
3. Weaver, K. D., Branch, C. A., Hernandez, L., Miller, C. H., and Quattrocchi, K. B. (2000) Effect of leukocyte–endothelial adhesion antagonism on neutrophil migration and neurologic outcome after cortical trauma. *J. Trauma* **48,** 1081–1090.
4. Cassel, W. A., Weidenheim, K. M., Campbell, W. G. Jr., and Murray, D. R. (1986) Malignant melanoma. Inflammatory mononuclear cell infiltrates in cerebral metastases during concurrent therapy with viral oncolysate. *Cancer* **57,** 1302–1312.
5. Eikelenboom, P., Rozemuller, A. J., Hoozemans, J. J., Veerhuis, R., and van Gool, W. A. (2000) Neuroinflammation and Alzheimer disease: clinical and therapeutic implications. *Alzheimer Dis. Assoc. Disord.* **14,** S54–S61.
6. Pettinelli, C. B. and McFarlin, D. E. (1981) Adoptive transfer of experimental allergic encephalomyelitis in SJL/J mice after in vitro activation of lymph node cells by myelin basic protein: requirement for Lyt1+2-T lymphocytes. *J. Immunol.* **127,** 1420–1429.
7. Traugott, U., Reinherz, E., and Raine, C. S. (1983) Multiple sclerosis: distribution of T cell subsets within active chronic lesions. *Science* **219,** 308–310.
8. Hauser, S. L. (1986) Immunohistochemical analysis of the cellular infiltrate in multiple sclerosis. *Ann. Neurol.* **19,** 578–587.
9. Barone, F. C., Knudsen, D. J., Nelson, A. H, Feuerstein, G. Z., and Willette, R. N. (1993) Mouse strain differences in susceptibility to cerebral ischemia are related to cerebral vascular anatomy. *J. Cereb. Blood Flow Metab.* **13,** 683–692.
10. Kidd, D., Barkhof, F., McConnell, R., Algra, P. R., Allen, I. V., and Revesz, T. (1999) Cortical lesions in multiple sclerosis. *Brain* **122,** 17–26.
11. Bakshi, R., Ariyaratana, S., Benedict, R. H., and Jacobs, L. (2001) Fluid-attenuated inversion recovery magnetic resonance imaging detects cortical and juxtacortical multiple sclerosis lesions. *Arch. Neurol.* **58,** 742–748.
12. Lassmann, H. and Vass, K. (1996) Are current immunological concepts of multiple sclerosis reflected by the immunopathology of its lesions? in *Immunoneurology* (Chofflon, M. and Steinman, L., eds.), Springer-Verlag, Heidelberg, p. 77.
13. Berger, T., Weerth, S., Kojima, K., Linington, C., Wekerle, H., and Lassmann, H. (1997) Experimental autoimmune encephalomyelitis: the antigen specificity of T lymphocytes determines the topography of lesions in the central and peripheral nervous system. *Lab. Invest.* **76,** 355–364.
14. Sun, D., Whitaker, J. N., Huang, Z., et al. (2001) Myelin antigen-specific CD8+ T cells are encephalitogenic and produce severe disease in C57BL/6 mice. *J. Immunol.* **166,** 7579–7587.
15. Huseby, E. S., Liggitt, D., Brabb, T., Schnabel, B., Ohlen, C., and Governman, G. (2001) A pathogenic role for myelin-specific CD8+ T cells in a model for multiple sclerosis. *J. Exp. Med.* **194,** 669–676.

16. Huo, Y., Hafezi-Moghadam, A., and Ley, K. (2000) Role of vascular cell adhesion molecule-1 and fibronectin connecting segment-1 in monocyte rolling and adhesion on early atherosclerotic lesions. *Circ. Res.* **87,** 153–159.
17. Ramos, C. L., Huo, Y., Jung, U., et al. (1999) Direct demonstration of P-selectin- and VCAM-1-dependent mononuclear cell rolling in early atherosclerotic lesions of apolipoprotein E-deficient mice. *Circ. Res.* **84,** 1237–1244.
18. Norman, K. E., Katopodis, A. G., Thoma, G., et al. (2000) P-Selectin glycoprotein ligand-1 supports rolling on E- and P-selectin in vivo. *Blood* **96,** 3585–3591.
19. Piccio, L., Rossi, B., Scarpini, E., et al. (2002) Molecular mechanisms involved in lymphocyte recruitment in inflamed brain microvessels: critical roles for P-selectin glycoprotein ligand-1 and heterotrimeric G(i)-linked receptors. *J. Immunol.* **168,** 1940–1949.
20. Constantin G., Majeed, M., Giagulli, C., Piccio, L., Kim, J. Y., and Laudanna, C. (2000) Chemokines trigger immediate beta2 Integrin affinity and mobility changes: differential regulation and roles in lymphocyte arrest under flow. *Immunity* **16,** 759–769.
21. Mazo, I. B., Gutierrez-Ramos, J. C., Frenette, P. S., Hynes R. O., Wagner, D. D., and von Andrian, U. H. (1998) Hematopoietic progenitor cell rolling in bone marrow microvessels: parallel contributions by endothelial selectins and vascular cell adhesion molecule 1. *J. Exp. Med.* **188,** 465–475.

16

Animal Models to Study Chemokine Receptor Function In Vivo

Mouse Models of Allergic Airway Inflammation

Clare M. Lloyd and Jose-Carlos Gutierrez-Ramos

1. Introduction

Animal models using guinea pigs, monkeys, rats, and mice have been employed to study the pathogenesis of asthma. More recently, mouse models of allergic lung disease have been used to dissect the complex pathophysiological mechanisms underlying the asthma phenotype. This increase in usage of mouse models stems from the range of tools available for outlining functional pathways for individual cells and mediators. Genetic technologies allow us to manipulate the expression of particular molecules of interest and, therefore, it is possible to dissect inflammatory pathways to investigate the functional roles of particular mediators or cells. Mice can be induced to display a range of the pathophysiological features that are hallmarks of the human disease, including inflammatory cell recruitment to the lung, mucus secretion from the bronchoepithelial surface, serum IgE, and IgG2a, accompanied by a Th2 cytokine profile. Importantly, these pathophysiological indicators are generally accompanied by changes in lung function, allowing correlation between changes in cell or mediator expression and lung physiology.

This chapter describes the generation of allergic airway inflammation in mice, initiated by two distinct methods. The first is by peripheral sensitization with allergen, followed by local allergen challenge, which results in changes in lung function in conjunction with a profound cellular pulmonary inflammation with a distinct Th2 profile—marked by pulmonary expression of interleukin (IL)-4, IL-5, IL-13, and serum IgE. In contrast, the other is initiated by the adoptive transfer of allergen-specific Th2 cells that have been generated in vivo. The transfer of relatively small numbers of these cells to naive mice followed by

From: *Methods in Molecular Biology, vol. 239: Cell Migration in Inflammation and Immunity*
Edited by: D. D'Ambrosio and F. Sinigaglia

local allergen challenge induces airway hyperreactivity, eosinophilia, and a Th2 cytokine profile, in the absence of peripheral IgE. This latter model has been useful in tracking Th2 cell recruitment because donor (Th2) cells can be differentiated from host cells by antibody staining of a clonotypic receptor if transgenic T-cells are used or by fluorescent labeling of cells prior to transfer if nontransgenic cells are used.

2. Materials

2.1. Mice

1. Pathogen-free mice, 6- to 8-wk-old female BALB/cJ mice (*see* **Note 1**).
2. Mice expressing the transgene for the DO11.10 αβ-TCR, which recognizes residues 323–339 of chicken egg ovalbumin (OVA) in association with I-Ad ***(1)***. These mice were originally generated by Dr. D. Loh (Washington University, St. Louis, MO) ***(1)***.

2.2. Induction of Inflammation

2.2.1. Sensitization Model

1. Chicken egg ovalbumin (OVA) (Sigma, Dorset UK, A-5503).
2. Aluminium hydroxide, 1.3% alum in water (Alu-Gel-S suspension; Serva, Heidelberg Germany; cat. no. 12261).
3. Nebuliser (e.g., Pariboy ultrasonic nebuliser [Pari, Germany]).

2.2.2. Adoptive Transfer Model

1. RPMI 1640 with 25 m*M* HEPES buffer without L-glutamine (Gibco-BRL; cat. no. 42401-018).
2. L-Glutamine, Pen/Strep, and fetal calf serum (FCS) (all from Gibco-BRL).
3. Nylon cell strainers (70 µm; Becton Dickinson; cat. no. 352350).
4. Mitomycin C (Sigma; cat. no. M-0503). Make a 10X stock by adding 4 mL sterile phosphate-buffered saline (PBS) to a 2-mg vial of mitomycin C. Store in aliquots at 4°C in the dark.
5. Mouse $CD4^+$ subset column kit (R&D Systems; cat. no. MCD4C-1000).
6. OVA peptide, residues 323–339 (from any peptide-generating facility).
7. Recombinant mouse IL-4 (Endogen; cat. no. RM-IL4-10). Make up 10 µg/mL stock in complete RPMI and store in 50-µL aliquots at −70°C.
8. Anti-mouse IL-12 monoclonal antibody (mAb) (Endogen; cat. no. MM-121). Aliquot neat stock and store in 50-µL aliquots at −70°C.
9. Anti-CD3ε mAb (Pharmingen; cat. no. 01080D).
10. Ficoll-Hypaque (Pharmacia Biotech, Uppsala, Sweden; cat. no. 17-1440-02).
11. Complete RPMI: To 500-mL bottle of RPMI, add 5 mL of 200 m*M* L-glutamine solution, 5 mL penicillin–streptomycin solution, 2 mL of 0.001% (v/v) 2-mercaptoethanol (Sigma; cat. no. M-7522) in PBS and 50 mL FCS.

12. Red cell lysis buffer: For 1 L buffer, combine 8.29 g NH_4Cl 0.15 *M*, 1.0 g $KHCO_3$ 1 m*M*, and 37.2 mg Na_2EDTA. Add 900 mL distilled H_2O, adjust pH to 7.2–7.4 with HCl, and make up volume to 1 L. Sterile-filter or autoclave.

2.3. Analysis

2.3.1. Airway Hyperreactivity

1. Whole-body plethysmograph system: Buxco® (Buxco Electronics, Hampshire, UK).
2. Methacholine (98% acetyl-β-methylcholine chloride, A-2251; Sigma, Dorset). For a dose–response curve, prepare a range of concentrations (typically, 1, 3, 10, 30, and 100 mg/mL) in PBS and store at −20°C.

2.3.2. Cell Recovery

1. Tracheal cannula: the plastic sheath around Venisystems Abbocath 23G needles is about the right size for 6- to 8-wk-old BALB/c mice (Abbott Laboratories, Kent). Discard the needle and cut the plastic down to about 1 cm.
2. Wright/Giemsa staining kit (Shandon Upshaw).
3. Collagenase (type D) (Boehringer Mannheim).
4. DNAse (type 1) (Boehringer Mannheim).
5. Penicillin and streptomycin (Gibco-BRL Life Technologies).
6. Digest reagent: 75 U/mL collagenase (type D; Boehringer Mannheim, UK), 50 U/mL DNAse (type 1; Boehringer Mannheim, UK), 100 U penicillin, and 100 mg/mL streptomycin (Gibco-BRL Life Technologies, UK) in 100 mL complete RPMI.

2.3.3. Histology

1. 10% Neutral-buffered formalin (NBF) (Shandon Upshaw, UK).
2. Cryomatrix compound or similar (BDH).
3. Isopentane (2-methylbutane) (Sigma).
4. Disposable plastic base molds, 15 × 15 × 5 mm (Shandon Upshaw).
5. Superfrost Slides (BDH).
6. Normal Donkey serum (Sigma).
7. KJ126 antibody (Morwell Diagnostics Ltd, Switzerland).
8. Vectashield mounting medium (Vector Laboratories, Burlingame, CA, USA).

3. Methods

3.1. Induction of Allergic Airway Inflammation

3.1.1. Antigen Sensitization

Mice are sensitized with 10 μg OVA injected intraperitoneally with alum. The OVA solution is made up fresh on the day of the protocol in sterile PBS at a concentration of 1 mg/mL. Alum is added to the OVA solution at a 1:2 ratio of 1X OVA/PBS solution:alum. For 9 mL of OVA/alum, add 300 μL of 10X

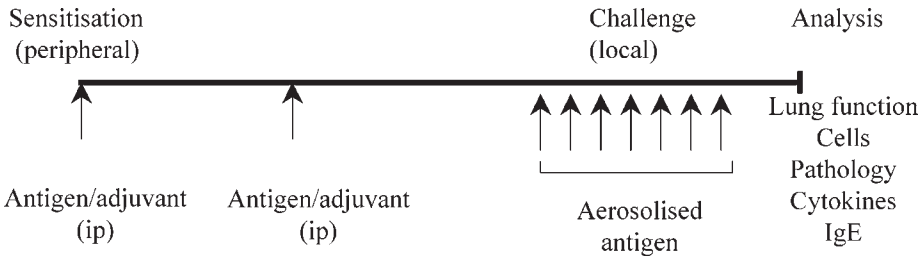

Fig. 1. Protocol to induce AHR and eosinophilic inflammation in mice.

OVA solution + 2.7 mL sterile PBS:6 mL alum. Vortex and leave for at least 1 h at room temperature on a roller, for the alum to absorb the OVA. Inject each mouse intraperitoneally with 300 µL OVA:alum solution.

3.1.2. Aerosol Challenge

Make up fresh on the day of the protocol approx 10 mL of 5% OVA in sterile PBS (w/v). The OVA solution is aerosolized using a nebulizer. Aerosolized OVA is delivered to a plastic box containing the mice via a plastic tube for 30 min each day according to the schedule in Fig. 1 (*see* **Note 2**).

3.2. Adoptive Transfer Model

*3.2.1. Preparation of OVA Transgenic Splenic Lymphocytes (*see ***Note 3****)*

1. Remove spleens aseptically from several (*see* **Note 3**) DO11 mice and collect in sterile 15-mL tubes in RPMI. Make single-cell suspensions from spleens using 70-µm nylon cell strainers and RPMI .
2. Centrifuge cell preps at 250*g* for 5 min.
3. Resuspend in 10 mL red cell lysis buffer and incubate on ice for 5 min.
4. Bring volume of tube up to 50 mL with complete RPMI and centrifuge to pellet.
5. Perform cell count and resuspend cells at 2×10^8 cells/mL in $CD4^+$ kit antibody solution (as per manufacturer's instructions). Incubate for 15 min at room temperature.
6. Meanwhile, equilibrate two $CD4^+$ Subset Enrichment columns with $CD4^+$ column buffer (prepared as per manufacturer's instructions, 10 mL each), collecting the flow through in 2 to 15-mL centrifuge tubes. After equilibration, replace the 15-mL waste tubes with fresh tubes.
7. After the 15-min incubation, wash the cells twice with 30 mL column buffer. Centrifuge the cells at 250*g* for 10 min and decant the supernatant after each wash. Resuspend the final cell pellet in column buffer and load 2 mL of cells onto each column (2×10^8 cells/column).
8. After the cells have entered into the column, incubate for 10 min at room temperature.

9. Elute the cells using 10 mL column buffer per column, then collect cells by spinning at 250*g* (1200 rpm) for 5 min. Resuspend the cells in complete RPMI, pool the tubes of eluted cells, and perform a viable cell count.
10. After counting, resuspend cells at 1×10^6/mL in complete RPMI and transfer to two separate T-25 or T-75 mm^2 tissue culture flasks.

3.2.2. Preparation of Antigen Presenting Cells (APC) for Lymphocyte Stimulation

1. Repeat steps 1–4 of **Subheading 3.2.1.** using BALB/c spleens.
2. Resuspend spleens cells in 9.5 mL in RPMI and treat with 0.5 mL of 1 mg/mL mitomycin C for 20 min at 37°C.
3. Wash cells three times in complete RPMI.
4. Perform cell counts, resuspend cells to 5×10^7 cells/mL in complete RPMI, and incubate with 100 µg/mL OVA peptide for 20 min at room temperature.
5. Store on ice until ready to use.

3.2.3. Polarization of Th2 Lymphocytes

1. Supplement cells with recombinant murine IL-4 and anti-IL-12 antibody at 50 ng/mL and 10 µg/mL, respectively.
2. Add an appropriate volume of OVA peptide-pulsed APC to yield a final APC:Th cell ratio of approx 4:1 and incubate at 37°C.

3.2.4. Maintenance of Cells

1. Examine cells after 3 d to check growth; if medium appears acidic, add fresh cytokine-supplemented medium equivalent to 50% of the culture volume.
2. After 5–6 d in culture, restimulate with fresh OVA-pulsed APC.
3. On day of restimulation, prepare APC as described in **Subheading 3.2.3.**
4. Remove Th2 cells from culture and count.
5. Centrifuge to pellet and resuspend cells in complete RPMI at a final concentration of 1×10^6/mL.
6. Supplment medium with rmIL-4 and anti-IL-12 as described above.
7. Add freshly pulsed APC at a final APC:Th ratio of 4:1.
8. Incubate at 37°C, 5% CO_2 as in **Subheading 3.2.3.**
9. Repeat restimulation every 5–6 d (*see* **Note 4**).

3.2.5. Preparation of Cells for Injection In Vivo

1. After the third round of antigen stimulation cells are centrifuged to pellet and resuspended in fresh unsupplemented RPMI; volumes will vary but should be in multiples of 35 (i.e., 35, 70, 105 mL, etc.)
2. Transfer each 35-mL volume of cells to a 50-mL centrifuge tube and underlay with 10 mL Ficoll-Hypaque.
3. Centrifuge for 20 min at room temperature at 850*g* with *no* brake to separate viable and nonviable cells.

4. After centrifugation, transfer the cells at the medium–Ficoll interface to a fresh tube.
5. Wash cells twice in 50-mL volumes of complete RPMI.
6. Count cells and resuspend at 1×10^6 mL in fresh complete RPMI.
7. Incubate cells in a flask and supplement with rmIL-2 to yield a final concentration of 10 U/mL.
8. Incubate for 48–72 h before injection in vivo.

3.2.6. Induction of T-Cell-Mediated Pulmonary Inflammation

1. Wash IL-2 rested cells in tissue culture medium and resuspend to give a concentration of 1×10^7cells/mL in sterile PBS or RPMI.
2. Inject recipient BALB/c mice with 100-µL cell solution through the tail vein, using an insulin syringe. After 24 h expose mice to an aerosol of OVA (50 mg/mL) for 20 min, as described in **Subheading 3.1.1.** Thereafter, challenge mice daily until sacrifice.
3. In each experiment, include control mice that receive cells but are challenged with aerosolized PBS.

3.3. Analysis of Inflammation

3.3.1. Airway Hyperactivity (AHR)

Airway responsiveness is measured in mice 24 h after the last aerosol challenge by recording respiratory pressure curves using whole-body plethysmography in response to inhaled methacholine at concentrations ranging from 1 to 100 mg/mL for 1 min. Airway responsiveness is expressed as enhanced pause (Penh), a calculated value that correlates with measurement of airway resistance, impedance and intrapleural pressure in the same mouse: Penh = (Te/Tr1) × Pef/Pif, where Te is the expiration time, Tr is the relaxation time, Pef is the peak expiratory flow, and Pif is the peak inspiratory flow. Data are analyzed by Biosystem XA software. Data are expressed as Penh over an increasing dose of methacholine (*see* **Fig. 2A**).

3.3.2. Cell Isolation and Analysis

1. Anesthetize mice 24 h after the final OVA challenge using an appropriate anesthetic drug, and bleed out by cardiac puncture.
2. Recovery of cells from the airway lumen. Estimation of cell recruitment to the airway lumen is made by analysis of the bronchoalveolar lavage (BAL).
3. Expose the trachea and lungs of the mouse and make a small incision into the trachea.
4. Insert a cannula into the trachea and instill 0.4 mL of PBS into the lungs (you should see the lungs inflate). Repeat twice and pool the three washes.
5. Centrifuge the BAL fluid at 700*g* for 5 min at 4°C.
6. Collect supernatant for cytokine analysis and resuspend pellet in 0.5 mL PBS.

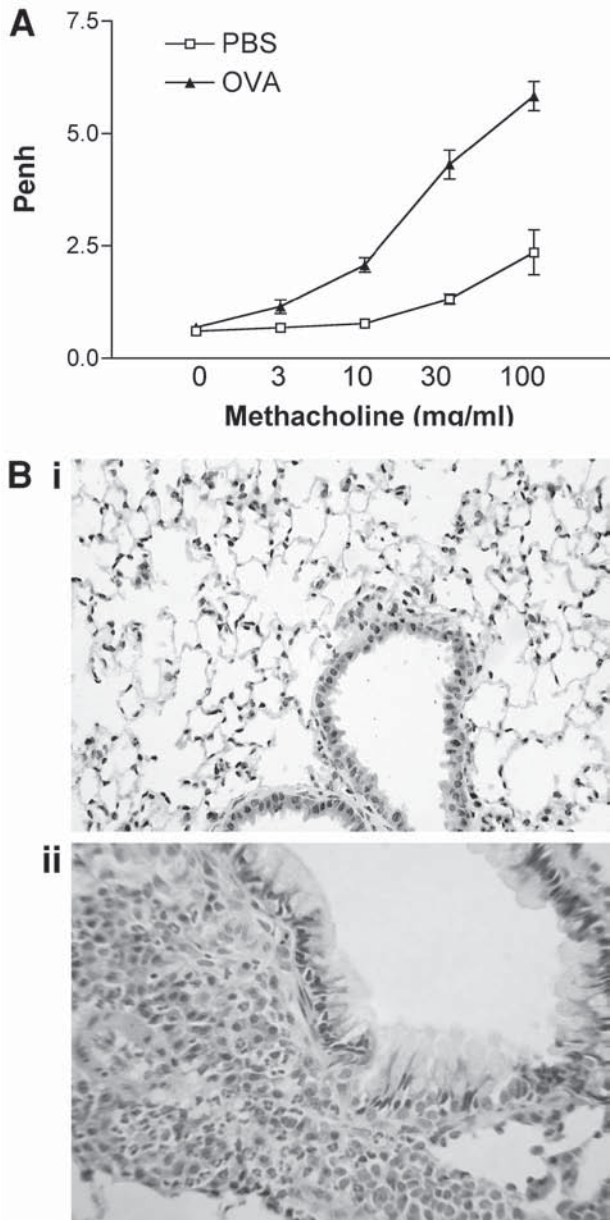

Fig. 2. Lung pathophysiology. (**A**) Mice sensitized with ova/ovums (triangles) showed increased Penh in comparison to sham immunized controls (squares). (**B)** OVA sensitization and challenge induces eosinophilic inflammation (ii) that is absent from sham immunized controls (i).

7. Count and then disperse 5×10^4 cells onto glass slides by cytocentrifugation.
8. Stain air-dried cytospins with Geimsa and perform differential cell counts at ×40 magnification. Count between 800 and 1000 cells and determine the percentages of eosinophils, neutrophils, macrophages, and lymphomononuclear cells (*see* **Note 6**). Calculate the absolute number of each population by multiplying percentages by the total cell count for each sample.

3.3.3. Recovery of Cells from the Lung Parenchyma

Estimation of cell recruitment to the airway tissue is made by analysis of the cells recovered from one lobe of the lung.

1. Take one lobe (around 100 mg) of lung and incubate at 37°C for 1 h in the digest reagent.
2. Filter the recovered cells through a 70-µm nylon sieve.
3. Wash twice and resuspend in complete RPMI.
4. Count cells, make cytospins, and perform differential counts as described in **Subheading 3.3.2., steps 7** and **8**. Total differential counts are expressed per milligram of tissue.
5. The remaining cells can be phenotyped by flow cytometry or used for in vitro assays (*see* **Note 7**).

3.3.4. Histology

1. After performing the bronchiolar lavage, inflate the lungs with 0.5 mL of 10% neutral-buffered formalin via tracheal cannula (as described in **Subheading 3.3.2., step 4**); secure by tying the trachea with cotton. Remove the lungs from the chest cavity and place in a cassette. Fix by placing the cassette in a pot of 10% neutral-buffered formalin solution for at least 24 h.
2. Lungs should be paraffin embedded and sectioned (4 µm) before staining with hematoxylin and eosin (H&E) to assess extent and phenotype of inflammatory infiltrates or periodic acid-Schiff (PAS) to show goblet cells, according to standard histological protocols.
3. Score the slides microscopically using a semiquantitative scoring system to grade the size of lung infiltrates. Typically, +5 signifies a large (more than three cells deep), widespread infiltrate around the majority of vessels and bronchioles (*see* **Fig. 2B**), and 0 signifies no inflammatory cell foci (*see* **Fig. 2A**).
4. Goblet cells can be counted on PAS-stained lung sections using a numerical scoring system (0 = <5% goblet cells; 1 = 5–25%; 2 = 25–50%; 3 = 50–75%; 4 = >75%) ***(2)***. The sum of the airway scores from each lung are divided by the number of airways examined (20–30 per mouse) and expressed as mucus score in arbitrary units.

3.3.5. Immunostaining

1. After performing the bronchiolar lavage, inject approx 0.5 mL of 1:1 mix of cryomatrix optimum cutting temperature (OCT):PBS via the tracheal cannula (*see* **Note 8**).

2. Remove lungs and separate each lobe. Place each lobe into a plastic mold with additional OCT to completely cover the tissue (making sure there are no air bubbles).
3. Drop mold into a beaker of prechilled isopentane (placed in a bucket of dry ice). Leave tissue in isopentane for approx 10 min until a solid white block has formed, then remove, wrap immediately in foil to prevent drying out, being careful not to thaw OCT, and store at –70°C.
4. To locate antigen-specific T-cells within lung tissue (for T-cell transfer model, *see* **Note 9**), cut frozen sections (4 µm) onto Superfrost slides.
5. Fix sections by incubation in ice-cold acetone for 15 min and air-dry.
6. Block nonspecific binding by incubation with 20% normal donkey serum for 15 min.
7. Tip off serum and add monoclonal antibody specific for transgenic TCR KJ126 labeled with fluorochrome. Incubate at room temperature in a humid chamber.
8. Wash off excess antibody and mount in Vectashield or similar apparatus.
9. Visualize positively stained cells under a fluorescent microscope.

3.3.6. Cytokine/Chemokine Analysis

Cytokines can be measured in either BAL samples or lung tissue homogenates. BAL must be kept on ice after sampling and cell-free supernatant left frozen until analyzed. Lung samples are prepared by homogenizing lung tissue (approx 100 mg) in 2 mL HBSS on ice using a tissue tearor. Centrifuge at 10,000*g* for 10 min, collect the supernatant, and store at –20°C prior to use. Cytokines such as IL-4, IL-5, interferon (IFN)-γ, and IL-13 are measured by standardized sandwich enzyme-linked immunosorbent assays (ELISAs) using paired antibodies according to the manufacturer's protocol. Alternatively, there are many kits available to measure a number of cytokines and other inflammatory mediators.

3.3.7. Circulating Immunoglobulins

Serum is prepared from cardiac bleeds and frozen until use. Levels of IgE, IgG1, and IgG2a are determined by ELISA using paired antibodies according to the manufacturer's instructions.

4. Notes

1. Allergen-induced pulmonary inflammation varies considerably between different strains of mice. In particular, AHR is dependent on the background strain of the mouse, consistent with the hypothesis that airway hyperresponsiveness is a heritable trait ***(3)***. AKR/J and A/J strains showed the greatest degree of airway responsiveness, whereas the C57BL/6J, SJL, and C3H/HeJ strains were the least responsive. BALB/c mice tend to be high-IgE responders, and in allergic protocols, this strain exhibits a more Th2-skewed response, compared to the same protocol used in C57BL/6 mouse. These aspects of model generation have been recently reviewed ***(4)***.

2. The sensitization model described here uses chicken egg ovalbumin as an allergen and mice are primed with allergen in conjunction with an adjuvant. However, it is possible to use other allergens, such as cockroach antigens, cat dander extracts, or parasite antigens ***(5)***. Moreover, we have given the local allergen challenge as an aerosol; other investigators have given soluble allergen to the airways by intransal or intratracheal instillation. We have found the protocol described here to give a robust Th2-dependent pulmonary inflammation characterized by tissue and lavage eosinophilia, Th2 cytokine production, allergen-specific IgE production, and airway hyperreactivity ***(6)***.
3. We have found that starting with spleens from five DO11 mice yields plenty of cells for an in vivo experiment after three rounds of expansion and polarization.
4. You can continue to stimulate the cells multiple times, although we have found that cells polarized three times induce eosinophillic airway inflammation when transferred in vivo ***(7)***.
5. Integrity of polarization should be determined by extracting a small sample of IL-2-rested cells (2×10^5 cells) and activating on immobilized anti-CD3 mAb (2C11, 10 µg/mL) in the presence of mIL-2 (10 U/mL). After 48 h, collect the supernatants to measure IL-4, IL-5, and IFN-γ levels by ELISA and cell pellets for RNA extraction and polymerase chain reaction (PCR) analysis. At this point, the cells should be polarized, expressing high levels of IL-4 but low levels of IFN-γ.
6. We have found that although it is relatively simple to identify eosinophils, neutrophils, and macrophages within differentially stained cytospins, it is more difficult to categorically distinguish between monocytes and lymphocytes. Therefore, we count them together as "lympho-mononuclear cells." To equivocally distinguish between these cells, the lavage cells can be immunophenotyped by staining cytospins or by flow cytometry.
7. After making cytospins from lavage and lung homogenate samples, the rest of the cells can be used for flow cytometry, in vitro functional assays, or RNA analysis.
8. In order to obtain the maximum amount of information from each mouse and to minimize the total numbers of mice used per experiment, we lavage each mouse and then use the lungs for histology or digestion and preparation of homogenates. We have found it preferable to use separate mice for histology because perfusion with NBF or OCT affects the digest or homogenate process.
9. Staining to identify KJ126-positive cells is described here, but we have also used sections to identify chemokine receptor expression ***(7)***, cellular localization of chemokines ***(8,9)*** and phenotype of leukocytes within infiltrates ***(10)***.

References

1. Murphy, K. M., Heimberger, A. B., and Loh, D. Y. (1990) Induction by antigen of intrathymic apoptosis of CD4+CD8+TCRlo thymocytes *in vivo*. *Science* **250,** 1720–1723.
2. Townsend, M. J., Fallon, P. G., Matthews, D. J., Smith, P., Jolin, H. E., and McKenzie, A. N. (2000) IL-9-deficient mice establish fundamental roles for IL-9

in pulmonary mastocytosis and goblet cell hyperplasia but not T cell development. *Immunity* **13,** 573.
3. Drazen, J. M., Finn, P. W., and De Sanctis, G. T. (1999) Mouse models of airway responsiveness: physiological basis of observed outcomes and analysis of selected examples using these outcome indicators. *Annu. Rev. Physiol.* **61,** 593.
4. Lloyd, C. M., Gonzalo, J. A., Coyle, A. J., and Gutierrez-Ramos, J. C. (2001) Mouse models of allergic airway disease. *Adv. Immunol.* **77,** 263–295.
5. Campbell, E. M. and Lukacs, N. W. (2000) Murine models of airway inflammation. *Methods Mol. Biol.* **138,** 295.
6. Lloyd, C. M., Gonzalo, J. A., Nguyen, T., et al. (2001) Resolution of bronchial hyperresponsiveness and pulmonary inflammation is associated with IL-3 and tissue leukocyte apoptosis. *J. Immunol.* **166,** 2033.
7. Lloyd, C. M., Delany, T., Nguyen, T., et al. (2000) CC Chemokine receptor (CCR)3/Eotaxin is followed by CCR4/monocyte-derived chemokine in mediating pulmonary T helper lymphocyte type 2 recruitment after serial antigen challenge *in vivo*. *J. Exp. Med.* **191,** 265.
8. Gonzalo, J. A., Pan, Y., Lloyd, C. M., et al. (1999) Mouse monocyte-derived chemokine is involved in airway hyperreactivity and lung inflammation. *J. Immunol.* **163,** 403.
9. Gonzalo, J. A., Lloyd, C. M., Peled, A., et al. (2000) Critical involvement of the chemotactic axis CXCR4/stromal cell-derived factor-1 alpha in the inflammatory component of allergic airway disease. *J. Immunol.* **165,** 499.
10. Gonzalo, J.-A., Lloyd, C. M., Kremer, L., et al. (1996) Eosinophil recruitment to the lung in a murine model of allergic inflammation. The role of T cells, chemokines and adhesion receptors. *J. Clin. Invest.* **98,** 2332.

17

Assessing the Role of Multiple Phosphoinositide 3-Kinases in Chemokine Signaling

Use of Dominant Negative Mutants Controlled by a Tetracycline-Regulated Gene Expression System

Adam P. Curnock, Yannis Sotsios, and Stephen G. Ward

1. Introduction

A combination of pharmacological, molecular, and genetic approaches have indicated the involvement of phosphoinositide 3-kinase (PI3K) in chemokine-stimulated cell migration. PI3Ks can be divided into three main classes on the basis of their in vitro lipid substrate specificity, structure, and likely mode of regulation ***(1)***. Hence, the class I PI3Ks can phosphorylate PI, PI(4)P, and PI(4,5)P_2 to yield the 3'-phosphorylated phosphoinositide (PI) lipids PI(3)P, PI(3,4)P_2, and PI(3,4,5)P_3 respectively. They also interact with Ras and form heterodimeric complexes with adaptor proteins that link them to different upstream signaling events ***(1)***. The prototypical class IA PI3Ks are heterodimers consisting of the 85-kDa regulatory/adaptor subunit and a catalytic 110-kDa subunit. The existence of multiple isoforms of both the regulatory (e.g., p85α/β, p55γ) and catalytic (e.g., p110α/β/δ) components provides considerable scope for specific variation between tissues as well as for coupling to different receptors and functional events. The class IB PI3K (PI3Kγ) is stimulated by G-protein βγ-subunits and associates with a unique p101 adaptor molecule ***(2,3)***. Nevertheless, there is some evidence that G-protein-coupled receptors (GPCRs) are also able to activate the p85/p110 PI3K ***(4)***. The class II PI3Ks (e.g., PI3K-C2α/β/γ) are characterized by the presence of a C-2 domain and utilize predominantly PI and PI(4)*P* as substrates. Recent evidence has indicated that clathrin functions as an adaptor for class II PI3K-C2α binding to its N-terminal region and stimulating its catalytic activity ***(5)***. The class III PI3Ks utilize only PI as a substrate ***(1)***.

The lipid products of PI3K activity, namely 3'-phosphorylated lipids such as PI(3,4,5)P_3 are known to accumulate in response to chemokines such as SDF-1/CXCL12 or MCP-1/CCL2. Such an accumulation of 3'-phosphorylated

From: *Methods in Molecular Biology, vol. 239: Cell Migration in Inflammation and Immunity*
Edited by: D. D'Ambrosio and F. Sinigaglia

PI lipids may be the result of the activation of more than one PI3K (e.g., the p85/p110 PI3K and/or PI3Kγ). Given that chemokine receptors are G-protein coupled ***(6,7)***, it is not surprising that the accumulation of PI(3,4,5)P_3 stimulated by SDF-1 and MCP-1 can be completely inhibited by pretreatment with pertussis toxin, strongly indicating that 3'-phosphoinositide lipid accumulation occurs via the G_i-protein-coupled PI3Kγ ***(8–10)***. Experiments using PI3Kγ knockout mice have revealed that leukocytes from such mice are unable to produce PI(3,4,5)P_3 in response to the CXC chemokine interleukin (IL)-8/CXCL8 ***(11)***, thus lending further evidence to the notion that PI3Kγ is the key mediator of PI(3,4,5)P_3 production in response to IL-8.

Despite strong biochemical and genetic evidence for activation of PI3Kγ by chemokines and its role in PI(3,4,5)P_3 accumulation and cell migration, there is a strong body of evidence to suggest that other classes of PI3K are activated by chemokines. First, there is incomplete reduction (e.g., 50–70%) in the capacity of neutrophils to migrate to a range of chemoattractants in PI3Kγ$^{-/-}$ mice ***(11–13)*** and the PI3Kγ knockout does not prevent chemoattractant-induced actin polymerization ***(12)***. Second, in vitro assays of immunoprecipitated p85 subunits of PI3K indicate that the p85/p110 heterodimer is activated by SDF-1 and RANTES in T-cells ***(8–10,14)*** and by MCP-1 in THP-1 cells ***(8)***. Moreover, p85 has been reported to coassociate with anti-CXCR4 immunoprecipitates after SDF-1 stimulation of human peripheral blood T-lymphocytes ***(15)***. Third, MCP-1 has been reported to activate class II PI3KC2α in a monocytic cell line ***(8)***.

Although the biochemical evidence for activation of multiple PI3K isoforms is strong, it has not been possible to accurately evaluate the functional consequences of activation of the class IA and class IB PI3Ks because available inhibitors do not exhibit sufficient isoform selectivity. In addition, genetic approaches have adopted strategies that have only deleted single α or β isoforms of the p85 subunit ***(16,17)***, so the p85α$^{-/-}$ and p85β$^{-/-}$ mice retained expression of at least one other isoform of the adaptor subunit that may be able to compensate for the lack of expression of one or other isoform.

A common molecular approach used to assess the role of an enzyme in cellular responses is to establish stable transfectants that overexpress dominant negative forms of the enzyme. However, given the importance of PI3K in cell growth and survival ***(1)***, overexpression of dominant negative PI3K constructs is likely to be toxic and result in the selection of clones with other compensatory mutations, thus rendering direct comparisons with nonexpressing cells meaningless. This chapter describes the use of the tetracycline-inducible gene system ***(18)*** as a tool to dissect the roles of class IA and IB PI3K in chemokine-mediated signaling and functional responses.

An inducible expression system has several advantages over a constitutive expression system. First, inducible expression reduces the potential for select-

ing transfectants, which have developed an additional phenotype in order to compensate for the effect of expressing the primary mutant. Second, gene expression can be shut down during the generation of stable transfectant, with a very low level of "leakiness" of the expression of proteins that would normally be toxic to the host cells. Third, expression can be tightly regulated and controlled by titrating the concentration of tetracycline used. Finally, the level of expression achievable using the tetracycline-inducible system has been reported to be greater than in a constitutive system using the same cytomegalovirus (CMV) promoter ***(19)***. The use of inducible expression systems such as that described here will provide an invaluable tool for assessing the role of individual PI3K isoforms and their downstream effector proteins in not only chemotaxis but also for distinct biochemical and functional responses such as regulation of transcription factors, actin polymerization, cytsoskeletal rearrangements, and adhesion molecule upregulation.

2. Materials

All reagents are from Sigma (Dorset, UK) unless otherwise stated; all cell culture media and supplements are from Life Technologies (Paisley, UK).

1. Standard molecular-biology reagents: restriction enzymes *Fsp*I, *Sac*II, *Eco*RI, *Kpn*I, and *Xba*I, T4 polymerase, Klenow, DNA ligase, calf intestinal phosphatase, and *Escherichia coli* strain DH5α and the response plasmid pUHD10.3-hygro (Promega, Southampton, UK).
2. Forward and reverse primers flanking the insertion site on pUHD10-3hygro (CTCC ATAGAAGACACCGGGA [forward] and GCATTCTAGTTGTGGTTTGT [reverse]) and primers flanking the catalytic domain region of KD and WT PI3Kγ: (CAGAA TTTGAATCTCCCCCA [forward], TGATAGAGCCGTAGGATCGG [reverse]) were obtained from MWG Biotech AG (Ebersberg, Germany).
3. Luria–Bertani (LB) broth, LB agar, agarose.
4. DNA purification kits (Qiagen, Crawley, West Sussex, UK).
5. TET-OFFJurkat T-cells, which stably express the regulatory plasmid pUHD15-1neo (Clontech, Basingstoke, Hants, UK).
6. Tissue culture medium, fetal bovine serum (FBS), penicillin, and streptomycin.
7. Selective antibiotics, G418 and hygromycin B (Calbiochem, Nottingham, UK)
8. Tetracycline.
9. Anti-myc 9E10 monoclonal antibody (mAb) (Santa Cruz Biotechnology (Santa Cruz, CA) and horseradish peroxidase (HRP)-conjugated rabbit anti-mouse Abs (Dako, Cambridge, U.K).
10. Lysis buffer: 1% (v/v) Nonidet P-40, 100 m*M* NaCl, 20 m*M* Tris-HCl pH 7.4, 10 m*M* iodoacetamide, 10 m*M* NaF. Prior to use, the buffer is supplemented with the protease inhibitors 1 m*M* phenylmethylsulfonyl fluoride (PMSF) (1 m*M*), aprotinin (2 μg/mL), leupeptin (2 μg/mL), pepstatin A (2 μg/mL), and the phosphatase inhibitors sodium orthovanadate (1 m*M*) and β-glycerophosphate (10 μg/mL).

11. Tris-buffered saline: 10 m*M* Tris, pH 7.5, 100 m*M* NaCl.
12. Enhanced chemiluminescence (ECL) Western blotting detection reagents (Amersham Biosciences).
13. XAR-5 film (Kodak), exposure cassettes, X-ray film developer.
14. 96-Well chemotaxis chambers (Neuroprobe Inc. Gaithersburg, MD).
15. Versene (Life Technologies, Paisley, UK).
16. Cell Titre 95 AQ_{ueous} Reagent (Promega, Southampton, UK).
17. SDF-1α or other chemokines (R&D Systems, Abingdon, UK).
18. Standard sodium dodecyl sulfate–polyacrylamide gel electrophoresis (SDS-PAGE) and Western blotting equipment.
19. Nitrocellulose membranes (BDH, Poole, UK).
20. 5-μm Pore size polyvinyl pyrolidine (PVP)-free polycarbonate membranes (Neuroprobe Inc., Gaithersburg, MD).

3. Methods

3.1. Principles of the Tetracycline-Inducible System

The tetracycline-inducible gene system is a two-vector system, comprising a regulatory plasmid (pUHD15-1) and response plasmid (pUHD10-3; *see* **Fig. 1**). The regulatory plasmid constitutively produces a tetracycline-sensitive transactivator (tTA) that is a chimera of the *E. coli* tetracycline repressor tetR and the transcriptional activator domain of the herpessimplex virus protein VP16. The response plasmid contains a tetracycline response element (TRE), which is a heptameric repeat of the tetR binding site (*tetO*), upstream of a minimal CMV promoter. In the absence of tetracycline, the tTA binds to *tetO* sites of the TRE on the response vector and activates expression of the gene of interest downstream of the minimal promoter. In the presence of tetracycline, the tTA undergoes a conformational change that prevents it from binding to the *tetO* sites, resulting in the inhibition of gene expression.

Two rounds of transfection and selection are required to obtain clones stably expressing both regulatory and response plasmids. It is possible to use a commercially available Jurkat cell line that stably expresses the regulatory plasmid pUHD15-1-neo, which contains a neomycin-resistance gene for selection of transfectants (Clontech, Basingstoke, Hants, UK). Other commonly used cell lines stably expressing the regulatory plasmid are also available from this supplier. This effectively halves the time required to obtain doubly-transfected, stably expressing clones.

3.2. Dominant Negative PI3K Cloning Strategy

Dominant negative constructs of class IA and IB PI3K must be sub-cloned into the response vector pUHD10-3hygro, which contains a hygromycin resistance gene for direct selection of transfectants. For class IA PI3K, a bovine

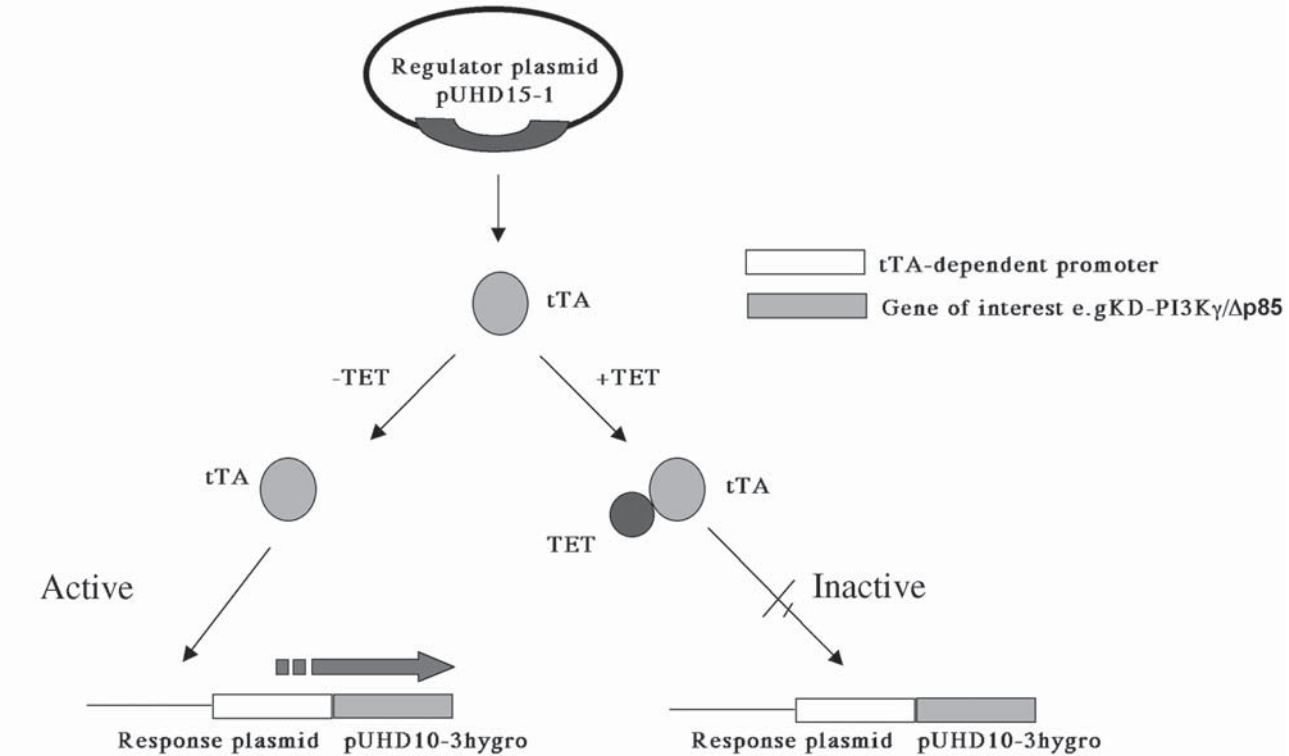

Fig. 1. Schematic of the tetracycline-inducible gene system. The regulatory plasmid constitutively produces tTA (tetracycline-controlled transactivator), which, in the absence of tetracycline, binds to the TRE (tetracycline-response element) on the response plasmid, promoting the transcription of the gene of interest downstream of a minimal CMV promoter. In the presence of tetracycline, tTA undergoes a conformational change, rendering it unable to bind to the TRE on the response plasmid and switches off expression of the gene of interest.

p85α regulatory subunit construct with a deletion of the inter-SH2 domain (amino acids 479–513, which constitute the p110-binding domain) can be used. This Δp85 is unable to bind to p110 catalytic domains ***(20)***, but retains its adapter function via its two SH2 domains, SH3, and proline-rich regions, and thus, overexpression of Δp85 prevents the recruitment and activation of the catalytic subunit, by out-competing endogenous p85 for binding sites. For the class IB PI3K, a bovine kinase-dead PI3Kγ construct (KD-PI3Kγ) is used. KD-PI3Kγ has a single point mutation in its catalytic domain, K799R, rendering it inactive ***(21)***. Both constructs were tagged by the decapeptide myc epitope recognized by the *c*-Myc monoclonal antiobody 9E10 to enable screening for expressing clones ***(21)***. Standard molecular-biology techniques were followed throughout ***(22)***.

1. Myc-tagged Δp85 (kindly provided by M. J. Welham, University of Bath, UK) is excised from the pBluescript-N-Myc2 vector using *Sac*II and *Eco*RI and Myc-tagged KD-PI3Kγ excised from the vector pCDNA3 using *Kpn*I and *Xba*I.
2. All inserts are blunt ended on both the 3' and 5' ends using T4 polymerase, followed by the Klenow fragment of DNA polymerase.
3. The response plasmid pUHD10-3-hygro is linearized with *Xba*I, followed by blunt ending and removal of 3'-OH groups by treatment with calf intestinal phosphatase to minimize resealing of empty pUHD10-3-hygro.
4. Ligation reactions of linearised, blunt-ended pUHD10-3-hygro with each of the blunt-ended myc-tagged PI3K constructs are carried out and ligation products used to transform *E. coli* strain DH5α.
5. Analytical restriction digests are performed to identify transformants with pUHD10-3-hygro containing myc-tagged PI3K constructs in the correct orientation.
6. The identity and orientation of the PI3K inserts is confirmed by sequencing using forward and reverse primers flanking the insertion site on pUHD10-3-hygro. The forward primer sequence was CTCCATAGAAGACACCGGGA and the reverse primer was GCATTCTAGTTGTGGTTTGT.
7. To confirm the identity of KD and wild-type (WT) PI3Kγ inserts, primers flanking the catalytic domain region were used: The forward primer sequence was CAGAA TTTGAATCTCCCCCA, whereas the reverse primer sequence was TGATAGAG CCGTAGGATCGG. A single guanosine to adenosine substitution in codon 799, resulting in a lysine to arginine substitution, confirmed the identity of the KD PI3Kγ construct.

3.3. Transfection and Selection of Tet-Off Dominant Negative PI3K Jurkat Clones

1. The pUHD10-3/dominant negative PI3K constructs are linearised with *Fsp*I and purified by gel electrophoresis, chloroform extraction, and ethanol precipitation by standard techniques ***(22)***.

2. The 2×10^7 Jurkat cells already stably expressing the pUHD15-1-neo plasmid (Tet-OFF Jurkats, Clontech) are transfected with 10 µg of purified DNA by electroporation at 950 µF and 300 V.
3. Transfer cells immediately to growth media (RPMI 1640 containing 25 m*M* HEPES and 2 m*M* glutamine, 10% FBS, and penicillin/streptomycin) containing 2 µg/mL tetracycline and culture for 48 h in the absence of selection agents.
4. Following this recovery period, wash the transfected cells three times and resuspend in growth media supplemented with 2 µg/mL tetracycline, 500 µg/mL G418, and 300 µg/mL hygromycin B. Aliquot cells into 96-well plates at 1×10^4 cells/well. (*See* **Note 1**.)
5. Replenish the tetracycline every 48 h. Replace the media on a weekly basis to maintain levels of G418 and hygromycin B.
6. From approx 2 wk posttransfection, selected colonies can be picked and transferred to 1 mL selective media in 24-well plates for expansion and then further expanded in 6-well plates.

3.4. Characterization of Tet-Off Dominant Negative PI3K Jurkat Clones

1. After appropriate expansion of the clones, the cells can be washed and incubated for 24 h in selective media, in the presence and absence of 2 µg/mL tetracycline, to test for inducible expression of the PI3K constructs.
2. Jurkat cells stably transfected with either KD-PI3Kγ or Δp85 are washed three times in RPMI 1640, resuspended, and incubated in the presence or absence of tetracycline for 48 h and lysed in sample buffer. Expression of the mutant PI3K isoforms is analyzed by performing Western blots with the anti-myc 9E10 monoclonal antibody (*see* **Notes 2–6**).
3. For experimentation, tetracycline is removed from cells by washing three times in RPMI 1640 and the cells are resuspended at 1×10^4 cells/mL in growth medium, with or without 2 µg/mL tetracycline. Cells are routinely cultured for 48 h to allow the mutant proteins to be expressed.
4. After 48 h, the cells are washed twice in RPMI and resuspended in RPMI 1640, and serum starved for a further 2 h at 37°C. Functional and/or biochemical responses to chemokine stimulation can then be assessed (*see* **Notes 7–10**).

4. Notes

1. Any remaining cells at this stage can be cultured in an 80-cm^2 tissue culture flask in selective media to obtain a polyclonal suspension of selected cells. These can be used for an alternative method of selection of individual clones by subsequently seeding them into 96-well plates at very low density (0.3 cells/well, i.e., 3 cells/mL) in Jurkat-cell-conditioned media, plus selective reagents and tetracycline.
2. We find that high-level expression of constructs is maintained from 24 to 72 h incubation, following the removal of tetracycline.

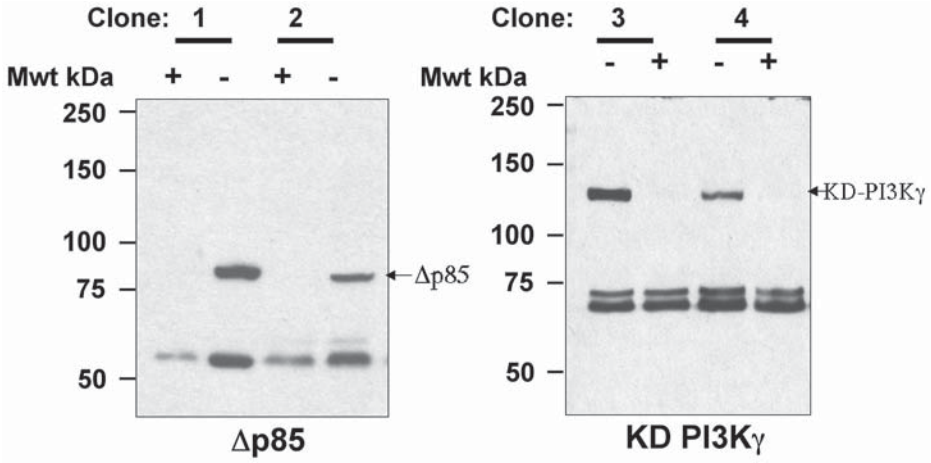

Fig. 2. Analysis of myc-KD-PI3Kγ and Δp85 expression. Clones of Tet-Off Jurkat cells (1×10^4 cells/mL) transfected with either (**A**) Δp85 clones 1 and 2 or (B) KD-PI3Kγ clones 3 and 4 were washed, incubated in the absence (–) or presence (+) of 2 μg/mL tetracycline for 48 h and cells lysed. The lysates were resolved by SDS-PAGE then transferred to nitrocellulose membranes. Membranes were probed with a myc epitope antibody and developed by enhanced chemiluminescence.

3. In our hands, the expression of either KD-PI3Kγ or Δp85 is critically dependent on initial seeding density. Hence, optimal expression is achieved when the cells are initially seeded at 1×10^4 cells/mL, whereas expression is markedly reduced at seeding densities of 5×10^4 cell/mL or higher.
4. The expressed mutants are fully regulatable in that once the protein has been induced upon removal of tetracycline, the subsequent readdition of tetracycline leads to a rapid downregulation of expression within 24 h.
5. The effects of tetracycline are concentration dependent, with marked abrogation of expression observed at concentrations in the range 0.03–3000 ng/mL. The concentration of tetracycline that gives 50% inhibition of expression (IC_{50}) is approx 0.3 ng/mL ($n = 3$).
6. It should be emphasised that cells should be routinely cultured in the presence of 2 μg/mL tetracycline prior to use to ensure that expression of the mutant proteins was adequately switched off (*see* **Fig. 2**).
7. We use a range of clones expressing differing levels of the constructs, but all exhibiting tight regulation of expression by tetracycline. We find that the functional responses (e.g., chemotactic responses to SDF-1) of different clones varies irrespective of construct expression, so it is important that the effect of the dominant negative PI3K constructs be determined within the same clone in the presence and the absence of expression. For this reason, it is important to use clones with tight regulation by tetracycline and to compare functional responses of several clones with and without tetracycline.

8. In all experiments, whole-cell lysates of induced and noninduced cells are retained for expression analysis by Western blotting ***(8,9)***. Cells (1×10^7/sample) are incubated in 1.5-mL Eppendorf tubes at 37°C, and after appropriate treatment regimens, the reactions are terminated by pelleting the cells in a microfuge for 10 s, supernatant is aspirated, and the cell pellet is resuspended in 500 µL ice-cold lysis buffer (20 m*M* Tris-HCl, pH 7.4, 137 m*M* NaCl, 1 m*M* $MgCl_2$, 1 m*M* $CaCl_2$, 10% glycerol (w/v), 1% NP-40 (w/v), and protease inhibitors 1 m*M* PMSF, 2 µg/mL aprotinin, 2 µg/mL leupeptin, 2 µg/mL pepstatin A, and 1 m*M* sodium orthovanadate). Lysates are incubated on a rotator for 20 min and nonsoluble material removed by spinning in a microfuge, at 13,000*g* for 10 min. The protein levels in supernatants are determined by the BCA protein assay (Pierce and Warriner, Chester, UK) and adjusted to equal protein concentration by dilution with lysis buffer, where necessary.
9. Cell lysates are boiled for 5 min in sample buffer and samples loaded, at volumes corresponding to equivalent amounts of protein, onto 7.5% SDS-PAGE gels. After electrophoresis, resolved proteins are transferred onto nitrocellulose membranes and probed with appropriate antibodies. Briefly, membranes are blocked in TBS (10 m*M* Tris-HCl, pH 7.5, 100 m*M* NaCl)/5% nonfat milk for 2 h, followed by overnight incubation with primary anti-myc antibody (at 0.5–1 µg/mL diluted in TBS/0.1% Tween/0.01% sodium azide) at 4°C on a platform shaker. After extensive washing in TBS/Tween, membranes are incubated with an appropriate HRP-conjugated secondary antibody for 1 h. After a further round of extensive washing in TBS/Tween, membranes are developed using the ECL Western blotting system.
10. Typical functional readouts that might be performed on these cells are chemotaxis assays, which are carried out in 96-well chemotaxis chambers (Neuroprobe Inc, Gaithersburg, MD). The wells of the 96-well plate in the lower chamber are filled with 355 µL RPMI 1640/0.1% bovine serum albumin (BSA), containing a range of SDF-1α concentrations and carefully overlaid with a PVP-free polycarbonate membrane (5 µm pore size). Tet-OFF Jurkat cells are added to the upper chambers (200 µL of a 1×10^6 cell/mL suspension in RPMI 1640/0.1% BSA) and the chamber incubated at 37°C for 3 h. The cell suspension is carefully aspirated off and 200 µL Versene (Life Technologies) added to each well and incubated for 20 min at 4°C. The 96-well plate and attached membrane was centrifuged at 1000*g* at 4°C, for 10 min and the supernatant carefully aspirated off. The remaining cells were resuspended in 100 µL RPMI/0.1% BSA and cell numbers determined from standard curves of the same cells using Cell Titre 96 AQ_{ueous} Reagent following the manufacturer's instructions.

References

1. Vanhaesebroeck, B., Leevers, S., Khatereh, A., et al. (2001) Synthesis and function of 3-phosphorylated inositol lipids. *Annu. Rev. Biochem.* **70,** 535–602.
2. Stephens, L. R., Smrcka, A. S., Cooke, F. T., Jackson, T. R., Sternweiss, P. C., and Hawkins, P. T. (1994) A novel phosphoinositide 3 kinase activity in myeloid cells is activated by G protein βγ subunits. *Cell* **77,** 83–93.

3. Stephens, L. R., Eguinosa, A., Erdjument-Bromage, H., et al. (1997) The Gβγ sensitivity of a PI3K is dependent upon a tightly associated adaptor, p101. *Cell* **89,** 105–114.
4. Stephens, L., Eguinoa, A., Corey, S., Jackson, T., and Hawkins, P. T. (1993) Receptor-stimulated accumulation of phosphatidylinositol-(3,4,5)-trisphosphate by G-protein mediated pathways in human myeloid derived cells. *EMBO J.* **12,** 2265–2273.
5. Gaidarov, I., Smith, M. E. K., Domin, J., and Keen, J. H. (2001) The class II phosphoinositide 3-kinase C2α is activated by clathrin and regulates clathrin-mediated membrane trafficking. *Mol. Cell* **7,** 443–449.
6. Ward, S. G., Bacon, K. B., and Westwick, J. (1998) Chemokines and T lymphocytes: more than an attraction. *Immunity* **8,** 1–9.
7. Ward, S. G. and Westwick, J. (1998) Chemokines: understanding their role in T lymphocyte biology. *Biochem. J.* **333,** 457–470.
8. Turner, S. J., Domin, J., Waterfield, M. D., Ward, S. G., and Westwick, J. (1998) The CC chemokine monocyte chemotactic peptide-1 activates both the class 1 p85/p110 phosphatidylinositol 3-kinase and the class II PI3K-C2γ. *J. Biol. Chem.* **73,** 25,987–25,995.
9. Sotsios, Y., Whittaker, G. C., Westwick, J., and Ward, S. G. (1999) The CXC chemokine stromal cell-derived factor activates a Gi-coupled phosphoinositide 3-kinase in T lymphocytes. *J. Immunol.* **163,** 5954–5963.
10. Sotsios, Y. and Ward, S. G. (2000) Phosphoinositide 3-kinase: a key biochemical signal for cell migration in repsonse to chemokines. *Immunol. Rev.* **177,** 217–235.
11. Hirsch, E., Katanaev, V. L., Garlanda, C., et al. (2000) Central role for G protein-coupled phosphoinositide 3-kinase-γ in inflammation. *Science* **287,** 1049–1053.
12. Li, Z., Jiang, H., Zie, W., Zhang, Z., Smrcka, A. V., and Wu, D. (2000) Roles of PLCβ2 and β-3 and PI3Kγ in chemoattractant-mediated signal transduction. *Science* **287,** 1046–1049.
13. Sasaki, T., Irie-Sasaki, J., Jones, R. G., et al. (2000) Function of PI3Kγ in thymocyte development, T cell activation and neutrophil migration. *Science* **287,** 1040–1045.
14. Turner, L., Ward, S. G., and Westwick, J. (1995) RANTES-activated human T lymphocytes: a role for phosphoinositide 3-kinase. *J. Immunol.* **155,** 2437–2444.
15. Vicente-Manzanares, M., Rey, M., Jones, D. R., et al. (1999) Involvement of phosphatidylinositol 3-kinase in stromal cell-derived factor-1α-induced lymphocyte polarisation and chemotaxis. *J. Immunol.* **163,** 4001–4012.
16. Fruman, D. A., Snapper, S. B., Yballe, C. M., et al. (1999) Impaired B cell development and proliferation in the absence of phosphoinositide 3-kinase p85α. *Science* **283,** 393–397.
17. Suzuki, H., Terauchi, Y., Fujiwara, M., et al. (1999) *Xid*-like immunodeficiency in mice with disruption of the p85 subunit of phosphoinositide 3-kinase. *Science* **283,** 390–392.
18. Gossen, M. and Bujard, H. (1992) Tight control of gene-expression in mammalian-cells by tetracycline-responsive promoters. *Proc. Natl. Acad. Sci. USA* **89,** 5547–5552.

19. Yin, D. X., Zhu, L., and Schimke, R. T. (1996) Tetracycline-controlled gene expression system achieves high level and quantitative control of gene expression. *Anal. Biochem.* **235,** 195–201.
20. Hara, K., Yonezawa, K., Sakaue, H., et al. (1994) 1-Phosphatidylinositol 3-kinase activity is required for insulin-stimulated glucose-transport but not for ras activation in CHO cells. *Proc. Natl. Acad. Sci. USA* **91,** 7415–7720.
21. Takeda, H., Matozaki, T., Takada, T., et al. (1999) PI3Kγ and protein kinase C-ζ mediate Ras-independent activation of MAP kinase by a Gi protein-coupled receptor. *EMBO J.* **18,** 386–392.
22. Sambrook, J., Fritsch, E. F., and Maniatis, T. (1989) *Molecular Cloning: A Laboratory Manual,* 2nd ed., Cold Spring Harbor Laboratory, Cold Spring Harbor, NY.

18

In Vitro and In Vivo Models to Study Chemokine Regulation of Angiogenesis

Giovanni Bernardini, Domenico Ribatti, Gaia Spinetti, Lucia Morbidelli, Marina Ziche, Angela Santoni, Maurizio C. Capogrossi, and Monica Napolitano

1. Introduction

Angiogenesis is defined as the generation of new blood vessels from preexisting ones. Physiologic angiogenesis is a controlled and fundamental process during embryonic development, being rare in the adult and limited to conditions such as wound healing and menstrual cycle. If regulation of the process is lost, persistent angiogenesis may occur and contribute to pathologic states such as cancer, rheumatoid arthritis, and diabetes mellitus.

Several chemokines have been described that regulate the angiogenic process, both positively and negatively, by directly modulating endothelial (EC) or smooth muscle cell activation and/or by interfering with angiogenic factor activity. Primary ECs are commonly used for in vitro studies and can be purified from human cord blood (human umbilical vein endothelial cells [HUVECs]) and dermis (human dermal microvascular endothelial cells [HDMECs]), mouse brain endothelium, and so forth.

In this chapter, we describe a method to isolate HUVECs and some in vitro and in vivo assays currently utilized to assess the role of chemokines in angiogenesis. Different types of in vitro assay have to be performed, because chemokines modulate only one or few of the many steps required for the angiogenic process to occur (endothelial or accessory cell proliferation, metalloproteases production, chemotaxis, adhesion, differentiation, etc.). On the contrary, in vivo assays allow the study of a specific factor in a more physiologic context, where additional roles are played by molecules produced by resident cells and by cell-to-cell interactions. Because of the high homology of their sequence among species, single chemokines often preserve their biological activity when

From: *Methods in Molecular Biology, vol. 239: Cell Migration in Inflammation and Immunity*
Edited by: D. D'Ambrosio and F. Sinigaglia

tested in a host of different classes. For this reason, their ability to modulate angiogenic processes can be assessed in models of angiogenesis that have been developed in different animals, including chick, rabbit, and mouse.

2. Materials

2.1. Endothelial Cell Isolation from Human Umbilical Cord Vein

1. Plastic syringes.
2. Sterile clamps.
3. Sterile phosphate-buffered saline (PBS).
4. Isolation medium: RPMI 1640; 10 ng/mL fibroblast growth factor (FGF), 20% heat-inactivated fetal calf serum (FCS), glutamine, amphotericine B, penicilline, and streptomicin.
5. Freshly prepared sterile solution of collagenase type 1 (0.2% in PBS with calcium and magnesium).
6. Complete medium: EBM (endothelial cell basal medium)-2 supplemented with 2% serum and growth factors by the company (Clonetics, UK).

2.2. Endothelial Cell Chemotaxis/Invasion and Differentiation Assay

1. Endothelial cells either purified following **Subheading 3.1.** or bought from Clonetics.
2. 8–12-µm pore-size polycarbonate filters (Neuroprobe, Cabin John, MD).
3. 48-Well chemotaxis chamber (Nucleopore, Cambridge, MA).
4. Murine collagen type IV (Beckton-Dikinson, Bedford, MA).
5. Matrigel IV (Beckton Dickinson, Bedford, MA).
6. Migration medium (MM): RPMI, 25mmol/L HEPES, 0.01% bovine serum albumin (BSA).
7. Chemokine (R&D System or Peprotech).
8. DiFF-Quick solutions (American Scientific Products, Edison, NJ, USA).
9. Glass slides.
10. Direct-light microscope.
11. Inverted-phase photomicroscope.

2.3. Rabbit Cornea Assay

1. New Zealand white rabbits.
2. Sodium pentothal.
3. 1.5-mm-Wide pliable iris spatula.
4. Absolute ethanol.
5. Ethylene-vinylacetate copolymer (Elvax-40) (DuPont de Nemours, Wilmington, DE).
6. Hematoxylin and eosine.
7. Slit-lamp stereomicroscope.

2.4. Chorioallantoic Membrane Assay

1. Elvax 40, hydron or gelatin sponge.

2. Fertilized chick eggs.
3. Scissors.
4. Paraffin or Epon 812.
5. Microtome or ultramicrotome.
6. 0.5% Aqueous solution of toluidine blue.
7. Light microscope or electron microscope.

3. Methods

3.1. In Vitro Assays

3.1.1. Isolation of Human Umbilical Cord Endothelial Cells (Modified from **refs. *1*** *and* ***2****)*

Use umbilical cord vein within 48 h of delivery.

1. Wash cords with tap water and insert a high-caliber syringe needle in the umbilical vein. Clamp and wash twice the inner part of the cord with PBS using a 20-mL syringe.
2. Connect the other edge of the cord to a second needle and fill the vein with collagenase solution using a syringe connected to it.
3. Incubate the cord for 30 min in a clean, distilled water bath at 37°C with frequent squeezing.
4. Collect the cell suspension in the first syringe and transfer to a sterile tube.
5. Pellet the cells by centrifuge at 250*g* for 15 min.
6. Resuspend the cell pellet in isolation medium and plate cells in a 75-cm^2 tissue culture flask precoated with 0.05% gelatine.
7. Replace 50% of medium every other day for a week and test cells for the expression of specific endothelial cell markers, such as CD31, von Willebrand factor, Webel–Palade bodies, uptake of acetylated low-density lipoprotein (LDL) expression and/or angiotensin-converting enzyme (ACE) activity.
8. Maintain cells in complete medium for further use.

3.1.2. Chemotaxis/Invasion Assay

Chemotaxis is the directional migration of cells in response to an increasing gradient of a chemotactic factor. To evaluate the ability of the cells to respond to a chemoattractant, cells are incubated in a compartment (upper chamber) of a chemotaxis chamber (*see* **Subheading 2.2., item 3**) connected to a second compartment (lower chamber) through the pores of a polycarbonate membrane (*see* **Subheading 2.2, item 2**). The size of the membrane pores (usually between one-half and two-thirds of the diameter of the cell) is chosen according to the size and plasticity of the cells under study and has to be small enough to counteract the passage of cells to the lower compartment by gravity. A 8 to 12-μm pore size is used to study HUVEC migration. A chemoattractant is placed in the lower chamber, and diffuses toward the upper chamber, forming a gradient. Migration

of cells in response to the chemotactic factor is determined by evaluating the number cells that cross the membrane to reach the lower compartment.

During angiogenesis, ECs cross the basement membrane, proliferate, and migrate to form the new blood vessel wall. Accordingly, chemotaxis of ECs in response to chemokines often correlates with the behavior of these molecules as angiogenesis regulators in vivo. Positive regulators of the process such as CXCL8 and CCL1 may promote endothelial cell migration in a dose-dependent manner, whereas angiostatic chemokines such as CXCL4 and CXCL10 can block growth-factor- or chemokine-induced chemotaxis. Doses of chemokines in the 48-well chemotaxis chamber usually range between 0.1 n*M* and 1 μ*M* ***(3)***.

1. Keep cells in the medium without growth factors for 36 h.
2. Coat the polycarbonate filter by evenly distributing 1 mL (20 μg/mL) of murine collagen type IV on the opaque side of the filter for 2 h at room temperature. It is important to use a flat surface to avoid irregular coating of the substrate.
3. If an invasive response of HUVEC has to be evaluated, **step 2** has to be followed by 1–2 h of coating with a solution of Matrigel (50 μg/mL) in sterile water.
4. Detach cells using 1 m*M* EDTA (in PBS without Ca^{2+} and Mg^{2+}) and dilute them in serum-containing medium. Detachment in EDTA solution prevents proteolytic cleavage of membrane receptors induced by a trypsin-based solution.
5. Place cells on a shaker and keep them at room temperature for 30 min to avoid clump formation. This step allows cells to recover from the detachment.
6. Wash and place cells in MM at 5×10^5 cells/mL.
7. Add 27–30 μL of medium containing different doses of chemokines to the lower wells in triplicate.
8. Lay the filter on the wells (with the coated side up) and place the rubber membrane of the chamber on it.
9. Immediately add the upper part of the chamber and seal the chamber with screw bolts to form the upper chamber.
10. Add 50 μL of ECs from **step 6** to the upper wells.
11. Leave the chamber at 37°C in 5% CO_2 for 3–5 h (time has to be optimized and is longer for the invasion assay).

During **steps 7–10** of the assay, the formation of air bubbles in the lower or upper compartment has to be avoided.

FGF-2 (10 ng/mL) can be used as a positive control. When a putative angiostatic effect of a chemokine has to be evaluated, increasing doses of chemokines are added to the lower wells in the presence or absence of growth factors such as vascular endothelial factor (VEGF) or FGF-2.

12. To stop the assay, the chamber is inverted on paper to discard the majority of the cells that have not migrated.
13. The membranes are then removed and the cells remaining on the upper side of the filter are scraped away, and the cells on the opposite side are fixed and stained

with Diff-Quick solution. After laying the filter on a glass slide, quantification of the assay is performed (within a week).

14. Migration of the cells in each well is quantified by counting and averaging the number of cells of six high-power fields (×400 magnification) by light microscopy. Results are expressed as the mean ± standard deviation of the triplicate well counts.

3.1.3. Matrigel Assay

Matrigel assay is an in vitro assay that allows one to determine the ability of ECs to adhere, migrate, and differentiate into capillarylike structures. ECs plated on this substrate form tubules that branch from a single cell and connect to each other when incubated in angiogenic-factor-containing medium.

Matrigel is an extract of murine basement membrane derived from the mouse Engelbreth–Holm–Swarm sarcoma containing laminin, collagen, heparan sulfate, and proteoglycan prepared as a sterile solution. It has the property of being liquid at 4°C and semisolid at 37°C. It contains stimulatory cytokines and growth factors, but preparations depleted of such factors are also commercially available. The latter preparations allow one to determine the activity of putative angiogenic factors, minimizing the basal level of differentiation often observed on the cells seeded in Matrigel.

1. Starve ECs (passage 3–5) in 0.5% EBM serum without growth factors (starvation medium) for 36 h.
2. Thaw Matrigel on ice to prevent premature polymerization.
3. Plate 250 µL on a 24-well tissue culture plate on ice and allow to polymerize at 37°C for 30–60 min.
4. Detach cells from the culture by treating the monolayer with EDTA (1 m*M*).
5. Wash twice in starvation medium and place 8×10^4 cells in each well in the same medium with or without chemokines.
6. Perform a time-course. The assay can be visually monitored for 1–24 h by an inverted-phase photomicroscope. After 4–6 h, "capillarylike" structures will become apparent and may increase in number in 48 h. Usually, after 48 h, the reticulate of cells start to regress and degenerate.
7. Quantification of the assay: cells are fixed in PBS containing 0.2% glutaraldehyde and 1% paraformaldehyde. Randomly selected fields are then photographed on low magnification (×50) and quantification of tubule/capillary formation can be carried out by counting tubules or using computer imaging. Several approaches can be followed:
   a. A standardized counting method can be performed by calculating a mean tubule length using computer imaging: A line is drawn along each tubule, and the total number of pixels of the lines obtained is divided by the number of tubules ***(4)***.
   b. Alternatively, the quantification can be performed calculating the number of intersections by counting the number of branches of each endothelial cell in the field ***(5)*.**

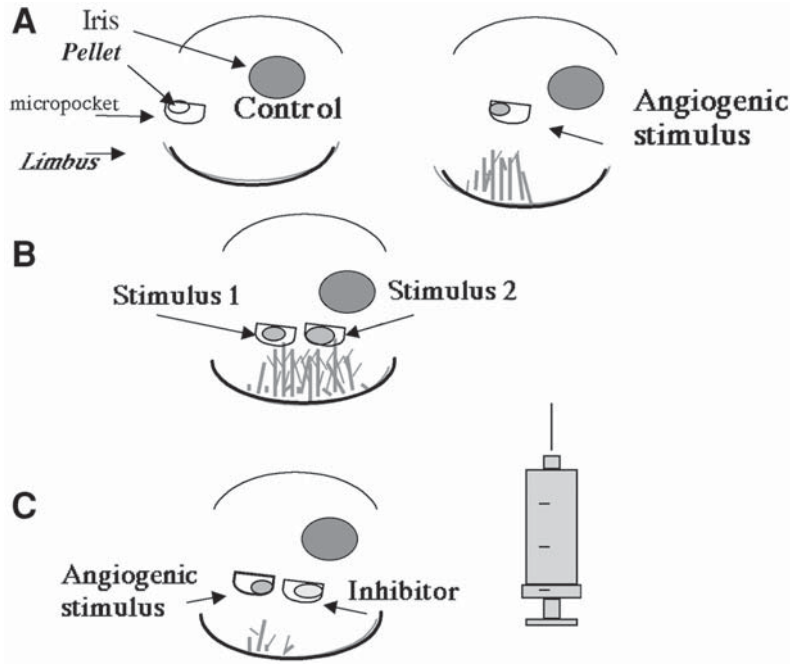

Fig. 1. Schematic of the different application of the rabbit cornea assay in the study of modulators of angiogenesis. (**A**) characterization of the angiogenic activity of a purified factor released in the corneal stroma from a slow release device. (**B,C**) Analysis of the interaction among factors. Two micropockets can be surgically produced in the same eye and the synergistic (**B**) or antagonistic (**C**) effect of two coreleased factors is monitored. The syringe represent the possibility of inhibiting aniogenesis through systemic administration of a soluble factor.

3.2. Micropocket Cornea Assay

In the cornea assay, a stimulus (tumor tissue, cell suspension, purified growth factor) is placed into a corneal pocket using rabbit, rat, and mouse as animal models (*see* **Fig. 1A**). If an angiogenic response is obtained, vascular outgrowth from the limbal vessels toward the implant will be evidenced. Because the cornea is normally avascular, only newly formed vessels will be measured to quantify the assay. In particular, in rabbits, manipulation is easy and neovascular growth and inflammatory reaction can be visually monitored over time.

In order to determine whether chemokines are acting as direct angiogenic factors or by means of their pro-inflammatory activity, it is important to be able to distinguish the neovessel formation from the inflammatory reaction. For this reasons, this assay is frequently utilized to assess angiogenic activity of chemokines in vivo.

The rabbit corneal assay is performed as firstly described by Gimbrone et al. ***(6)***.

3.2.1. Choice of the Implant

The material under test can be in the form of slow-release pellets incorporating recombinant growth factors, cell suspensions, or tissue samples:

3.2.1.1. Slow-Release Preparations of Purified Factors

Recombinant growth factors are prepared as slow-release pellets by incorporating the protein under test into an ethylene-vinylacetate copolymer (Elvax-40).

1. Elvax-40 has to be carefully prepared by extensive washing of the beads in absolute alcohol, 100-fold, at 37°C, and a casting solution is prepared in methylene chloride and tested for its biocompatibility. This step is critical for avoiding inflammatory reactions.
2. Mix a predetermined volume of Elvax-40 casting solution with a given amount of the compound to be tested on a flat surface.
3. Allow the polymer to dry under a laminar-flow hood.
4. After drying, cut the film sequestering the compound into $1 \times 1 \times 0.5$-mm pellets. Empty pellets of Elvax-40 are used as controls.

3.2.1.2. Cell and Tissue Implants

Trypsinize confluent cell monolayers. Five microliters containing 2×10^5 cells in medium supplemented with 10% serum are used in the corneal micropocket. When the overexpression of growth factors by stable transfection of specific cDNA is studied, one eye is implanted with the wild-type cells and the other with the transfected cells ***(7)***.

When tissue samples are implanted, 2–3 mg samples are obtained by cutting the original fragments under sterile conditions. The angiogenic activity of pathological samples is compared with macroscopically healthy tissues. In order to reduce corneal tension, it is crucial to drain a small amount of the aqueous humor when implanting cells or tissue fragments.

3.2.2. Implantation of the Stimulus

1. Anesthetize the rabbit by intravenous injection of sodium pentothal (30 mg/kg).
2. Surgically produce a micropocket (1.5×3 mm) using the pliable iris spatula in the lower half of the cornea.
3. Position the implant 2.5–3 mm from the limbus to avoid false positives as a result of mechanical procedure and to allow the diffusion of test substances in the tissue, with the formation of a gradient for the endothelial cells of the limbal vessels. Implants sequestering the test materials and the controls are coded and implanted in a double-masked manner.

When two factors are released simultaneously, two independent micropockets are produced in the same cornea ***(8)*** (**Fig. 1B,C**). In other experimental settings,

the corneal tissue can be enriched with one substance and then a second stimulus can be added to test the interference between two different stimuli.

3.2.3. Evaluation and Quantification of Angiogenic Activity

To quantify the assay, subsequent daily observation of the implants is made with a slit-lamp stereomicroscope without anesthesia by an independent operator. Several parameters such as neovascular growth, edema, and cellular infiltration have to be evaluated and recorded with the aid of an ocular grid. An angiogenic response is scored positive when budding of vessels from the limbal plexus occurs after 3–4 d and capillaries progress to reach the implanted pellet in 7–10 d. Implants that do not induce a neovascular growth within 10 d are considered negative, whereas implants showing an inflammatory reaction are discarded.

The potency of angiogenic activity is evaluated on the basis of the number and growth rate of newly formed capillaries, and an angiogenic score is calculated by the formula: Vessel density × Distance from limbus ***(7,8)***. A density value of 1 corresponds to 0–25 vessels per cornea, 2 from 25–50, 3 from 50–75, 4 from 75–100, and 5 for more than 100 vessels. The distance from the limbus is graded in millimeter with the aid of an ocular grid. The number of positive implants over the total implants performed is scored during each observation.

Corneas are removed at the end of the experiment as well as at defined intervals after surgery and/or treatment and fixed in formalin for histological examination. Newly formed vessels and the presence of inflammatory cells are detected by hematoxylin and eosin staining or specific immunohistochemical procedure (i.e., anti-rabbit macrophages [RAM11], anti-CD31 for endothelium) ***(7)***.

3.3. Chick Embryo Chorioallantoic Membrane Assay

The avian chorioallantoic membrane (CAM) is a useful model for studying angiogenesis and antiangiogenesis in vivo ***(9)***. It arises by the fusion of allantois and chorion on d 4 of incubation, and primitive blood vessels begin to take shape. Until d 8 of incubation, primitive vessels continue to proliferate and to differentiate into an arteriovenous system and thus originate a network of capillaries that migrate to occupy an area next to the chorion epithelium and mediate gas exchanges with the outer environment. The CAM vessels show rapid cell proliferation until d 11, after which the rate of proliferation experiences a rapid decline, after which the endothelial cell mitotic index decreases. The vascular system attains its final setup on d 18 of incubation, just before hatching.

1. Incubate fertilized chick eggs at 37°C, under condition of constant humidity.
2. On d 3 of incubation, remove 2–3 mL albumin at the more pointed end of the egg, so that the CAM can be detached from the shell itself.
3. Cut a square window into the shell with the aid of scissors; when this is done, the underlying CAM vessels are exposed.

4. Seal the window with a glass of the same dimension and return the egg to the incubator.
5. On d 8 of incubation, introduce, on the top of growing CAM, the type of implant that is more suitable for your studies. Precisely, these vessels were first used to study tumor angiogenesis by grafting tumors, or fractions of tumors, onto the CAM surface. Alternatively, fluid substance or cell suspensions can be directly inoculated into the cavity of the allantoic vescicle so that their activity covers the whole vascular area in a uniform manner or incorporated in gelatin sponges treated with a stimulator or inhibitor of blood vessel formation in the CAM ***(9,10)***. In the latter case, inert synthetic polymers, similar to those used in the rabbit's cornea and soaked with the macromolecule one wants to test, are laid on the CAM surface. Elvax-40 and hydron are commonly used.
6. Fix the embryos and their membranes *in ovo* in 3% phosphate-buffered glutaraldehyde, dehydrate in serial alcohols, postfix in 1% phosphate-buffered OsO_4, and embed in Epon 812. One-micrometer semithin and ultrathin sections are cut on a ultramicrotome. The semithin sections are stained with a 0.5% aqueous solution of toluidine blue and observed under a light microscope. The ultrathin sections are stained with uranyl acetate, followed by lead citrate, and examined under a transmission electron microscopy.

   Unfixed sponges can be utilized for chemical studies, such as the determination of DNA, protein, and collagen content, as well as for reverse transcription–polyacrylamide gel electrophoresis (RT-PCR) analysis of gene expression by infiltrating cells, including endothelial cells.
7. The angiogenic response can be evaluated as the microvessel area by using a morphometric method of "point counting" ***(10)***. This method allows one to quantify blood vessels, growing vertically into the sponge and at the boundary between the sponge and surrounding CAM mesenchyme. With a double-headed photomicroscope, two investigators simultaneously identify the transversally cut microvessels (diameter ranging from 3 to 10 μm), and each identification is agreed upon in turn. Microvessels are studied at a magnification of ×250 with a square mesh inserted in the eyepiece. The mesh consisted of 12 lines per side, giving 144 intersection points. Six randomly chosen microscopic fields of each section (every third section within 30 serial slides from an individual specimen are analyzed) are evaluated for the total number of intersection points that are occupied by microvessels. For vessel counts, the mean values ± 1 standard deviation are determined for each analysis. The microvessel area is indicated by the final mean number of the occupied intersection points, expressed, again, as the percentage of the total number of intersection points. Statistically significant differences between the mean values of the intersection points in the experimental CAMs and control ones are determined by the Student's *t*-test for unpaired data.

3.3.1. Critical Parameters of the CAM Assay

1. Inflammatory reaction is a major issue for the consideration of the angiogenic effect of chemokines as well as other factors in the CAM assay. A study of histological

CAM sections would help in detecting the possible presence of a perivascular inflammatory infiltrate together with a hyperplastic reaction, if any, of the chorion epithelium. However, the possibilities of causing nonspecific inflammatory response are much lower when the test material is grafted as soon as CAM begins to develop, because the host's immune system is relatively immature.

2. The test material is placed on pre-existing vessels and newly formed blood vessels grown within the CAM mesenchyme. It follows that the actual neovascularization can hardly be distinguished from a falsely increased vascular density because of the rearrangement of pre-existing vessels that follows contraction of the membrane.
3. Timing of the CAM angiogenic response is essential. Many studies determine angiogenesis after 24 h, a time at which there is no angiogenesis—only vasodilatation. It would be worthwhile to point out that measurements of vessel density are really measurements of visible vessel density and that the distinction between vasodilatation and neovascularization is not easy to make. To circumvent this drawback, it is useful to utilize sequential photography to document new vessel formation.

References

1. Jaffe, E. A., Nachman, R. L., Becker, C. G., and Minick, C. R. (1973) Culture of human endothelial cells derived from umbilical veins. Identification by morphologic and immunologic criteria. *J. Clin. Invest.* **52,** 2745–2756.
2. Bachetti, T. and Morbidelli, L. (2000) Endothelial cells in culture: a model for studying vascular functions. *Pharmacol. Res.* **42,** 9–19.
3. Bernardini, G., Spinetti, G., Ribatti, D., et al. (2000) I-309 binds to and activates endothelial cell functions and acts as an angiogenic molecule in vivo. *Blood* **96,** 4039–4045.
4. Hudetz, A. G., Greene, A. S., Feher, G., Knuese, D. E., and Cowley, A. W. Jr. (1993) Imaging system for three-dimensional mapping of cerebrocortical capillary networks in vivo. *Microvasc. Res.* **46,** 293–309.
5. Donovan, D., Brown, N. J., Bishop, E. T., and Lewis, C. E. (2001) Comparison of three in vitro human "angiogenesis" assays with capillaries formed in vivo. *Angiogenesis* **4,** 113–121.
6. Gimbrone, M. A. Jr., Cotran, R. S., Leapman, S. B., and Folkman, J. (1974) Tumor growth and neovascularization: an experimental model using the rabbit cornea. *J. Natl. Cancer Inst.* **52,** 413–427.
7. Ziche, M., Maglione, D., Ribatti, D., et al. (1997) Placenta growth factor-1 is chemotactic, mitogenic, and angiogenic. *Lab. Invest.* **76,** 517–531.
8. Ziche, M., Morbidelli, L., Masini, E., et al. (1994) Nitric oxide mediates angiogenesis in vivo and endothelial cell growth and migration in vitro promoted by substance P. *J. Clin. Invest.* **94,** 2036–2044.
9. Ribatti, D., Vacca, A., Roncali, L., and Dammacco, F. (1996) The chick embryo chorioallantoic membrane as a model for in vivo research on angiogenesis. *Int. J. Dev. Biol.* **40,** 1189–1197.
10. Ribatti, D., Gualandris, A., Bastaki, M., et al. (1997) New model for the study of angiogenesis and antiangiogenesis in the chick embryo chorioallantoic membrane: the gelatin sponge/chorioallantoic membrane assay. *J. Vasc. Res.* **34,** 455–463.

19

Real-Time In Vitro Assay for Studying Chemoattractant-Triggered Leukocyte Transendothelial Migration Under Physiological Flow Conditions

Guy Cinamon and Ronen Alon

1. Introduction

Leukocyte recruitment to inflamed and lymphoid tissues is mediated by sequential adhesive interactions between specialized vascular receptors and their endothelial counterligands ***(1–3)***. Following rolling and arrest on the endothelium, circulating immune cells locomote on and extravasate through the endothelial cell (EC) barrier ***(4–6)***. These steps must be delicately coordinated to allow leukocyte motility while maintaining leukocyte resistance to detachment by the high shear forces constantly exerted at the vessel wall. The key signals, which trigger leukocyte arrest on endothelial integrin ligands, are elicited by chemokines, presented on the apical surface of the endothelial lining at sites of leukocyte diapedesis ***(7–9)***. Recent observations from our lab ***(10)*** as well as from other labs ***(11–13)*** have pointed out that shear forces may transduce, together with endothelial chemokines, potent promigratory signals to adherent leukocytes at endothelial interfaces. These studies suggest that in vitro transendothelial migration (TEM) model systems should incorporate both the physiological blood flow conditions and chemokine presentation profiles that exist at sites of leukocyte emigration in the vasculature.

Traditional transwell Boyden chamber assays are performed in shear-free conditions and assess slow cell migration processes across chemotactic gradients established across various endothelial barriers ***(14,15)***. These assays therefore appear inadequate for in vitro characterization of TEM processes in the circulation but may represent cell migration across nonendothelial cellular barriers under shear-free conditions. Here, we describe an alternative real-time assay to study cell TEM in vitro. The assay is conducted in a parallel-plate flow chamber setup simulating physiological shear flow conditions and monitors leukocyte

From: *Methods in Molecular Biology, vol. 239: Cell Migration in Inflammation and Immunity*
Edited by: D. D'Ambrosio and F. Sinigaglia

interactions with defined endothelial barriers reconstituted with apical chemokines. Video-recorded segments are analyzed off-line either manually or by computerized cell tracking ***(16)***. This assay allows the resolution of separate steps in the adhesive and migratory cascades of leukocyte subsets interacting with differently treated endothelial monolayers under defined shear flow conditions. Both morphological changes and detailed motion patterns of all leukocytes adhered to the endothelial monolayer are monitored at a single-cell level in the field of view. This system can be used to test how specific chemokines or chemoattractants stably overlaid on apical surfaces of the endothelial cell monolayer, in defined compositions, promote migration of leukocyte populations on and across the monolayer (*see* **Notes 1–3**).

2. Materials

1. Human umbilical vein endothelial cells (HUVEC, primary culture, two to four passages, 1:3 split ratio).
2. HUVEC culture medium: M-199 (Sigma; cat. no. M-4530) supplemented with 10% lipopolysaccharide (LPS)-free fetal calf serum (FCS), penicillin (100 ng/mL), streptomycin (100 U/mL), endothelial mitogen (25 µg/mL) (Biomedical Technologies Inc., Stoughton, MA; cat. no. BT-203), and porcine heparin (5 U/mL) (Sigma; cat. no. 3393).
3. Human plasma fibronectin (FN) (Sigma; cat. no. F-2006) dissolved in sterile phosphate-buffered saline (PBS) at 20 µg/mL.
4. Petri polystyrene dishes, 60 × 15 mm (Falcon; Becton Dickinson; cat. no. 351007).
5. Trypsin–EDTA solution (Sigma; cat. no. 03-053-1B).
6. Recombinant human tumor necrosis factor-α (TNF-α) (2 ng/mL) (R&D Systems, Minneapolis, MN; cat. no. 210-TA).
7. Human T-lymphocytes isolated from whole blood and cultured overnight in RPMI 1640 (Sigma; cat. no. R-8758) supplemented with 10% LPS-free FCS, penicillin (100 ng/mL), streptomycin (100 U/mL), L-glutamine (2 m*M*), and sodium pyruvate (1 m*M*).
8. Cell-binding medium: Cation-free Hank's balanced salt solution (HBSS) (Sigma; cat. no. H-2387) supplemented with 10 m*M* HEPES, pH 7.4, containing 2 mg/mL of bovine serum albumin (BSA) and 1 m*M* of Ca^{2+} and Mg^{2+}. The medium is kept at 37°C throughout the assay.
9. Human recombinant stromal cell-derived factor-1α (SDF-1, CXCL12, 100 ng/mL), or EBI-1 molecular ligand chemokine (ELC, CCL19, 1 µg/mL) (both from R&D), dissolved in binding medium (*see also* **Notes 4** and **5**).
10. Inverted microscope with ×20 phase-contrast objectives (Diaphot 300; Nikon, Japan) (*see also* **Note 6**) connected to a high-resolution CCD video camera (LIS-700; Applitech, Israel), a time-lapse SVHS video recorder (AG-6730, Panasonic, Japan), and a monitor (Sony). The system is kept at 35–37°C.
11. Parallel-plate flow chamber kit (gasket thickness 0.01 in., channel width 2.5 mm, 1/16-in. tubes; GlycoTech, Rockville, MD; cat. no. 31-003) connected to an auto-

mated syringe pump (Harvard Apparatus, Natick, MA) and a vacuum pump (Master-Flex; Cole-Palmer Instrument Co., Niles, IL, (*see also* **Fig. 1**).
12. Disposable 1.5-mL test tubes, disposable 10-mL plastic syringe without a needle, 30-mL glass syringe greased with vacuum silicon grease (Beckman, Palo Alto, CA; cat. no. 335148) and connected to a three-way Luer-lock (Sigma).
13. EDTA washing solution (10 m*M* in PBS, pH 7.4).

3. Methods

The assay is composed of three parts:

1. Preparation of the HUVEC monolayers.
2. The flow chamber TEM assay.
3. Analysis and quantification of video-recorded segments. The assay is described primarily for human lymphocyte migration across inflamed human endothelial monolayers. However, this assay can be readily modified to follow other human or animal leukocytes and corresponding EC barriers (*see* **Notes 3** and **5**).

3.1. Prior Experimental Preparations

The HUVECs should be plated on Petri dishes at least 24 h prior to the planned experiment. This allows the cells to form a confluent monolayer and acquire, upon cytokine activation (*see* **Subheading 3.1.5.**) the adhesion and junctional molecule repertoire found on inflamed endothelial cells. Each migration assay is performed on a separate HUVEC-containing dish.

1. Spot a 10 µL drop of FN (*see* **Subheading 2., item 3**) in the center of the dish under sterile conditions and incubate at 37°C for 1 h.
2. Wash the spot three times with 15 µL PBS (sterile). Avoid dehydration.
3. Harvest HUVEC from a long-term tissue culture plate by standard trypsinization. Collect cells by gentle pipetting, suspend in HUVEC medium and centrifuge (300*g* for 4 min). Resuspend cell pellet in HUVEC medium, count cells, and adjust volume to reach final concentration of 3×10^6 cells/mL.
4. Add a 15-µL drop of HUVEC on the FN spot and incubate for 45 min in a humidified incubator. This procedure is aimed at minimizing the quantities of seeded ECs. We have also found out that the chamber attaches more tightly to unseeded areas of the Petri dish, thereby keeping a better vacuum sealing of the chamber (*see* **Subheading 3.2.**).
5. Add 3 mL of HUVEC medium to the plate and incubate for 24 h with TNF-α-supplemented or control medium.

3.2. Transendothelial Migration Assay Under Shear Flow

1. Place the lower part of a test Petri dish on the microscope stage (*see* **Fig. 1**). Place the flow chamber in the dish. Connect the inlet hole of the chamber through the inlet tube to a 50-mL reservoir tube filled with binding medium. Attach the outlet

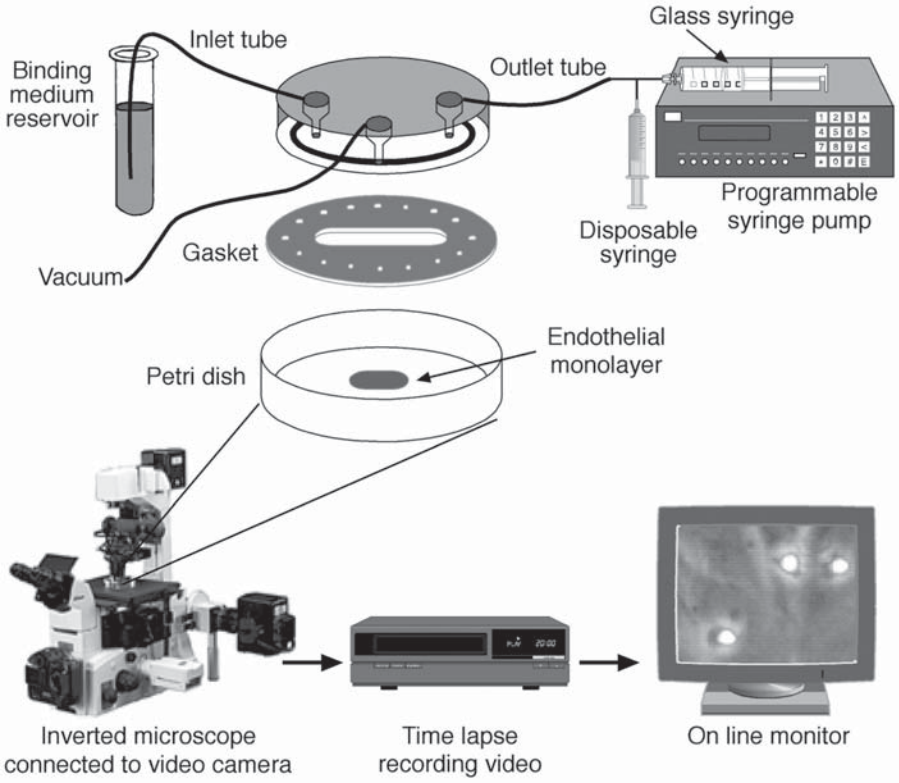

Fig. 1. Scheme of the flow chamber setup. Note that individual items are not drawn to scale. (Reprinted with permission from **ref. *21***.)

tube to a three-way Leur-lock that is connected to the glass syringe of the automated pump. Connect a 10-mL disposable syringe to the third end of the lock. Use this syringe to manually pump binding medium through the system. Connect the vacuum pump to the vacuum outlet of the chamber. Pump binding medium throughout the system. Ensure that the vacuum tightly seals the chamber to the dish. Refer to **Fig. 1** for further clarifications.

2. Disconnect the vacuum and remove the test dish. Place a new dish plated with a HUVEC monolayer on the microscope stage. Locate a field of view on the monolayer. The field should be confluent and placed near the edge of the monolayer to minimize leukocytes rolling or crawling into the field of view from upstream fields not recorded by the videocamera (*see* **Subheading 3.3.**).
3. Place the flow chamber on the coated monolayer. Connect the chamber to the vacuum pump and ensure that the chamber is tightly sealed to the dish. Make sure that no air bubbles are introduced through the chamber. Any air perfused over the HUVEC monolayer will irreversibly damage it. Use the disposable syringe (*see* **Fig. 1**) to wash the monolayer with binding medium.

4. To absorb a chemokine of interest on the HUVEC monolayer, perfuse 200 µL of chemokine-containing binding medium using the disposable syringe. Let the entire volume of chemokine enter the chamber and keep air out. Incubate for 5 min. Use the disposable syringe to collect back the unbound chemokine by backpumping the chemokine-containing medium in the reverse direction, so that it is completely discarded from the system. Return the inlet tube to the binding medium reservoir and extensively wash the system to remove any traces of unbound chemokine.
5. Place 1×10^6 of cultured lymphocytes in a 1.5-mL tube and mix with an equal volume of EDTA solution to remove cell-bound integrin ligands. Centrifuge cells (400*g* for 4 min) and resuspend pellet in 50 µL binding medium. Pump in the lymphocyte suspension until the entire volume enters the inlet tube (*see* **Fig. 1**). Return the tube to the 50-mL binding-medium-containing reservoir tube. Ensure that no air bubbles enter the inlet tube during this manipulation.
6. Set the automated pump to provide a constant shear flow of 5 dyn/cm^2 for the required time period. Start video recording in real-time mode. Once the cell flux enters the field of view, pause the pump and immediately set it to the program mode and activate the program (*see* **Note 7**). Record the migration phase (*see* **Note 4**) at 1 frame/s.

3.3. Analysis and Quantification of Interacting Cells

1. Motion analysis is performed manually on all cells interacting with the endothelial monolayer in the microscopic field of view. Lymphocytes are individually tracked from their site of interaction with the endothelial surface at the end of the accumulation phase and throughout the migration phase (*see* **Fig. 2**). Only leukocytes that have accumulated in the field of view during the accumulation phase are analyzed. Lymphocytes entering the field of view from upstream fields or crawling out of the field to downstream fields, as well as lymphocytes captured to the EC during the migration phase, are not included in the analysis.
2. Four distinct categories of accumulating lymphocytes are defined in this analysis (*see* **Fig. 2**): (1) Lymphocytes that roll away or detach from the ECs during the migration phase are considered detaching; (2) lymphocytes that remain stationary throughout the migration phase, or locomote less than their diameter, are considered arrested; (3) lymphocytes that spread and migrate over the EC surface throughout the assay without crossing the EC barrier are considered locomoting. (4) Lymphocytes that migrate for variable distances on the ECs and eventually transmigrate through the monolayer are considered transmigrating. Because lymphocytes (and other leukocytes) may turn dark and falsely counted as transmigrating cells, only lymphocytes that undergo stepwise darkening of their leading edge and retain their dark images while locomoting underneath the ECs are considered transmigrating cells.
3. The different categories are recorded as a percentage of the originally accumulated lymphocytes.
4. To evaluate transmigration kinetics, the time that elapses from the beginning of the migration phase until the completion of a TEM process of an individual leukocyte

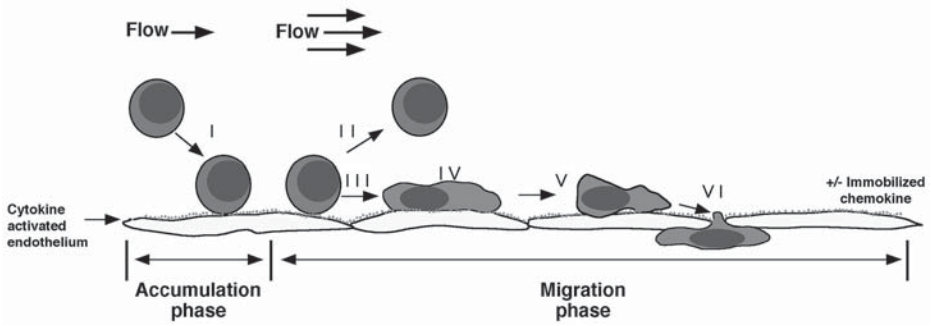

Fig. 2. Analysis of leukocyte TEM under physiological shear flow in a parallel-plate flow chamber assay. This assay analyzes separate steps in the migratory cascade of leukocytes interacting with a cytokine-activated EC monolayer under shear flow, in the presence of chemokines reconstituted on the apical surface of the monolayer. To allow leukocytes to accumulate on the monolayer, leukocytes are perfused at low physiological shear flow (accumulation phase, recorded by real-time videomicroscopy). The flow is then increased to higher rates, generating shear stresses of interest and kept constant throughout the assay (migration phase, recorded in time-lapse videomicroscopy). Motion analysis is performed manually on all adherent cells from their initial point of capture onto the endothelial surface (I) and throughout the entire assay period. Both the morphological changes and migratory patterns of the leukocytes adhering to the endothelial monolayers are monitored at a single cell level. The indicated steps (I–VI) are monitored: (I) rolling and arrest; (II) detachment from original adhesion site; (III) spreading; (IV) firm stationary adhesion; (V) locomotion over the EC; (VI) transmigration through the EC. (Reprinted from **ref. *21*** with permission from Elsevier Science.)

is recorded for each transmigrating leukocyte. The accumulative number of transmigrating leukocytes at a given time-point is expressed as a fraction of the accumulated leukocytes in the beginning of the migration phase. Other parameters such as crossing time through the EC barrier and migration velocities over and beneath the ECs can also be determined (*see* **Note 8**).

5. Although the number of lymphocytes entering the system is kept fixed for all experiments, their distribution within the leukocyte flux and, hence, the fraction of lymphocytes making direct contact with the endothelium-coated plate can vary considerably. Therefore, it is recommended to enumerate only lymphocytes in the plane of view closest to the endothelial barrier.

4. Notes

1. Lymphocyte TEM also depends on both the basal and junctional adhesive and chemotactic information of the endothelial barrier. It is, therefore, essential to define the background TEM capacity of a given lymphocyte or leukocyte population before exogenously introducing the chemoattractant of interest on the endothelial barrier. This background activity can vary with cell donor and passage and should be carefully taken into consideration when performing the TEM experiments. ECs

might, for example, present, on both their basal and apical surfaces, a variety of endogenous chemokines upon inflammatory stimulation. Although TNF-α-activated HUVECs do not produce and immobilize major T-cell chemokines on their surface, they readily produce and present other proadhesive and promigratory chemokines such as Groα (CXCL1) and MCP-1 (CCL2) ***(11)***. These mediators might induce monocyte and neutrophil TEM even under shear-free conditions ***(11,12)***. These leukocytes may use both apical and sublumenal chemokine pools for their TEM with variable dependence on shear forces.

2. The main limitation of the assay is the inability to manipulate either the leukocyte or the endothelial cell populations assayed in the system with reversible pharmacological reagents (e.g., by pretreatment of either the leukocyte or the EC with inhibitors to signaling kinases or cytoskeletal drugs) because of the extensive washing conditions existing in the flow chamber throughout the assay ***(17,20)***. A continuous infusion of the inhibitor through the binding medium is generally not advisable. Genetic manipulation of cells (e.g., transient or stable transfection) is an appropriate solution for this experimental limitation.
3. Endothelial cell lines constructed with defined adhesion molecules, chemokines, or junctional components might be used in this assay to evaluate the role of these molecules in leukocyte TEM under shear flow conditions. Nonendothelial cells might also be used as control cell barriers.
4. Lymphocyte TEM not only depends on the type of chemokine but also on its dose. We could show that low-level SDF-1 or ELC sufficient for triggering rapid integrin-mediated adhesion strengthening of accumulated lymphocytes was insufficient to trigger their subsequent TEM. Thus, two distinct thresholds of EC-bound chemokine, one for adhesion and a higher one for TEM, can be defined ***(17)***. Different chemokines might induce TEM at different concentrations because of differences in efficacy of immobilization on the endothelial surface. For example, SDF-1 could induce maximal lymphocyte TEM at 100 ng/mL, whereas ELC had a similar effect only at concentration of 1 μg/mL. Notably, not all chemokines adsorbed to the HUVEC monolayers at sufficient levels or stability to promote lymphocyte adhesion or TEM. SLC (CCL21), a coligand to the CCR7 receptor, the major receptor for ELC on resting T-lymphocytes, only weakly adsorbed to the HUVEC monolayers. Other chemokines for resting or activated T-cells such as IP-10 (CXCL10), MIP-1β (CCL4), and RANTES (CCL5) bound transiently to the HUVEC but were readily washed out during the early phases of the migration assay and could not be assessed for their TEM potential.
5. Although the assay described here is designed to study lymphocyte TEM across cytokine-activated HUVEC, it can be modified and used to monitor real-time TEM of other leukocytes and endothelial cells under any inflammatory stimulatory condition of interest. For example, Cuvelier et al. took a similar approach to study eosinophil migration across interleukin (IL)-4 activated HUVEC in vitro ***(13)***. Interestingly, shear-promoted eosinophil TEM was mediated by an eosinophil-specific endothelial chemokine, eotaxin (CCL11), that was endogenously produced and apically displayed by IL-4-treated HUVEC.

6. Normally, a ×20 phase contrast objective is used for all microscopic recordings. The optical properties of the lens and the microscope condenser should be optimized to provide proper phase-contrast images of leukocytes such that bright images of leukocytes positioned on the apical side of the endothelial layer can be readily distinguished from the dark images of leukocytes positioned at the basal side of the monolayer. The ×20 magnification also allows tracking both motion and morphological changes (*see* **Subheading 3.3.**) of a reasonable number of leukocytes, 40–80 in a typical field of view. CCD cameras with a particularly large recording area are advisable.
7. The automated pump program used to study lymphocyte TEM is set to provide a shear stress of 0.75 dyn/cm^2 for 40 s (accumulation phase; *see* **Fig. 2**) and then a mid-range physiological shear stress of 5 dyn/cm^2 for an additional 15-min period (migration phase; *see* **Fig. 2**). The geometry of the flow chamber does not allow lymphocytes to accumulate on adhesive endothelial surfaces at this shear stress, but once accumulated, lymphocytes remain adhesive and shear resistant for prolonged periods at a very broad range of shear flow rates. For control experiments, the flow can be stopped after the short accumulation phase, and lymphocyte motion can be monitored for 15 min under shear-free conditions. The accumulation phase is required to select a representative fraction of adhesive lymphocytes within the heterogenous T-cell preparation. Accumulation of lymphocytes conducted at a too high shear flow might bias the system toward highly activated subsets and should be avoided.
8. The assay can be adapted for immunostaining of leukocytes or ECs by confocal microscopy. The Petri dishes should be replaced by glass cover slips with a diameter that exceeds the chamber size to allow proper vacuum sealing of the chamber. Cover slips (40 mm) from Bioptechs (Butler, PA; cat. no. 40-1313-0319) are recommended. The cover slips should be sterilized by autoclave or ethanol wash. Each slide is placed in a sterile Petri dish, coated with FN, seeded with endothelial cells and activated as described in **Subheading 3.**). The chamber is mounted on the endothelial-coated cover slip and connected to the vacuum source. A fixative solution should be infused through the chamber at desired time-points during the TEM assay. This is achieved by transferring the inlet tube from the binding medium reservoir to a test tube containing the fixative (e.g., 3% paraformaldehyde). Once the perfused fixative reaches the chamber, the flow can be halted and the fixative is left for an additional 5-min incubation. The chamber is then disconnected from the vacuum and carefully separated from the cover slip that is taken for further processing. The chamber must be extensively washed from all traces of fixative before the following run. If the fixation is to be performed under shear-free conditions or if the fixative is highly toxic (e.g., gluteraldehyde), the assay must be stopped, the chamber quickly and carefully removed, and the cover slip immediately incubated with the fixative. Immunostaining can be proceeded according to a standard staining protocol. The same method can be used for electron microscopy analysis of samples ***(17)***. For real-time fluorescence imaging of leukocyte TEM under shear flow using a similar setup, please refer to **refs. 18** and **19**.

References

1. Springer, T. A. (1994) Traffic signals for lymphocyte recirculation and leukocyte emigration: The multistep paradigm. *Cell* **76,** 301–314.
2. Butcher, E. C. and Picker, L. J. (1996) Lymphocyte homing and homeostasis. *Science* **272,** 60–66.
3. Campbell, J. J. and Butcher, E. C. (2000) Chemokines in tissue-specific and microenvironment-specific lymphocyte homing. *Curr. Opin. Immunol.* **12,** 336–341.
4. Bianchi, E., Bender, J. R., Blasi, F., and Pardi, R. (1997) Through and beyond the wall: late steps in leukocyte transendothelial migration. *Immunol. Today* **18,** 586–591.
5. Johnson-Leger, C., Aurrand-Lions, M., and Imhof, B. A. (2000) The parting of the endothelium: miracle, or simply a junctional affair? *J. Cell. Sci.* **113,** 921–933.
6. Worthylake, R. A. and Burridge, K. (2001) Leukocyte transendothelial migration: orchestrating the underlying molecular machinery. *Curr. Opin. Cell. Biol.* **13,** 569–577.
7. Middleton, J., Neil, S., Wintle, J., et al. (1997) Transcytosis and surface presentation of IL-8 by venular endothelial cells. *Cell* **91,** 385–395.
8. Peled, A., Grabovsky, V., Habler, L., et al. (1999) The chemokine SDF-1 stimulates integrin-mediated arrest of $CD34^+$ cells on vascular endothelium under shear flow. *J. Clin. Invest.* **104,** 1199–1211.
9. Stein, J. V., Rot, A., Luo, Y., et al. (2000) The CC chemokine thymus-derived chemotactic agent 4 (TCA-4, secondary lymphoid tissue chemokine, 6Ckine, Exodus-2) triggers lymphocyte function-associated antigen 1-mediated arrest of rolling T lymphocytes in peripheral lymph node high endothelial venules. *J. Exp. Med.* **191,** 61–76.
10. Cinamon, G., Grabovsky, V., Winter, E., et al. (2001) Novel chemokine functions in lymphocyte migration through vascular endothelium under shear flow. *J. Leukocyte Biol.* **69,** 860–866.
11. Weber, K. S., von Hundelshausen, P., Clark-Lewis, I., Weber, P. C., and Weber, C. (1999) Differential immobilization and hierarchical involvement of chemokines in monocyte arrest and transmigration on inflamed endothelium in shear flow. *Eur. J. Immunol.* **29,** 700–712.
12. Kitayama, J., Hidemura, A., Saito, H., and Nagawa, H. (2000) Shear stress affects migration behavior of polymorphonuclear cells arrested on endothelium. *Cell. Immunol.* **203,** 39–46.
13. Cuvelier, S. L. and Patel, K. D. (2001) Shear-dependent eosinophil transmigration on interleukin 4-stimulated endothelial cells: a role for endothelium-associated eotaxin-3. *J. Exp. Med.* **194,** 1699–1709.
14. Roth, S. J., Carr, M. W., Rose, S. S., and Springer, T. A. (1995) Characterization of transendothelial chemotaxis of T lymphocytes. *J. Immunol. Methods* **188,** 97–116.
15. Ding, Z., Xiong, K., and Issekutz, T. B. (2000) Regulation of chemokine-induced transendothelial migration of T lymphocytes by endothelial activation: differential effects on naive and memory T cells. *J. Leukocyte Biol.* **67,** 825–833.

16. Franitza, S., Alon, R., and Lider, O. (1999) Real-time analysis of integrin-mediated chemotactic migration of T lymphocytes within 3-D extracellular matrix-like gels. *J. Immunol. Methods* **225,** 9–25.
17. Cinamon, G., Shinder, V., and Alon, R. (2001) Wall shear forces promote lymphocyte migration across inflamed vascular endothelium presenting apical chemokines. *Nature Immunol.* **2,** 515–522.
18. Shaw, S. K., Bamba, P. S., Perkins, B. N., and Luscinskas, F. W. (2001) Real-time imaging of vascular endothelial-cadherin during leukocyte transmigration across endothelium. *J. Immunol.* **167,** 2323–2330.
19. Barreiro, O., Yanez-Mo, M., Serrador, J. M., et al. (2002) Dynamic interaction of VCAM-1 and ICAM-1 with moesin and ezrin in a novel endothelial docking structure for adherent leukocytes. *J. Cell. Biol.* **157,** 1233–1245.
20. Kuijpers, T. W., Hoogerwerf, M., and Roos, D. (1992) Neutrophil migration across monolayers of resting or cytokine-activated endothelial cells. Role of intra-cellular calcium changes and fusion of specific granules with the plasma membrane. *J. Immunol.* **148,** 72–77.
21. Cinamon, G. and Alon, R. (2003) A real time in vitro assay for studying leukocyte transendothelial migration under physiological flow conditions. *J. Immunol. Methods* **273,** 53–62.

20

Generation of Monoclonal Antibodies Against Chemokine Receptors

Leonor Kremer and Gabriel Márquez

1. Introduction

Chemokines are a family of structurally related, small chemoattractant proteins that interact with specific seven-transmembrane, G-protein-coupled receptors that mediate cell migration in chemotactic gradients ***(1,2)***. Chemokine-receptor expression is finely regulated during leukocyte differentiation, maturation, and activation, causing each cell subpopulation to express a specific set of chemokine receptors. Although they were initially considered as simple leukocyte chemoattractants, chemokines are now known to be implicated in diverse phases of the immune response, and their significance is becoming apparent in many areas of biomedicine, including cancer, human immunodeficiency virus (HIV)-1 infection, asthma, and cardiovascular disease ***(3)***. This has greatly increased interest in studying how chemokines exert their activities at the molecular level, which obviously requires specific reagents. Monoclonal antibodies (mAbs) that recognize chemokines or chemokine receptors are among the most useful tools for this purpose, particularly for cell expression and neutralization studies.

The production of specific anti-chemokine-receptor antibodies is a difficult task, because of their integral membrane structure and the sequence similarity among the members of this protein family. Recognition of extracellular receptor domains is necessary for most experimental approaches, but typically less than 30% of the protein (the average length is approx 360 amino acids) is exposed at the cell surface, separated into four regions: the N-terminal (approx 30–50 amino acids) and three extracellular domains, each of approx 10–30 amino acids. These extracellular domains adopt a tertiary structure stabilized by disulfide bonds and are frequently postranslationally modified by *N*- and *O*-glycosylation and/or tyrosine sulfation. Thus, the use as immunogens of synthetic peptides based on the amino acid sequence of these regions does not guarantee generation of appropriate antibodies against the extracellular chemokine-receptor domains.

From: *Methods in Molecular Biology, vol. 239: Cell Migration in Inflammation and Immunity*
Edited by: D. D'Ambrosio and F. Sinigaglia

Because murine models of many human diseases are widely used, it would be quite convenient to have chemokine and/or chemokine-receptor blocking mAbs to study the contribution of these proteins to different pathologies. The production of anti-mouse chemokine-receptor mAbs is, nonetheless, an especially demanding challenge. Current technology uses myeloma lines of rodent origin, and both the close phylogenetic origin and the constitutive presence of circulating chemokine-receptor-expressing cells in rats and hamsters severely hinder the development of a strong immune response when these animals are immunized with mouse antigens. In consequence, antibodies against murine chemokine receptors are very scarce, despite the time that has passed since their amino acid sequences were first reported.

Here, we describe a general methodology for the generation of mAbs against chemokine receptors, including the preparation of synthetic peptides and transfectant cells expressing the receptor of interest to be used as immunogens, fusion protocols, as well as strategies for screening positive hybridomas and selecting blocking mAbs. The strategy followed to generate an anti-mouse CCR8 blocking mAb will be used as an example to illustrate a general approach to the generation and characterization of mAbs against murine chemokine receptors.

2. Materials

2.1. Facilities and General Equipment

1. Pathogen-free animal facilities.
2. Standard cell culture facilities, with laminar hoods (Bio-II-A; Telstar, Terrassa, Spain), freezers (−20°C and −80°C) (Sanyo Electric Biomedical Co, Osaka, Japan), humidified CO_2 incubators (Stericult 200, Forma Scientific, Marietta, OH, USA), inverted microscopes (Leitz, Wetzlar, Germany), and bench-top centrifuge (Heraeus Instruments, Hanau, Germany).
3. Liquid-nitrogen storage containers (Air Liquide, Paris, France).
4. Enzyme-linked immunosorbent assay (ELISA) plate reader (Titertek multiscan MCC/340; Flow Lab, McLean, VA, USA).
5. Flow cytometer (EPICS XL; Coulter, Palo Alto, CA, USA).
6. Spectrofluorimeter (SLM-8000C).
7. Electroporator (Gene pulser II, BIORAD, Hercules, CA, USA).

2.2. Animals

1. Lou rats (Charles River Laboratories, Roven, France).
2. BALB/c mice (Charles River).

2.3. Cell Lines

The following cell lines are cultured at 37°C in a humidified 5% CO_2 atmosphere, using the cell growth medium specified.

1. The murine myeloma P3X63Ag8.653 (ATCC CRL-1580), derived from the BALB/c mineral oil-generated plasmacytoma MOPC 21, can be obtained from the American Type Culture Collection (ATCC, Manassas, VA, USA). The cells are cultured in RPMI 1640 complete medium.
2. The rat hybridoma clone YB2/O (ATCC CRL-1662), derived from a cell fusion between a Lou myeloma and AO spleen cells, can also be obtained from the ATCC. Cells are cultured in Dulbecco's modified Eagle's medium (DMEM) complete medium.
3. Murine interleukin (IL)-3-dependent Ba/F3 cells were obtained from Dr. D. Milligan (Arris Pharmaceuticals, San Francisco, CA, USA). These cells are cultured in RPMI 1640 complete medium, supplemented with 10% conditioned medium from the IL-3-producing cell line WEHI-3B.
4. The mouse thymic lymphoma line BW5147.3 (ATCC TIB-47) cells can be obtained from the ATCC. Cells can be grown in RPMI 1640 complete medium.
5. The human embryonic kidney cell line (HEK) 293 (ATCC CRL-1573) was obtained from the ATCC. These cells are cultured in DMEM complete medium.

2.4. Cell Culture

1. Tissue culture flasks (5, 25, and 125 cm^2; Costar, Cambridge, MA, USA).
2. Flat-bottom tissue culture plates (24 and 96 wells, Costar).
3. Tissue culture Petri dishes (60 mm) (Costar).
4. Conical centrifuge tubes (15 and 50 mL) (Costar).
5. DMEM with 4.5 g/L glucose (BioWhittaker, Verviers, Belgium).
6. RPMI 1640 (BioWhittaker).
7. Clonacell™ H, medium E: Hybridoma growth medium (StemCell Technologies Inc, Vancouver, BC, Canada).
8. Fetal calf serum (FCS) (Sigma Chemical Co., St. Louis, MO, USA).
9. 1 *M* HEPES, pH 7.4 (Sigma).
10. 100 m*M* Sodium pyruvate (Sigma).
11. 200 m*M* L-glutamine (BioWhittaker).
12. 10,000 U/mL Penicillin–streptomycin (BioWhittaker).
13. Dimethyl sulfoxide (DMSO) (Sigma).
14. Trypan blue (Sigma).
15. Ammonium chloride (Sigma).
16. Azaserine (Sigma).
17. Hypoxanthine (Sigma).
18. Polyethylene glycol (PEG 4000, Merck, West Point, PA, USA).
19. Neomycin (G418, Sigma).

2.5. Immunization

1. Syringes (1, 2, and 5 mL) (Discardit; Becton Dickinson, Franklin Lakes, NJ, USA).
2. 19-, 23-, and 25-G needles (Microlance; Becton Dickinson).
3. Heparinized capillary tubes (Propper Manufacturing Co., Long Island City, NY, USA).

4. Keyhole limpet hemocyanin (KLH, Sigma).
5. Complete Freund's adjuvant (Sigma).
6. Incomplete Freund's adjuvant (Sigma).
7. 2,6,10,14-Tetramethylpentadecane (Pristane, Sigma).
8. Glutaraldehyde (Sigma).
9. 4-(Maleidomethyl)-cyclohexane-1-carboxylic acid (Pierce, Rockford, IL, USA).
10. *N*-Hydroxysuccinimide ester (Pierce).
11. Surgical instruments (scissors, forceps).

2.6. Monoclonal Antibody Characterization and Screening Assays

1. Polystyrene 96-well microtiter plates (Maxisorb; Nunc, Copenhagen, Denmark).
2. Carbonate buffer: 50 m*M* sodium carbonate, pH 9.0 (Sigma).
3. Bovine serum albumin (BSA) (Fraction V; Sigma).
4. Peroxidase-labeled rabbit anti-rat immunoglobulins (DAKO A/S, Glostrup, Denmark).
5. Streptavidin–horseradish peroxidase (HRPO) (Sigma).
6. *O*-Phenylenediamine dihydrochloride (OPD) (Sigma).
7. 0.15 *M* Sodium citrate, pH 5.0 (Sigma).
8. Hydrogen peroxide, 30% (w/w).
9. Sulfuric acid (Merck).
10. Recombinant chemokines (PharMingen, San Diego, CA, USA; R&D Systems, Minneapolis, MN, USA).
11. SFLLR-amide (Bachem, Torrence, CA, USA).
12. Transwell inserts, 5-μm pore diameter (Costar).
13. Polyvinyl pyrrolidone-free filters with 10-μm pore (Poretics; Osmonics, Livermore, CA, USA).
14. Mouse immunoglobulins (Sigma).
15. Fluorescein isothiocyanate (FITC)-labeled goat anti-rat immunoglobulins, mouse adsorbed (Southern Biotechnology, Birmingham, AL, USA).
16. R-Phycoerythrin (PE)-labeled goat anti-rat immunoglobulins, mouse adsorbed (Southern Biotechnology).

2.7. mAb Purification and Labeling

1. Ammonium sulfate (Sigma).
2. Sulfo-NHS-LC-biotin (Pierce, Rockford, IL, USA).
3. *N*-Hydroxysuccinimidobiotin (Sigma).
4. Protein-A- and Protein-G-coupled Sepharose (Amersham Pharmacia Biotech, Cerdanyola, Spain).
5. Rat isotyping kit (ICN Pharmaceuticals, Costa Mesa, CA, USA).

2.8. Reagents and Solutions

1. Complete media: DMEM or RPMI 1640 medium, supplemented with 10% FCS, 2 m*M* L-glutamine, 1 m*M* sodium pyruvate, 10 m*M* HEPES, pH 7.4, and antibiotics.

2. Selection media:
   a. DMEM supplemented with 20% FCS, 2 m*M* L-glutamine, 1 m*M* sodium pyruvate, 10 m*M* HEPES, pH 7.4, 0.1 m*M* hypoxanthine, and 10 μ*M* azaserine.
   b. Clonacell™ H, medium E supplemented with 10 μ*M* azaserine.
3. Phosphate-buffered saline (PBS): 10 m*M* Sodium phosphate, pH 7.4, 150 m*M* sodium chloride.
4. Staining PBS (sPBS): PBS containing 2% BSA, 2% FCS, and 0.05% sodium azide. Store at 4°C.

3. Methods

3.1. Preparation of Synthetic Peptides

Synthetic peptides can be used to generate antibodies when the native protein is not available or is difficult to purify in its native conformation, as is the case of the membrane-embedded chemokine receptors. The immunizing peptides normally correspond to the hydrophilic regions of the receptors (i.e., the N-terminal region and the extracellular domains) (*see* **Notes 1** and **2**).

Mouse CCR8 is a 353-amino-acid chemokine receptor (*see* **Fig. 1**). One of the approaches we followed to generate mAbs specific for this chemokine receptor used peptides as immunogens. We synthesized peptides covering almost the entire exposed extracellular sequence of murine CCR8; peptides corresponded to N-terminal domain residues 2–21 and 9–36, peptides 170–181 and 181–197 represented the second extracellular loop, and peptides 259–277 were based on the third extracellular domain (*see* **Fig. 1**). Peptides can be obtained from different commercial sources, but in the case of mouse CCR8 peptides, they were synthesized in-house in the solid phase using standard Fmoc chemistry ***(4)*** in a multiple-peptide synthesizer (Abimed, Langefeld, Germany). Peptides were then purified by high-performance liquid chromatography (HPLC) (Waters, Millipore Corporation, Bedford, MA, USA) and analyzed by mass spectrometry. Finally, they were KLH-coupled using either the two-step glutaraldehyde method or the heterobifunctional reagent 4-(maleidomethyl)-cyclohexane-1-carboxylic acid *N*-hydroxysuccinimide ester ***(5)***.

3.2. Generation of Stable Transfectant Cell Lines Expressing mCCR8

Transfectant cells expressing the desired receptor can be used as immunogens to generate antibodies specific for that protein. The probability of obtaining appropriate antibodies depends on the number of receptor molecules expressed by the transfectant cells and the degree of identity in the receptor amino acid sequences between the immunizing and the immunized species. To prepare a transfectant cell line expressing the chemokine receptor, the cDNA encoding this receptor is cloned in an expression plasmid, which is then transfected into

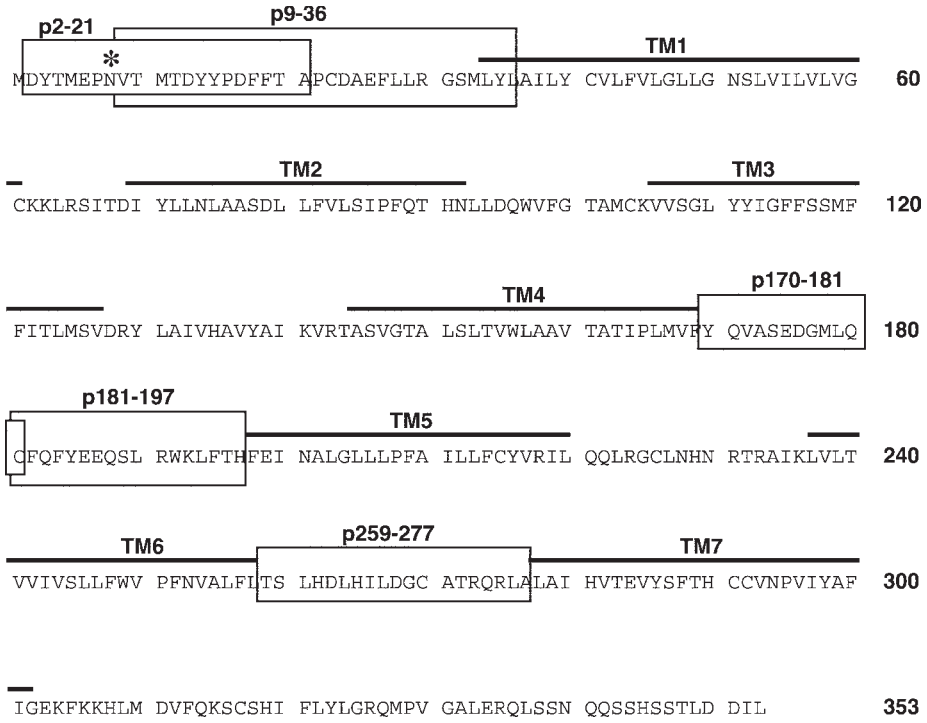

Fig. 1. Amino acid sequence of mouse CCR8. Predicted transmembrane domains (TM) are marked with bold lines. The amino acid sequences of the peptides used for immunization are boxed. The potential *N*-glycosylation site at N8 is marked with an asterisk.

an appropriate host cell line. To maximize the immune response against the chemokine receptor and diminish recognition of other cell surface determinants, it is advantageous that the host cell and the animal to be immunized are syngeneic.

3.2.1. Plasmid Construction

Regarding mouse CCR8, its cDNA was cloned by standard molecular-biology procedures and inserted into the pCIneo expression vector (Promega Corp., Madison, WI, USA), which contains the neomycin (G418)-selectable drug marker. In general, later selection of transfectant clones expressing the desired chemokine receptor is greatly facilitated if the cDNA is tagged with a marker such as the *c*-myc tag ***(6)*** that can later be recognized by a specific antibody. For this reason, a 5'-myc-tagged version of mouse CCR8 (myc-mCCR8) cDNA was also prepared and cloned into the pCIneo vector.

3.2.2. Generation of Stable Transfectants

Two different cell lines were used as hosts to generate stable mouse CCR8 transfectants. Human embryonic kidney (HEK) 293 cells were transfected with 15 µg of myc-mCCR8 cDNA cloned in pCIneo using the standard calcium phosphate method *(7)*. In addition, rat lymphoblast YB2/O cells resuspended at 10 $\times 10^6$ cells/mL were mixed with 20 µg of the myc-mCCR8 cDNA. After 5 min incubation at room temperature, the cells were transferred to an electroporation cuvet (Bio-Rad) and pulsed at 250 V and 950 µF on a Bio-Rad Gene pulser II.

For both cell types, stable transfectants were selected in the presence of 1 mg/mL G418 for 14 d and were then analyzed for mouse CCR8 expression by immunostaining and flow cytometric analysis using an anti-myc mAb (9E10, Santa Cruz Biotechnology, Santa Cruz, CA, USA). Selected transfectant cells were cloned by limiting dilution and again analyzed for a high, stable receptor expression level before immunization.

3.3. Immunization

Many antigens and immunization methods can be employed. In the case of chemokine receptors, their use as purified proteins in native conformation is not feasible, as these receptors are integral membrane proteins. The best approaches include immunization with synthetic peptides, fusion proteins covering part or all of the receptor sequence, and chemokine-receptor-expressing transfected cells. A caveat in using synthetic peptides as immunogens is that the antibodies generated may then not recognize the native protein. To maximize the chances of generating antibodies with the desired specificity, four to six animals are usually immunized for each antigen chosen.

3.3.1. Peptides as Immunogens

Eight-week-old Lou rats were injected subcutaneously (sc) with the mouse CCR8 KLH-coupled peptide. For each rat, 30 µg of the conjugated peptide were dissolved in 150 µL of PBS, mixed with the same volume of Freund's complete adjuvant and injected in several sites. Animals were boosted sc at d 30 and 60, with the same amount of antigen in incomplete Freund's adjuvant (*see* **Note 3**).

Serum samples were taken from rat tails on d 38 and 68 to test the polyclonal anti-mouse CCR8 response. The presence of specific antibodies was studied by ELISA using synthetic peptides and by flow cytometry with receptor-expressing cells. Serial dilutions of sera (1:100 to 1:10,000) were tested.

Animals with a high polyclonal anti-mouse CCR8 response were selected for fusion and received two additional intraperitoneal (ip) booster injections with 40–60 µg of the KLH-coupled peptide immunogen at d −3 and −2 before cell fusion (approx 90–120 d after starting the immunization protocol) (*see* **Note 4**).

3.3.2. Transfectant Cell Lines as Immunogens

Stably transfected YB2/0 and HEK 293 cells expressing myc-tagged mouse CCR8 in exponential growth were recovered and washed twice with PBS. Cells were then irradiated (10 Gy) and injected ip into 10-wk-old Lou rats (20×10^6 cells/0.3 mL sterile PBS). Rats were boosted on d 30 and 60 with the same number of cells.

In the case of rats immunized with HEK 293 cell transfectants, only a strong, nonspecific immune response developed against human proteins expressed on the cell membranes. This negative result illustrates the convenience of using syngeneic cell hosts for immunization purposes.

For rats immunized with mouse CCR8-expressing YB2/0 cells, serum samples were collected 7–10 d after each boost, and the presence of specific antibodies was tested by flow cytometry using mouse CCR8-transfected HEK 293 cells. As a negative control, HEK 293 cells transfected with the void pCIneo vector were used. Not less than 1 mo after the last boost, rats with a high specific anti-CCR8 response received an iv injection with 20×10^6 cells in 0.2 mL sterile PBS on d −3 and −2 before fusion.

3.4. Cell Fusion

Selected rats were sacrificed by CO_2 inhalation, and spleen and peripheral lymph nodes were removed aseptically. Lymphocytes were fused with the P3X63Ag8.653 murine plasmacytoma, using PEG 4000 essentially as described ***(8)***. Myeloma cells are deficient in the gene for the hypoxanthine–guanine phosphoribosyltransferase (HPRT) enzyme, which is involved in the salvage pathway utilized when the *de novo* nucleotide synthesis pathway is blocked. After fusion with splenocytes, hybridoma cells are selected by the addition of azaserine, a drug that blocks the *de novo* purine synthesis and inhibits the growth of the myeloma fusion partner, forcing the hybrid cells to use the salvage pathway. The selective medium must be supplemented with hypoxanthine. Serum and PEG batches must be carefully selected for optimal cell-fusion efficiency. The general procedure is as follows.

1. Collect, count, and centrifuge (400*g* for 6 min) murine P3X63Ag8.653 plasmacytoma cells in exponential growth. Cell viability at the time of cell collection should be greater than 95%. Resuspend the cells in DMEM complete medium at 2×10^6 cells/mL.
2. Aseptically remove the spleen and inguinal and axillary lymph nodes from the rats selected, place the cell suspension in a 60-mm-diameter Petri dish with 6 mL of complete medium, and tease apart. Allow clumps to settle and filter the resulting cell suspension through a fine mesh screen. Transfer the cells to a 50-mL Falcon tube.

3. Centrifuge cells (400*g* for 6 min), resuspend the pellet in 4 mL of prewarmed 0.83% ammonium chloride, and incubate (4 min at 37°C) to lyse erythrocytes. Add 10 mL of complete medium and centrifuge again.
4. Resuspend the cells in 10 mL of complete medium and count.
5. Mix myeloma and lymphocytes at a 1:4 ratio.
6. Wash the lymphocyte–myeloma cell mixture by centrifugation (400*g* for 5 min). Resuspend the cells in serum-free medium and centrifuge again (400*g* for 10 min). Repeat this washing step.
7. Remove all of the supernatant and disaggregate the cell pellet by gently tapping the bottom of the tube. Add 1 mL of warmed (37°C) 50% PEG 4000 slowly, drop by drop, for 1.5 min with continuous gentle mixing.
8. Two minutes after starting PEG 4000 addition, add 10 mL of serum-free DMEM. This must be done slowly, at a rate of approx 1–2 mL/min, with constant gentle mixing. Centrifuge (400*g* for 5 min).
9. Carefully resuspend the cells in complete DMEM medium, supplemented with 20% FCS, at 2×10^6 cell/mL, avoiding excessive pipetting. Allow the cells to recover by culturing them in a flask (24 h at 37°C).
10. Collect and centrifuge the cells, resuspend them in selective DMEM medium or Clonacell HY at $(0.5–1) \times 10^5$ cells/mL and plate 200 µL/well of the cell suspension in a 96-well flat-bottom tissue culture plate. The number of viable cells obtained is usually around $(3–6) \times 10^7$, corresponding to approx 15–30 plates. It is convenient to seed fewer than 10 plates, however, to facilitate the screening assays. The remainder of the cells can be frozen and plated later.
11. Place plates in a 5% CO_2/air incubator at 37°C. Feed cells every 4 d with the same medium. To change the medium, remove half the volume of each well and add prewarmed fresh medium.
12. Ten to 14 d after fusion, supernatants from wells with growing hybrids are tested in screening assays (*see* **Note 5**).
13. Hybridomas from positive wells with colonies that cover more than 10% of the well bottom are expanded to 24-well plates for further characterization and stabilization.
14. Uncloned hybridomas in exponential growth can be stored frozen in liquid nitrogen while their conditioned media are analyzed to determine which of them will be selected and cloned.

3.5. Screening Positive Hybridomas

Sera from animal bleedings can be used to develop screening assays. Because of the large number of samples to be analyzed, usually approx 1000 wells, screening assays are performed sequentially, first to select positive hybrids and second to eliminate false positive or crossreactive antibody-producing hybrids (*see* **Note 6**). To economize efforts, combined supernatants from 5–10 wells can first be tested. In our case, the hybridomas producing anti-mouse CCR8 mAbs were detected by ELISA using peptide-coated plates when synthetic peptides were used as immunogens and by flow cytometry using mouse CCR8-transfected

HEK 293 cells when the immunogen used was mouse CCR8-transfected YB2/0 cells. Supernatants from positive hybridoma cell cultures were subsequently confirmed by flow cytometry using murine BW5147.3 cells, a thymoma cell line that naturally expresses mouse CCR8. Mock-transfected HEK 293 cells were used as a negative control.

3.5.1. ELISA

Microtiter plates were coated with 100 µL/well of the appropriate synthetic peptide at 1 µg/mL in PBS or carbonate buffer and stored overnight at 4°C. After blocking with 200 µL of 0.5% BSA in PBS (1 h at 37°C), culture supernatants and peptide-immunized rat serum dilutions, as positive control, were added. After incubation (1.5 h at 37°C) and three washes with PBS, 100 µL of a peroxidase-labeled rabbit anti-rat immunoglobulin antibody (1:2000 dilution) was added. After a new incubation (1 h at 37°C), plates were washed with PBS and developed with 100 µL of a solution containing OPD and H_2O_2. Color development was terminated by adding 50 µL of 2 *M* H_2SO_4. Results were quantified by measuring absorbance at 492 nm.

3.5.2. Flow Cytometry

Flow cytometry was used to select hybridomas producing mAbs specifically recognizing mouse CCR8-expressing cells. For staining $(0.1–3) \times 10^5$ transfectant or control mock-transfected cells were centrifuged in V-bottom 96-well plates and washed with sPBS. To prevent nonspecific binding, cells were preincubated with mouse IgG (40 µg/mL; 20 min at 4°C). The same concentration of mouse IgG was used in all staining steps. After centrifugation and washing with sPBS, the cells were incubated with 100 µL of the hybridoma cell culture supernatant tested, diluted 1:2 in sPBS, and incubated (40 min at 4°C). Cells were then washed twice with sPBS, incubated (30 min at 4°C) with 50 µL fluorescent anti-rat second antibody. Finally, samples were washed and analyzed in a flow cytometer.

3.6. Stabilization of Hybrids by Limiting Dilution Cloning

Because more than one hybridoma colony might be growing in a plate well, cells that give a positive result in the screening assays must be isolated (*see* **Note 7**). A general procedure for cloning individual hybridomas is as follows.

1. Mix and resuspend the cells growing in the well homogeneously, remove an aliquot, dilute it 1:2 in 0.2% trypan blue in PBS, and count the cells.
2. In serial dilutions, dilute a sample of the culture cells to be cloned such that approx 200 live cells are suspended in 40 mL of Clonacell HY medium E. Plate 200 µL/well in two 96-well flat-bottom tissue culture plates (approx 1 cell/well). Hybri-

domas are usually cloned by limiting dilution, using a feeder layer of BALB/c mouse thymocytes (2×10^6 cells/mL), until stable antibody production is achieved. In the case of the anti-mouse CCR8 fusion, we used a specific hybridoma grown medium (Clonacell HY), because thymocytes express CCR8.

3. Change the medium every fourth day for 10–14 d. At this time, take samples from the supernatants to repeat the screening assays.
4. For cells confirmed as positive, check visually with a microscope that only one clone is growing in the well. Expand single-clone positive cells to a 24-well plate.
5. Repeat the cloning procedure until >95% of the wells with growing cells give positive signals in the screening assays.
6. Clones that secrete the desired antibody are expanded and several aliquots of them are frozen before proceeding to large-scale antibody production.

3.7. Large-Scale Production of mAbs

Monoclonal antibodies can be produced either in culture medium or in mouse ascites fluid. Antibody production in culture supernatants ranges from 5 to 60 µg/mL. To achieve this production level, hybridomas are overgrown until cells in the culture begin to die. Ascites tumors were established by ip injection of $(1–1.5) \times 10^6$ exponentially growing cells into 4.5-Gy-irradiated BALB/c mice. The mice must be primed previously (14 d before injecting the hybridoma cells) by an ip injection of 0.5 mL Pristane. After 10–20 d, ascites fluid can be collected (approx 8 mL of ascites can be produced by one mouse). The mAb concentration in ascites ranges from 1 to 6 mg/mL. The mAb can be partially purified from ascites fluid or from tissue culture medium by precipitation with 50% ammonium sulphate, or by affinity chromatography using protein A– or protein G–Sepharose (Amersham Pharmacia Biotech), as recommended by the supplier.

3.8. Monoclonal Antibody Characterization

The monoclonal isotypes can be determined by radial immunodiffusion or ELISA using some of the mAb typing kits (Sigma, Southern Biotechnology, Pharmingen), as recommended by the manufacturers.

To confirm mAb specificity—in particular, their lack of recognition of other chemokine receptors—cells that express different chemokine receptors such as T-cells, neutrophils, eosinophils, and so forth can be used. Plasmids encoding other chemokine receptor cDNAs can also be used to generate transfectant cell lines, useful for verifying antibody specificity. The expression of transfected chemokine receptors in these cells has necessarily to be verified with appropriate antibodies and/or calcium mobilization and migration assays. For other purposes, such as immunoprecipitation and antigen-capture ELISA, mAbs need to be not only specific but also have a high affinity for the antigen. Antibody

affinity can be tested by competitive ELISA or radioimmunoassay, followed by the Scatchard analysis of the data.

3.8.1. Assaying the Neutralizing Activity of Anti-Chemokine-Receptor mAbs

Antibodies able to antagonize the activity of the proteins they recognize specifically are very valuable tools for studying their in vivo role in animal models of pathologies. Indeed, validation of therapeutic targets using neutralizing mAbs mimics the clinical situation closely, as the antibodies can be administered once the disease has already been established. In the case of anti-chemokine-receptor mAbs, there are several simple in vitro assays that can be used to analyze the antagonist activity of the specific immunoglobulins generated. As an example, the approach followed to characterize the blocking activity of anti-mouse CCR8 mAbs is described.

3.8.1.1. Chemokine–mAb Competition for Receptor Binding

For competition experiments, CD4 single-positive mouse thymocytes were preincubated (40 min at 4°C) in parallel with several chemokines before staining with the anti-mouse CCR8 mAb, using a fluorescent anti-rat immunoglobulin as second antibody. Samples were analyzed by flow cytometry as described in **Subheading 3.5.2.** Binding of an anti-mouse CCR8 mAb antibody to CCR8-expressing mouse thymocytes is clearly blocked by previously added CCL1 (*see* **Fig. 2**). For this analysis, we used 8F4, one of the mAbs generated by immunizing rats with CCR8-expressing YB2/0 cells ***(9)***.

3.8.1.2. Inhibition of Calcium Mobilization by mAb

After CCL1 addition to stable transfected HEK 293 cells expressing mouse CCR8, we analyzed variations in the intracellular calcium concentration by fluorometry, registering alterations in the F395/F500 ratio ***(10)***. Cells were loaded with Indo-1 AM and preincubated (20 min at 4°C) with several mAb dilutions (0.1–100 n*M*), prior to stimulation with 1–10 n*M* mouse CCL1. Control incubations were performed with chemokines specific for other receptors, with no antibody or with an isotype-matched, irrelevant mAb. SFLLR-amide (1.4 m*M*) was also added to confirm the cell's ability to mobilize Ca^{2+} via a chemokine-independent mechanism. The anti-mouse CCR8 mAb 8F4 clearly blocks CCL1-induced Ca^{2+} mobilization mediated by CCR8 (*see* **Fig. 3**).

3.8.1.3. Inhibition of Chemotaxis by mAb

Migration assays with thymocytes and BW5147.3 cells were performed in Transwell inserts with a 5-µm pore diameter. Cells were resuspended in RPMI 1640 with 1% BSA and 25 m*M* HEPES, pH 7.3 (10^7 cells/mL), and 100-µL ali-

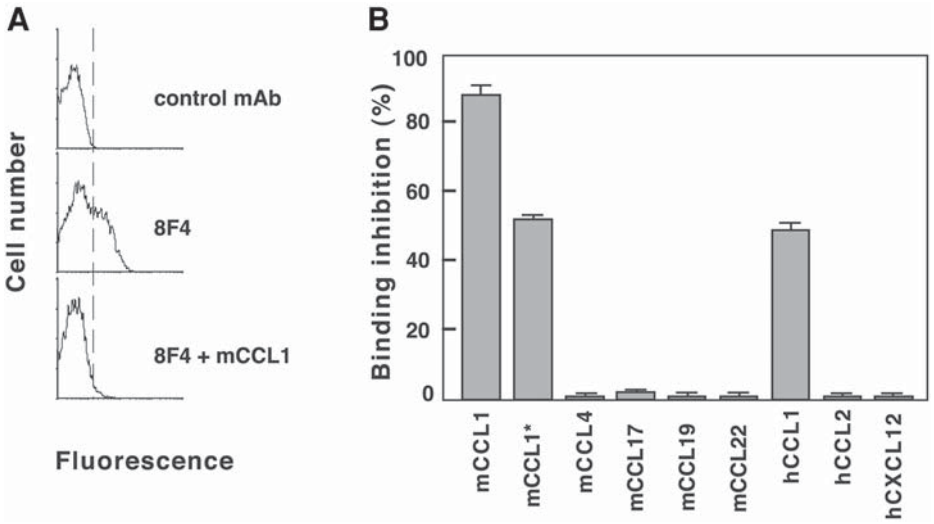

Fig. 2. Mouse CCL1/TCA3 blocks binding of mAb 8F4 to mouse CCR8 in thymocytes. (**A**) Mouse thymocytes were preincubated (40 min at 4°C) with 100 n*M* mouse CCL1, then stained with anti-CD4, anti-CD8, and mAb 8F4. The results are shown for gated CD4 single-positive thymocytes, the subset with the highest CCR8 expression. Control staining is shown using an isotype-matched irrelevant antibody and mAb 8F4 in the absence of competitor chemokine. (**B**) Results of similar experiments with thymocytes preincubated with different mouse or human chemokines (100 n*M*) and analyzed with mAb 8F4. Data are presented as the percentage of inhibition of mAb 8F4 binding to CD4 single-positive thymocytes not preincubated with chemokines. Mouse CCL1 was also tested at 1 n*M* (CCL1*) and showed approx 50% inhibition. Similar results were obtained with a 100-fold excess of human (h) CCL1. (Data reproduced from **ref. *9***. Copyright 2001. The American Association of Immunologists, Inc.)

quots were loaded into upper inserts. Samples of 0.2 n*M* mouse CCL1, prepared in 600 µL of the same medium, were placed in the lower wells. After 2 h incubation, inserts were removed and migrated cells were counted in a flow cytometer.

For chemotaxis assays with HEK 293/CCR8 cells, a 48-well microchamber (Neuroprobe, Cabin John, MD, USA) was used. Lower wells were loaded with 1 n*M* mouse CCL1 (27 µL/well), and cells (50 µL/well, 10^6 cells/mL) were placed in the upper wells. Polyvinyl pyrrolidone-free filters (10-µm pore; Poretics) were used, precoated (2 h at 37°C) with type VI collagen (Sigma). The chamber was incubated (5–6 h at 37°C) in a humidified atmosphere with 5% CO_2. Cells in the migration assays were first preincubated (20 min at 4°C) with increasing amounts of the anti-mouse CCR8 mAb 8F4 or an isotype-matched irrelevant antibody. Quadruplicate wells were used for each point. A migration

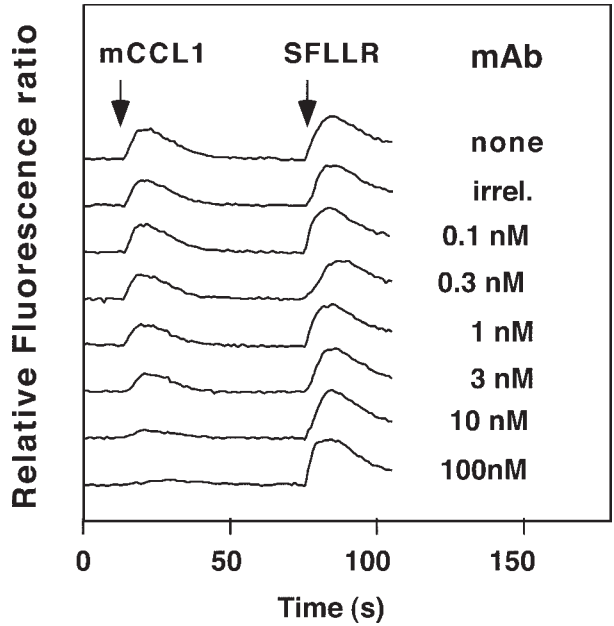

Fig. 3. The mAb 8F4 blocks murine CCL1-mediated calcium mobilization by HEK 293/CCR8 transfectant cells. HEK 293 cells expressing mouse CCR8 were loaded with 5 μ*M* Indo-1 AM and preincubated for (20 min at 4°C) with the indicated amounts of 8F4 prior to stimulation with 1 n*M* mouse CCL1. Control incubations were performed without antibody (none) or with an isotype-matched irrelevant mAb (100 n*M*, irrel.). The cell's ability to mobilize Ca^{2+} by a chemokine-independent mechanism was assayed by addition of 1.4 μ*M* SFLLR-amide. (Data reproduced from **ref. *9***. Copyright 2001. The American Association of Immunologists, Inc.)

index was established as the ratio of the cell number migrated in response to the chemokine and the cell number migrated to buffer. This index was used to estimate the percentage of migration inhibition caused by the preincubation with the mAbs.

To study the antibody-blocking activity of mouse CCL1-induced migration of HEK 293/CCR8 transfectants and BW5147.3 T cell lymphoma cells, the cells were preincubated with different amounts of 8F4 or an irrelevant isotype-matched mAb before loading into the migration device. As a chemoattractant, 1 n*M* (HEK 293/CCR8 transfectants) or 0.2 n*M* (BW5147.3 cells) mouse CCL1 was used. The 8F4-blocking activity of the CCR8-mediated chemotaxis of CCR8-expressing cells was clearly observed (*see* **Fig. 4**).

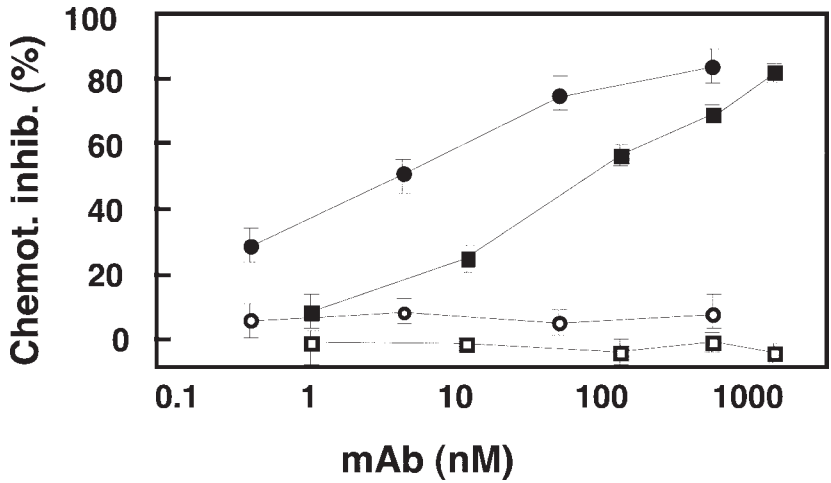

Fig. 4. The mAb 8F4 blocks mouse CCL1-induced migration of HEK 293/CCR8 transfectants and BW5147.3 T-cell lymphoma cells. In vitro migration experiments were performed in a microchamber (HEK 293/CCR8 transfectants, circles) or Transwell inserts (BW5147.3 cells, squares). Before loading into the migration device, cells were preincubated with the indicated amounts of mAb 8F4 (filled symbols) or an irrelevant isotype-matched mAb (empty symbols). As a chemoattractant, 1 n*M* (HEK 293/CCR8 transfectants) or 0.2 n*M* (BW5147.3 cells) mouse CCL1 was used. (Data reproduced from **ref. *9***. Copyright 2001. The American Association of Immunologists, Inc.)

3.8.2. Other Uses of mAb Against Chemokine Receptors

The number of studies that can be done using anti-chemokine-receptor mAb is limited only by the characteristics of the antibodies and the researcher's imagination. As some examples, mAbs are excellent tools to study chemokine-receptor expression in physiological and pathological situations in flow cytometry, immunohistochemistry, and Western blotting. Their use in confocal microscopy and coimmunoprecipitation assays can aid the analysis of receptor endocytosis and recycling to the cell membrane, as well as receptor intracellular signaling events. Combinations of mAbs, each recognizing a different chemokine-receptor epitope, can be used to map important functional domains of the receptor, such as the ligand-binding site or effector docking sites.

3.9. Monoclonal Antibody Labeling

Monoclonal antibodies are often labeled to increase the sensitivity of the detection techniques and the possibility of using them in combination with other

differently labeled or unlabeled antibodies. One of the most commonly used markers for mAb is biotin, a small molecule that can be conjugated to proteins without altering their biological activity. Biotin interacts with avidin, and the avidin–biotin interaction is the strongest noncovalent biological interaction known. There are many commercial sources of enzyme- or fluorescence-modified avidin. Given the broad applications of biotin-labeled antibodies, we describe here the method followed to biotinylate the anti-mouse CCR8 mAb 8F4 (*see* **Note 8**). This general approach can be used to biotinylate other antibodies.

1. Dialyze the antibody against 0.1 *M* sodium bicarbonate ($NaHCO_3$), pH 9, containing 0.15 *M* NaCl. The final concentration should be around 1 mg/mL.
2. For each milligram of protein, add 100 µL of 1 mg/mL *N*-hydroxysuccinimidobiotin in DMSO, prepared immediately prior to use. Alternatively, 74 µL of sulfo-NHS-LC-biotin (1 mg/mL in water, prepared just before use) can be used.
3. Mix the contents gently and allow the reaction to proceed in the dark (2 h at room temperature).
4. Dialyze the sample against your assay buffer to remove unreacted biotin.
5. Store at −80°C. Alternatively, dilute the conjugate with an equal volume of 98% glycerol, aliquot, and store at −20°C.

4. Notes

1. Special attention should be paid when choosing the sequence of the synthetic peptides to be used as immunogens. If peptides contain amino acid residues susceptible to posttranslational modifications in the native receptor, antibodies with high affinity for the immunizing peptide might not be able to recognize the receptor on cells that express it. Posttranslational modifications are usually cell- or tissue-specific; the host cell line should therefore be selected carefully if transfectant cells will be used as immunogens.
2. Immunization with synthetic peptides corresponding to receptor intracytoplasmic sequences are useful not only for cell expression studies but also for analysis of receptor interaction with its effectors and receptor localization in endocytic compartments. Antibodies raised against such intracytoplasmic peptides can often be used for immunohistochemistry, immunofluorescence of fixed cells, immunoprecipitation, and Western blot.
3. When preparing complete Freund's adjuvant for immunization, it is important to mix the commercial oil by vortexing vigorously until all of the *Mycobacterium tuberculosis* cells are resuspended. Then, dissolve the protein antigen in PBS, mix with the same volume of adjuvant, and vortex the mixture until an emulsion is formed. Freund's adjuvants are potentially harmful; take care during preparation and injection.
4. Several final antigen boosts are needed before carrying out the cell fusion to generate hybridomas, but these injections should be performed at least 1 mo after the previous ones. This period is necessary to allow a reduction in blood antibody levels. If blood antibody levels are high, these antibodies will compete with B-

lymphocytes for antigen binding, reducing the number of antigen-specific lymphocytes available for cell fusion.

5. Unfused B-lymphocytes will die several days after cell fusion, but until they die, some continue to secrete antibody that could give false-positive results in the screening assays. To dilute the antibody produced by these cells, the selective medium should be changed at least three times. With this procedure, the antibody produced by the hybridomas will increase simultaneously, because of cell proliferation.
6. Screening assays for antibody detection should be developed before starting the cell-fusion process. Growing hybrids will be ready for screening 10–14 d after plating, allowing little time to work out technical problems.
7. Positive hybridomas should be cloned as soon as possible. More than one colony may grow in each well, each derived from an independent fusion event, and non-immunoglobulin-producing hybrids may growth faster than immunoglobulin-producing cells. Moreover, during the first cell divisions after fusion, chromosomes are frequently lost while the new genetic complement is being stabilized. Even within the same colony, there could, thus, be cells that have ceased antibody production.
8. A variety of fluorescent compounds, enzymes, and radioactive products can be used for antibody labeling ***(8)***. In some cases, labeling amino groups inactivates mAbs that have lysines in or near their active sites. Monoclonal antibodies can also be labeled directly with enzymes and fluorescent compounds through other group-specific reagents, such as tyrosyl and histidyl amino acid side chains (*p*-diazobenzoylbiocytin), sulfhydryl groups [3-(*N*-maleimidopropionyl)biocytin] or sugar residues and carboxyl groups (biocytin hydrazide). Several commercial kits (Sigma, Pierce, Amersham Pharmacia Biotech) are available as potential alternatives to labeling with amine-specific reagents.
9. Now that a number of chemokine receptor knockout mice are available, they can be immunized appropriately to generate antibodies against the receptor they do not express.

Acknowledgments

The authors thank C. Mark for editorial assistance. The Department of Immunology and Oncology was founded and is supported by the Spanish Council for Scientific Research (CSIC) and by the Pharmacia Corporation.

References

1. Mackay, C. R. (2001) Chemokines: immunology's high impact factors. *Nature Immunol.* **2,** 95–101.
2. Zlotnik, A. and Yoshie, O. (2000) Chemokines: a new classification system and their role in immunity. *Immunity* **12,** 121–127.
3. Gerard, C. and Rollins, B. J. (2001) Chemokines and disease. *Nature Immunol.* **2,** 108–115.
4. Gausepohl, H., Boulin, C., Kraft, M., and Frank, R. W. (1992) Automated multiple peptide synthesis. *Peptide Res.* **5,** 315–320.

5. Tijssen, P. (1985) Preparation of enzyme-antibody or other enzyme-macromolecule conjugates, in *Laboratory Techniques in Biochemistry and Molecular Biology* (Burdon, R. H. and van Knippenberg, P. H., eds.), Elsevier Science, New York, pp. 221–296.
6. Martin-Belmonte, F., Kremer, L., Albar, J. P., Marazuela, M., and Alonso, M. A. (1998) Expression of the MAL gene in the thyroid: the MAL proteolipid, a component of glycolipid-enriched membranes, is apically distributed in thyroid follicles. *Endocrinology* **139,** 2077–2084.
7. Ausubel, F. M., Brent, R., Kingston, R. E., et al. (1989) *Current Protocols in Molecular Biology,* Green Publishing Associates, New York.
8. Harlow, E. and Lane, D. E. (1988) *Antibodies: A Laboratory Manual*, Cold Spring Harbor Laboratory, Plainview, NY.
9. Kremer, L., Carramolino, L., Goya, I., et al. (2001) The transient expression of C–C chemokine receptor 8 in thymus identifies a thymocyte subset committed to become $CD4^+$ single-positive T cells. *J. Immunol.* **166,** 218–225.
10. Didsbury, J. R., Uhing, R. J., Tomhave, E., Gerard, C., Gerard, N., and Snyderman, R. (1991) Receptor class desensitization of leukocyte chemoattractant receptors. *Proc. Natl. Acad. Sci. USA* **88,** 11,564–11,568.

21

Detection of High-Affinity α4-Integrin Upon Leukocyte Stimulation by Chemoattractants or Chemokines

Jason R. Chan and Myron I. Cybulsky

1. Introduction

On circulating leukocytes, including monocytes and lymphocytes, α4-integrins are expressed in a low-affinity conformation. Low-affinity interactions with its ligand, vascular cell adhesion molecule-1 (VCAM-1), result in leukocyte tethering and rolling under flow ***(1,2)***, whereas high-affinity interactions mediate leukocyte arrest ***(3)***. Rapid triggering of integrin-mediated arrest occurs upon leukocyte stimulation with chemoattractants and chemokines ***(4,5)***. In monocytes, α4-integrin affinity is rapidly upregulated and mediates arrest ***(6)***. Changes in affinity may be monitored by binding of a soluble ligand because high-affinity α4-integrins form stable interactions with a soluble ligand, unlike low-affinity α4-integrins ***(7)***. In this protocol, binding of recombinant chimeric human VCAM-1 is used to identify high-affinity α4-integrins by flow cytometry. In addition, a recently reported method for monitoring α4-integrin affinity in real time using a ligand-mimetic peptide, which contains the leucine, aspartic acid, valine (LDV) consensus binding sequence for α4-integrin, is described ***(8)***. The cell line U937, transfected with the human formyl peptide receptor (FPR), and stimulated with fMLP or SDF-1α is used as a model. These methods allow for analysis of α4-integrin activity without the complications of post-ligand-binding events inherent in cell adhesion-based assays.

2. Materials

1. U937-FPR cells.
2. Recombinant chimeric human VCAM-1/Fc (ICOS Corporation, Bothell, WA).
3. Nonimmune human IgG1 (Sigma Chemical Company, St. Louis, MO).
4. 4-((*N*′-2-Methylphenyl)ureido)-phenylacetyl-L-leucyl-L-α-aspartyl-L-valyl-L-prolyl-L-alanyl-L-alanyl-L-lysine conjugated to fluorescein isothiocyanate (LDV-FITC)

From: *Methods in Molecular Biology, vol. 239: Cell Migration in Inflammation and Immunity*
Edited by: D. D'Ambrosio and F. Sinigaglia © Humana Press Inc., Totowa, NJ

(synthesized by Commonwealth Biotechnologies, Richmond, VA). Stock solution should be 15 μ*M* with dimethyl sulfoxide (DMSO) as the solvent.
5. fMLP (from Sigma).
6. Human SDF-1α (from Peprotech, Rocky Hill, NJ).
7. 4% Paraformaldehyde.
8. Hank's balanced salt solution (HBSS) (Invitrogen Canada Inc., Burlington, Ontario, Canada).
9. 1 *M* HEPES solution (from Sigma).
10. Phycoerythrin (PE)-conjugated $F(ab')_2$ fragments of goat anti-human IgG (Jackson Immunoresearch Labs, West Grove, PA).
11. Propidium iodide (Molecular Probes, Eugene, OR).
12. Manganese chloride ($MnCl_2$, from Sigma).
13. EDTA (from Sigma).
14. Epics® XL-MCL flow cytometer with Expo™ 32 analysis software (Beckman Coulter Inc., Miami, FL).
15. Microsoft® Excel (Redmond, WA).

3. Methods

Methods are described here to detect high-affinity α4 integrins by binding of recombinant chimeric human VCAM-1/Fc or ligand-mimetic peptide (LDV-FITC). Cell fixation is required for the former method, whereas the latter can be performed in real time with live cells.

*3.1. Recombinant Chimeric VCAM-1/Fc (***see** *Notes 1–6)*

1. U937-FPR cells are resuspended in assay buffer (HBSS containing 1 m*M* Mg^{2+}/Ca^{2+}, 20 m*M* HEPES, and 0.5% fetal bovine serum [FBS]) at a concentration of 1×10^6/mL.
2. For 100 μL of cells, soluble VCAM-1/Fc or nonimmune IgG1 (negative control) are added to a final concentration of 20 μg/mL and allowed to equilibrate for at least 5 min.
3. Each sample is then stimulated with fMLP (100 n*M*), SDF-1α (12.5 n*M*), $MnCl_2$ (0.5 m*M*), or vehicle control for 30 s.
4. To terminate agonist stimulation, the sample is quickly diluted with 3.5 mL assay buffer, followed immediately by 500 μL of 4% paraformaldehyde.
5. After 15 min, samples are washed twice by centrifugation with assay buffer.
6. Binding of soluble VCAM-1/Fc or nonimmune IgG is detected by flow cytometry using a PE-conjugated anti-human IgG secondary antibody (*see* **Fig. 1**).

*3.2. Ligand-Mimetic Peptide (LDV-FITC) (***see** *Notes 7–12)*

This experimental method was adapted from Chigaev et al. ***(8)***, with some modifications. Expo™ 32 software is used for data analysis. However, any flow cytometry software capable of exporting raw data into a spreadsheet format will suffice.

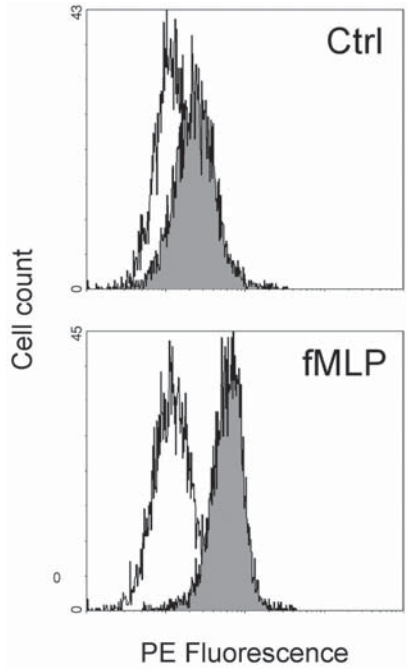

Fig. 1. Flow cytometry histogram plots for detection of soluble VCAM-1/Fc binding in U937-FPR cells. Binding of soluble VCAM-1/Fc (closed curve) or nonimmune IgG negative control (open curve) is detected by PE-conjugated anti-human IgG secondary antibody in U937-FPR cells stimulated with vehicle control (top) or 100 n*M* fMLP for 30 s.

1. Resuspend U937-FPR cells in assay buffer at a concentration of 0.5×10^6/mL. Add LDV-FITC peptide to achieve a final concentration of 3 n*M*. Allow cells to equilibrate with peptide for 15 min at room temperature.
2. Aliquot U937-FPR cells into 500-µL samples in polypropylene flow cytometry tubes. To determine nonspecific binding of the LDV-FITC peptide, add EDTA to one sample (5 m*M* final concentration).
3. Configure flow cytometer to detect FITC versus time. Gate on live cells as determined by propidium iodide exclusion.
4. Add propidium iodide to the sample and run in flow cytometer for 30–60 s to obtain a baseline fluorescence reading.
5. Pause flow cytometer, remove sample, and add FP, SDF-1α, $MnCl_2$ (100 n*M*, 12.5 n*M*, and 0.5 m*M*, respectively, all final concentrations), or vehicle control.
6. Return sample to flow cytometer and resume data collection for selected amount of time.
7. Run 10% bleach for 5 min and use the cleaning cycle in between each sample to remove any agonist contaminating the flow cytometer.
8. Save all data for off-line analysis.

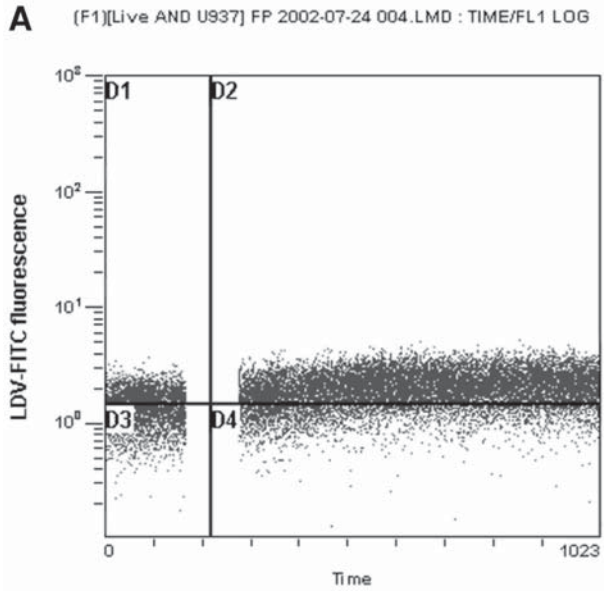
A
(F1)[Live AND U937] FP 2002-07-24 004.LMD : TIME/FL1 LOG
D1
D2
D3
D4
LDV-FITC fluorescence
Time
0
1023

B

C For *y*-axis:
LDV–FITC fluorescence = $10^{\text{RowNumber}/16}$
For *x*-axis:
Time = Time of assay ÷ 64 × column number

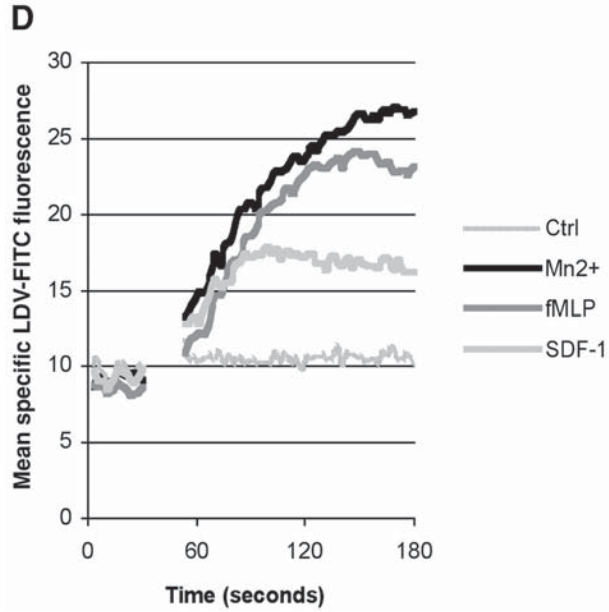

Fig. 2. Analysis of LDV-FITC binding in real time upon agonist stimulation of U937-FPR cells. An example of data acquisition, transformation, and graphing is shown in (**A**) (*opposite page*). Flow cytometer data are exported directly to a spreadsheet as a 64 × 64 grid (**B**) (*opposite page*). Each point in the grid refers to the number of events that have a particular LDV-FITC fluorescence value and time interval that can be mathematically determined according to formulas shown in (**C**). The mean LDV-FITC fluorescence of all events at each time interval is calculated. The mean LDV-FITC fluorescence of the negative control is subtracted from each sample and data are plotted as mean specific LDV-FITC fluorescence versus time. Sample curves are shown in (**D**) for U937-FPR cells stimulated with vehicle control, 0.5 m*M* $MnCl_2$, 100 n*M* fMLP, or 12.5 n*M* SDF-1.

3.2.1. Ligand-Mimetic Peptide (LDV-FITC: Data Analysis)

1. Open list mode file. Cut data from LDV-FITC versus time plot (*see* **Fig. 2A**) and paste into Microsoft Excel spreadsheet. Data are exported as a 64 × 64 density grid where each value represents the number of events with a particular LDV-FITC fluorescence accumulated over a specific time interval, Fig. 2B.
2. The units of the 64 × 64 grid are arbitrary. Convert the scale of the *y*-axis to LDV-FITC fluorescence. This can be done mathematically because the scale of the original plot covers a defined range of LDV-FITC fluorescence. In a similar manner, convert the *x*-axis to time (*see* **Fig. 2C**).

3. For each point defined by the 64 × 64 grid, calculate the total fluorescence by multiplying the LDV-FITC fluorescence value by the number of events.
4. Determine mean FITC fluorescence at each time point by summing the total fluorescence at each time-point and dividing by the total number of events.
5. Subtract FITC fluorescence values for nonspecific binding from each sample to obtain mean specific LDV-FITC fluorescence. Plot specific mean LDV-FITC fluorescence versus time (*see* **Fig. 2D**).

4. Notes

1. α4-Integrin affinity is modulated by the divalent cation environment. Therefore, $MnCl_2$ (0.5 mmol/L), which artificially puts integrins into high affinity ***(7)***, should be used as a positive control.
2. The assay may be performed either at room temperature or in a 37°C water bath.
3. Transient effects of chemoattractant or chemokine stimulation on α4-integrin affinity can be detected by varying the amount of time prior to terminating the assay by dilution and fixation.
4. The specificity of the VCAM-1/α4-integrin interaction can be determined by preincubating cells with function blocking α4-integrin antibodies prior to assay.
5. A major disadvantage is the requirement for cell fixation.
6. This method can be modified, in principle, to examine the affinity of other integrins. For example, recombinant ICAM-1/Fc could be used to detect high-affinity αLβ2- and αMβ2-integrins. However, the K_d of high-affinity αLβ2-integrin appears to be below the limits of conventional assays ***(9)***. Therefore, very high concentrations of ICAM-1/Fc may be required. In contrast, a more sensitive technique using radiolabeled ICAM-1 has been reported ***(10)***.
7. Integrin–ligand interactions require divalent cations. Therefore, preincubation of cells with EDTA, a divalent cation chelator, serves as an ideal negative control to determine nonspecific binding of the fluorescent peptide (background).
8. Special attention must be given to potential contamination of the flow cytometer with agonists. For example, it is our experience that stimuli such as SDF-1α and thapsigargin can cause spurious results in subsequent samples if the flow cytometer is not properly cleaned between samples. It is imperative that baseline readings be flat prior to sample stimulation. We recommend running nonstimulated cells as a "reporter" to ensure that the system is clean between experimental samples.
9. Best results are obtained when samples are run at room temperature. Qualitatively similar results can be obtained when samples are prewarmed to 37°C in a water bath prior to data collection. However, baseline readings tend to be inconsistent with a general downward trend. Flatter baseline readings are obtained when the entire experiment is performed at room temperature. This temperature sensitivity could be the result of a change in sample temperature because most commercial flow cytometers are operated with sheath fluid at room temperature.
10. Data are most reliable when the event rate is around 200 per second. Lower event rates lead to choppy curves when data are plotted as mean FITC fluorescence versus time. This is particularly apparent for leukocytes isolated from blood.

11. Unless the flow cytometer is equipped with a stir bar, 10 min appears to be the longest time that a sample can be run because event rates decline significantly over the time of the assay as a result of settling of cells within the tube.
12. A significant disadvantage of this method is the loss of approx 5–10 s of data collection immediately after sample stimulation. This occurs because the tube is removed from the flow cytometer and can only be circumvented if an injection port is present so that data collection can be uninterrupted. Unfortunately, most commercially available flow cytometers do not have such a capability.

Acknowledgments

The authors thank Dr. G. P. Downey, from the University of Toronto, and Dr. D. E. Staunton, from the ICOS Corporation, for generously providing U937-FPR cells and recombinant chimeric human VCAM-1/Fc, respectively.

This work was supported by the Canadian Institutes of Health Research, grant MT-14151. J. R. Chan is the recipient of a Doctoral Research Award from the Heart and Stroke Foundation of Canada.

References

1. Alon, R., Kassner, P. D., Carr, M. W., Finger, E. B., Hemler, M. E., and Springer, T. A. (1995) The integrin VLA-4 supports tethering and rolling in flow on VCAM-1. *J. Cell. Biol.* **128,** 1243–1253.
2. Berlin, C., Bargatze, R. F., Campbell, J. J., et al. (1995) alpha 4 integrins mediate lymphocyte attachment and rolling under physiologic flow. *Cell* **80,** 413–422.
3. Chen, C., Mobley, J. L., Dwir, O., et al. (1999) High affinity very late antigen-4 subsets expressed on T cells are mandatory for spontaneous adhesion strengthening but not for rolling on VCAM-1 in shear flow. *J. Immunol.* **162,** 1084–1095.
4. Campbell, J. J., Qin, S., Bacon, K. B., Mackay, C. R., and Butcher, E. C. (1996) Biology of chemokine and classical chemoattractant receptors: differential requirements for adhesion-triggering versus chemotactic responses in lymphoid cells. *J. Cell. Biol.* **134,** 255–266.
5. Campbell, J. J., Hedrick, J., Zlotnik, A., Siani, M. A., Thompson, D. A., and Butcher, E. C. (1998) Chemokines and the arrest of lymphocytes rolling under flow conditions. *Science* **279,** 381–384.
6. Chan, J. R., Hyduk, S. J., and Cybulsky, M. I. (2001) Chemoattractants induce a rapid and transient upregulation of monocyte alpha4 integrin affinity for vascular cell adhesion molecule 1 which mediates arrest: an early step in the process of emigration. *J. Exp. Med.* **193,** 1149–1158.
7. Jakubowski, A., Rosa, M. D., Bixler, S., Lobb, R., and Burkly, L. C. (1995) Vascular cell adhesion molecule (VCAM)-Ig fusion protein defines distinct affinity states of the very late antigen-4 (VLA-4) receptor. *Cell Adhes. Commun.* **3,** 131–142.
8. Chigaev, A., Blenc, A. M., Braaten, J. V., et al. (2001) Real time analysis of the affinity regulation of alpha 4-integrin. The physiologically activated receptor is intermediate in affinity between resting and Mn(2+) or antibody activation. *J. Biol. Chem.* **276,** 48,670–48,678.

9. Takagi, J., Petre, B., Walz, T., and Springer, T. (2002) Global conformational rearrangements in integrin extracellular domains in outside-in and inside-out signaling. *Cell* **110,** 599–611.
10. Constantin, G., Majeed, M., Giagulli, C., et al. (2000) Chemokines trigger immediate beta2 integrin affinity and mobility changes: differential regulation and roles in lymphocyte arrest under flow. *Immunity* **13,** 759–769.

Index

A

Actin polymerization, *see* F-actin
Adhesion, *see* α4-Integrin; Integrin-dependent rapid adhesion assays; Leukocyte migration assays
Allergic airway inflammation,
  mouse models for in vivo studies,
    adoptive transfer model,
      antigen-presenting cell preparation, 203
      cell preparation for injection, 203, 204, 208
      inflammation induction, 204
      ovalbumin transgenic splenic lymphocyte preparation, 202, 203, 208
      Th2 cell polarization, 203
    aerosol challenge, 202, 208
    airway hyperreactivity analysis, 204
    antigen sensitization, 201, 202
    cell isolation, 204, 206, 208
    chemokine assays, 207
    cytokine assays, 207
    histology, 206
    immunoglobulin assays, 207
    immunostaining, 206–208
    lung parenchymal cell isolation, 206
    materials, 200, 201, 207
    overview, 199, 200
Angiogenesis,
  chemokine regulation assays,
    chemotaxis/invasion assay, 225–227
    chorioallantoic membrane assay, 230–2332
    human umbilical cord endothelial cell isolation for in vitro assay, 225
    materials, 224, 225
    Matrigel assay, 227
    micropocket cornea assay,
      implant selection, 229
      interpretation, 230
      principles, 228
      stimulus implantation, 229, 230
    overview, 223, 224
  definition, 223
Antigen-specific lymphocyte tracking in vivo,
  adoptive transfer of transgenic lymphocytes,
    animals,
      cell suspension preparation, 136
      DO11.10 transgenic mice, 135
      MD4 B-cell transgenic mice, 135
      recipient mice, 135, 136
    antigen preparation, 138, 139
    carboxyfluorescein diacetate labeling of transgenic lymphocytes, 136
    principles, 134, 135
    T-cell purification, 137, 138, 143

T-helper cell differentiation, 137, 138
flow cytometry,
lymphocyte division history analysis, 141
one-color, 139
three-color, 140, 141, 143, 144
two-color, 139, 143, 144
immunohistochemistry tracking,
DO11.10 staining using tyramide signal amplification system, 142
double staining, 143
slide preparation, 142, 144
lymphocyte function assessment, 141, 142
materials, 133, 134
overview, 133

B

B-cell, *see* Antigen-specific lymphocyte tracking in vivo
Boyden chamber, *see* Leukocyte migration assays
Brain microvessels, *see* Intravital microscopy

C

CAM, *see* Chorioallantoic membrane
Chemokines,
actin polymerization induction in chemokine-stimulated lymphocytes, *see* F-actin
angiogenesis regulation, *see* Angiogenesis
conditional expression in transgenic mice,
applications, 117, 118
overview, 105, 106
tetracycline-inducible system, 107–109
tissue-specific expression system, 115, 116
ubiquitous KC expression system and tissue distribution, 110–115, 117
history of study, 1, 2
inhibitors, *see* Viral chemokine-binding proteins
leukocyte chemoattraction, *see* Integrin-dependent rapid adhesion assays; Leukocyte migration assays
posttranslational processing analysis,
chemical synthesis of truncated chemokines, 35, 37, 41
identification by sizing and sequencing, 34, 35, 41
isolation of cleaved natural chemokines,
affinity purification, 32, 34, 41
concentrating of conditioned media and biological fluids, 30–32
ion-exchange chromatography, 34, 41
principles, 29, 30
reversed-phase chromatography, 34, 41
materials, 28, 29
overview, 27, 28
protease processing in vitro, 37–42
profiling of CD4 T cell response specificity,
cell labeling, 47, 51
cell purification, 46, 50

chemotaxis assay, 46, 47, 50, 51
materials, 45, 46, 50
migration analysis,
chemotactic index, 50
percentage of input, 50
specific cell migration, 48, 50
overview, 45
receptors, *see* Chemokine receptors
redundancy, 182
Chemokine receptors,
antagonist screening,
binding assays, 185
chemotaxis assay, 185–187
high-throughput screening, 184
materials, 183, 184
strategy, 182, 183
immune disease modulation, 181, 182
monoclonal antibody generation,
antigens, 243
applications, 244
characterization,
calcium mobilization inhibition, 254
chemotaxis inhibition, 254–256
competition assay, 254
enzyme-linked immunosorbent assay, 253, 254
hybridomas,
enzyme-linked immunosorbent assay screening, 251, 252
flow cytometry screening, 252
preparation, 250, 251
stabilization by limited dilution cloning, 252, 253, 259
immunization,
peptides, 249
transfected cell lines, 250
labeling of antibodies, 257–259
large-scale production, 253
materials, 244–247
stable transfection of CCR8, 247–249
synthetic peptide preparation, 247, 258
mouse models of allergic airway inflammation for in vivo studies,
adoptive transfer model,
antigen-presenting cell preparation, 203
cell preparation for injection, 203, 204, 208
inflammation induction, 204
ovalbumin transgenic splenic lymphocyte preparation, 202, 203, 208
Th2 cell polarization, 203
aerosol challenge, 202, 208
airway hyperactivity analysis, 204
antigen sensitization, 201, 202
cell isolation, 204, 206, 208
chemokine assays, 207
cytokine assays, 207
histology, 206
immunoglobulin assays, 207
immunostaining, 206–208
lung parenchyma cell isolation, 206
materials, 200, 201, 207
overview, 199, 200
redundancy, 182
regulation of expression, 243

signaling, *see* Phosphoinositide 3-kinase
T-cell chemokine response profiling, *see* Chemokines
T-cell homing receptor
expression detection in disease states,
combination
immunohistochemistry/nonradioactive *in situ* hybridization, 159, 160, 164
double immunofluorescence,
blocking, 160
primary antibody incubation, 160, 161, 164
secondary antibody incubation, 161
tissue preparation, 160
visualization of signal, 161, 162
washing, 161
immunohistochemistry,
avidin–biotin amplification signal, 159, 163
blocking, 158
nuclei counterstaining, 159, 163, 164
primary antibody incubation, 158, 159, 163
secondary antibody incubation, 159
tissue preparation, 158, 163
visualization of signal, 159, 163, 164
materials, 148–150
nonradioactive *in situ* hybridization,
hybridization, 156
immunostaining, 157
nuclei counterstaining, 157, 158
prehybridization treatment, 155, 156
probe synthesis, 154, 155
tissue preparation, 154
visualization of signal, 157, 162, 163
washing, 156, 157
radioactive *in situ* hybridization,
counterstaining, 154
hybridization, 152
paraffin-embedded tissue preparation, 150
prehybridization treatment, 151, 152
riboprobe synthesis, 150, 151, 162
visualization of signal, 153, 154, 162
washing, 153
T-helper cell subtype profiles, 147, 148
therapeutic targeting, 182
Chemotaxis,
Dicyostelium discoideum, *see* *Dicyostelium discoideum* chemotaxis
leukocyte chemoattraction, *see* Chemokines; Integrin-dependent rapid adhesion assays; Intravital microscopy; Leukocyte migration assays; Three-dimensional extracellular matrix leukocyte migration assay
Chorioallantoic membrane (CAM), angiogenesis assay, 230–232

D

Dicytostelium discoideum
chemotaxis,
advantages as model system, 94, 95
aggregation process, 91
gene disruption,
clone isolation, 97, 98
genomic DNA isolation, 99
screening for targeted disruptant, 98, 99
targeting vector construction, 96, 97
transformation, 97, 103
materials for assays, 95
neutrophil homology, 93, 94
null mutant analysis,
DB agar development assay, 100, 101
development in suspension with exogenous cAMP addition, 101, 102
overview, 99, 100
receptors and signal transduction, 91–93
signaling protein localization,
intracellular localization, 102
pathway localization, 102, 103

E

EAE, *see* Experimental autoimmune encephalomyelitis
ELISA, *see* Enzyme-linked immunosorbent assay
Endothelial migration assays, *see* Leukocyte migration assays
Enzyme-linked immunosorbent assay (ELISA), chemokine receptor monoclonal antibodies, characterization, 253, 254
hybridoma screening, 251, 252
Experimental autoimmune encephalomyelitis (EAE), leukocyte migration through blood–brain barrier, 189, 190

F

F-actin,
flow cytometry assays of
chemokine-induced formation,
cell pretreatment with signaling inhibitors, 56, 57
chemokine treatment, 57
fixation, permeabilization, and F-actin staining, 57, 65
flow cytometry of F-actin levels, 57, 59, 65, 66
Jurkat T-cell culture, 55
materials, 54, 55
peripheral blood lymphocyte preparation, 56
transfected Jurkat T-cell
studies using proteins in–green fluorescent protein fusion protein,
fixation, permeabilization, and F-actin staining, 61, 63
flow cytometry of F-actin levels, 63, 65, 66
plasmid constructs, 59
transient transfection, 61, 66
formation in leukocyte migration, 53
phalloidin binding, 54
signal transduction in formation, 53, 54
FlashPlate assay, chemokine binding to viral chemokine-binding proteins, 176, 178, 179

Flow assays, *see* Integrin-dependent rapid adhesion assays; Leukocyte migration assays
Flow cytometry,
antigen-specific cell tracking, *see* Antigen-specific lymphocyte tracking in vivo
F-actin, *see* F-actin
hybridoma screening, 252
α4-integrin binding assays on activated leukocytes, 265, 266

G

Glutathione *S*-transferase pull-down assay, *see* Rho

H

Human umbilical cord endothelial cell,
isolation for in vitro angiogenesis assay, 225
monolayer preparation, 235

I

In situ hybridization, *see* Chemokine receptors
α4-Integrin,
adhesion assays on stimulated leukocytes,
ligand-mimetic peptide,
flow cytometry and data analysis, 265, 266
preparation, 262, 263, 266, 267
materials, 261, 262
vascular cell adhesion molecule-1/Fc fusion protein preparation, 262, 266
affinity regulation, 261
leukocyte arrest mediation, 261
vascular cell adhesion molecule-1 interactions, 261
Integrin-dependent rapid adhesion assays,
adhesion molecule affinity purification,
affinity column preparation, 20, 24
chromatography, 20, 24
tissue disruption, 19, 20, 24
capillary tube coating with adhesion molecules and chemokines, 21, 22, 24
interacting cell analysis and quantification, 22, 23, 25
laminar flow assay, 22, 25, 26
materials, 17–19, 23, 24
overview, 17
Integrin signaling, *see* Rho
Intravital microscopy, leukocyte recruitment and chemotaxis,
brain microvessel studies,
adhesion molecule staining, 196
artery ligation, 192, 196
endothelial activation, 191, 192, 196
leukocyte–endothelium interaction analysis, 194–196
lymphocyte preparation for injection, 192
materials, 190, 191
skull preparation, 192, 193, 196
statistical analysis, 196
superficial vessel visualization, 193, 194, 196
chemokine in agarose gel preparation, 126, 127

cremaster muscle,
chemokine application, 127, 129, 130
microscopy, 125, 128, 129
data analysis, 127, 128
integrins in rolling and adhesion, 123
liver microscopy, 125, 126, 129
materials, 124
mouse preparation, 124, 125
overview, 123, 124

L

Laminar flow, *see* Integrin-dependent rapid adhesion assays
Leukocyte migration assays,
actin polymerization, *see* F-actin
air-pouch model, 6, 7
chemotaxis across porous membrane in Boyden microchamber, 5
data analysis, 85, 86
endothelial adhesion assay, 7, 8
endothelial cell generation for study,
lymphatic endothelial cell isolation and culture, 11–13
materials, 4
polyoma middle T-transformed mouse vascular endothelial cells, 10, 11
α4-integrin detection on stimulated leukocytes, *see* α4-Integrin
intravital microscopy, *see* Intravital microscopy, leukocyte recruitment and chemotaxis
materials, 2–4
polarization assay, 5, 6
profiling of specific chemokine responses, *see* Chemokines
reverse transendothelial migration assay, 9, 10
three-dimensional extracellular matrix studies, *see* Three-dimensional extracellular matrix leukocyte migration assay
transendothelial migration assay, 8, 9
transendothelial migration assay under physiologic flow conditions,
applications, 234, 238, 239
chamber setup and shear flow conditions, 235–237, 239, 240
human umbilical cord endothelial cell monolayer preparation, 235
interacting cell analysis and quantification, 237, 238, 240
materials, 234, 235, 239, 240
rationale, 233, 234

M

Macrophage colony-stimulating factor (M-CSF), chemoattractant activity, 1
M-CSF, *see* Macrophage colony-stimulating factor
Micropocket cornea angiogenesis assay,
implant selection, 229
interpretation, 230
principles, 228
stimulus implantation, 229, 230
MS, *see* Multiple sclerosis

Multiple sclerosis (MS), leukocyte migration through blood–brain barrier, 189, 190

N

Neutrophil, *Dicyostelium discoideum* chemotaxis homology, 93, 94

O

Ovalbumin, *see* Allergic airway inflammation, mouse models for in vivo studies

P

Phosphoinositide 3-kinase (PI3K),
adaptor molecules, 211
classes, 211
products, 211, 212
tetracycline-inducible expression in mice for chemokine receptor signaling studies,
characterization of dominant negative clones, 217–219
dominant negative cloning strategy, 214, 216
materials, 213, 214
principles, 212–214
transfection and selection of dominant negative clones, 216, 217
PI3K, *see* Phosphoinositide 3-kinase

R

Rho,
associated proteins in activation, 70
GTPase activity, 69
integrin activation pull-down assay,
bead coupling to antibody or protein, 71, 73
cell stimulation and lysate preparation, 71, 72
glutathione *S*-transferase fusion protein, preparation, 72–74
pull-down assay, 72, 74
materials, 70, 71
Western blot analysis, 73, 74
members, 69

S

Scintillation proximity assay (SPA), chemokine binding to viral chemokine-binding proteins, 174, 176, 179
SPA, *see* Scintillation proximity assay

T

T-cell,
actin polymerization, *see* F-actin
antigen-specific cell tracking, *see* Antigen-specific lymphocyte tracking in vivo
chemokine response profiling, *see* Chemokines
homing receptor expression detection in disease states, *see* Chemokine receptors
Three-dimensional extracellular matrix leukocyte migration assay,
collagen culture, 79, 80, 86
computer-assisted cell tracking, 81, 82, 84, 85, 88
materials, 78, 86
migration chamber construction, 78, 79, 86

principles, 77, 78
rationale, 77
time-lapse video or digital microscopy, 80, 81, 87
Time-lapse video microscopy, *see* Three-dimensional extracellular matrix leukocyte migration assay
Transgenic mouse,
antigen-specific cell tracking, *see* Antigen-specific lymphocyte tracking in vivo
conditional chemokine expression,
applications, 117, 118
overview, 105, 106
tetracycline-inducible system, 107–109
tissue-specific expression system, 115, 116
ubiquitous KC expression system and tissue distribution, 110–115, 117
inducible phosphoinositide 3-kinase expression, *see* Phosphoinositide 3-kinase

V

Vascular endothelial growth factor (VEGF), chemoattractant activity, 1
vCKBPs, *see* Viral chemokine-binding proteins
VEGF, *see* Vascular endothelial growth factor
Viral chemokine-binding proteins (vCKBPs),
binding assays,
cell binding assays, 172, 174
crosslinking with radiolabeled chemokines, 170
FlashPlate assay, 176, 178, 179
ligand blot assay, 170–172
materials, 168, 169
scintillation proximity assay, 174, 176, 179
generation from virus-infected cell cultures, 169, 170, 178
types, 167

W

Western blot, Rho pull-down assay, 73, 74

METHODS IN MOLECULAR BIOLOGY™ • 239
Series Editor: *John M. Walker*

Cell Migration in Inflammation and Immunity

Methods and Protocols

Edited by

Daniele D'Ambrosio and **Francesco Sinigaglia**
BioXell S.p.A., Milan, Italy

Cell migration is now well recognized as a critical component of the inflammatory disease process, so that its proper understanding promises to generate both ground-breaking basic discoveries and the development of novel therapeutics. In *Cell Migration in Inflammation and Immunity: Methods and Protocols,* leading cell biologists and immunologists present their most widely useful and innovative techniques for studying the molecular and cellular basis of this phenomenon. Describing each method in step-by-step detail, the authors provide a series of focused, cutting-edge techniques proceeding from the in vitro analysis of cell migration and the molecular mechanisms underlying this process, to methodologies for the analysis of cell migration in vivo. Methods for the analysis of rapid leukocyte adhesion under flow conditions in vitro are described, which may prove especially fruitful for scientists exploring the molecular mechanisms underlying both vascular recognition and leukocyte–endothelium interaction. Experimental approaches useful in establishing the role of cell migration in the pathogenesis of both acute and chronic inflammatory diseases are emphasized. Each fully tested protocol includes an introduction explaining the principle behind the technique, equipment and reagent lists, and tips on troubleshooting and how to avoid known pitfalls.

Comprehensive and cutting-edge, *Cell Migration in Inflammation and Immunity: Methods and Protocols* offers novice and experienced investigators alike a collection of powerful techniques for studying the molecular basis and pathophysiological significance of cell migration in inflammatory and immune diseases, as well as for the development of novel therapeutics.

FEATURES

- **Comprehensive collection of easy-to-use techniques for the study of cell migration**
- **Methods for analyzing rapid leukocyte adhesion under flow conditions in vitro**
- **Balanced combination of established experimental protocols with new methodologies**
- **Assays for analyzing the mechanisms of cell migration in vivo**

CONTENTS

Chemotaxis and Interaction with Vascular or Lymphatic Endothelium. Analysis of Integrin-Dependent Rapid Adhesion Under Laminar-Flow Conditions. Posttranslational Processing of Chemokines. Chemotactic Profiling of Lymphocyte Subpopulations. Measurement of the Levels of Polymerized Actin (F-Actin) in Chemokine-Stimulated Lymphocytes and GFP-Coupled cDNA Transfected Lymphoid Cells by Flow Cytometry. Evaluation of Rho Family Small G-Protein Activity Induced by Integrin Ligation on Human Leukocytes. Reconstructing Leukocyte Migration in 3D Extracellular Matrix by Time-Lapse Videomicroscopy and Computer-Assisted Tracking. Analyzing Chemotaxis Using *Dictyostelium discoideum* as a Model System. Conditional Transgenic Models to Study Chemokine Biology. Intravital Microscopy as a Tool for Studying Recruitment and Chemotaxis. Tracking Antigen-Specific Lymphocytes In Vivo. Analysis of Homing-Receptor Expression on Infiltrating Leukocytes in Disease States. Interaction of Viral Chemokine Inhibitors with Chemokines. Discovery of Small-Molecule Antagonists of Chemokine Receptors: *Screening Strategy and Assays*. Visualization and Analysis of Adhesive Events in Brain Microvessels by Using Intravital Microscopy. Animal Models to Study Chemokine Receptor Function In Vivo: *Mouse Models of Allergic Airway Inflammation*. Assessing the Role of Multiple Phosphoinositide 3-Kinases in Chemokine Signaling: *Use of Dominant Negative Mutants Controlled by a Tetracycline-Regulated Gene Expression System*. In Vitro and In Vivo Models to Study Chemokine Regulation of Angiogenesis. Real Time In Vitro Assay for Studying Chemoattractant-Triggered Leukocyte Transendothelial Migration Under Physiological Flow Conditions. Generation of Monoclonal Antibodies Against Chemokine Receptors. Detection of High-Affinity α4-Integrin Upon Leukocyte Stimulation by Chemoattractants or Chemokines. Index.

Methods in Molecular Biology™ • 239
CELL MIGRATION IN INFLAMMATION AND IMMUNITY
METHODS AND PROTOCOLS
ISBN: 1-58829-102-2 E-ISBN: 1-59259-435-2
ISSN: 1064–3745 humanapress.com

ISBN 1-58829-102-2
9 781588 291028 90000